

Durham E-Theses

Thermodynamics of polymer mixtures

Robin John MacDonald

How to cite:

MacDonald, Robin John (1991) Thermodynamics of polymer mixtures. Doctoral thesis, Durham University.

Use policy

The full-text may be used and/or reproduced, and given to third parties in any format or medium, without prior permission or charge, for personal research or study, educational, or not-for-profit purposes provided that:

- a full bibliographic reference is made to the original source
- a <https://etheses.durham.ac.uk/id/eprint/6096/> is made to the metadata record in Durham E-Theses
- the full-text is not changed in any way

The full-text must not be sold in any format or medium without the formal permission of the copyright holders.

Please consult the [full Durham E-Theses policy](#) for further details.

Abstract

Research into the thermodynamic behaviour of copolymer blends has been stimulated by the increasing number of applications in which these materials can be used. In this work, it was intended to characterise the thermodynamics of mixtures of two industrial copolymers and to review the experimental techniques and theoretical analyses currently used in this field.

The copolymers used were poly(ethylene - co - vinyl acetate), with $\bar{M}_n = 3290$, and poly(tetradecyl fumarate - co - vinyl acetate), with $\bar{M}_n = 10400$.

The thermodynamics of these mixtures was studied using Differential Scanning Calorimetry, Inverse Phase Gas Chromatography, Solvent Vapour Sorption, Heats of Mixing Calorimetry and Phase Contrast Optical Microscopy. The results of these experiments were interpreted using Flory - Huggins Lattice fluid theory and Flory - Prigogine equation of state theory. Additionally, the results of the calorimetry and chromatography experiments were used to predict the theoretical phase boundary with the intention of comparing the phase boundaries determined experimentally with those predicted theoretically. Unfortunately this comparison could not be made because none of the techniques listed above located a miscibility limit between 303 and 393K. Although some of the experimental results are in conflict, it has been concluded that these materials are immiscible in all proportions in this temperature range. The theoretically simulated spinodal condition occurs between 5 and 50K and is of little practical use in the absence of its experimental equivalent and its extreme temperature.

The free energy change which occurs on mixing these copolymers is dominated by the entropic contribution and the equation of state was concluded to be inadequate to interpret this type of behaviour. It is believed that this is the first work which uses experimental data and a partition function to calculate directly a phase boundary without the inclusion of a fixing parameter.

Thermodynamics of Polymer Mixtures

Robin John MacDonald

Department of Chemistry

University of Durham

April 1991

Submitted for the Degree of Doctor of Philosophy of the University of Durham

The copyright of this thesis rests with the author.
No quotation from it should be published without
his prior written consent and information derived
from it should be acknowledged.


10 FEB 1992

To The Angel - Heaven can wait

Acknowledgements

I would like to acknowledge the support and aid that I have been given during the course of this work and the period over which this thesis was prepared. To Dr. R.W. Richards, for whom the obligatory, glib, statements of respect and thanks would be insulting, I prefer to remember a very alcoholic plane journey from Strasbourg to Newcastle. To Dr. R.D. Tack and all those at Abingdon for their warmth and assistance. To Professor J.S. Higgins and her staff at Imperial College for access to their facilities, and to Mr. G. Woods at the University of Strathclyde for the density measurements and his patience. The financial support of both the SERC and Exxon Chemicals are gratefully acknowledged.

I would also like to thank Mrs. Kelly and the staff of the Malinson Rd. guesthouse in Clapham who made Chapter 5 possible, and Dr. B.B. MacDonald at the University of Strathclyde who facilitated Chapter 8, and acted as Executive Producer in the preparation of this thesis.

Finally, I would like to thank the Three Bears at 107 and all of my friends for their love and support over the most demanding and traumatic period that I hope I will ever have to face,

"Ooh, I get by with a little help from my friends"

"You play, you win, you play, you lose, you play"

- Jeanette Winterton, *The Passion*

Contents	Page
Abstract	1
Title Page	2
Contents	6
List of Tables	9
List of Figures	13
Chapter 1 - Introduction	
Chapter 2 - Theories of Polymer Miscibility	16
2.0 - Introduction	22
2.1 - Flory-Huggins-Miller-Chang Theory	23
2.2 - Equation of State Theory	32
2.3 - Summary	41
2.4 - References	42
Chapter 3 - General Experimental Work	44
3.0 - Characterisation of materials	44
3.1 - Elemental Analysis of EVA	45
3.2 - Gel Permeation Chromatography	47
3.3 - Density Measurements	47
3.4 - Differential Scanning Calorimetry	52
3.5 - Laser Turbidimetry	62
3.6 - General discussion	66
3.7 - References	68
Chapter 4 - Inverse Phase Gas Chromatography	69
4.1 - Introduction	69
4.2 - Theoretical	69
4.3 - Apparatus and materials	74
4.4 - Experimental procedure	76
4.5 - Results	78
4.6 - Discussion	95
4.7 - References	107

	Page
Chapter 5 - Heats of Mixing	110
5.1 - Introduction	110
5.2 - Theoretical	110
5.3 - Materials	111
5.4 - Apparatus	111
5.5 - Experimental procedure	114
5.6 - Results	119
5.7 - Discussion	129
5.8 - References	132
Chapter 6 - Solvent Vapour Sorption	133
6.1 - Introduction	133
6.2 - Theoretical	133
6.3 - Materials	136
6.4 - Apparatus	136
6.5 - Experimental procedure	138
6.6 - Results	139
6.7 - Discussion	155
6.8 - References	165
Chapter 7 - Optical Microscopy	166
7.1 - Introduction	166
7.2 - Apparatus and materials	166
7.3 - Refractive Index calculation	167
7.4 - Results	168
7.5 - Discussion	176
7.6 - Reference	176
Chapter 8 - Simulation of the Phase Boundary	177
8.1 - Introduction	177
8.2 - Procedure	177
8.3 - Results	192
8.4 - Discussion and evaluation of the sensitivity of the model	203
8.5 - General discussion	216
8.6 - References	220

	Page
Chapter 9 - Final Conclusions	222
Appendix 1 - Full report of the IGC data from a Lattice Theory analysis	
Appendix 2 - Full report of the Simulation data from Chapter 8	
Appendix 3 - Listing of external lectures, colloquia and seminars given in 1990-91	
Appendix 4 - Listings of the BASIC programs employed in the IGC experiments	
Appendix 5 - Listings of the Modula2 programs used in Chapter 8.	

Tables	Page
3.1 Elemental analysis of EVA	45
3.2 GPC analysis of EVA and FVA molecular weight	47
3.3 Temperature-Composition-Density relationships of EVA and FVA mixtures	49
3.4 DSC miscibility results	55
3.5 DSC melting point depression results	57
3.6 Turbidimetry results for EVA	64
4.1 IGC Polymer-Solvent Interaction Parameters at 353K	89
4.2 IGC Polymer-Solvent Interaction Parameters at 373K	90
4.3 IGC Polymer-Solvent Interaction Parameters at 393K	91
4.4 IGC Polymer-Polymer Interaction Parameters at 353K	92
4.5 IGC Polymer-Polymer Interaction Parameters at 373K	93
4.6 IGC Polymer-Polymer Interaction Parameters at 393K	94
4.7 Mean values of the Polymer-Solvent Interaction Parameters	97
4.8 Mean values of the Polymer-Polymer Interaction Parameters	98
4.9 Comparison of Polymer-Solvent and Polymer-Polymer-Solvent Interaction Parameters at 353K	101
4.10 Comparison of experimental Net Retention Volumes and those calculated for a heterogeneous mixture	106
5.1 Calorimeter calibration at 348.7K	121
5.2 Calorimeter calibration at 359.3K	121
5.3 Heat of Mixing data at 348.7K	124
5.4 Heat of Mixing data at 359.3K	124
5.5 Heat of Mixing Polymer-Polymer Interaction Parameters at 348.7K	126

	Page
5.6 Heat of Mixing Polymer-Polymer Interaction Parameters at 359.3K	126
5.7 Free Energy of Mixing calculated from Heat of Mixing data at 348.7K	127
5.8 Free Energy of Mixing calculated from Heat of Mixing data at 359.3K	129
6.1 Saturation vapour pressures of Hexane	140
6.2 Reproducibility of the SVS spring extension data	141
6.3 SVS Calibration function	143
6.4 Hexane-FVA Interaction Parameters at 313K	146
6.5 Hexane-EVA Interaction Parameters at 313K	148
6.6 Hexane-20%EVA mixture Interaction Parameters at 313K	150
6.7 Hexane-40%EVA mixture Interaction Parameters at 313K	152
6.8 Hexane-FVA Interaction Parameters at 353K	152
6.9 Hexane-EVA Interaction Parameters at 353K	155
6.10 Polynomial fits of Hexane-EVA data at 313K	157
6.11 SVS Polymer-Solvent Interaction Parameters	158
6.12 Comparison of SVS and IGC Polymer-Polymer Interaction Parameters	159
6.13 Polynomial Fits of Hexane-EVA data at 353K	160
6.14 Polynomial Fits of Benzene-PS-PVME data at 298K	160
6.15 Polynomial Fits of Carbon Tetrachloride-PVC-PCL data at 338K	163
7.1 Refractive Index values for EVA and FVA	167
8.1 Solubility Parameter values for EVA and FVA	182

	Page
8.2 Measured and recalculated Heat of Mixing values at 348.7K	184
8.3 Comparison of Heat of Mixing values from the literature	186
8.4 List of the surface area to volume ratios for the IGC solvents	190
8.5 EOS Parameters for EVA	192
8.6 EOS Parameters for FVA	192
8.7 Comparison of EOS Parameters from the literature	193
8.8 Mean Interaction Parameter and Spinodal Temperature values at 353K	195
8.9 Mean Interaction Parameter and Spinodal Temperature values at 373K	196
8.10 Mean Interaction Parameter and Spinodal Temperature values at 393K	196
8.11 to 8.13 Effect of Molecular Weight on the Spinodal Prediction	204, 206
8.14 to 8.16 Effect of the surface area/volume ratio on the Spinodal Prediction	207, 209
8.17 to 8.21 Effect of the Thermal Expansion coefficient on the Spinodal Prediction	210-212
8.22 Effect of the Q Parameter on the Spinodal Prediction	214
8.23 Relationship between Q and the Spinodal Temperature	216
8.24 Measured and Recalculated Heat of Mixing values at 359.3K	218

Figures	Page
2.1 Idealised phase diagram of UCST behaviour	30
3.1 Unit Structure of EVA	46
3.2 Unit Structure of FVA	46
3.3 Density-Composition functions of mixtures of EVA and FVA	50
3.4 Phase diagram of EVA/FVA as determined by DSC	56
3.5 DSC thermogram of EVA	59
3.6 DSC thermogram of FVA	60
3.7 Schematic diagram of Turbidimetry apparatus	63
3.8 Schematic diagram of Turbidimetry sample cell	65
3.9 Plot of Turbidimetry results for EVA	67
4.1 Schematic diagram of IGC apparatus	75
4.2 Elution Curve of Dichloromethane on an FVA column at 353K	77
4.3 IGC Polymer-Polymer Interaction Parameters at 353K	99
4.4 IGC Polymer-Polymer Interaction Parameters at 373K	103
4.5 IGC Polymer-Polymer Interaction Parameters at 393K	104
5.1 Schematic diagram of the original sample cell for Heats of Mixing measurements	113
5.2 Graphical representation of the dependence of Calorimeter angle and baseline response	115
5.3 Schematic diagram of new sample cell design	116
5.4a Cross-sectional view of Calorimeter	117
5.4b Schematic diagram of the operation of the Calorimeter	118
5.5 Calorimeter calibration function	123
5.6 Heat of Mixing data	125

	Page
5.7 Polymer-Polymer Interaction Parameters and Free Energy of Mixing at 348.7K	128
5.8 Idealised phase diagram for EVA/FVA mixture from Heat of Mixing Data	131
6.1 Schematic diagram of SVS apparatus	137
6.2 SVS calibration function	144
6.3 Hexane-FVA Interaction Parameters at 313K	147
6.4 Hexane-EVA Interaction Parameters at 313K	149
6.5 Hexane-20%EVA mixture Interaction Parameters at 313K	151
6.6 Hexane-40%EVA mixture Interaction Parameters at 313K	153
6.7 Hexane-FVA Interaction Parameters at 353K	154
6.8 Hexane-EVA Interaction Parameters at 353K	156
6.9 Hexane-20%EVA mixture Interaction Parameters at 313K	161
6.10 Hexane-40%EVA mixture Interaction Parameters at 313K	162
6.11 Comparison of polynomial fits of the Carbon Tetrachloride-PVC-PCL data at 338K	164
7.1 Four Optical Micrographs of EVA being heated from 313.2 to 343.3K	170
7.2 a&b: Eight Optical Micrographs of a 50%EVA mixture being heated from 313.2 to 373.2K	171, 172
c: Four Optical Micrographs of 50%EVA mixture, after being annealed at 373K, being heated from 303.2 to 373.2K	173
7.3 Four Optical Micrographs of a 17%EVA mixture being heated from 313 to 343K	174
7.4 Four Optical Micrographs of a solution cast 17%EVA mixture being heated from 313.1 to 364.3K	175

	Page
8.1 Measured and recalculated Heat of Mixing values at 348.7K	185
8.2 Mean Interaction Parameter values at 353K	197
8.3 Mean Interaction Parameter values at 373K	198
8.4 Mean Interaction Parameter values at 393K	199
8.5 Simulated Spinodal from data at 353K	200
8.6 Simulated Spinodal from data at 373K	201
8.7 Simulated Spinodal from data at 393K	202
8.8 Effect of molecular weight on the Spinodal prediction	205
8.9 Effect of the surface area/volume ratio on the Spinodal prediction	208
8.10 Effect of the Thermal Expansion coefficient on the Spinodal prediction	213
8.11 Effect of the Q Parameter on the Spinodal prediction	215
8.12 Relationship between Q and the Spinodal temperature	217

Declaration and Copyright

I hereby declare that none of the material contained in this thesis has been submitted for any other degree, at this or any other University, and unless stated otherwise the material is original and the work of the author.

The copyright of this thesis rests with the author. No quotation from it should be published without his prior written consent and information derived from it should be acknowledged.

Chapter 1 Introduction

The last four decades have seen significant research into the occurrence and characterisation of mutually soluble polymeric species. This effort was initiated and has been sustained by both academic interest and the many commercial applications where either an averaging of pure polymer properties or a useful combination of different properties has been sought.

Until the 1960s very few polymer pairs were known to be miscible and, conceptually, polymer miscibility was always considered to be unusual since high molecular weight materials have a negligibly small entropic contribution to mixing energetics and consequently a small, unfavourable enthalpic contribution would preclude miscibility. The majority of the early polymer blends were found to be miscible because of some strong specific interaction between components in different chains, *e.g.* hydrogen bonding, which dominated the free energy change on mixing. However, a wide range of materials has been studied and a host of compatible pairs identified⁽¹⁾, including poly(vinylchloride) with poly(acrylates)⁽²⁾, vinyl acetate copolymers⁽³⁾ and butadiene-acrylonitrile copolymers⁽⁴⁾, all of which have found applications as additives in the industrial manufacture of PVC, and polystyrene and poly(2,6-dimethyl-1,4-phenylene oxide) which form a strong engineering plastic which is sold under copyright as 'Noryl'⁽⁵⁾. There are essentially three methods of preparing miscible polymer blends,

- (a) mechanical mixing,
- (b) mixing in a common solvent, and
- (c) *in situ* polymerisation.

Although physically mixing two polymers is the simplest and most widely utilised method of producing blends in industry it has several inherent disadvantages. Firstly, polymeric materials often have relatively low thermal stability and the lengthy periods, at elevated temperatures, necessary for the inter-diffusion of viscous polymers often cause degradation of the product. Secondly, efficient mixing can be extremely difficult and when this is not achieved the resulting blend often contains regions of heterogeneous polymer and degraded material, caused by prolonged exposure to excessive temperatures in the reactor. Dissolution and mixing of polymers in a common solvent is the preferred academic method as it is suitable for small-scale preparations and generally forms more homogeneous mixtures since the viscosity and mobility problems of physically contacting the polymers are avoided.

However, this is not necessarily true, since the introduction of a common solvent results in a ternary system which has its own miscibility limits and subsequent evaporation of the solvent may cause the entire system to become thermodynamically unstable and completely phase separate, *e.g.* polystyrene and poly(vinyl methyl ether) form two-phase systems when cast from chlorinated solvents but homogeneous blends when cast from toluene. Finally, *in situ* polymerisation involves reacting a monomer in the presence of another polymer. This technique is particularly attractive in industrial processes because it can be used to fabricate both engineering plastics, which are essentially insoluble, and base polymers which have poor thermal stability and/or a high glass-transition temperature. It has also found favour as an alternative to existing large scale commodity processes which generate enormous solvent effluents. However, this approach does not guarantee a miscible blend since two-phase regions can exist within the polymer/polymer/monomer phase diagram, and frequently this approach involves a series of reaction steps which are designed to maintain the composition within the miscibility window.

Owing to the limited number of monomeric species which can be polymerised, and the processing difficulties which arise while attempting to manufacture miscible polymer blends, significant interest has developed in copolymers, *i.e.* species which are formed from more than one monomer. Copolymers have a distinct advantage over homopolymer blends because the monomers are part of the same molecular chain, and hence their intimate contact is guaranteed. Although these materials often display the complementary properties desired in the corresponding polymer blend, they have also been found to have completely unique properties, *e.g.* synthetic rubber is commonly prepared as a terpolymer comprising butadiene for elasticity, styrene for rigidity and acrylonitrile for solvent resistance. In this material the polystyrene molecules are segregated spatially and form supporting cross-linked structures which can be thermally decomposed. This reversibility may lead to a synthetic alternative to natural rubber which would be capable of being recycled. Copolymers have also found applications as 'compatibilisers', where an AB copolymer can be used to solubilise a mixture of A and B bulk polymers in a similar manner to the way that a soap molecule behaves at the oil/water interface. They have also found applications as crystal structure modifiers where the incorporation of a minute quantity of a copolymer contaminant disrupts the order of the crystallising bulk polymer chains.

Some confusion is evident when the terms compatibility and miscibility are used with reference to polymer systems. The academic literature describes a mixture which behaves as a single phase as being compatible, whereas the same term is frequently used in an industrial context to describe materials, capable of being processed, which are heterogeneous and phase separated. Similarly, many commercially available materials which are described as being miscible actually are micro-phase separated dispersions. To eliminate this confusion, miscibility is most clearly defined on a thermodynamic basis where the essential, unambiguous criterion for its existence is a negative and favourable free energy of mixing. The original theories of polymer-polymer thermodynamics were derived from liquid-liquid and polymer-solvent theories^(6,7,8,9,10) and Flory's lattice theory⁽¹¹⁾. The latter remains the most successful of the simple approaches and retains many of the original features of the small molecule theories. More recently, an equation of state approach has been developed which links all of the state parameters, and hence physical characteristics, of a polymer or a mixture of polymers, by a single partition function. This type of theory is generally agreed to provide a more accurate description of blend behaviour but its application requires a considerable data input which in some cases appears to outweigh its advantages. However, both of these types of theory include a term which characterises the energetic interaction between two heterospecies and, by the numerical value or sign of this term, gives an indication of whether these materials are likely to be miscible. This term is generally defined as the interaction parameter. A host of analytical techniques has been applied, or developed, to determine the value of these interaction parameters for a wide range of polymer mixtures.

The simplest method of measuring the enthalpic interaction of two fluids is to measure their heat of mixing. The main advantage of this type of experiment are that the operation is being measured directly and only the enthalpic contribution to the free energy of mixing is detected. The theoretical and experimental simplicity of this measurement should provide data which are both accurate and absolute. Unfortunately, it is almost impossible to determine the heat of mixing of polymeric materials owing to their physical state, and consequently the existing heat of mixing studies on polymer blends have used either a common solvent as a third component and extracted the polymer-polymer contribution using a Hess's law⁽¹²⁾ type calculation, or they have used low molecular weight analogues and attempted to modify these values for the high molecular weight case^(13,14). Not surprisingly, neither approach has been particularly successful as the enthalpy of mixing of macromolecular species tends to be small, and consequently the errors in a

Hess's law calculation are significant, and the corrections to oligomeric determinations are extremely crude. Another classical and simple technique which has been applied to polymer systems is solvent vapour sorption⁽¹⁵⁾ which comprises exposing a homopolymer or blend to solvent vapour and measuring the uptake as a function of solvent vapour pressure. As with heats-of-mixing experiments, this technique also has the advantage of providing absolute thermodynamic information and does not require the polymer phase to be either mobile or volatile. The main disadvantage of SVS is that it is a static equilibrium method and consequently a measurement can only be taken once the solvent has diffused into the bulk polymer structure and an absorption equilibrium has been established. This can take a period of days or even weeks and during this period complete control of temperature and vapour pressure are required. The polymer-polymer interaction is calculated from SVS data by measuring each homopolymer-solvent response, the blend-solvent response and then extracting the difference algebraically and defining this as the polymer-polymer contribution. This method of analysis is also used in inverse phase gas chromatography which involves eluting a volatile solvent of known physical characteristics over a polymeric stationary phase, the inverse situation to conventional gas chromatography. This technique was first reported in 1969⁽¹⁶⁾ and stimulated considerable interest as it appeared to be a rapid, cheap and reliable method of studying the thermodynamics of polymer-solvent and polymer-polymer systems. However, this initial optimism soon waned when it became clear that the polymer-polymer interaction parameters which were derived from IGC measurements exhibited a clear dependence on the nature of the solvent probe. Much of the subsequent research into the application of IGC to polymer blends has been devoted to characterising this solvent dependence but a definitive solution has not yet been found and this remains an inherent weakness.

If one of the components of a polymer blend is amorphous while the other is crystalline at any particular temperature, the depression of the crystalline component's melting point can be used to evaluate an interaction parameter^(11,17) and the most convenient techniques to follow this effect are differential scanning calorimetry and turbidity measurements. Although this approach is appealing theoretically it has been found to be difficult in practice owing to heterogeneity and diffusion limitation on sample heating and supercooling in reverse. Another technique which can be used to evaluate polymer-polymer interaction parameters is intrinsic viscosity measurements, which have been used for some time to determine the interaction parameters of dilute polymer-solvent-non-solvent systems, but some work has also been

carried out to examine its suitability to polymer blends⁽¹⁸⁾. The scattering of radiation, *i.e.* X-rays and light, has also been widely used to characterise the thermodynamics of polymer blends but since this area is so large, and the techniques were not applicable in this work, it was felt that further discussion was outwith the scope of this study.

The equation of state theory can also be used to evaluate interaction parameters by fitting theoretical spinodal functions to experimental data, using Q , the entropic correction factor, as the adjustable parameter⁽¹⁹⁾. This approach assumes that the free energy of mixing can be represented by an enthalpic component, which is constant for any polymer pair, and an entropic correction factor. The value of the enthalpic component dictates the position of the spinodal and small adjustments are then made to Q in order to improve the fit. However, as Q has no physical significance, and was incorporated into the equation of state model to improve the original predictions, this arbitrary fitting procedure is difficult to justify since it assumes that the adopted partition function upon which the EOS is based represents exactly the thermodynamic mixing of polymer molecules and any poor correlation between theoretical and experimental results can be ascribed to entropic effects which are not accounted for by the model.

The intentions behind this current work were to characterise the mixing of two copolymers on the basis that they were homopolymers and examine the applicability and accuracy of the homopolymer models to this system. This study was to include determination of the free energy polymer-polymer interaction parameter from an indirect technique, *e.g.* IGC or SVS, determination of the enthalpic interaction parameter from heats of mixing experiments and then, for the first time, directly calculating the value of Q . From this information the phase boundary can be simulated. It was then hoped to measure the experimental phase boundary using phase contrast optical microscopy or differential scanning calorimetry and compare these results to the simulated condition.

REFERENCES

- (1) O.Olabisi, L.M.Robeson and M.T.Shaw,
"Polymer-Polymer Miscibility", Academic Press, N.Y. (1979).
- (2) K.Adler, K.P.Paul, *Kunststoffe*, 7, 70, (1980).
- (3) D.J.Walsh and J.G.McKeown, *Polymer*, 21, 1330, (1980).
- (4) R.A.Emmett, *Ind. Eng. Chem.*, 36, 730, (1979).
- (5) E.P.Cizek, US Patent 3,383,435, (General Electric Co.), (1968).
- (6) J.J.Van Laar, *Z. Physik. Chem.*, 72, 723, (1910).
- (7) J.H.Hildebrand and S.E.Wood, *J.Chem.Phys.*, 1, 817, (1933).
- (8) G.Scatchard, *Chem Rev.*, 8, 321, (1931).
- (9) G.Scatchard, *Trans. Faraday Soc.*, 33, 160, (1937).
- (10) J.H.Hildebrand, J.M.Prausnitz and R.L.Scott,
'Regular and Related Solutions', Van Nostrand Reinhold Co., (1970).
- (11) P.J.Flory, 'Principles of Polymer Chemistry',
Cornell University Press, (1953).
- (12) A.A.Tager, T.T.Scholokhovich and Yu.S.Bessanov,
Eur. Polym. J., 11,321, (1975).
- (13) Z.Chai, S.Rouna, D.J.Walsh and J.S.Higgins, *Polymer*, 24, 263, (1983).
- (14) S.Rostami and D.J.Walsh, *Macromolecules*, 17, 315, (1984).
- (15) C.Panayiotou and J.H.Vera, *Polymer J.*, 16:2, 89, (1984).
- (16) J.E.Guillet and O.Smidsrod, *Macromolecules*, 2, 272, (1969).
- (17) T.Nishi and T.T.Wang, *Macromolecules*, 8, 909, (1975).
- (18) J.W.A.van Den Berg and F.W.Altena, *Macromolecules*, 15, 1447, (1982).
- (19) Z.Chai, S.Rouna, D.J.Walsh and J.S.Higgins, *Polymer*, 24, 263, (1983)

Chapter 2 Theories of Polymer Miscibility

2.0 Introduction

Solution thermodynamics⁽¹⁾ forms the basis for many of the theories of polymer- polymer miscibility. These theories normally involve modelling the mixture and interpreting its behaviour with statistical techniques.

The difference in many of the theories lies in either the nature and sophistication of the initial model, or the statistical mechanics with which it is interpreted. This chapter aims to describe and discuss the salient features and areas of application of some of the more widely used theories without explicitly deriving them from first principles since these procedures are well documented elsewhere.

The equilibrium properties of a material can be fully characterised by a knowledge of the Gibbs free energy, G , as a function of the independent state variables, *e.g.* temperature, T , pressure, P , and composition. The change in this function must be negative for a potential mixing process, *i.e.* $\Delta G_{mix} < 0$, and this is a necessary, although not sufficient, criterion for miscibility.

For the process,



this change is defined as,

$$\Delta G_{mix} = G_{12} - (n_1 G_1^0 + n_2 G_2^0) \quad (2.1)$$

where, G_{12} = Gibbs free energy of mixture, J

n_i = number of moles of component 'i', mol

G_i^0 = molar Gibbs function of pure component 'i' at the temperature and pressure of the system, J

This study has used both classical Flory⁽²⁻⁴⁾ - Huggins⁽⁵⁻⁸⁾ - Chang⁽⁹⁾ - Miller⁽¹⁰⁻¹²⁾ theory, which is based on a lattice model, and Prigogine^(13,14) - Flory^(15,17) theory, which uses an arbitrary partition function to interpret the changes in the Gibbs free energy in terms of an equation of state, and their relative merits are considered. The discussion of Prigogine - Flory theory concentrates on the concepts involved rather than the mathematical treatment as a full description of how to apply this theory is detailed in chapter 8.

2.1 Flory - Huggins - Chang - Miller Theory (FHCM)

Flory - Huggins - Chang - Miller theory considers ΔG_{mix} as the sum of enthalpic and entropic contributions and develops these terms independently, *i.e.* from the classical expansion,

$$\Delta G_{mix} = \Delta H_{mix} - T \Delta S_{mix} \quad (2.2)$$

where, ΔH_{mix} = change in enthalpy of the system on mixing, J mol⁻¹

ΔS_{mix} = change in entropy of the system on mixing, J mol⁻¹ K⁻¹

T = absolute temperature, K

The fundamentals of this approach will be derived initially for small molecules and then developed for polymers.

The Enthalpic Contribution, (ΔH_{mix})

Intermolecular forces between uncharged molecules decrease rapidly as the separation distance increases and thus this model considers the effect of mixing only on neighbouring molecules. The enthalpic change, defined as the heat of mixing, ΔH_{mix} , is considered to originate from the difference in contact energy between like and unlike molecules, *e.g.* for a system comprising species 1 and 2,

$$W = 0.5 \left| (E_{11} + E_{22} - 2E_{12}) \right| \quad (2.3)$$

where

W = change in contact energy for the formation of a molecule of '12', J

E_{ij} = contact energy between species 'i' and 'j', J

If a single arrangement of molecules on the lattice is specified, in which there are N_c unlike contacts, the heat of formation, $\Delta H_{conformation 1}$, of this particular configuration, from the pure components is,

$$\Delta H_{conformation 1} = N_c W \quad (2.4)$$

An average value of N_c is now required to represent random mixing in the solution. This term is the product of the number of contact sites available and the probability that neighbouring molecules are different,

$$N_c = z n_1 p_{12} \quad (2.5)$$

where

z = the coordination number of the lattice

n_1 = the number of molecules of 'species 1'

p_{12} = the probability that the neighbour of a molecule of component 1 is a molecule of component 2

This probability term is difficult to evaluate since the frequency of different contacts is governed by Boltzmann factors. Instead it is replaced with the probability, p_2 , that any molecule in the solution is of component 2 irrespective of its position. If it is assumed that the arrangement of the molecules on the lattice is completely random, this probability is equal to the mole fraction of component 2,

$$p_{12} = p_2 = N_2 / (N_1 + N_2) = x_2 \quad (2.6)$$

where

N_i = the number of molecules of species 'i'

x_i = mole fraction of 'i'

and hence,

$$\Delta H_{\text{conformation 1}} = \frac{z W N_1 N_2}{N_1 + N_2} = z W N_{AV} n_1 x_2 \equiv \Delta H_{\text{mix}} \quad (2.7)$$

where

n_i = number of moles of 'i'

N_{AV} = Avogadro's number, $6.023 \times 10^{23} \text{ mol}^{-1}$

The product $z W N_{AV}$ represents the enthalpy change that occurs when 1 mole of pure A is infinitely diluted in a solution of B, or *vice versa*. This theory then simplifies the situation by introducing the 'interaction parameter', χ_{12} ,

$$\chi_{12} \equiv z W N_{AV} / RT \equiv z W / kT \quad (2.8)$$

where

R = General gas constant, $8.31441 \text{ J mol}^{-1} \text{ K}^{-1}$

k = Boltzmann constant, $1.38066 \times 10^{-23} \text{ JK}^{-1}$

and therefore

$$\Delta H_{mix} = zW N_{AV} n_1 x_2 = RT n_1 x_2 \chi_{12} \quad (2.9)$$

This dimensionless quantity, χ_{12} , incorporates the difference in energy that a molecule possesses when it is surrounded by molecules of another species, compared to that of the pure state. χ_{12} can be either positive or negative and theoretically is inversely proportional to temperature. It should be noted that none of the original parameters of the hypothetical lattice is retained in this final expression as they have been incorporated into the χ_{12} parameter.

This predicted independence was supported by the work of Longuet-Higgins⁽¹⁸⁾ who derived the same expression, starting from the free energy of mixing, and derived on a classical basis.

The Entropic Contribution, (ΔS_{mix})

Using statistical mechanics, the entropy of any system can be subdivided conceptually into several components:

- (a) external degrees of freedom, *e.g.* translational movement
- (b) internal degrees of freedom, *e.g.* vibration and rotation
- (c) intermolecular interactions, and
- (d) configurational entropy

Configurational entropy, S_{conf} , plays a significant role in the thermodynamics of polymer chains, because of the numerous orientations that these molecules can adopt, and Flory-Huggins-Chang-Miller theory assumes that it is the only significant entropic effect that occurs during mixing of polymers,

i.e. $\Delta S_{mix} \equiv S_{conf}$. This can be calculated from the Boltzmann relation,

$$S_{conf} = k \ln C \quad (2.10)$$

where C = the number of different molecular arrangements compatible with the same macroscopic state of the system.

The relationship above implies total randomness and thus C can be equated to the total number of configurations that N_1 molecules of substance 1 can assume upon a lattice comprising molecules of 1 and 2 arranged over $N_1 + N_2$ locations.

From this concept C can be redefined as,

$$C = (N_1 + N_2)! / (N_1! N_2!) \quad (2.11)$$

From which (2.10) becomes,

$$S_{conf} = k \text{Ln} \left\{ (N_1 + N_2)! / (N_1! N_2!) \right\} \quad (2.12)$$

If the factorial terms are simplified by Stirling's approximation,

$$\text{i.e. } \text{Ln}(N!) = N \text{Ln}(N) - N,$$

Equation 2.10 becomes,

$$S_{conf} = -k \left\{ N_1 \text{Ln} \left(N_1 / (N_1 + N_2) \right) \right\} + N_2 \text{Ln} \left\{ N_2 / (N_1 + N_2) \right\} \quad (2.13a)$$

This can now be re-expressed in terms of moles and mole fractions,

$$\text{i.e. } R = kN_{AV} \text{ and } N_i / (N_1 + N_2) = x_i,$$

$$\text{then } S_{conf} = -R \left\{ n_1 \text{Ln}(x_1) + n_2 \text{Ln}(x_2) \right\} \quad (2.13b)$$

From the assumption stated earlier, that this term represents the only contribution to entropic change during mixing,

$$\Delta S_{mix} = -R \left\{ n_1 \text{Ln}(x_1) + n_2 \text{Ln}(x_2) \right\} \quad (2.13c)$$

This is the general form of the entropic contribution to the mixing from FHCM theory. If equations 2.9 and 2.13c are substituted into equation 2.2, an expression for the free energy change is obtained,

$$\Delta G_{mix} = n_1 x_2 \chi_{12} RT - \left\{ -RT \left(n_1 \text{Ln}(x_1) + n_2 \text{Ln}(x_2) \right) \right\}$$

or,

$$\Delta G_{mix} / RT = n_1 x_2 \chi_{12} + n_1 \text{Ln}(x_1) + n_2 \text{Ln}(x_2) \quad (2.14a)$$

or

$$\Delta G_{mix} = RT \left\{ n_1 \text{Ln}(x_1) + n_2 \text{Ln}(x_2) + n_1 x_2 \chi_{12} \right\} \quad (2.14b)$$

This is the classical FHCM expression for the free energy of mixing of small molecules which, in turn, requires to be modified to represent the mixing of polymeric species.

In order to place both solvent molecules and macromolecules on the same lattice it is necessary to subdivide the polymer chains into segments, each of which have the same volume as a solvent molecule. If the ratio of the molar volumes of the polymer, subscript 2, and solvent, subscript 1, is defined as f , the number of sites available on the lattice is now $N_1 + fN_2$ and these must accommodate N_1 molecules of solvent and N_2 macromolecules. In this system the configurational entropy is equal to the number of different arrangements in which these species can coexist in the lattice. In this case the calculation is more complex than for a small molecule, since each segment of the macromolecule is not discrete. The optimum solution to this problem is again obtained by the use of probabilities. In the small molecule derivation, it was assumed that the probability of a specific neighbouring cell already being occupied was equal to that of any other cell already being occupied, which is also equal to the number of cells occupied at any given time in the lattice filling process. For simplicity this assumption is also applied to macromolecular systems. It is adequate for highly concentrated polymer solutions and polymer blends, but renders the theory useless for dilute solutions where the local density of the polymeric segments may be high even though the overall concentration may be approaching infinite dilution. Since the polymer dimension which is now of interest is the volume of the segment, which is equivalent to the volume of each cell in the lattice, the mole fractions used in equation 2.14b are replaced by volume fractions, ϕ_i

$$\Delta G_{mix} = RT \left\{ n_1 \ln(\phi_1) + n_2 \ln(\phi_2) + n_1 \phi_2 \chi_{12} \right\} \quad (2.14c)$$

$$\text{where } \phi_1 = 1 - \phi_2 = n_1 / (n_1 + f n_2) \text{ and } \phi_2 = f n_2 / (n_1 + f n_2)$$

This is the classical FHCM theory expression for the free energy change on mixing polymeric species. Since the enthalpic and entropic contributions have been developed separately they will now be examined separately to investigate their predicted individual effects on this free energy change.

The influence of the enthalpic component

From equation 2.3,

$$i.e. \quad W = 0.5 \left| (E_{11} + E_{22} - 2 E_{12}) \right|$$

the enthalpy change on mixing non-polar materials will unfavourable since E_{12} is equivalent to the geometric mean, *i.e.* $E_{12} = (E_{11} E_{22})^{0.5}$, which is smaller than the arithmetic mean, *i.e.* $0.5(E_{11} + E_{22})$.

The influence of the entropic component

From equation 2.13c it is apparent that the magnitude of the entropic change is highly dependent on the molecular weight of the materials being mixed.

As the molecular weight of the components increases, the number of moles decreases, (for a constant mass of mixture), hence as $M \rightarrow \infty$ then $n_i \rightarrow 0$ and hence $\Delta S_{mix} \rightarrow 0$. In polymeric systems the component molecular weights are usually high and consequently the entropic effect is assumed to be extremely small.

In view of these two predictions it is not surprising that very few polymers are miscible. Three exceptions exist to this general condition.

- (a) If the molecular weights of the components are relatively small, the negative entropic contribution may dominate the enthalpic effect and produce a favourable free energy.
- (b) If the polymer pair are chemically and physically very similar the heat of mixing is likely to be very small and again the miscibility will be determined by the favourable entropic contribution.
- (c) The enthalpy of mixing for species with specific interactions, *e.g.* hydrogen bond, is significantly negative, which dominates the ΔG_{mix} term.

To examine the temperature dependence of the free energy change, it is convenient to replace the interaction parameter, χ_{12} , with the interaction energy density characteristic of the polymer pair, B , defined as,

$$B = \chi_{12} RT/V_1 \quad (2.15)$$

where,

$$V_1 = \text{the molar volume of component 1, cm}^3 \text{mol}^{-1}$$

If equation 2.15 is substituted into equation 2.9, we have,

$$\Delta H_{mix} = B n_1 V_1 \phi_2 \quad (2.9b)$$

and consequently (2.14) becomes,

$$\Delta G_{mix} = \underbrace{RT \{n_1 \text{Ln}(\phi_2) + n_2 \text{Ln}(\phi_{12})\}}_{\text{[Entropic]}} + \underbrace{B n_1 V_1 \phi_2}_{\text{[Enthalpic]}} \quad (2.14c)$$

In this form the effect of temperature is apparent. The favourable entropic component is directly dependent on absolute temperature and thus becomes increasingly large as T increases. Conversely, the enthalpic component is

independent of temperature and constant for a specific polymer pair, thus ΔG_{mix} has the same temperature dependence as the entropic component and becomes increasingly negative and favourable as the temperature is increased. This gives rise to the limits of miscibility and a phase diagram as shown in Figure (2.1). This type of phase behaviour, called Upper Critical Solution Temperature, (UCST), is typical of blends which have low molecular weight constituents. At T_3 , Figure (2.1), the polymers are miscible in all proportions and the second derivative of the free energy with respect to composition is always positive,

$$\frac{d^2(\Delta G_{mix})}{d\phi_b^2} > 0 \quad (2.16)$$

This is the essential criterion for miscibility. At T_1 all compositions between ϕ_a and ϕ'_a can phase separate to reduce the overall energy. This produces two discrete phases whose compositions are ϕ_a and ϕ'_a and which have equal free energy/composition first derivatives,

$$\frac{d(\Delta G_{mix})_a}{d\phi_a} = \frac{d(\Delta G_{mix})_{a'}}{d\phi_{a'}} \quad (2.17)$$

The maximum temperature at which miscibility occurs in monodisperse polymers is T_2 . At T_2 the critical point is given by,

$$\frac{d^2(\Delta G_{mix})_a}{d\phi_a^2} = \frac{d^3(\Delta G_{mix})_{a'}}{d\phi_{a'}^3} = 0 \quad (2.17)$$

Between ϕ_a and ϕ_b and between ϕ'_a and ϕ'_b a region of metastability occurs since any small fluctuation in composition produces an increase in the free energy, which prevents phase separation. In this region phase separation can only proceed *via* a mechanism of nucleation and growth. This mechanism involves the growth of phases which have constant composition and consequently results in an irregular pattern of separation. Between compositions ϕ_b and ϕ'_b a small fluctuation in composition causes a lowering of the free energy and phase separation occurs by spinodal decomposition. The mechanism of spinodal decomposition involves the growth of a preferred concentration fluctuation which causes a continuous change in the composition of the phases. In the early stages of spinodal decomposition the spacing of the phases remains constant while the composition varies.

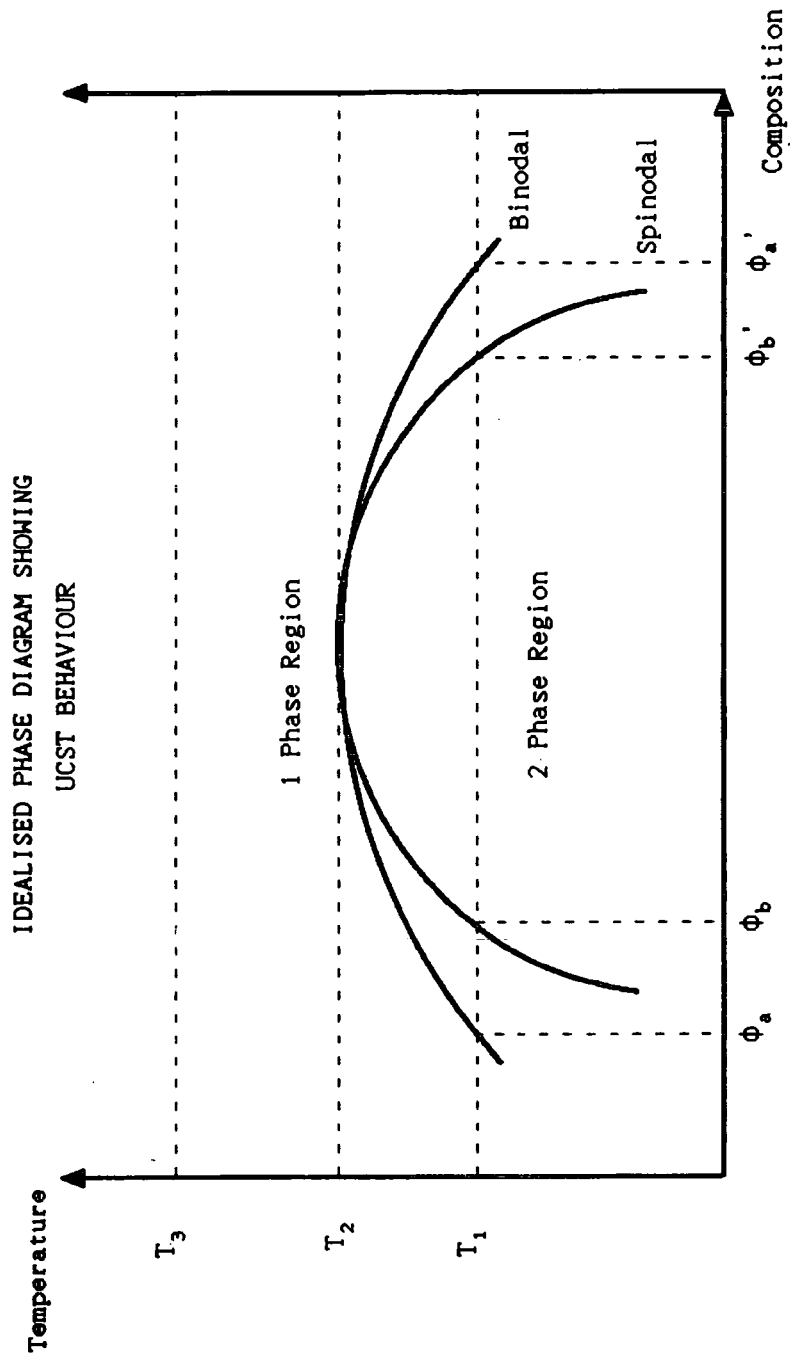


Figure 2.1

The spinodal condition is given by,

$$\frac{d^2(\Delta G_{mix})}{d\phi^2} = 0 \quad (2.19)$$

and the line satisfying this condition and connecting all points of composition ϕ_b is the spinodal. This function has the physical significance of being the systems limit of stability to small concentration fluctuations.

The line connecting points at various temperatures at composition ϕ_a satisfying equation 2.17 is the binodal which represents the limit of two phase coexistence. However, the majority of polymeric systems exhibit a Lower Critical Solution Temperature, (LCST), type behaviour rather than an UCST and the resulting phase diagram is the inverted parabola of Figure 2.1. Simple Flory - Huggins - Chang - Miller theory cannot predict LCST behaviour unless the interaction parameter is redefined as the sum of both enthalpic and entropic contributions,

$$i.e., B = B_H - TB_S \quad (2.20)$$

This equation treats the interaction energy density characteristic as a temperature dependent free energy term, and can be directly compared to equation 2.2. LCST behaviour is thought to arise for several reasons.

- (a) The true free energy change contains a contribution from the volume change on mixing, and this becomes increasingly unfavourable as temperature increases. Simple FHCM theory assumes that the lattice is always completely filled and consequently there is no volume change on mixing.
- (b) If the miscibility of the polymer pair arises from specific interaction, this can lead to a strong dependence of the heat of mixing on temperature.
- (c) If the mixing in the blend is not truly random, *e.g.* specific interactions causing some degree of ordering, unfavourable entropic contributions may arise, and a temperature dependence other than that described in equation 2.20 may exist.

These conditions all demonstrate a different inadequacy of the lattice model. To avoid the assumptions necessary for the FHCM theory, and to prevent the thermodynamic treatment of polymer blends becoming a series of *ad hoc* additions to simple lattice theory, it was recognised that another model was required.

It was perceived that this new theory must provide the entropy and enthalpy change on mixing in addition to the relationship between pressure, volume and temperature of the system. These parameters are often described as the state variables and consequently these theories have become known as the equation of state theories. There exists a number of different approaches but they all rely on Prigogine's original hypothesis that a polymer can be adequately described by a partition function.

2.2 Prigogine-Flory: (EOS or Equation of State theory)^(13-17, 19-26)

The central quantity in statistical thermodynamics is the canonical partition function, Q . This parameter arises from quantum theory and contains the systems thermodynamic information. All of the thermodynamic functions can be derived from this quantity *via* the Helmholtz function, A ,

$$\text{e.g. } A = -kT \ln(Q) \quad (2.21a)$$

The Helmholtz function for solids and liquids at low pressures is approximately equal to the Gibbs function, *i.e.*

$$G = A = -kT \ln(Q) \quad (2.21b)$$

and,

$$U = \left\{ \frac{\partial(A/T)}{\partial(1/T)} \right\}_v \quad (2.22a)$$

where,

$$U = \text{internal energy of the system, J}$$

However, in non-gaseous systems, the internal energy - which is the time average molecular energy - can be approximated to the enthalpy, H ,

$$H = U = \left\{ \frac{\partial(A/T)}{\partial(1/T)} \right\}_v \quad (2.22b)$$

The entropy of the system, S , is given by

$$S = \left(\frac{\partial A}{\partial T} \right)_V \quad (2.23)$$

and the pressure by

$$P = - \left(\frac{\partial A}{\partial V} \right)_T \quad (2.24)$$

The EOS theories generally abandon the lattice model, although some useful features are retained, and instead aim to model statistically the movements of macromolecules. This theory rests upon three important assumptions.

- (1) The internal degrees of freedom of a molecule do not change during mixing and do not contribute to the mixing process, and consequently can be neglected. However, because the contributions which enable sections of the molecule to move from one volume to another are closely associated to the entropy, they must be included. If each section of the molecule is considered independently it has 3 external degrees of intermolecular motion. However, because of the constraints of the chain, the number of degrees of freedom are reduced and this is represented in the model by introducing c , the coefficient of segmental constraint. The intermolecular motion is thus $3c$, ($0 < c < 1$).
- (2) All molecules can be subdivided into segments of arbitrary but equal size. There are r segments per molecule and the volume required for each segment under normal conditions is v . However, it is also assumed that these segments have an orientation which occupies a minimum volume, below which they cannot be compressed, *i.e.* a hard core. The volume required to accommodate a segment under this condition is described as the core volume, v^* . This criterion was intended to enable the theory to cope with mixtures comprising components of greatly differing size, *e.g.* high homopolymer-solvent systems.
- (3) The partition function of a pure liquid is postulated as,

$$Z = Z_{comb} \left\{ g (v^{1/3} - v^{*1/3}) \right\}^{3Nrc} \text{Exp} (-E/kT) \quad (2.25)$$

where,

N = the number of molecules in the system

g = a geometric factor

E = the intermolecular energy of the liquid

Z_{comb} = a factor representing the number of ways of arranging the molecules in the liquid; this term has been derived from the lattice model and can be equated to S_{conf} , eqn (2.10), by

$$Z_{comb} = \text{Exp}(S_{conf}/k) \quad (2.26)$$

$v^{1/3}$ is the linear space in which the segment can move and $v^{*1/3}$ is the characteristic linear dimension, of the segment, hence $(v^{1/3} - v^{*1/3})$ is the free volume in which the segment can move. Like Lattice theory, the intermolecular energy of the liquid, E , is based on the concept of contact energies and can be subdivided into energetic and geometric contributions,

$$E = -Nrs\eta/2v \quad (2.27)$$

where,

η = contact energy parameter,

s = number of contact sites per segment, and

$-s\eta/2v$ = intermolecular energy per segment.

If expressions (2.25) and (2.27) are substituted for the respective terms in equation 2.21a,

$$A = -kT \left\{ \text{Ln}(Z_{comb}) + 3Nrc \text{Ln} \left(g(v^{1/3} - v^{*1/3}) \right) \right\} - Nrs/2v \quad (2.28)$$

The volume of the system is $V = Nrv$, thus equation 2.24 becomes,

$$P = ckTv^{-2/3} (v^{1/3} - v^{*1/3}) - s\eta/2v^2 \quad (2.29)$$

These expressions are of little practical use since they contain the arbitrary parameters s , η and c . These parameters are removed by defining the characteristic pressure, P^* , and temperature, T^* , such that

$$P^* = s\eta/2v^{*2} \quad (2.30)$$

$$T^* = s/2v^*ck \quad (2.31)$$

P^* and T^* are related to the physical parameters by the 'reduced state parameters',

$$\text{Reduced pressure} = \tilde{P} = P/P^* \quad (2.32)$$

$$\text{Reduced volume} = \tilde{v} = v/v^* \quad (2.33)$$

$$\text{Reduced temperature} = \tilde{T} = T/T^* \quad (2.34)$$

Prigogine-Flory theory postulates that the equation of state for pure liquids is,

$$\tilde{P}\tilde{v} = \left(\frac{\tilde{v}^{1/3}}{\tilde{v}^{1/3} - 1} - \frac{1}{\tilde{T}} \right) \quad (2.35)$$

However, at ambient pressures the product comprising the left hand side of the equation is insignificant and thus equation 2.35 reduces to,

$$\tilde{T} = (\tilde{v}^{1/3} - 1)/\tilde{v}^{4/3} \quad (2.36)$$

To solve this equation it is necessary to know the values of P^* , T^* and \tilde{v} . The best estimations of these parameters are obtained when the equation of state is fitted to pure component PVT data when available. A less satisfactory procedure involves calculating these parameters from other characteristic properties, e.g. using the thermal expansion coefficient to obtain \tilde{v} and the thermal pressure coefficient γ to obtain P^* .

(1) The thermal expansion coefficient α

The thermal expansivity, or expansion coefficient, is defined as,

$$\alpha \equiv \frac{1}{v} \left(\frac{\partial v}{\partial T} \right)_{P,N} \quad (2.37)$$

and the reduced volume can be calculated from,

$$\tilde{v} = \left(1 + \frac{\alpha T}{3(1 + \alpha T)} \right) \quad (2.38)$$

The thermal expansion coefficient is normally calculated from density data measured as a function of temperature.

- (2) The thermal pressure coefficient, γ

The thermal pressure coefficient, defined as,

$$\gamma \equiv \left(\frac{\partial P}{\partial T} \right)_v \quad (2.39)$$

can be used to calculate the hard core pressure characteristic as follows,

$$P^* = \gamma T \tilde{V}^2 \quad (2.40)$$

The thermal pressure coefficient is not often known and hence is estimated from the Hildebrand solubility parameter, δ , using,

$$\gamma \approx \delta^2 / T \quad (2.41)$$

- (3) The reduced temperature can be calculated from equation (2.36) by introducing the value of the reduced volume calculated from equation (2.38).

With this information the equation of state can be solved. If the equation is solved by using the approximate expressions the results have been found to be in only approximate agreement with experiment. The main fault of the treatment is that the characteristic temperature, T^* , which although defined constant, increases as the data measurement temperature increases.

The main advantage of the theory is in its application to mixtures. To enable this theory to be applied to mixtures two further assumptions are required.

- (1) The core volumes of the components are additive, and the specification of the dimensions of a segment remains arbitrary. It is convenient to choose segments of equal size such that,

$$v_1^* = v_2^* = v^* \quad (2.42)$$

- (2) The intermolecular energy of the mixture only depends on the surface area of contact between these segments, as intermolecular attractions are short range relative to the molecular diameter of most liquids.

On the basis of this extended model, some of the previous expressions require to be redefined. The number of external degrees of intermolecular motion is now the appropriate sum over all the components, *e.g.* for a binary mixture,

$$3 N r c = 3 (N_1 r_1 c_1 + N_2 r_2 c_2) \quad (2.43)$$

The intermolecular energy also requires to be altered to include heterogeneous contacts and this is done using the contact energy parameter η_{ij} and the surface fraction θ_i , defined by equations 2.46a and 2.46b. Contacts between identical molecules are designated by η_{11} and η_{22} while a contact between differing molecules is designated by η_{12} . Equation 2.27 becomes,

$$E = -(N_1 r_1 s_1 \theta_1 \eta_{11} + N_2 r_2 s_2 \theta_2 \eta_{22} + 2N_1 r_1 s_1 \theta_2 \eta_{12}) / 2v \quad (2.44a)$$

or

$$E / (N_1 r_1 + N_2 r_2) = P^* v^* / v \quad (2.44b)$$

$$\text{(from equation 2.30, } P^* = s \eta / 2v^{*2}\text{)}$$

The volume fractions are redefined using the hard core volume of the components, ϕ_i^* ,

$$\phi_1^* \equiv 1 - \phi_2^* \equiv N_1 r_1 / (N_1 r_1 + N_2 r_2) \quad (2.45a)$$

or,

$$\phi_1^* \equiv w_1 V_1^* / (w_1 V_1^* + w_2 V_2^*) \quad (2.45b)$$

where,

w_i = weight fraction of component 'i'

V_i^* = molar hard core volume of component 'i'

Hard core volume fractions are more useful than normal volume fractions because they are, by definition, independent of temperature, pressure and any volume changes that may occur during mixing. Since the characteristic dimension is now a segment and the intermolecular energy is dependent on the surface area of this quantity, it is convenient to introduce the surface fraction, θ ,

$$\theta_1 \equiv 1 - \theta_2 \equiv N_1 r_1 s_1 / (N_1 r_1 s_1 + N_2 r_2 s_2) \quad (2.46a)$$

or,

$$\theta_1 \equiv \frac{(s_2/s_1) \phi_1^*}{(s_2/s_1) \phi_1^* + \phi_2^*} \quad (2.46b)$$

where, s_2/s_1 = surface area per unit volume ratio

With these modifications the mixture can again be described by the equations of state as defined by (2.35) and (2.36). The hard core parameters, P^* and T^* , now describe the properties of the mixture and can be related to the pure component data as follows,

$$P^* = \phi_1 P_1^* + \phi_2 P_2^* - \phi_1 \theta_2 X_{12} \quad (2.47)$$

$$T^* = \frac{\phi_1 P_1^* + \phi_2 P_2^* - \phi_1 \theta_2 X_{12}}{\phi_1 P_1^*/T_1^* + \phi_2 P_2^*/T_2^*} \quad (2.48)$$

where,

X_{12} = an interaction term which reflects the difference in energies of the homo/heterogeneous contacts and is comparable with the zW term in equation (2.8).

and X_{12} is defined as,

$$X_{12} \equiv (\eta_{11} + \eta_{22} - 2\eta_{12})(s_1 / 2v^*)^2 \quad (2.49)$$

The change in enthalpy, *i.e.* excess enthalpy, on mixing is equal to the energy change on mixing at low pressure,

$$\Delta H_{mix} = E_{12} - (E_{11} + E_{22}) \quad (2.50)$$

From equation (2.44b), this equation can be defined in terms of the hard core and reduced parameters,

$$\Delta H_{mix} = (N_1 r_1 + N_2 r_2) v^* \left\{ \phi_1 P_1^* / \tilde{v}_1 + \phi_2 P_2^* / \tilde{v}_2 - P^* / \tilde{v} \right\} \quad (2.51)$$

and substitution of P^* from (2.47) gives,

$$\begin{aligned} \Delta H_{mix} = (N_1 r_1 + N_2 r_2) v^* \left\{ \phi_1 P_1^* (1/\tilde{v}_1 - 1/\tilde{v}) + \phi_2 P_2^* (1/\tilde{v}_2 - 1/\tilde{v}) \right\} \\ + \phi_1 \theta_2 X_{12} / \tilde{v} \end{aligned} \quad (2.52a)$$

$$\Delta H_{mix} = v^* \left\{ N_1 r_1 \theta_2 X_{12} / \tilde{v} - N_1 r_1 P_1^* (1/\tilde{v} - 1/\tilde{v}_1) - N_2 r_2 P_2^* (1/\tilde{v} - 1/\tilde{v}_2) \right\} \quad (2.52b)$$

$$\Delta H_{mix} = n_1 V_1^* \left\{ \theta_2 X_{12} / \tilde{v}_1 + P_1^* (1/\tilde{v} - 1/\tilde{v}_1) - (\phi_2^* / \phi_1^*) P_2^* (1/\tilde{v} - 1/\tilde{v}_2) \right\} \quad (2.52c)$$

The first term inside the braces in equation 2.52c corresponds to the contact enthalpy term in FHCM theory, *i.e.* equation 2.9. The two remaining contributions, called the equation of state terms, are still significant even if $X_{12} = 0$, *i.e.* there is no difference in the chemical nature of the components, as the magnitude of their contribution is determined by the reduced volume of the mixture. From equation 2.38 it is apparent that the reduced volume is a function of the thermal expansion coefficient and consequently a significant excess enthalpy may still occur on mixing materials which have a small degree of interaction but very different thermal expansivities.

The entropy of mixing can be obtained from the partial derivative in equation 2.23,

$$\Delta S_{mix} - \Delta S_{comb} = 3(N_1 r_1 + N_2 r_2) v^* \left\{ \frac{\phi_1^* P_1^*}{T_1^*} \text{Ln} \left\{ \frac{\tilde{v}^{1/3} - 1}{\tilde{v}_1^{1/3} - 1} \right\} + \frac{\phi_2^* P_2^*}{T_2^*} \text{Ln} \left\{ \frac{\tilde{v}^{1/3} - 1}{\tilde{v}_2^{1/3} - 1} \right\} \right\} \quad (2.53a)$$

$$\Delta S_{mix} - \Delta S_{comb} = 3n_1 V_1^* \left\{ \frac{P_1^*}{T_1^*} \text{Ln} \left\{ \frac{\tilde{v}^{1/3} - 1}{\tilde{v}_1^{1/3} - 1} \right\} + \frac{\phi_2^* P_2^*}{\phi_1^* P_1^*} \text{Ln} \left\{ \frac{\tilde{v}^{1/3} - 1}{\tilde{v}_2^{1/3} - 1} \right\} \right\} \quad (2.53b)$$

For macromolecular solutions the FHCM entropy of mixing, equation 2.13, is equated to ΔS_{comb} and the difference $\Delta S_{mix} - \Delta S_{comb}$ is called the residual entropy of mixing ΔS^R .

A general expression for the free energy of mixing can now be constructed,

$$\Delta G_{mix} = \Delta H_{mix} - T(\Delta S_{comb} + \Delta S^R) \quad (2.54)$$

and,

$$\Delta G_{mix} = RT \left\{ n_1 \text{Ln}(\phi_1^*) + n_2 \text{Ln}(\phi_2^*) + n_1 \phi_2^* (\chi_H^* + \chi_S^*) \right\} \quad (2.55)$$

where,

$$\chi_H^* = \frac{v_1^*}{RT} \left\{ \frac{\theta_2}{\phi_2^*} X_{12} \tilde{v}^{-1} - \frac{P_1^*}{\phi_2^*} (\tilde{v}^{-1} - \tilde{v}_1^{-1}) - \frac{P_2^*}{\phi_1^*} (\tilde{v}^{-1} - \tilde{v}_2^{-1}) \right\} \quad (2.56)$$

and

$$\chi_s^* = \frac{3V_1^*}{R} \left\{ \frac{P_1^*}{T_1^* \phi_2^*} \text{Ln} \left\{ \frac{\tilde{v}_1^{1/3} - 1}{\tilde{v}_1^{1/3} - 1} \right\} + \frac{P_2^*}{T_2^* \phi_1^*} \text{Ln} \left\{ \frac{\tilde{v}_2^{1/3} - 1}{\tilde{v}_2^{1/3} - 1} \right\} \right\} \quad (2.57)$$

These two terms are the enthalpic and entropic interaction coefficients which give some indication of which thermodynamic effect is dominant in any mixing process.

When applied on a qualitative basis, this form of the Prigogine-Flory theory had some success in explaining the behaviour of many systems but its quantitative success was only moderate and significant variation was observed in the theoretically constant quantities, *e.g.* v^* , P^* and T^* . An improvement in its quantitative performance was achieved by adding a correction term to the enthalpic exchange parameter. In this term, $Q_{12}T\tilde{v}_1$, Q_{12} is an adjustable parameter characterising excess entropic effects. This additional parameter has no physical meaning and consequently many derived relationships are no longer directly related to the original model.

The Phase Diagram

McMaster⁽²⁷⁾ considered both internal and external degrees of freedom in addition to polydispersity while developing a generalised form of this relationship which simulated both the binodal and spinodal curves of a hypothetical polymer mixture. From this he showed that it was possible to predict both UCST and LCST behaviour both individually and simultaneously. McMaster, and Walsh and Rostami⁽²⁸⁾, have examined the influence of a variety of the parameters on the miscibility limits of hypothetical mixtures. Their conclusions can be summarised as follows.

- (a) The largest range of miscibility, with respect to temperature is found when the components have similar thermal expansion coefficients. This is equivalent to having similar values of \tilde{v} and T^* .
- (b) Variations in γ have less effect on miscibility than changes in α . High values of γ reduce the range of miscibility and a difference in the thermal pressure between components affects the shape of the limits and the position of the minimum.

- (c) If the molecular weight of the components is increased the mixture will become less miscible, as also predicted from FHCM theory.
- (d) As X_{12} becomes increasingly positive the mixture becomes less miscible while conversely as it becomes more negative the mixture becomes more miscible.
- (e) The value of the surface area to volume ratio, s_2/s_1 , is only significant for large values of either Q_{12} or X_{12} . Under these circumstances, the miscibility limit is skewed by an amount proportional to the deviation of s_2/s_1 from unity.
- (f) A negative value of Q_{12} makes the mixture less miscible.

This theory has also been used to simulate the phase diagrams of real polymer mixtures⁽²⁹⁻³³⁾ using Q_{12} as an adjustable parameter. This work has simulated the phase diagram of the EVA/FVA mixture using calculated values of both X_{12} and Q_{12} and this is described and discussed in chapter 8.

Other free volume approaches, such as the 'lattice-fluid' theory of Sanchez and Lacombe⁽³⁴⁾ and the equation of state theory of Simha and Somcynski⁽³⁵⁾, are based on the lattice model and all or part of the free volume arises from vacancies on the lattice unlike Prigogine-Flory theory where the free volume arises from an overall increase in molecular separations. These theories may prove to be valuable, because their description of the pure component properties is superior but to date their main application has been to polymer solutions.

2.3 Summary

In this chapter two quite different approaches to the thermodynamics of polymer mixtures have been discussed. The FHCM lattice theory, which has been the basis of much research for the last forty years, has been shown to be inadequate for understanding and predicting many of the phenomena routinely observed in polymer blends. The equation of state treatment is seen to be an improvement on the lattice model, although the necessary introduction of the adjustable Q_{12} parameter is an indication that the initial model is inadequate. It should also be apparent that the latter theory requires substantially more information about both the pure components and the mixture than the FHCM theory, and consequently the choice of which approach to use should be based on a balance between the relative input required and the information obtained.

2.4 REFERENCES

- (1) J.H.Hildebrand and S.E.Wood, *J. Chem. Phys.* **1**, 817, (1933).
- (2) P.J.Flory, *J. Chem. Phys.*, **9**, 660, (1941).
- (3) P.J.Flory, *J. Chem. Phys.*, **10**, 51, (1942).
- (4) P.J.Flory, 'Principles of Polymer Chemistry',
Cornell University Press, (1953).
- (5) M.L.Huggins, *J. Chem. Phys.*, **9**, 440, (1941).
- (6) M.L.Huggins, *J. Chem. Phys.*, **46**, 151, (1942).
- (7) M.L.Huggins, *Ann. N. Y. Acad. Sci.*, **43**, 1, (1942).
- (8) M.L.Huggins, *J. Am. Chem Soc.*, **64**, 1712, (1942).
- (9) T.S.Chang, *Proc. Cambridge Philos. Soc.*, **38**, 109, (1939).
- (10) A.R.Miller, *Proc. Cambridge Philos. Soc.*, **38**, 109, (1942).
- (11) A.R.Miller, *Proc. Cambridge Philos. Soc.*, **39**, 54, (1943).
- (12) A.R.Miller, 'The theory of Solutions of High Polymers',
Clarendon Press, Oxford, (1948).
- (13) I.Prigogine, N.Trappeniers and V.Mathot,
Discuss. Faraday Soc., **15**, 93, (1953).
- (14) I.Prigogine, 'The Molecular Theory of Solutions',
North-Holland Pub., Amsterdam, (1957).
- (15) P.J.Flory, R.A.Orwell and A.Vrij, *J. Am. Chem. Soc.*, **86**, 3507, (1964).
- (16) P.J.Flory, R.A.Orwoll and A.Vrij, *J. Am. Chem. Soc.*, **86**, 3515, (1964).
- (17) P.J.Flory, *J. Am. Chem. Soc.*, **87:9**, 1833, (1965).
- (18) H.C.Longuet-Higgins, *Discuss. Faraday Soc.*, **15**, 73, (1953).
- (19) A.Abe and P.J.Flory, *J. Am. Chem. Soc.*, **87:9**, 1838, (1965).
- (20) A.Abe and P.J. Flory, *J. Am. Chem. Soc.*, **88:13**, 2887, (1966).
- (21) R.A.Orwoll and P.J.Flory, *J. Am. Chem. Soc.*, **89**, 6814, (1967).
- (22) B.E.Eichinger and P.J.Flory, *Trans. Faraday Soc.*, **64**, 2035, (1968).

- (23) B.E.Eichinger and P.J.Flory, *Trans. Faraday Soc.*, 64, 2053, (1968).
- (24) B.E.Eichinger and P.J.Flory, *Trans. Faraday Soc.*, 64, 2061, (1968).
- (25) B.E.Eichinger and P.J.Flory, *Trans. Faraday Soc.*, 64, 2065, (1968).
- (26) H.Shih and P.J.Flory, *Macromolecules*, 5, 758, (1972).
- (26) H.Shih and P.J.Flory, *Macromolecules*, 5, 761, (1972).
- (27) L.P.McMaster, *Macromolecules*, 6, 760, (1973).
- (28) D.J.Walsh and S.Rostami, *Adv. Polym. Sci.*, 70, 119, (1985).
- (29) O.Olabisi, *Macromolecules*, 8, 316, (1975).
- (30) Z.Chai, S.Ruona, D.J.Walsh and J.S.Higgins,
Polymer, 24, 263, (1983).
- (31) D.J.Walsh and S.Rostami, *Polymer*, 26, 418, (1985).
- (32) S.Rostami and D.J.Walsh, *Macromolecules*, 17, 315, (1984).
- (33) S.Rostami and D.J.Walsh, *Macromolecules*, 18, 1228, (1985).
- (34) I.C.Sanchez and R.H.Lacombe, *Macromolecules*, 11, 1145, (1978).
- (35) R.Simha and T.Sonmcynsky, *Macromolecules*, 2, 342, (1969).

Chapter 3 General Experimental Work

This chapter describes experimental work which gave ambiguous results or which is subsidiary to another part of the project. Included are the initial characterisation of the materials, their density-temperature functions and a DSC study of their blends. Each series of experiments has been reported as a brief introduction, description, list of results and discussion. The final section reviews the value of all the information obtained.

3.0 Characterisation of materials

Three copolymers have been used in this work,

- (a) poly(ethylene-vinyl acetate) or EVA
- (b) poly(tetradecyl/hexadecyl fumarate-vinyl acetate) or $C_{14/16}$ FVA
- (c) poly(tetradecyl fumarate-vinyl acetate) or C_{14} FVA (or simply FVA).

EVA was a random copolymer which was prepared industrially by a free radical process in a mixed solvent of cyclohexane and oligomeric poly(iso-butylene). It was necessary to anneal the polymer at 353K under vacuum for 12 hours to remove the residual processing solvents and any water or air which had been absorbed. The polymer was analysed elementally to determine the structure of the statistical repeat unit, *i.e.* the ratio of ethylene to vinyl acetate in the polymer.

The polymer was a viscous, opaque liquid which became less turbid when it was heated. Provisional experiments in a test tube showed that the sample became transparent when it was heated to approximately 323-328K. It was unclear whether this was the final melt of any crystallinity present resulting from long sequences of polyethylene in the statistical composition or if the copolymer did not exist as a single homogeneous phase at ambient temperature owing to the disperse nature of its composition.

This effect was investigated

- (a) thermally: using differential scanning calorimetry, (3.4), and
- (b) optically: by
 - (i) a laser/photo-multiplier tube arrangement, (3.5), and
 - (ii) a microscope fitted with a hot stage, (7.0).

The FVA samples were also prepared industrially by a free radical process and had an alternating structure of (fumarate-vinyl acetate). The $C_{14/16}$ FVA was a yellowish wax which began to melt at approximately 300K: the C_{14} FVA was a viscous yellow liquid at room temperature. The behaviour of the EVA/ $C_{14/16}$ FVA blend was of prime industrial interest and was studied initially. Unfortunately the ratio of tetradecyl to hexadecyl substitution in the fumarate was unknown and this blend was eventually discarded in favour of the simpler EVA/ C_{14} FVA mixture.

3.1 Elemental Analysis of EVA

Duplicate EVA samples were analysed for carbon, hydrogen and, by difference, oxygen. The results were as follows:-

Table 3.1

Mass Fraction	Carbon	Hydrogen	Oxygen
EVA1	0.749	0.127	0.124
EVA2	0.750	0.129	0.121

From these results the average structure was determined by a mass balance calculation as that given in Figure 3.1. This structure contains six ethylene units per vinyl acetate and although it represents only the statistical average of the composition distribution it has been used as the unit structure for this work.

The general structure of the FVA samples is given in Figure 3.2, where $R = C_{14}H_{29}$ or $C_{16}H_{33}$.

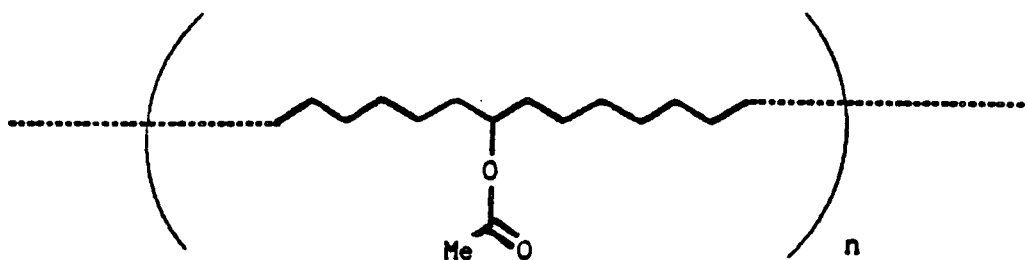
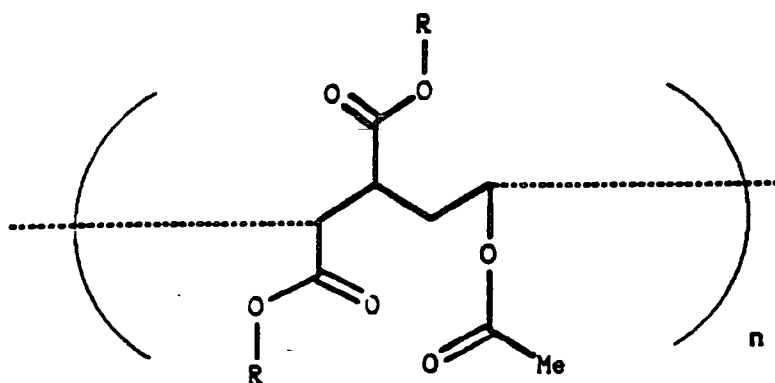


Figure 3.1: Macro structure of EVA



where $R = C_{14}H_{29}$ or $C_{16}H_{33}$

Figure 3.2: Macro structure of C₁₄FVA

3.2 Gel Permeation Chromatography (GPC)

The GPC measurements were performed by Exxon Chemicals using polystyrene as the calibrant.

Table 3.2

Sample	\bar{M}_n	\bar{M}_w	\bar{M}_w/\bar{M}_n
EVA1	3290	9704	2.948
C ₁₄ FVA	10400	28543	2.756

3.3 Density Measurements

These measurements were undertaken to determine the densities and the thermal expansion coefficients of EVA and C₁₄FVA from which were derived many of the pure component parameters needed for an Equation of State analysis (Chapter 8).

Additionally it was hoped that the optically observed apparent phase change that EVA exhibits (section 3.0) might result in a discontinuity in the relationship between density and temperature.

The density measurements were carried out using an Anton Paar KGDMA60 densitometer with a DMA602 external cell⁽¹⁾. This apparatus comprises a vibrating U-tube whose frequency of oscillation alters when filled with different fluids. This change is converted into an absolute value by calibrating the apparatus with materials of known density. The temperature of the cell was controlled by the circulation of heated water from a Townson and Mercer bath, but the range of the study was restricted by the operational limits of the sample tube.

3.3.1 Experimental Procedure

The experimental procedure involved equilibrating the water bath at the desired temperature and ensuring that a stable temperature, ($\pm 0.01\text{K}$), was observed for a minimum of 30 minutes. The cell was calibrated with doubly distilled water and dry air before and after each density measurement and the calibration constant calculated from the expression below,

$$K = (e_w - e_a)/(T_w - T_a) \quad (3.1)$$

where,

K = calibration constant

ρ_w = density of water⁽²⁾, g cm^{-3}

ρ_a = density of air⁽²⁾, g cm^{-3}

T_w = period of oscillation measured for water, s

T_a = period of oscillation measured for air, s

A sample of approximately 4g was injected into the cell but because of the viscosity of these materials, the standard practice was to heat the mixture under vacuum at 353K for a minimum of 12 hours and inject the samples hot.

A reading was taken when the frequency of oscillation was constant.

Each measurement was repeated several times and a mean value calculated.

The sample density was then evaluated from the following equation:-

$$\rho = \rho_w - K(T_w - T_s) \quad (3.2)$$

where,

ρ = density of sample, g cm^{-3}

T_s = period of oscillation for sample, s

3.3.2 Density - Temperature Results:

Table 3.3

The relationship between temperature, composition and density (g cm^{-3}) for mixtures of EVA and C_{14} FVA

Mass Fraction EVA	Temperature / K			
	303	313	323	333
0.0000 (FVA)	0.95001	0.94320	0.93669	0.92993
0.1181	0.94935	0.94239	0.93558	0.92885
0.2426	0.94877	0.94176	0.93483	0.92794
0.3620	0.94780	0.94056	0.93325	0.92623
0.4836	0.94755	0.93992	0.93267	0.92552
0.6940	0.94582	0.93816	0.93071	0.92328
0.8013	0.94528	0.93722	0.92979	0.92224
0.9060	0.94466	0.93669	0.92884	0.92141
1.0000 (EVA)	0.94416	0.93618	0.92830	0.92060

These results are shown graphically in Figure 3.3.

A least-squares fit was performed on these data and the results were found to be essentially linear with respect to composition and temperature thus the coefficients of the composition-density fit could be linearised with the temperature-density function reducing these data to the following expression,

$$1/\rho = v = (b_0 + b_1T) + (c_0 + c_1T + c_2T^2)w \quad (3.3)$$

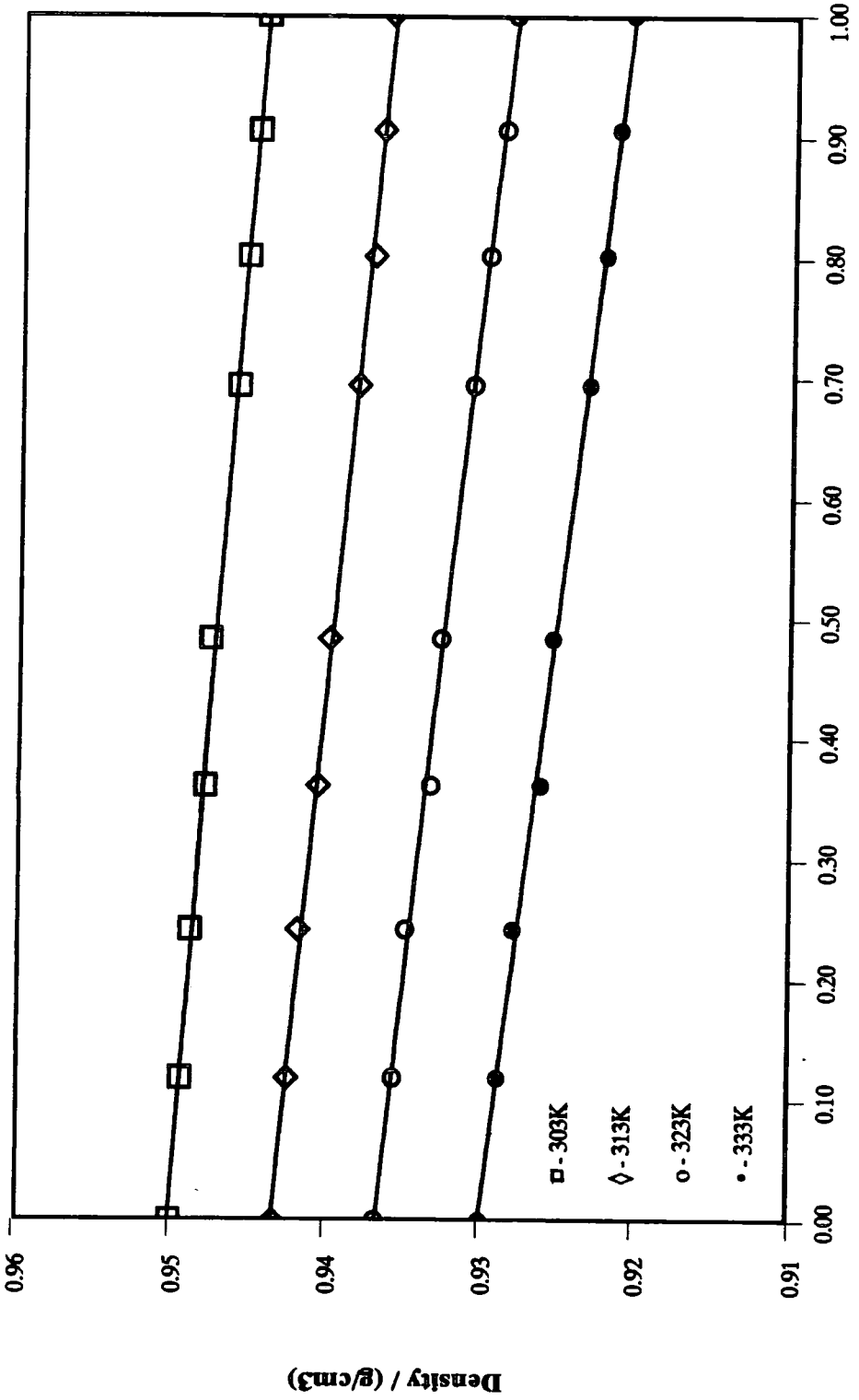
where,

v = specific volume, $\text{cm}^3 \text{g}^{-1}$

T = temperature, degrees Celcius

w = mass fraction of EVA

Density-Composition Functions of EVA/FVA



Mass Fraction EVA

Figure 3.3

with

$$\begin{aligned}
 b_0 &= 1.029764 && \text{cm}^3 \text{ g}^{-1} \\
 b_1 &= 7.582750 \times 10^{-4} && \text{cm}^3 \text{ g}^{-1} \text{ K}^{-1} \\
 c_0 &= 2.255139 \times 10^{-3} && \text{cm}^3 \text{ g}^{-1} \\
 c_1 &= 1.484851 \times 10^{-4} && \text{cm}^3 \text{ g}^{-1} \text{ K}^{-1} \\
 c_2 &= 3.291172 \times 10^{-11} && \text{cm}^3 \text{ g}^{-1} \text{ K}^{-2}
 \end{aligned}$$

(b_0 , b_1 , c_0 , c_1 and c_2 were evaluated from the least-squares calculations)

3.3.3 Discussion

It was assumed that no further phase changes, or other processes which were likely to radically alter the density, would occur, and thus the density-temperature-composition function could be extrapolated linearly to 393K for the inverse phase gas chromatography (Section 4.0) and vapour sorption (Section 6.0) analyses. No change in the EVA density was observed at around 325K, where the optically observed phase change had been detected, suggesting that whatever its origin, it had no effect on the density of the bulk material.

The linearity of these functions describes a system which demonstrated an additive change in volume when the components were mixed. This is an unusual effect since species which demonstrate electron-donor-acceptor interactions often display a volume contraction when mixed⁽³⁾, whereas the majority of normal liquids expand, (these effects arising from whether the intermolecular interactions of the mixture are greater or less than those of the pure components, respectively). The physical significance of this apparent volume additivity is that, either the intermolecular forces of each pure copolymer are essentially equal, or that these materials do not truly mix on a molecular level. Since neither of these materials were likely to have strong or specific intermolecular forces, *e.g.* dipole-dipole or hydrogen bonding, and that miscibility was likely to arise from the cohesion of alkyl groups, it was assumed that mixing did occur and that it was additive.

3.4 Differential Scanning Calorimetry, (DSC)

3.4.1 Introduction

All materials store energy in the form of thermal movement and this quantity changes with the state of the material. This is reflected by the heat capacity of the material and its magnitude is dependent on the number of modes of thermal movement that are available. Consequently, the heat capacity of glassy and crystalline polymers is small because of the morphological restrictions and larger for viscoelastic materials.

This change is defined as the glass transition temperature, T_g . Numerous other morphological changes and state transitions are accompanied by a heat flux into or out of the system, *e.g.* melting, crystallisation, vapourisation, polymerisation and decomposition. Differential scanning calorimetry measures this flux by measuring the amount of thermal energy required to increase the temperature of a sample by ΔT over that required by a reference, *e.g.* an empty sample vessel. A temperature sensor provides feedback control to electrical heaters which ensures that a constant rate of temperature change is maintained in both the sample and the reference. The electrical supply to the heaters is measured precisely and, after correction, provides a record of the heat capacity of the sample as a function of temperature. The technique has two distinct applications in polymer science,

- (a) the determination of the miscibility limits of the blend, and,
- (b) the quantitative evaluation of the Flory-Huggins interaction parameter.

3.4.2 Theoretical

3.4.2.1 Miscibility limits

Although the exact nature of the glass transition is still in some dispute the following definition is adequate for this work:-

"For every amorphous polymer there exists a narrow temperature region in which it changes from a viscous or rubbery condition at temperatures above this region, to a hard and relatively brittle one below it. This transformation is equivalent to the solidification of a liquid to a glass; it is not a phase transition. Not only do hardness and brittleness undergo rapid changes in the vicinity of the glass transition temperature, T_g , but other properties such as the thermal expansion coefficient, the heat capacity, and the dielectric constant (in the case of a polar polymer) also change markedly over an interval of a few degrees. T_g is regarded variously as the brittle temperature, the critical temperature for the glassy state, or the second-order transition temperature, although as mentioned above no phase transition is involved and reference to a transition may therefore be misleading"

- P. J. Flory⁽⁴⁾

Immiscible mixtures of polymeric materials retain the individual T_g values of the homopolymers: miscible polymer blends which behave as a single homogeneous phase have a single glass transition temperature, commonly between the T_g values of the pure components. The miscibility limits of a blend can be found by annealing various compositions at a arbitrary temperature then quenching the sample in liquid nitrogen and running a thermogram. This process freezes the blend in its equilibrium state at the temperature at which it was annealed, and the number of T_g values observed in the thermogram indicates whether it was homogeneous or heterogeneous at that temperature. By varying this temperature the limits of miscibility can be found.

3.4.2.2 The Flory - Huggins Interaction Parameter, χ'_{23}

When crystals of one component are in equilibrium with a mixed amorphous phase, the melting point will be lower than when the equilibrium is with a pure amorphous phase of the same component comprising the crystals⁽⁴⁾. This depression of melting point can be used to measure the Flory-Huggins interaction parameter of the mixture using the expression derived by Flory,

$$\frac{1}{T_m} - \frac{1}{T_m^0} = \frac{R}{\Delta H_2} \frac{V_0}{V_1} (\phi_3 - \chi'_{23} \phi_3^2) \quad (3.4)$$

where, subscript 2 refers to a repeat unit of crystalline polymer, and subscript 3 to the diluent, *i.e.* amorphous polymer.

T_m = equilibrium melting temperature, K

T_m^0 = equilibrium melting temperature of the pure crystalline polymer, K

ΔH_2 = heat of fusion per repeating unit, J

ϕ_i = volume fraction of species 'i'

R = universal gas constant, (8.3144 J mol⁻¹ K⁻¹)

V_i = molar volume of species 'i' m³ mol⁻¹

The interaction parameter can be obtained from the slope of a plot of

$$\frac{1}{\phi_3} \left\{ \frac{1}{T_m} - \frac{1}{T_m^0} \right\} \text{ versus } \phi_3$$

A significant amount of work has subsequently been done to refine this technique both experimentally and theoretically⁽⁵⁻¹⁰⁾.

3.4.3 Apparatus and Materials

The thermograms were recorded on a DuPont 9900 DSC apparatus, which could be fitted with a mechanical cooling head. It was calibrated regularly on a single point basis with Indium. The polymers were annealed at 353K in a vacuum oven for 12 hours and stored in a desiccator containing silica.

It should be noted that all of the DSC work was carried out on the EVA - C_{14/16} FVA blend.

3.4.4 Experimental Procedures and Results

3.4.4.1 Miscibility

Typically 10mg of each mixture of interest was annealed at a series of temperatures between 298 and 353K for 10 minutes. Several pretreatments were tried in an attempt to improve the reproducibility of the data and these are discussed in section 3.4.6. Thereafter, a thermogram was obtained at a scanning rate of 10 K min⁻¹ for the temperature range 133 - 373K.

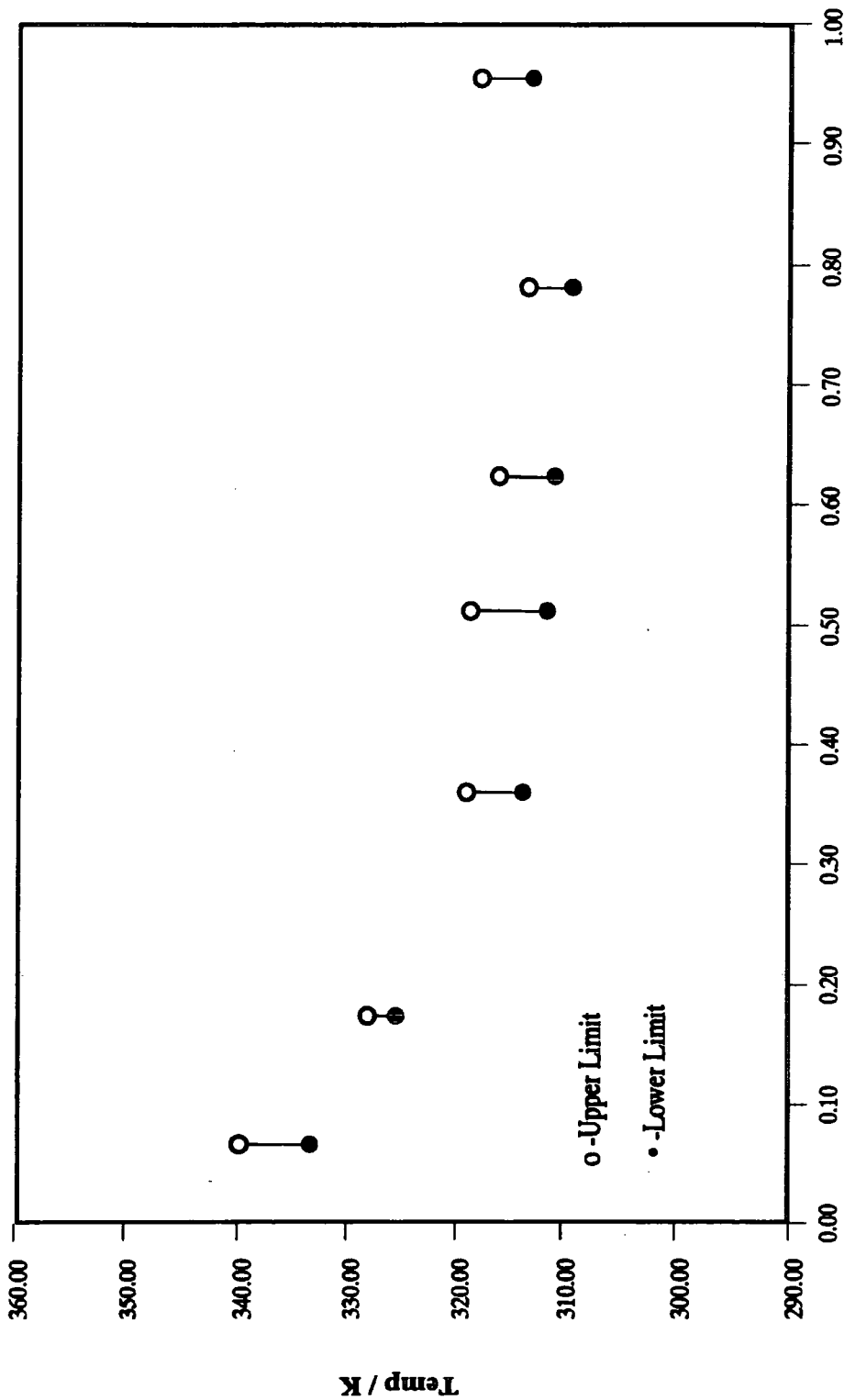
The number of T_g values identified was recorded and the process repeated until the limits of miscibility were obtained. The phase diagram was established by repeating this procedure for the entire composition range.

Table 3.4
DSC Miscibility Results

Mass Fr. EVA	No. T_g vals	$T_{\text{anneal}} / \text{K}$
0.066	2	333.6
0.066	1	340.0
0.174	2	325.5
0.174	1	328.1
0.360	2	313.8
0.360	1	319.1
0.512	2	311.5
0.512	1	318.8
0.623	2	310.8
0.623	1	316.1
0.781	2	309.2
0.781	1	313.4
0.954	2	313.0
0.954	1	317.9

If the limiting points for each composition are plotted the phase diagram is obtained, Figure 3.4

*Phase Diagram of EVA/FVA Mixture
as determined by DSC*



Mass Fraction EVA

Figure 3.4

The phase diagram obtained from the T_g analysis, Figure 3.3, suggests that this copolymer pair is miscible in all proportions up to $\sim 308\text{K}$ at which they undergo lower critical solution temperature type behaviour, (LCST), and phase separate. These results are discussed more fully in section 3.4.6.

3.4.4.2 Melting Point Depression

All of the results were obtained at a scanning rate of 10K min^{-1} in the range $223 - 353\text{K}$ and each experiment comprised both a heating and cooling cycle. Approximately 10mg of material were annealed at 353K for 10 minutes to ensure that it was amorphous and in thermal equilibrium before scanning to 223K , where it was maintained for 10 minutes before the cycle was completed. $\text{C}_{14/16}\text{FVA}$ melts at $\sim 302\text{K}$ and this was the endotherm which was followed: EVA was defined as the amorphous phase.

Melting Point Depression Results

Table 3.5

Sample	Mass Frn.EVA	Melting Point / K
1	0.0000	303.30
2	0.0843	301.99
3	0.2094	301.43
4	0.2287	302.49
5	0.2422	303.11
6	0.3062	300.98
7	0.3389	301.18
8	0.4541	303.09
9	0.5305	300.45
10	0.6275	301.19
11	0.7003	301.47
12	0.8471	300.12

From the data in table 3.5 it can be seen that there is virtually no depression in the melting point of $C_{14/16}$ FVA when it is mixed with EVA.

3.4.6 Discussion

The applicability of DSC to this system was in some doubt owing to the complexity and non-reproducibility of the thermograms obtained. In an attempt to improve and simplify these signals a variety of pretreatments was investigated, these included,

- (1) Heating approximately 1g of the materials to 393K, in the bulk state, and then sealing into DSC cells.
- (2) Dissolving the polymers in chloroform and re-precipitating from methanol.
- (3) Applying (1) to the re-precipitated polymers.
- (4) Quenching the 'canned' samples by crash-cooling within the DSC.
- (6) Physically plunging the cans into liquid nitrogen and placing these in the DSC at $\sim 133K$.

All these procedures had significant effects on the thermograms obtained and consequently it was concluded that a consistent pretreatment was required to ensure comparable results. Additional variation of the thermal histories was carried out and the following protocol was finally established:-

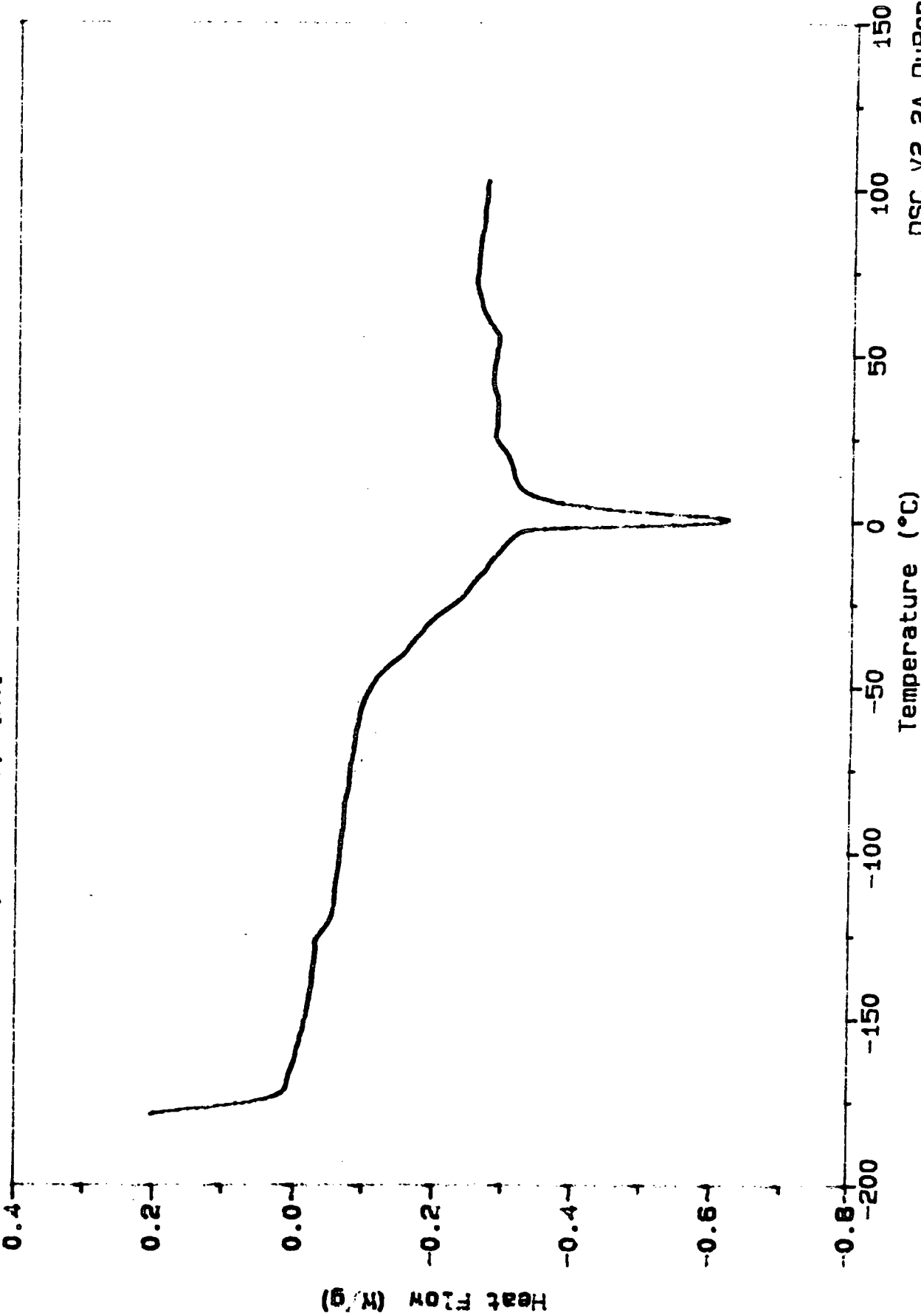
- (1) Heat the samples to 393K in the bulk.
- (2) 'Can' at room temperature.
- (3) Ramp at $20K\ min^{-1}$ to 393K and maintain isothermally for 10 minutes.
- (4) Cool to the temperature of annealing and hold for 10 minutes.
- (5) Crash-cool within the DSC, (include maximum rate), to 133K.
- (6) Heat at $10K\ min^{-1}$ to 373K.

Even when this convoluted procedure was used the degree of reproducibility was not particularly good and the resulting traces were still difficult to interpret. Figures 3.5 and 3.6 are typical results and their salient features are described below.

Sample: PPT PORE EVA, SAMS, HUNI, [HI]
Size: 13.0000 mg
Method: MACDONALD
Comment: 100%EVA, RE-PPT, 1ST RUN, [HT]

DSC

File: B:EVA100.03
Operator: MACDONALD
Run Date: 03/31/88 16:02



FILE: B:FVA-3-100.02

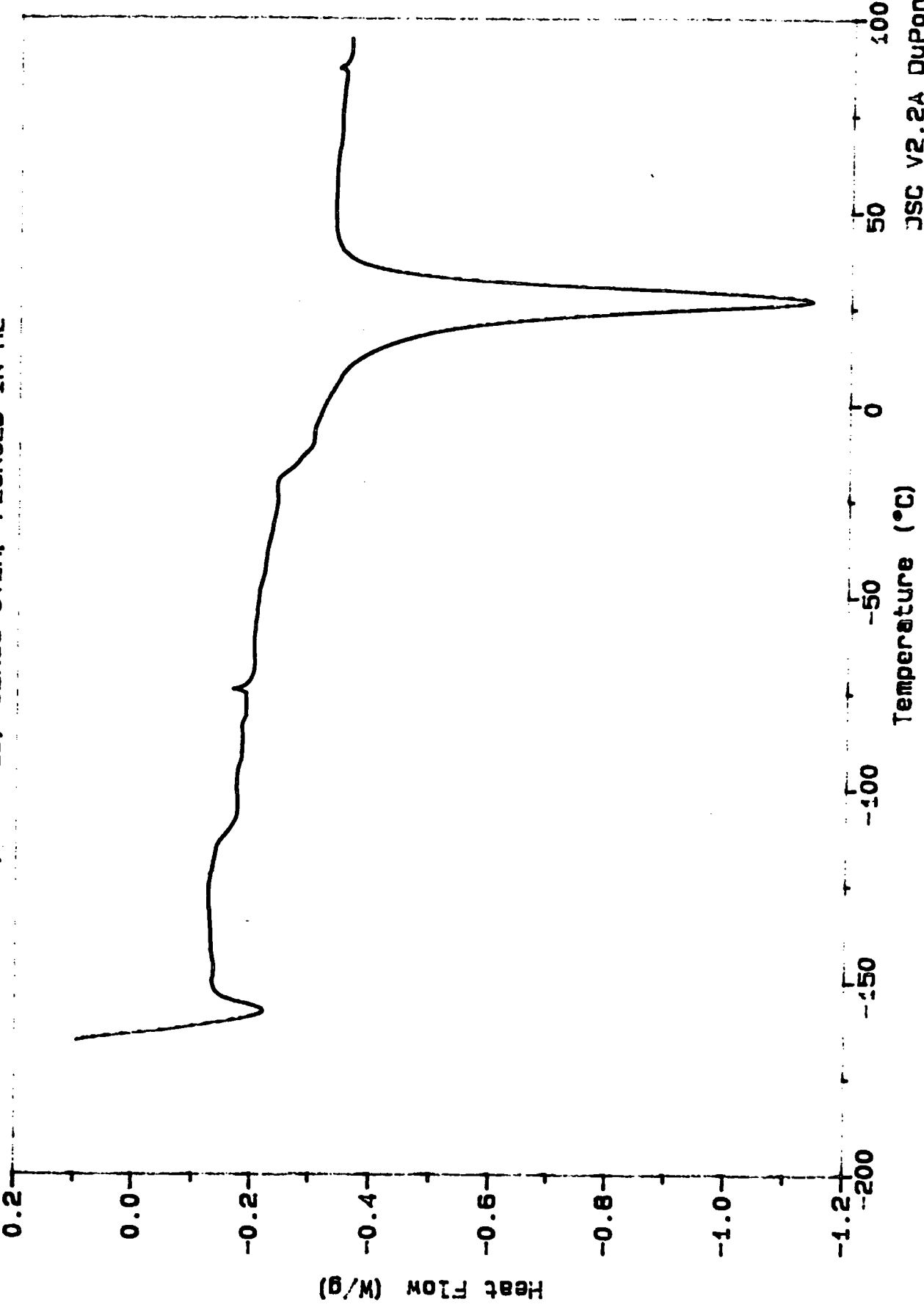
Operator: MACDONALD

Run Date: 05/13/88 11:04

Size: 16.2000 mg

Method: MACDONALD

Comment: DRIED IN VAC-OVEN, TINNED, GLASS-OVEN, PLUNGED IN 12



JSC V2.2A DuPont 9900

From Figure 3.4

Temperature Range / K	Effect
148 to 158	T_g
223 to 263	This effect is non-reproducible and its origin is unknown.
268 to 278	This sharp endotherm is produced by the melting of ice which has accumulated either in the sample vessel or in the DSC cell

From Figure 3.5

Temperature Range / K	Effect
153 to 163	Unknown non-reproducible effect
248 to 263	T_g
293 to 303	Sharp endotherm of the FVA melt

It should be noted that the EVA signal, (excluding the ice peak), shows a variation of only $\sim 0.25 \text{ W g}^{-1}$ over the temperature range 100 to 373K while the $C_{14/16}$ FVA sample is only slightly more responsive at $\sim 1.0 \text{ W g}^{-1}$: the data listed in Table 3.2 show a variation of $\pm 20\text{K}$ in the identified position of the respective T_g values. The interpretation of such small and fickle effects is consequently difficult. Additionally, both copolymers have a discontinuity in the range -125 to -110 °C that resembles a glass transition, (although this effect is not always observed in $C_{14/16}$ FVA). Since the whole construction of the phase diagram is based on the reliable identification of the T_g values in the blend, it is apparent that this may not have been done and consequently the validity of the phase diagram is questionable.

This diagram shows lower critical solution temperature type behaviour which is common amongst polymeric materials, and is characteristic of exothermic mixing and associated entropy effects⁽¹⁰⁾. A Flory-Huggins interaction parameter can qualitatively be assumed to have a negative or small positive value below $\sim 308\text{K}$, where the blend is miscible at all compositions. This parameter then becomes more positive as the temperature is increased and phase separation occurs. From the melting point data it appears that no depression occurs despite the apparent miscibility.

The variation in melting point observed, ($\pm 3\text{K}$), was considered to be within the experimental error. In view of the data and the accepted restrictions of this type of analysis, *e.g.* the dependence of the results on the heating/cooling rates, the effects of diffusion limitation, supercooling and non-homogeneity within the sample, it was felt that the evaluation of a χ parameter would be pointless. The data suggest that no interaction exists between EVA and $\text{C}_{14/16}\text{FVA}$ and thus the polymer - polymer interaction parameter would be unfavourable and positive. This leads to a discrepancy with the qualitative conclusions reached from the T_g work. However, the melting point depression results may also be misleading since Flory's original derivation requires one of the materials to be completely amorphous, *i.e.* EVA. The turbid nature of the EVA may have resulted from some crystallinity in the material.

As a result of the ambiguous nature of these experiments, and the close proximity of the estimated phase limit to the unidentified transition in EVA at 325K , it was decided to investigate this effect further using laser turbidimetry, and to use alternative techniques to obtain more information about the phase diagram of this blend.

3.5 Laser Turbidimetry

This experiment was done to obtain an accurate temperature profile of the EVA sample between 313 and 338K . Approximately 1.5g of EVA was charged to an optical cell immersed in a bath of xylene. A spectra physics 124B Helium/Neon laser was directed through this cell and the 90° scattering intensity measured with a photon-multiplier tube connected to a Malvern K7025 photo-correlator, Figure 3.7. The xylene bath was set to a series of temperatures and numerous determinations made of the intensity, from which the arithmetic mean and standard deviation were calculated.

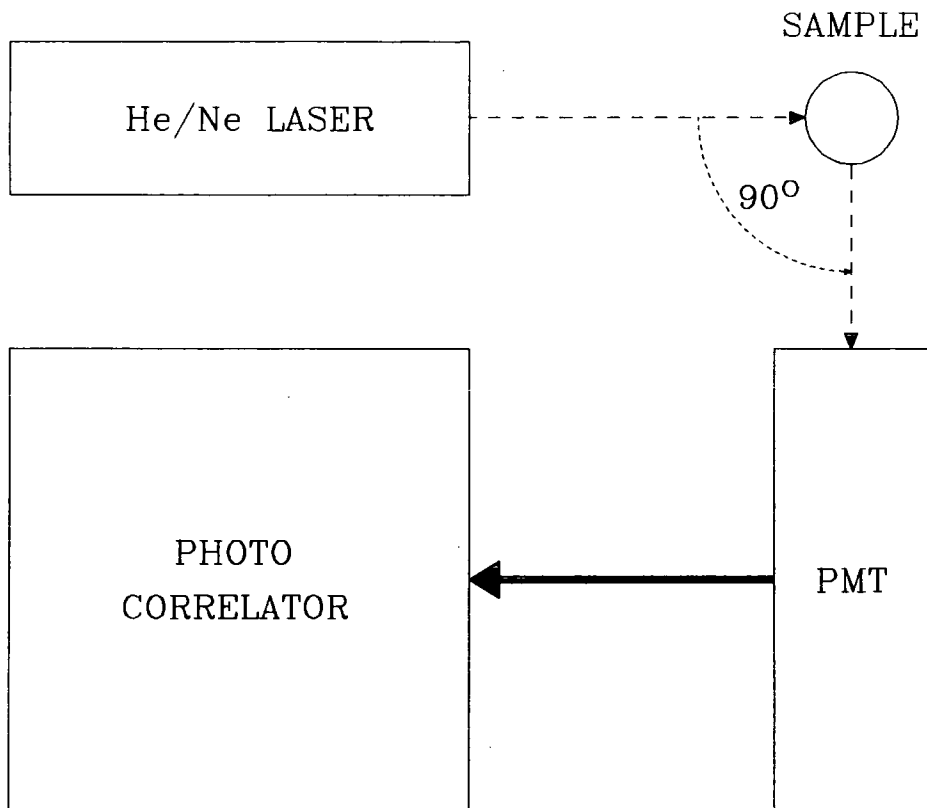


Figure 3.7: Schematic Diagram of Turbidimetry Apparatus

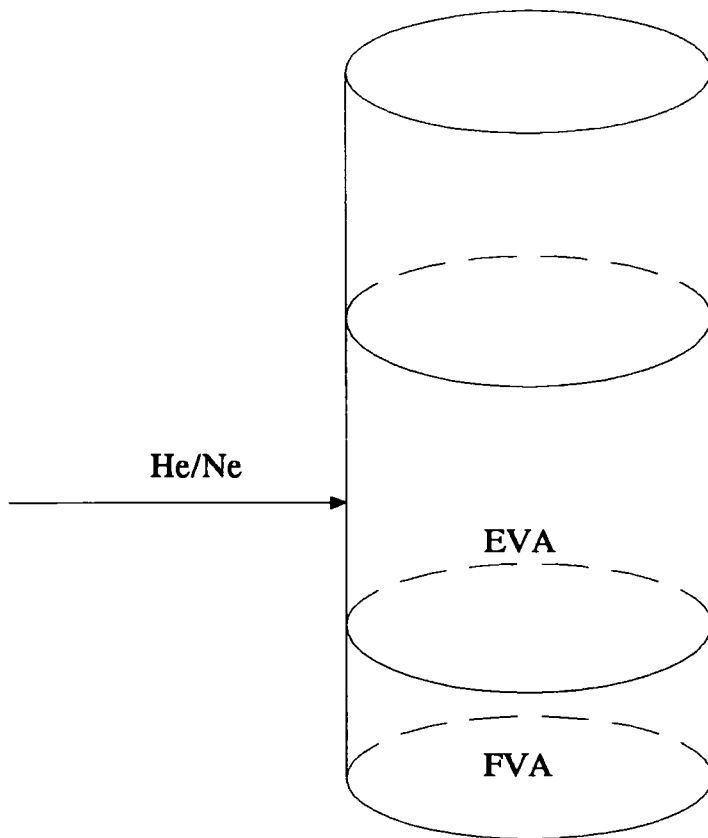
This apparatus could not be used for studying blends because the beam only collided with a very small area of the vertically mounted sample and since blends were observed to separate into two distinct layers when left at $\sim 353\text{K}$ for 12 hours⁽¹¹⁾, this prohibited any further work as shown in Figure 3.8.

3.5.1 Turbidimetry Results

Table 3.6

Temperature / K	Arbitrary Intensity	Standard Deviation
313.2	14133	959
315.9	13223	866
319.1	11887	766
323.2	9762	597
324.6	8418	506
325.6	8170	482
326.0	6626	467
326.1	8827	533
326.5	5128	421
326.9	3199	456
327.7	2752	403
328.2	3299	459
329.1	1853	226
330.2	1208	176
331.4	975	144
332.4	757	126
333.2	344	39
338.2	90	19

These results show that the intensity of the scattered light decreases evenly between 313 and 326 K and then falls dramatically between 326 and 329 K before reaching a minimum at approximately 333 K. This suggests that the clarification of the sample starts below 326 K though this effect is not



Optical Cell containing Sample

Figure 3.8: Schematic Diagram of Turbidimetry Sample Cell

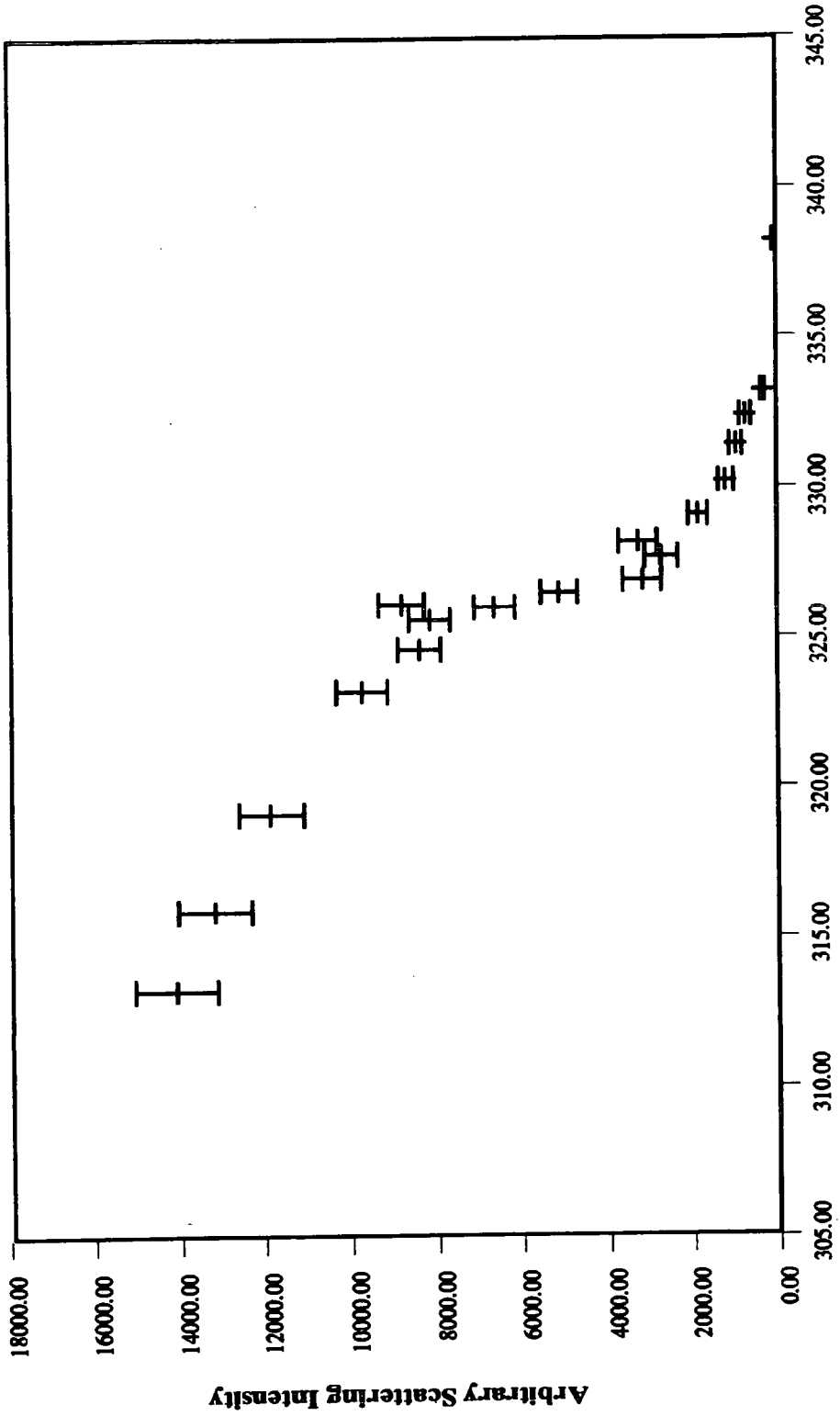
apparent to the naked eye. These results are expressed graphically in Figure 3.9.

3.6 General Discussion

The initial characterisation showed that both of these materials comprised long alkyl sequences and ester groups. If the macro structures are considered, (Figs. 3.1 and 3.2), it appears likely that any interaction between these species was likely to arise between substituted alkyl groups of the fumarate and the backbone of EVA, rather than between the ester linkages which are substantially protected. Any intermolecular interaction which existed between the alkyl chains was likely to be weak and thus difficult to measure. The volume additivity observed from the density measurements, and the insignificant depression of the C_{14} FVA melting point as determined by DSC, support this simple hypothesis. The GPC data show that both of these copolymers are polydisperse and of low molecular weight, the degree of polymerisation being 13 and 17 for EVA and C_{14} FVA respectively. Additionally, the EVA sample underwent some type of transition which the turbidimetry measurements showed as starting at temperatures of less than 313K and continuing towards a maximum at about 325-327K. No corresponding effect was seen with DSC. These factors complicated this work since many of the thermodynamic models and theories assume a monodisperse system of infinitely high molecular weight, and all further experiments had to be carried out above 353K to ensure that the EVA was in a stable state. These factors together with the non-reproducibility of the T_g data were considered to be sufficient evidence to doubt the value of the phase diagram as obtained in section 3.4.

Other experimental and theoretical techniques, which were used in an attempt to characterise this problematic blend, are described in subsequent chapters of this thesis.

90 Degree Scattering Intensity Profile of EVA



Temperature/K
Figure 3.9

3.7 REFERENCES

- (1) Anton Paar KG (Densimeter) Instruction manual.
- (2) G.F.C. Rogers and Y.R. Mayhew, 'Thermodynamic and Transport Properties of Fluids', 3rd Edition, Blackwell, (1980).
- (3) C.H.H.Jacques and H.B.Hapfenberg, Polym. Eng. Sci., 14, 441, (1974).
- (4) P.J.Flory, 'Principles of Polymer Chemistry', Cornell University, (1954).
- (5) J.D.Hoffman and J.J.Weeks, J. Res. Natl. Bur. Stand. U.S., 66, 13, (1962).
- (6) T.Nishi and T.T.Wang, Macromolecules, 8, 909, (1975).
- (7) J.J.Ziska, J.W.Barlow and D.R.Paul, Polymer, 22, 918, (1981).
- (8) J.E.Harris, S.H.Goh, D.R.Paul and J.W.Barlow
J. Appl. Polym. Sci., 27, 839, (1982).
- (9) J.E.Harris, D.R.Paul and J.W.Barlow,
Polym. Eng. Sci., 23, 676, (1983).
- (10) T.K.Kwei and H.L.Frisch, Macromolecules, 11, 1276, (1978).
- (11) D.R.Paul, 'Polymer Blends and Mixtures',
NATO ASI Series E: Applied Sciences, No.89.
- (12) Private communication from EXXON Chemicals.

Chapter 4 Inverse Phase Gas Chromatography

4.1 Introduction

The technique of Inverse Phase Gas Chromatography, (IGC), was first devised approximately twenty years ago⁽¹⁾ and was so-called because it uses the properties of an known volatile phase to examine the properties of an unknown stationary phase. This has particular application in polymer science because the vapour pressure of most polymers is effectively zero at practical temperatures, making conventional Gas Liquid Chromatography, (GC), unsuitable. IGC involves depositing the polymer onto an inert chromatographic support which forms the stationary phase in a GC column. A small quantity of volatile probe is vaporised and passed through this column and the time required to elute this probe gives a measure of the polymer-solute interaction. IGC has been used to study a variety of physico-chemical parameters⁽²⁻⁴⁾ which can all be derived from this elution time.

This technique measures the total free energy of interaction and consequently includes combinatorial and residual interactions in addition to any residual entropy contributions. Although it serves as an inexpensive, rapid and simple method which yields reproducible qualitative and relative information, *i.e.* between individual experiments, the quantitative reliability has often been found lacking, owing to the intrinsic but unpredictable surface adsorption and diffusion of the solvent probe in the stationary phase.

4.2 Theoretical

The time between injection of the probe on to the column and its elution peak maximum is defined as the elution time, Δt . In common with most dynamic techniques, Δt is normally converted to a more flexible parameter which normalises for many of the experimental conditions, *e.g.* the inlet pressure and volumetric flow rate of the carrier gas, and the mass of polymer on the support. The preferred parameter is the elution volume⁽⁵⁾, V_r , defined as,

$$V_r = 1.5 F \Delta t \left\{ \frac{(P_{inlet}/P_{outlet})^2 - 1}{(P_{inlet}/P_{outlet})^3 - 1} \right\} \left\{ \frac{273.16}{T_r} \right\} \quad (4.1)$$

where,

F = Carrier gas volumetric flow rate, $\text{cm}^3 \text{s}^{-1}$

T_r = Temperature at which data were recorded, K

P_{inlet} = Carrier gas pressure at inlet, mmHg

P_{outlet} = Carrier gas pressure at outlet, mmHg

However, this term contains contributions from both the void volume of the column, V_o , and the retention volume of the chromatographic support, V_s . The void volume is a characteristic of the column which is determined by passing a sample of inert, non-interacting gas, usually methane, through the column and recording its elution time. This value is then assumed to be the minimum time required to pass an unretentive species through a particular column. However, this procedure has been found to introduce a significant systematic error since the retention volume of methane is often of a similar magnitude to that of many of the solvent probes. To avoid this error Munk *et al* ⁽⁶⁾ suggested eluting a series of hydrocarbons and extrapolating the natural logarithm of their elution volumes to zero carbon number. The exponent of this value represents the elution volume of a true unretentive species. This current work used CH_4 , and C_5H_{12} to C_8H_{18} , and observed a linear relationship between $\text{Ln}(V_r)$ and carbon number for all of the columns employed. It has also been reported⁽⁷⁾ that the chromatographic support can make a substantial contribution to the elution time. This effect can be removed by duplicating each experiment on an uncoated column and subtracting this contribution from the retention volume of the probe.

If both of these effects are removed, then

$$V_g = V_r - V_o - V_s \quad (4.2)$$

where, V_o = column void volume, cm^3

V_s = retention volume of support, cm^3

The support retention volume can be further reduced as it contains a contribution from the void volume of the blank column, $V_{o(Blank)}$, *i.e.*,

$$V_s = V_{r(Blank)} - V_{o(Blank)} \quad (4.3)$$

If equations (4.2) and (4.3) are combined, and the result normalised for the mass of polymer on the stationary phase, w , equation (4.4) is obtained,

$$V_{gc} = \left\{ V_r - V_o - (V_{r(Blank)} - V_{o(Blank)}) \right\} / w \quad (4.4)$$

where,

V_{gc} = corrected net retention volume, $\text{cm}^3 \text{g}^{-1}$

V_r = elution volume of solvent on coated column, cm^3

V_o = void volume of the coated column, cm^3

$V_{r(Blank)}$ = elution volume of solvent on blank column, cm^3

$V_{o(Blank)}$ = void volume of blank column, cm^3

w = mass of polymer on coated column, g

It should be noted that these corrections are made as retention volumes rather than elution times because the experimental conditions often differ. The corrected net retention volume is the experimental parameter which is used in the following thermodynamic treatment. In this chapter the results are considered only in terms of Flory-Huggins-Miller-Chang theory: a full equation of state analysis is included in Chapter 8.

Calculation of Flory-Huggins-Chang-Miller Interaction Parameters

Since IGC measures the free energy of interaction the interaction parameters are denoted as $\bar{\chi}$ as opposed to χ which has been used elsewhere in this thesis to denote interaction parameters based solely on the enthalpic mixing contribution. The first interaction to be considered is that between the infinitely dilute solvent probe and the bulk polymeric stationary phase, $\bar{\chi}_{11}$,

$$\bar{\chi}_{11} = \text{Ln} \left\{ \frac{RTV_i}{V_{gc} V_1 P_1^o} \right\} - \left\{ 1 - \frac{V_1}{\bar{M}n_i V_i} \right\} - \frac{P_1^o}{RT} \left\{ B_{11} - V_1 \right\} \quad (4.5)$$

where,

$\bar{M}n_i$ = number average molecular weight of polymer, g mol⁻¹

R = Universal Gas Constant, 82.057 cm³ atm K⁻¹ mol⁻¹

T = operating temperature, K

V₁ = molar volume of solvent at T, cm³ mol⁻¹

P₁^o = saturated vapour pressure of solvent at T, atm

v_i = specific volume of polymer at T, cm³ g⁻¹

B₁₁ = second virial coefficient of solvent vapour phase at T,
cm³ mol⁻¹

Note: The subscripts used here denote the following quantities

1 - solvent

2 - EVA

3 - C₁₄FVA,

From equation 4.5 the two solvent-polymer interaction parameters, $\bar{\chi}_{12}$ and $\bar{\chi}_{13}$, together with the the solvent-polymer-polymer interaction parameter, $\bar{\chi}_{1,23}$, can be stated explicitly as,

$$\bar{\chi}_{12} = \text{Ln} \left\{ \frac{RTv_2}{V_{gc} V_1 P_1^o} \right\} - \left\{ 1 - \frac{V_1}{\bar{M}n_2 v_2} \right\} - \frac{P_1^o}{RT} \left\{ B_{11} - V_1 \right\} \quad (4.5a)$$

$$\bar{\chi}_{13} = \text{Ln} \left\{ \frac{RTv_3}{V_{gc} V_1 P_1^o} \right\} - \left\{ 1 - \frac{V_1}{\bar{M}n_3 v_3} \right\} - \frac{P_1^o}{RT} \left\{ B_{11} - V_1 \right\} \quad (4.5b)$$

$$\begin{aligned} \bar{\chi}_{1,23} = \text{Ln} \left\{ \frac{RT(w_2 v_2 + w_3 v_3)}{V_{gc,23} V_1 P_1^o} \right\} - \left\{ 1 - \frac{V_1}{\bar{M}n_2 v_2} \right\} \phi_2 \\ - \left\{ 1 - \frac{V_1}{\bar{M}n_3 v_3} \right\} \phi_3 - \frac{P_1^o}{RT} \left\{ B_{11} - V_1 \right\} \quad (4.5c) \end{aligned}$$

The polymer-polymer interaction parameter, $\bar{\chi}_{23}$, can be evaluated from the three equations above by considering the solvent effect to be additive,

$$\bar{\chi}_{23} = \frac{1}{\phi_2\phi_3} \left\{ \phi_2\bar{\chi}_{12} + \phi_3\bar{\chi}_{13} - \bar{\chi}_{1,23} \right\} \quad (4.6)$$

If the common factors are removed from the individual interaction parameters in equation 4.6,

$$\bar{\chi}_{23} = \frac{V_2}{V_1} \left\{ \frac{1}{\phi_2\phi_3} \text{Ln} \left(\frac{V_{gc,23}}{w_2V_2 + w_3V_3} \right) - \phi_2 \text{Ln} \left(\frac{V_{gc,2}}{V_2} \right) - \phi_3 \text{Ln} \left(\frac{V_{gc,3}}{V_3} \right) \right\} \quad (4.7)$$

where,

$\bar{\chi}_{23}$ = true polymer-polymer interaction parameter.

V_2 = molar volume of polymer, $\text{cm}^3 \text{mol}^{-1}$

ϕ_i = volume fraction of component 'i'

w_i = weight fraction of component 'i' in blend

(the subscripts on the corrected retention volumes denote which column was used to derive the data)

An alternative definition of interaction parameter, $\bar{\chi}'_{23}$, is sometimes used, namely,

$$\bar{\chi}'_{23} = \bar{\chi}_{23} (V_1/V_2) \quad (4.8)$$

This form is favoured because the molar volumes of both the solvent and the polymer need not be known. Another definition arises defined by removing the molar volume of the solvent from equation 4.8.

$$\bar{\chi}'_{23,app} = \bar{\chi}_{23} / V_2 \quad (4.9)$$

This was introduced to remove the intrinsic solvent effects from IGC data by normalising the interaction parameter for the molar volume of the probe used. However, it has been found to be a scaling factor rather than a correlation.

Another definition involves the interaction energy density characteristic of the polymer-polymer pair, B_{23}

$$B_{23} = \bar{\chi}'_{23} RT/V_1 \quad (4.10)$$

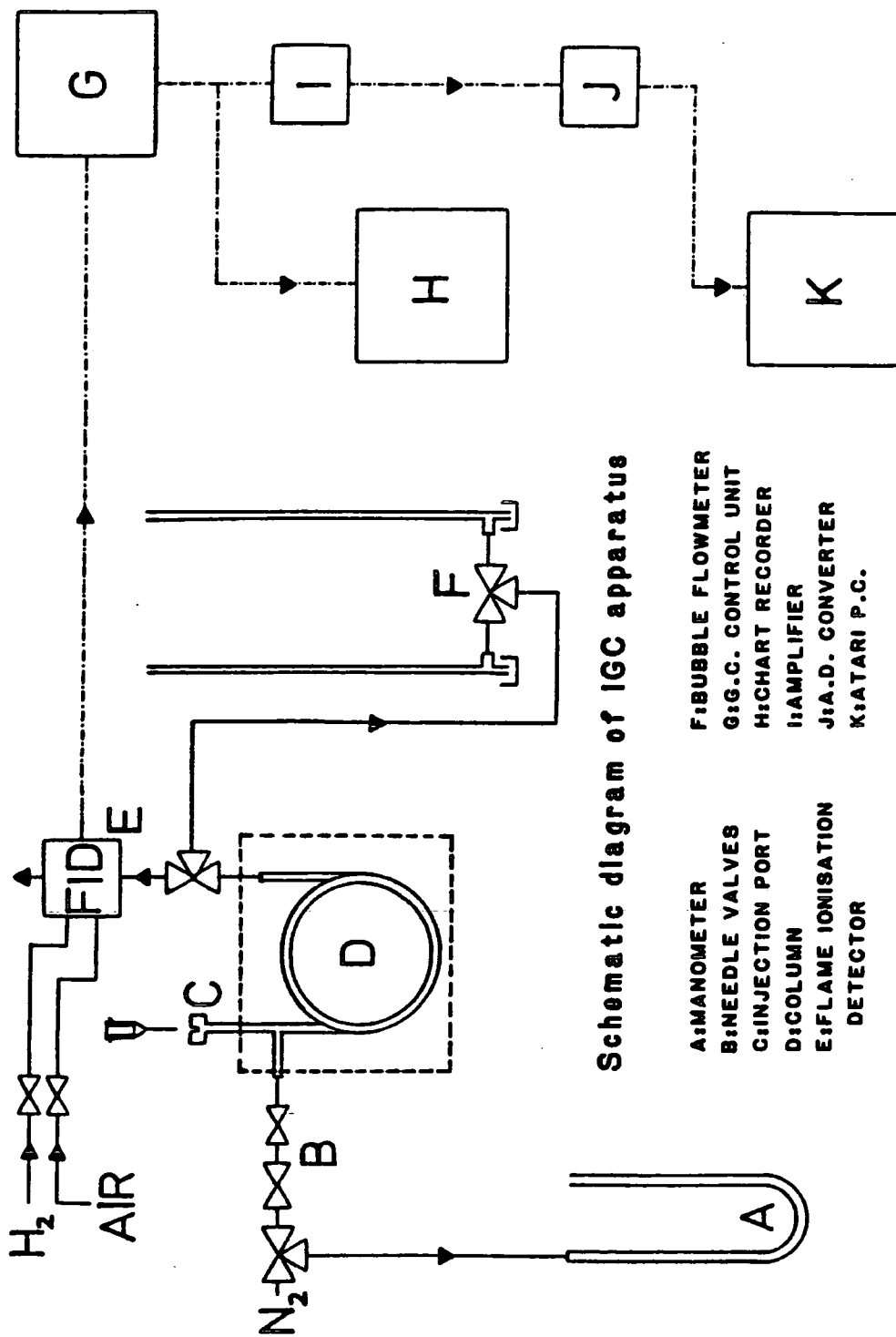
These definitions of interaction parameter are related, *i.e.*

$$\bar{\chi}_{23} = \bar{\chi}'_{23} (V_2/V_1) = \bar{\chi}'_{23app} V_2 = B_{23} V_2/RT$$

and the final choice is usually made on the basis of the information available about the polymer and the probe. Munk *et al*⁽⁹⁾ reported an empirical correlation between the B_{23} values obtained for blends of poly(ϵ -caprolactone) and poly(epichlorohydrin), and the Hildebrand solubility parameters of the eluents. It was originally hoped that this function could be used to predict and/or remove the obvious solvent dependence in the data. The same procedure was also attempted in this work but no correlation was apparent and consequently the results of this work have been presented in terms of $\bar{\chi}'_{23}$.

4.3 Apparatus and Materials

A PYE Unicam G.C.D. chromatograph equipped with flame ionisation detector, (FID), was adapted to perform the IGC measurements in this work,⁽⁹⁾ Fig.(4.1). Oxygen-free-nitrogen, (OFN), was used as the carrier gas which was supplied to the system through a 3-way valve, allowing the flow to be directed either to a mercury manometer, (A), which determined the inlet pressure, or to a pair of needle valves, (B), which accurately controlled the volumetric flow rate to the column. Approximately $0.5 \mu\text{L}$ of solvent was injected through a silicon rubber septum into section (C) which was maintained at 523K. As the solvent was vaporised it became entrained in the entering OFN stream and was propelled through the column as a molecular plug. An additional 3-way valve was inserted at the exit of the column to allow the stream to be directed either to a pair of 100 cm^3 bubble flowmeters, (F), or the FID, (E) : two independent flowmeters were used to reduce the time required to determine the flow rate and to ensure the reproducibility of the measurement. The electrical output from the GC control unit, (G), was sent simultaneously to a chart recorder, (H), and an Atari personal computer, (K). This arrangement provided both accurate information on the shape of the elution profile and the time at which the elution maxima occurred. The output to the Atari was processed initially by an amplifier, (I), which optimised the gain of the signal, and was then fed to a 8-bit Analog - Digital converter⁽¹⁰⁾, (J).



Schematic diagram of IGC apparatus

- | | |
|------------------------------|----------------------|
| A: MANOMETER | F: BUBBLE FLOWMETER |
| B: NEEDLE VALVES | G: G.C. CONTROL UNIT |
| C: INJECTION PORT | H: CHART RECORDER |
| D: COLUMN | I: AMPLIFIER |
| E: FLAME IONISATION DETECTOR | J: A.D. CONVERTER |
| | K: ATARI P.C. |

Figure 4.1

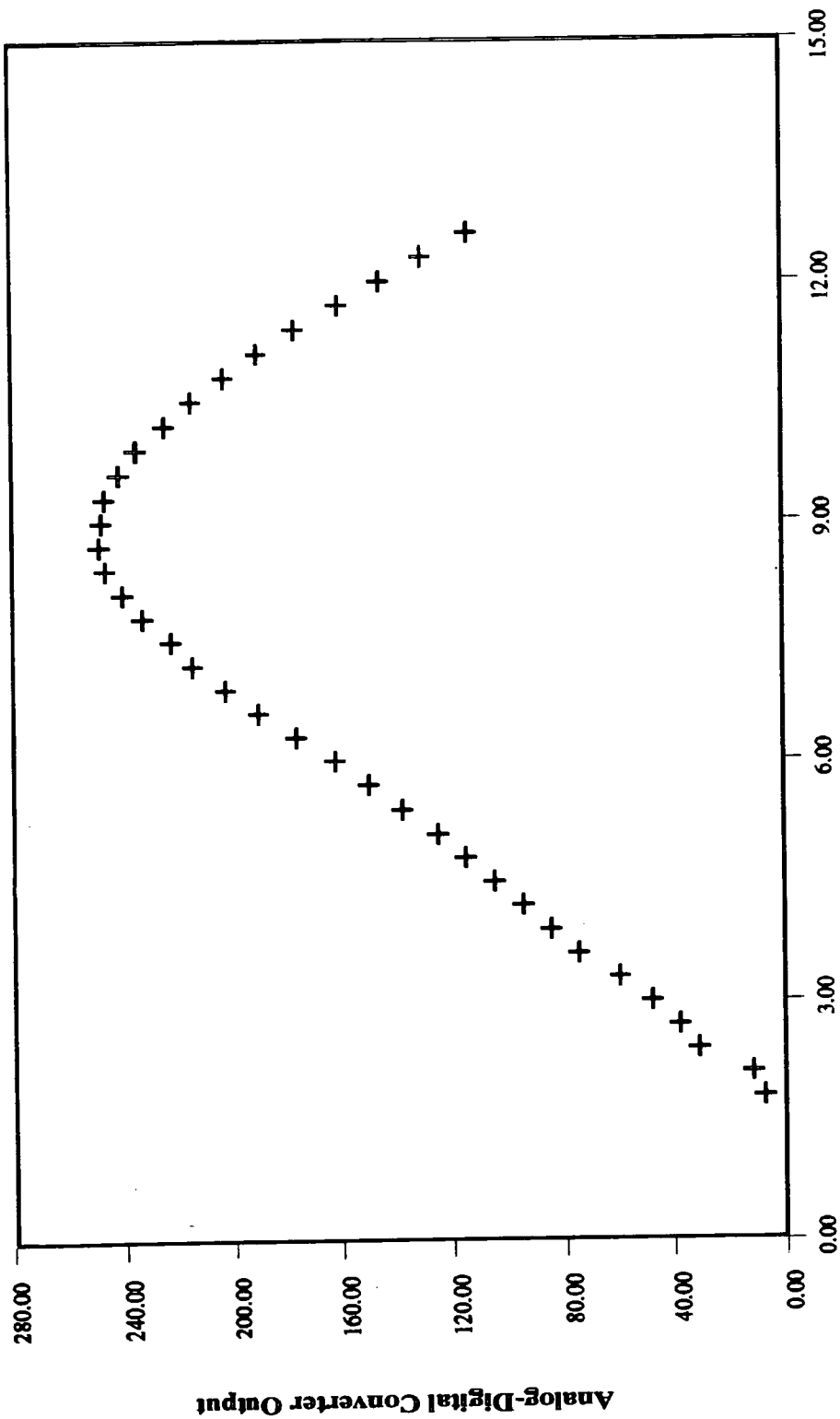
An Atari 1040 ST, (K), was chosen for this task as it has an internal clock which could be accessed to provide sampling intervals down to 0.01s. Previous workers⁽⁸⁾ used a sampling interval of 0.5 s and obtained the elution - peak maximum by fitting a quadratic to the data. This quadratic was then differentiated and set equal to zero; the maximum was found by solving the resulting equation. This method assumes that the profile is entirely symmetrical which is frequently not the case as may be seen from Fig.4.2. Using a sampling interval of 0.01s eliminates the need for such an assumption. The data acquisition software was developed for this apparatus using GFA Basic (version 3.2). The data was then stored as a series of values between 0 and 256 on floppy disk, and was immediately available for further manipulation *e.g.* graphical representation, integration of the area under the peak or estimation of the baseline stability. Additionally, a series of programs was written in Pascal and Modula 2 to reduce the data and to calculate the relevant physico-chemical parameters.

4.4 Experimental Procedure

The stationary phase which was packed into the columns comprised the polymeric material, at typically 7% loading, which had been deposited onto approximately 15g of the chromatographic support from a suitably volatile solvent using the method suggested by Al-Saigh and Munk⁽¹¹⁾: 30/80 mesh PTFE⁽¹²⁾ (which had been re-sieved, acid washed and treated with dichloro-methyl-siloxane) was used as the support. The coated material was drawn into glass columns⁽¹³⁾ of dimensions 2m x 4mm (i.d.) by an aspirator pump and left under vacuum until no further compression of the support could be detected. Approximately 0.05cm³ of 1mm diameter beads were then inserted on top of the packing at the inlet to the column, to aid solvent vaporisation and distribution, and the column was then placed in the G.C. oven and conditioned for 24 hours at 10K above the nominal operating temperature.

The solvent probes were of AnalaR grade and were used as supplied, as any contaminants were effectively separated on the column. At hourly intervals during experimentation the inlet pressure and volumetric flow rate were recorded to ensure that the carrier gas stream remained constant. It was found that over any 12 hour period the variation in these conditions lay within the resolution of the measuring devices. Similarly, the temperature of the GC oven was independently measured with a platinum resistance thermometer and was found to remain virtually constant over periods of up to 6 weeks although a 0.2K variation was found within the oven.

***IGC Elution Curve of Dichloromethane at 353K
on an FVA Column***



Time/s
Figure 4.2

The carrier gas flow rate was measured a minimum of 5 times on each occasion, and a mean value recorded. Once these parameters had been measured the elution times of the solvents could be studied. Each solvent was injected a minimum of 5 times and a mean value recorded. Elution times for different solvents varied from a minimum of 30 seconds to a maximum of 6 minutes. The reproducibility for any given solvent was typically 1%.

One disadvantage of sampling at an interval of 0.01s was that enormous quantities of irrelevant data could be accumulated with slowly eluting solvents. To eliminate this, the data acquisition program examined a predetermined number of consecutive samples which were required to increase by a given percentage before data logging began, (both of these parameters were variable and were set at the start of each run). The program then sampled the GC output for a specified duration and recorded the time at which the maximum signal was recorded. At the end of each run the data were transferred from RAM to a floppy disc and the process repeated.

4.5 Results

A sample calculation has been included to illustrate the calculation of interaction parameters from the IGC data.

4.5.1 Sample calculation and estimation of errors.

At each stage of the calculation an error has been estimated so that the significance of each term and its associated error can be examined, and to assist in estimating a total error for the interaction parameters. Owing to the limited number of results, a standard deviation analysis was not attempted and instead a simple best/worst case treatment has been used.

The specimen calculation uses the results for chloroform with the 0.3589 (wt/wt) EVA column at 373K; this was a random choice. This calculation illustrates the evaluation of the terms required for the processing of the IGC data which ultimately gives a value of $\bar{\chi}'_{1,23}$

(1) Carrier gas volumetric flow rate.

Start / cm	Stop / cm	Total / cm	Time / s	Flow / cm ³ s ⁻¹
98	68	30	88.39	0.3394
64	34	30	87.82	0.3416
30	0	30	88.38	0.3394

Mean = 0.3401 cm³ s⁻¹

Error: (+ve value = 0.3416, -ve value = 0.3394 cm³s⁻¹)

(2) Inlet and outlet carrier gas pressures

The inlet pressure was measured using a 2m manometer which was attached to a millimetre calibrated scale. The associated error in reading this scale was approximately 0.5mmHg. The inlet pressure was always measured at equilibrium. Hence in this case only a single point was ever recorded.

Inlet Pressure = 2327.0 ± 0.5 mmHg

Error: (+ve value = 2327.5, -ve value = 2326.5 mmHg)

The outlet pressure was always taken as the atmospheric condition, measured on a mercury barometer fitted with a Vernier scale. The error in reading this scale was 0.1mmHg, thus,

Outlet Pressure = 760 ± 0.1 mmHg

Error: (+ve value = 760.1, -ve value = 759.9 mmHg)

(3) Elution Times

These data were recorded at an interval of 0.01 s between points

Run	Elution time / s
1	164.17
2	164.59
3	164.07
4	164.33
5	164.21

$$\text{Mean} = 164.27 \text{ cm}^3 \text{ s}^{-1} \text{ (standard deviation 0.18)}$$

$$\text{Error: (+ve value} = 164.45, \text{-ve value} = 164.09 \text{ cm}^3 \text{ s}^{-1})$$

This value now requires to be converted into an elution volume which normalises the result for the conditions of the experiment, using equation 4.1,

$$V_r = 1.5 F \Delta t \left\{ \frac{(P_{inlet}/P_{outlet})^2 - 1}{(P_{inlet}/P_{outlet})^3 - 1} \right\} \left\{ \frac{273.16}{T_r} \right\}$$

substituting,

$$V_r = 1.5 \times (0.3401) \times (164.27) \left\{ \frac{(2327/760)^2 - 1}{(2327/760)^3 - 1} \right\} \left\{ \frac{273.16}{373.16} \right\}$$

$$V_r = 18.544 \text{ cm}^3$$

$$\text{Error: (+ve value} = 18.657, \text{-ve value} = 18.489 \text{ cm}^3)$$

To simplify the error calculation, the difference between the +ve value and the mean value has been assumed to represent the typical error associated with measuring a retention volume. If this is expressed as a percentage of the mean value, *i.e.*

$$\text{Difference} = 18.657 - 18.544 = 0.1126 \text{ or } 0.6\% \text{ (expressed as a \%age)}$$

It is now assumed that this magnitude of error is present in all retention volume measurements and the high/low values quoted for the following values represent 0.6% of the mean values given. This retention volume now requires to be corrected for the contributions from the PTFE support and the void volume in accordance with equation 4.4.

(3a) PTFE Contribution

The elution time of chloroform on a blank column was determined as,

$$\Delta t = 46.52 \text{ s}$$

under the following experimental conditions

$$P_i = 2302 \text{ mmHg} : P_o = 760 \text{ mmHg} : F = 0.2606 \text{ cm}^3\text{s}^{-1}$$

which gives a gross retention volume of,

$$V_{r(\text{blank})} = 5.549 \text{ cm}^3$$

However, this term includes the blank column void volume contribution which was evaluated by the extrapolation process described below, as 1.487 cm^3 , *i.e.*

$$\begin{aligned} V_s &= V_{r(\text{blank})} - V_{o(\text{blank})} \\ &= 5.549 - 1.487 = 4.062 \text{ cm}^3 \end{aligned}$$

Error: (+ve value = 4.086, -ve value = 4.038 cm^3)

(3b) Column void volume

The void volume of each column was determined by eluting methane, pentane, hexane, heptane and octane, at each temperature, and extrapolating the natural logarithm of their retention volume, as a function of carbon number, to give an intercept with the y-axis, and thus an estimate of the retention volume of a hypothetically non-interacting solvent probe.

Under the same conditions that are quoted above for the support contribution, the following elution times were measured,

Solvent	Carbon No.	$\Delta t / s$	$\ln(\Delta t)$
Methane	1	30.71	3.43
Pentane	5	57.85	4.06
Hexane	6	90.78	4.51
Heptane	7	161.03	5.08
Octane	8	304.73	5.72

The following values of slope and intercept were obtained from a linear least-squares fit for this data:

Intercept = 1.23, Slope = 0.56 with a correlation coefficient of 0.9971

Thus for a carbon number of 1, $\ln(\Delta t)$ was recalculated as 1.79; hence the void elution time was estimated as $\text{Exp}(1.79)$ or 5.96 s

Void Volume = $V_o = 1.015 \text{ cm}^3$

Error: (+ve value = 1.021, -ve value = 1.009 cm^3)

If the non-polymer contributions are now removed from V_r and the result normalised for the weight of material on the column, the net retention volume can be obtained from equation 4.2,

$$V_g = (V_r - V_o - V_s)/w$$

where, $w = 0.9996 \text{ g}$

Error: (+ve value = 0.99965, -ve value = 0.99955g)

$$\begin{aligned} V_{gc} &= (18.544 - 4.062 - 1.015)/0.9996 \\ &= 13.472 \text{ cm}^3 \text{ g}^{-1} \end{aligned}$$

Error: (+ve value = 13.5561, -ve value = 13.3907 $\text{cm}^3 \text{ g}^{-1}$)

This value is the retention volume arising from only the polymer-polymer-solvent interaction.

Equation 4.5 requires the estimation of a number of physical properties of both the polymer and the solvent. The methods that were used to calculate or measure these parameters are listed below:

$$\bar{\chi}_{1i} = \text{Ln} \left\{ \frac{RTv_i}{V_{gc} V_1 P_1^o} \right\} - \left\{ 1 - \frac{V_1}{M\bar{n}_i v_j} \right\} - \frac{P_1^o}{RT} (B_{11} - V_1) \quad (4.5)$$

solvent properties: V_1 , P_1^o and B_{11}

polymer properties: v_{23} and M_{23}

Solvent Properties

(a) molar volumes of solvents: V_1

These were calculated from an abbreviated form of the Gunn and Yamada expression ⁽¹⁴⁾,

$$V = V_{Ref} \frac{V_r^{(0)}(T_r) \{1 - \omega g(T_r)\}}{V_r^{(0)}(T_{r,Ref}) \{1 - \omega g(T_{r,Ref})\}} \quad (4.11)$$

where,

T = temperature for which the molar volume is required, K

T_c = critical temperature of the solvent, K

T_r = reduced temperature, T/T_c

T_{Ref} = reference temperature, K

$T_{r,Ref}$ = reduced reference temperature, T_{Ref}/T_c

V_{Ref} = molar volume of material at T_{Ref} , $\text{cm}^3 \text{mol}^{-1}$

ω = Pitzer and Curl acentric factor

$V_r^{(0)}$ and g are empirical functions of reduced temperature, such that

For $0.2 \leq T_r \leq 0.8$

$$V_r^{(0)} = 0.33593 - 0.33953 T_r + 1.51941 T_r^2 - 2.02512 T_r^3 + 1.11422 T_r^4 \quad (4.12)$$

and for $0.2 \leq T_r \leq 1.0$

$$g = 0.29607 - 0.09045 T_r - 0.04842 T_r^2 \quad (4.13)$$

For the sample data V_1 was calculated from the Gunn and Yamada correlation as $89.8 \text{ cm}^3 \text{ mol}^{-1}$

This method is recommended as one of the most accurate available for calculating the molar volume of a saturated liquid. It is said to be applicable for non-polar and slightly polar compounds although acetonitrile and alcohols have also been fitted. Another recommended correlation is a modified version of the Rackett equation⁽¹⁵⁾ which replaces the critical compressibility factor, Z_{cr} , with an empirical constant characteristic of the compound under study, Z_{Ra} .

$$V = \frac{RT_c}{P_c} \text{Exp} \left\{ (1 - T_r)^{2/7} \text{Ln} (Z_{Ra}) \right\} \quad (4.14)$$

where,

P_c = critical pressure of the solvent, and

$$Z_{Ra} = 0.29056 - 0.08775 \omega \quad (4.15)$$

For the sample data, the calculated specific volume using the Rackett equation was $89.9 \text{ cm}^3 \text{ mol}^{-1}$.

Both methods were used, where empirical data was available, to ensure reproducibility and although very little difference was observed between the results the modified Rackett equation was used preferentially. The error associated with this calculation is reported to be smaller than 1%, and this was taken as the worst possible case, *i.e.*

Error: (+ve value = 90.8, -ve value = 89.0 $\text{cm}^3 \text{ mol}^{-1}$)

(b) saturated vapour pressure, P_1^o

P_1^o was calculated preferentially from the Wagner equation⁽¹⁴⁾, where data were available,

$$P_1^o = \text{Exp} \left\{ (w_1 \tau + w_2 \tau^{1.5} + w_3 \tau^3 + w_4 \tau^6) / T_r \right\} \quad (4.16)$$

where $\tau = 1.0 - T_r$ and

w_i = the Wagner coefficients from Reid, Prausnitz and Polling⁽¹⁴⁾

or from the Antoine equation⁽¹⁴⁾,

$$P_1^o = \text{Exp} \left\{ A_0 - A_1 / (T + A_2) \right\} \quad (4.17)$$

where, A_i = the Antoine coefficients from Reid, Prausnitz and Polling⁽¹⁴⁾

For chloroform at 373.16 K, the Wagner equation gave a vapour pressure of 2325 mmHg. Although the error in the calculated vapour pressure will vary for different solvents, Reid, Prausnitz and Polling include a specimen calculation for acetone where the typical error does not exceed 0.2%. It was concluded that errors in vapour pressure calculations could be neglected when compared with other sources of error.

(c) Second virial coefficient of the solvent in the vapour phase : B_{11}

Gaseous second virial coefficients can be calculated either from the integration of theoretical expressions, which relate intermolecular energy to the distance of molecular separation, or by employing corresponding-states relations to experimental data. The latter approach is usually favoured owing to the limited information on the energetic relationships of molecules. This work has employed two techniques to estimate the vapour phase virial coefficients of the solvent probes from the collected data of Dymond and Smith⁽¹⁶⁾. The Tsonopoulos⁽¹⁴⁾ correlation is a modified version of the Pitzer and Curl expansion,

$$\frac{B_{11} P_c}{RT_c} = f^{(0)} + \omega f^{(1)} \quad (4.18)$$

$$\begin{aligned} \text{where, } f^{(0)} = & 0.1445 - 0.330/T_r - 0.1385/T_r^2 \\ & - 0.0121/T_r^3 - 0.000607/T_r^8 \end{aligned} \quad (4.19)$$

$$\text{and } f^{(1)} = 0.0637 + 0.331/T_r^2 - 0.423/T_r^3 - 0.008/T_r^8 \quad (4.20)$$

for the data in the specimen calculation, B_{11} is $-663 \text{ cm}^3 \text{ mol}^{-1}$

Where possible it is preferable to use experimental results for B_{11} and to permit this least-squares techniques were employed to derive a relationship between the reduced second virial coefficient, B_r and a function of reduced temperature (MacDonald⁽¹⁷⁾). The function chosen makes use of the fact that a plot of $\ln(x)/x$ versus x has a very similar shape to a plot of B_r versus T_r ; thus a plot of B_r versus $\ln(T_r)/T_r$ is substantially linear and hence a least-squares quadratic gives a very good fit over the temperature range of immediate interest.

This method gave a value of $-675 \text{ cm}^3 \text{ mol}^{-1}$ for the second virial coefficient.

The error is dependent on the quality of the experimental data which varies from solvent to solvent but for the specimen calculation it is convenient to use Dymond and Smith's estimate of $\pm 30 \text{ cm}^3 \text{ mol}^{-1}$.

Error: (+ve value = -705 , -ve value = $-645 \text{ cm}^3 \text{ mol}^{-1}$)

Polymer Characteristics

(a) Specific Weights of Polymers : v_2 and v_3

These values were extrapolated from the least-squares fit of the data relating the reciprocal of density to temperature and composition for each material, section 3.3, thus

$$v_{EVA.373K} = 1.1227 \text{ cm}^3 \text{ g}^{-1}$$

$$v_{FVA.373K} = 1.1056 \text{ cm}^3 \text{ g}^{-1}$$

The errors associated with these measurements were considered to be insignificant in relation to the other errors and consequently it has been neglected.

(b) number average molecular weight of the polymer phase: \bar{M}_n and \bar{M}_n

The number average molecular weights were obtained from the GPC measurements described in section 3.2. It is difficult to estimate the accuracy of the GPC measurements since the Mark-Houwink parameters were not known for either polymer and the calibrant was polystyrene, which is unrepresentative of poly(alkyl) materials.

For the purpose of testing the significance of this term in the final answer it has been estimated liberally as 20%, *i.e.*

$$\bar{Mn}_{EVA} = 3290 \text{ g mol}^{-1} \text{ and } \bar{Mn}_{FVA} = 10400 \text{ g mol}^{-1}$$

$$\text{Error}_{EVA}: (+\text{ve value} = 3948, -\text{ve value} = 2632 \text{ g mol}^{-1})$$

$$\text{Error}_{FVA}: (+\text{ve value} = 12480, -\text{ve value} = 8320 \text{ g mol}^{-1})$$

If the values calculated from all of the expressions above are now substituted into the equation 4.5c,

$$\begin{aligned} \bar{\chi}_{1,23} = & \text{Ln} \left\{ \frac{RT(w_2v_2 + w_3v_3)}{V_{gc,23} V_1 P_1^o} \right\} - \left\{ 1 - \frac{V_1}{M\bar{n}_2v_2} \right\} \phi_2 \\ & - \left\{ 1 - \frac{V_1}{M\bar{n}_3v_3} \right\} \phi_3 - \frac{P_1^o}{RT} (B_{11} - V_1) \end{aligned}$$

$$w_2v_2 + w_3v_3 = (0.3588)(1.1227) + (0.6412)(1.1056) = 1.1117$$

$$\begin{aligned} \text{term 1} &= \text{Ln} \left\{ (83.144)(273.16)(1.1117) / (13.472)(89.9)(2325/750) \right\} \\ &= 1.9058 \end{aligned}$$

$$\begin{aligned} \text{term 2} &= \left\{ 1.0 - (89.9)/(3290)(1.1227) \right\} (0.3588) \\ &= 0.3501 \end{aligned}$$

$$\begin{aligned} \text{term 3} &= \left\{ 1.0 - (89.9)/(10400)(1.1056) \right\} (0.6412) \\ &= 0.6362 \end{aligned}$$

$$\begin{aligned} \text{term 4} &= (2325/750)/(83.144)(373.16) \{-675 - 89.9\} \\ &= -0.0764 \end{aligned}$$

$$\begin{aligned} \bar{\chi}_{1,23} &= 1.9055 - 0.6326 - 0.3536 - (-0.0764) \\ &= 0.9960 \end{aligned}$$

This calculation was repeated for chloroform on the pure EVA and C₁₄FVA columns to evaluate $\bar{\chi}_{12}$ and $\bar{\chi}_{13}$ respectively,

$$\bar{\chi}_{12} = 1.057$$

$$\bar{\chi}_{13} = 1.069$$

These three values can now be used to calculate the polymer-polymer interaction parameter in equation 4.6, *i.e.*

$$\bar{\chi}'_{23} = \frac{1}{\phi_2\phi_3} \left\{ \phi_2\bar{\chi}_{12} + \phi_3\bar{\chi}_{13} - \bar{\chi}_{1,23} \right\} \quad (4.6)$$

$$\text{term1} = (0.3588)(1.057) = 0.3793$$

$$\text{term2} = (0.6412)(1.069) = 0.6854$$

$$\begin{aligned} \bar{\chi}'_{23} &= (0.3793 + 0.6852 - 0.9957)/(0.3588)/(0.6412) \\ &= 0.2999 \end{aligned}$$

Alternatively, the net retention volumes of the three experiments can be used directly in equation 4.7 which yields,

$$\bar{\chi}'_{23} = 0.2972$$

The discrepancy between the values of $\bar{\chi}'_{23}$ as calculated from equations 4.6 and 4.7 can be attributed to the different method of calculation.

4.5.2 Tabulated Results

Table 4.1

Polymer-solvent interaction parameters at 353K

Solvent	$\bar{\chi}_{13}$	$\bar{\chi}_{12}$	$ \Delta\bar{\chi} $
Pentane	1.7156	1.8708	0.1552
Hexane	1.5361	1.7963	0.2602
Heptane	1.2541	1.5804	0.3263
Octane	1.3074	1.6320	0.3246
Methanol	3.4880	3.4908	0.0028
Isopropyl alcohol	2.5467	2.5287	0.0180
Acetone	2.2106	2.3111	0.1005
Methylethylketone	1.8528	1.9495	0.0967
Methyl Acetate	2.0115	2.1549	0.1434
Ethyl Acetate	2.5140	2.5817	0.0677
Dichloromethane	1.2237	1.2796	0.0559
Chloroform	0.7962	0.8461	0.0499
Carbon Tetrachloride	1.1198	1.3096	0.1898
Benzene	1.1927	1.2983	0.1056
Toluene	1.1038	1.2283	0.1245
Cyclohexane	1.2690	1.5692	0.3002

Mean 0.1428

Standard Deviation 0.1062

Table 4.2

Polymer-solvent interaction parameters at 373K

Solvent	$\bar{\chi}_{13}$	$\bar{\chi}_{12}$	$ \Delta\bar{\chi} $
Pentane	2.0067	2.5196	0.5129
Hexane	1.6421	2.0567	0.4146
Heptane	1.4121	1.7131	0.3010
Octane	1.3889	1.7487	0.3598
Methanol	4.1420	4.0805	0.0615
Isopropyl alcohol	2.7015	2.6436	0.0579
Acetone	2.5519	2.6258	0.0738
Methylethylketone	2.0512	2.1226	0.0714
Methyl Acetate	2.3642	2.3653	0.0011
Ethyl Acetate	2.5087	2.5661	0.0574
Dichloromethane	1.5225	1.5515	0.0290
Chloroform	1.0687	1.0568	0.0119
Carbon Tetrachloride	1.3165	1.4471	0.1306
Benzene	1.3145	1.4695	0.1550
Toluene	1.2189	1.3595	0.1406
Cyclohexane	1.4484	1.6663	0.2179

Mean 0.1459

Standard Deviation 0.1667

Table 4.3

Polymer-solvent interaction parameters at 393K

Solvent	$\bar{\chi}_{13}$	$\bar{\chi}_{12}$	$ \Delta\bar{\chi} $
Pentane	2.3689	3.4446	1.0757
Hexane	1.8190	2.2782	0.4592
Heptane	1.5399	1.8471	0.3072
Octane	1.4889	1.7709	0.2820
Methanol	7.3473	6.8630	0.4843
Isopropyl alcohol	2.8418	2.7749	0.0669
Acetone	2.9218	2.9627	0.0409
Methylethylketone	2.1646	2.2186	0.0540
Methyl Acetate	2.6963	2.7535	0.0572
Ethyl Acetate	2.4985	2.5754	0.0769
Dichloromethane	1.7300	1.8012	0.0712
Chloroform	1.2208	1.2290	0.0082
Carbon Tetrachloride	1.4032	1.5754	0.1722
Benzene	1.3978	1.5584	0.1606
Toluene	1.2556	1.4092	0.1536
Cyclohexane	1.5094	1.7774	0.2680

Mean 0.2169

Standard Deviation 0.2595

Table 4.4

 $\bar{\chi}'_{23}$ versus wt. fraction EVA in the mixture at 353K

Solvent	Wt. Fraction EVA in the mixture						
	0.0904	0.2516	0.2906	0.3589	0.5001	0.7497	0.8033
C_5H_{12}	-2.0049	-2.7918	0.6587	1.1671	0.5123	0.2420	-0.4680
C_6H_{14}	-2.1632	-2.1051	0.6679	0.7427	0.4916	0.3706	0.2779
C_7H_{16}	-2.4872	-1.9846	-0.6169	0.9536	0.4164	0.4036	0.1477
C_8H_{18}	-2.6731	-1.9864	0.4816	0.8276	0.3776	0.2589	-0.1385
CH_3OH	-2.6796	-0.5957	0.7056	0.8309	0.1648	0.1865	-0.2099
C_3H_7OH	-2.1632	-2.1051	0.6679	0.7427	0.4916	0.3706	0.2779
C_3H_6O	-0.2194	-0.9679	0.6394	0.8585	0.4757	0.1955	-2.0500
C_4H_8O	-0.1580	-0.7952	0.6595	0.8680	0.5559	0.2981	-0.2636
$C_3H_6O_2$	-2.7010	-0.8607	0.6985	0.9485	0.6034	0.4453	-1.6321
$C_4H_8O_2$	0.3554	-0.5495	0.9276	1.0843	0.7322	0.5379	-1.2722
CH_2Cl_2	-0.2539	-0.8377	0.6189	0.6584	0.4964	0.1302	-0.5462
$CHCl_3$	-0.5703	-1.0256	0.5825	0.6548	0.5449	0.3918	-0.0256
CCl_4	-0.4438	-0.7359	0.6624	0.7812	0.6493	0.4718	-0.1998
C_6H_6	0.7243	-0.5799	0.7488	0.8128	0.6957	0.3919	-0.0586
C_7H_8	0.6616	-0.6151	0.7544	0.8315	0.7001	0.3989	-0.2943
C_6H_{12}	-0.2563	-0.7426	0.6579	0.8464	0.7062	0.6699	-0.0991
Mean	-0.9973	-1.1071	0.6001	0.8600	0.5351	0.3508	-0.4527
S.Dev	1.2621	0.6763	0.3273	0.1300	0.1441	0.1385	0.6261

Table 4.5

 $\bar{\chi}_{23}'$ versus wt. fraction EVA in the mixture at 373K

Solvent	Wt. Fraction EVA in the mixture					
	0.0904	0.2516	0.2906	0.3589	0.5001	0.7497
C_5H_{12}	-1.8814	0.2442	0.4548	0.3652	1.1918	1.3503
C_6H_{14}	-0.7363	0.4394	0.4830	0.2444	0.7136	1.1801
C_7H_{16}	-0.2244	0.5646	0.4135	0.1865	0.5927	1.0155
C_8H_{18}	-0.4871	0.4342	0.3488	0.2003	0.4349	1.1075
CH_3OH	-0.6407	0.4583	0.1838	0.2031	1.6022	1.3510
C_3H_7OH	0.2999	0.8047	0.4040	0.6599	0.8903	1.0822
C_3H_6O	-0.6545	0.4932	0.3183	0.2154	0.9729	1.0239
C_4H_8O	0.2023	0.7129	0.5089	0.4078	0.8751	1.1312
$C_3H_6O_2$	-0.3208	0.4689	0.2451	0.1512	0.9275	1.8315
$C_4H_8O_2$	-0.0237	0.5295	0.3844	0.2827	0.8469	1.0268
CH_2Cl_2	-0.7293	0.4932	0.3592	0.2747	0.7492	0.9319
$CHCl_3$	0.5848	0.6210	0.4691	0.2972	0.6845	1.0131
CCl_4	0.5772	0.5705	0.4983	0.3064	0.5588	0.9755
C_6H_6	0.1107	0.4725	0.4640	0.2928	0.7006	1.1337
C_7H_8	0.6655	0.5414	0.5283	0.3098	0.5962	0.2825
C_8H_{12}	0.6358	0.5817	0.5005	0.4086	0.7380	1.1540
Mean	-0.1639	0.5269	0.4103	0.3004	0.8172	1.0369
S.Dev	0.6652	0.1216	0.0960	0.1180	0.2701	0.2350

Table 4.6

 $\bar{\chi}'_{23}$ versus wt. fraction EVA in the mixture at 393K

Solvent	Wt. Fraction EVA in the mixture					
	0.0904	0.2516	0.2906	0.3589	0.5001	0.7497
C_5H_{12}	-2.4971	0.3264	0.8498	1.3513	2.3402	3.1209
C_6H_{14}	-0.9706	0.2245	0.6738	0.6964	0.8005	1.3243
C_7H_{16}	-0.0048	0.3665	0.6483	0.6189	0.5519	1.0069
C_8H_{18}	0.2779	0.3403	0.7247	0.6631	0.4963	0.9863
CH_3OH				5.5397	10.4675	0.6785
C_3H_7OH	0.0850	0.0353	0.3314	0.5691	1.3033	0.8045
C_3H_6O	0.1484	-0.1253	0.3513	0.7613	1.5513	0.7709
C_4H_8O	0.7448	0.2654	0.5593	0.6012	0.9381	0.9056
$C_3H_6O_2$	0.2899	-0.0552	0.4883	0.7873	1.2463	0.6947
$C_4H_8O_2$	0.6007	0.2335	0.5942	0.6766	0.9182	0.9429
CH_2Cl_2	0.5154	0.3904	0.4554	0.4908	0.8441	0.8907
$CHCl_3$	0.8401	0.7394	0.6513	0.6388	0.6717	1.0842
CCl_4	0.8032	0.4883	0.6732	0.7016	0.5138	1.1447
C_6H_6	0.7156	0.5709	0.6141	0.6943	0.5316	1.1581
C_7H_8	0.8326	0.5416	0.6577	0.6211	0.4757	1.0449
C_6H_{12}	0.8443	0.5143	0.7053	0.7943	0.4726	1.2639
Mean	0.4088	0.3236	0.5805	0.6653	0.8082	1.0014
S.Dev	0.4814	0.2392	0.1223	0.0813	0.3366	0.1770

4.6 Discussion

The preparative technique and experimental apparatus employed in this study produced highly consistent net retention volumes. These volumes were found to be independent of the carrier gas flowrate and thus these flowrates did not require extrapolation to zero, as required by some authors⁽¹⁹⁾. The net retention volumes were also found to be independent of the volume of solvent injected in the range 0.2 - 0.8 μL . Small volumes of solvent were used to ensure essentially symmetrical elution peaks and to satisfy the infinite dilution condition of equation 4.5. The elution peaks were generally symmetrical around the maxima, with the exception of methanol at 393K, confirming the infinite dilution condition⁽²⁰⁾ and the attainment of equilibrium between the vapour and stationary phase. However, a truly Gaussian distribution was seldom seen as the tails of the elution peak were generally asymmetric.

An investigation of this effect was not attempted. The reproducibility of the V_{gc} values was also examined by preparing two columns from a single batch of stationary phase, and, under a variety of experimental conditions, were found to yield values within a 1% error. From these experiments it was concluded that the measured results were extremely reliable. This conclusion is particularly relevant when the obvious solvent dependence of the $\bar{\chi}_{23}$ values is considered. Most data obtained from IGC experiments show some solvent dependence^(4,21-27) and considerable effort has been made to understand and correlate what is, without doubt, the greatest disadvantage of this technique. The origin of these effects has been the focus of some attention, with some workers arguing that the variation in values between solvents lies within their experimental error and are thus artifacts, while others maintain that the effects are real and can be related to either some physical attribute of the probe or to a limitation of the theoretical treatment.

Munk *et al*⁽⁸⁾ reported that a correlation could be made between the B_{23} values obtained from a blend of poly(ϵ -caprolactone) and poly(epichlorohydrin) and the Hildebrand solubility parameters of the probe species. In view of this apparent relationship they argued that the true B_{23} value of the blend would only be obtained if its solubility parameter, as estimated by Guillet's method^(2,28), was equal to that of the solvent. This study re-analysed Munk's data both by rescaling the results, and recalculating the solubility parameter using Price's method⁽²⁹⁾. Both procedures were found to distort the proposed correlation. The data obtained here were also treated in this manner but no correlation was observed. This study also attempted to correlate the variation in both the $\bar{\chi}_{23}$ and B_{23} values with other physical characteristics of the solvent probes,

- e.g.*
- (a) molar volume,
 - (b) second virial coefficient of the vapour phase,
 - (c) boiling point,
 - (d) saturated vapour pressure, and
 - (e) molecular weight.

None of the physical attributes mentioned above was found to influence the interaction parameters in any systematic manner. The $\Delta\bar{\chi}$ effect⁽³⁰⁻³²⁾ has also been reported to have a significant effect on the thermodynamics of ternary mixtures. $\Delta\bar{\chi}$ is calculated from,

$$\Delta\bar{\chi} = \left| \bar{\chi}_{12} - \bar{\chi}_{13} \right| \quad (4.21)$$

This parameter arises from the idea that the compatibility of polymers in solution is dependent both on the polymer-polymer interaction and the difference between the interactions of the homopolymers and the solvent. The similarity between the $\bar{\chi}_{12}$ and $\bar{\chi}_{13}$ values obtained from the EVA and C₁₄FVA experiments shows that the $\Delta\bar{\chi}$ effect is not significant in this case.

It has also been suggested that hydrogen bonding, or some other preferential specific interactions, between the probe and, either one or both, of the polymers may cause short-range ordering or non-random mixing in the ternary solution^(33,34) giving rise to these effects. Galin and Rapprecht⁽³⁵⁾ suggested that the solvent dependence of $\bar{\chi}'_{23}$ may be a consequence of non-molecular mixing, which supports Olabisi's concept that polymeric blends are at best micro-heterogeneous⁽²²⁾.

Another widely reported source of the solvent dependence of $\bar{\chi}'_{23}$ was the limited ability of Flory-Huggins theory to account for all the polymer-probe interactions in a ternary system^(11,36). Prolongo *et al*⁽³⁷⁾ argue that a true interaction parameter can never be obtained from this theory because the residual chemical potential of the probe in the ternary system is approximated to the sum of binary contributions. Instead they have applied an equation of state treatment, which does not rely on this approximation, and concluded that the solvent dependence arises from the assumption that the Gibbs mixing function for the polymer-polymer-solvent system is additive with respect to the binary contributions and thus true interaction parameters are only obtained from experiments where $\Delta\bar{\chi}$ is either zero or constant.

Another potentially fruitful approach may utilise moment analyses to interpret the elution peak obtained from IGC. The shape and position of this peak is known to depend on the column characteristics and the dynamic processes which occur, *e.g.* the diffusion of the probe into the stationary phase, the partitioning of the probe between the phases, the void volume of the column and the adsorption of the probe on the surface of the polymer and the support. This technique has always had theoretical appeal as it potentially would provide a wealth of information but in practice it has found relatively little favour owing to the large experimental errors generated in the measurement of the moments^(38,39). Some improvements to the technique have been published recently and more information is promised^(40,41).

It is now apparent that these solvent effects cannot be removed easily and that a full study of the processes involved in IGC, from both a chromatographic and a theoretical perspective, would be beneficial. Within this context, the results obtained in this study are discussed below.

The polymer-solvent interaction values are considered first, then the polymer-polymer results, which have been considered at each temperature separately and the overall implications and temperature dependences are discussed at the end.

4.6.1 Polymer-Solvent Interaction Parameters

The arithmetic means of $\bar{\chi}_{12}$ and $\bar{\chi}_{13}$ for all of the solvents at 353K, 373K and 393K are given in Table 4.7. Although these mean values have no physical significance they have been calculated and included to show the general trends in polymer-solvent behaviour.

Table 4.7

Mean value of polymer-solvent interaction parameter

Temperature / K	$\bar{\chi}_{13}$	s dev	$\bar{\chi}_{12}$	s dev	$ \Delta\bar{\chi} $
353	1.6964	0.6854	1.8392	0.6384	0.1428
373	1.9162	0.7689	2.0620	0.7141	0.1459
393	1.8920	0.5889	2.0380	0.5355	0.2169

All of the mean values are small and positive, and show a small positive increase as the temperature is increased. Although these results reflect the

bulk properties of the polymers at infinitely dilute solvent, their magnitude gives some indication of the solubility of the copolymers in the bulk solvent, *e.g.* at 353K octane ($\bar{\chi}_{13} = 1.2898$) is a known solvent for FVA whereas MEK ($\bar{\chi}_{13} = 1.8098$) is a known non-solvent. The polymer-solvent interaction parameters for FVA are generally smaller, suggesting that it is the more soluble in this range of solvents, particularly in the hydrocarbons. This may result from an interaction between the hydrocarbons and the pendant alkyl groups of FVA. These data show that both polymers behave similarly to a wide variety of other molecules and are consequently chemically similar, and thus liable to be miscible. Additionally, the $\Delta\bar{\chi}$ effect is small and unlikely to dominate the thermodynamics of blends of these materials.

4.6.2 Polymer-Polymer Interaction Parameters

From the data in Table 4.8 it is apparent that the polymer-polymer interaction parameter varies significantly with blend composition and temperature. Results are not quoted for the 0.8033 (wt/wt) EVA column at either 373 or 393K because it was damaged prior to completion of the experimental programme.

Table 4.8

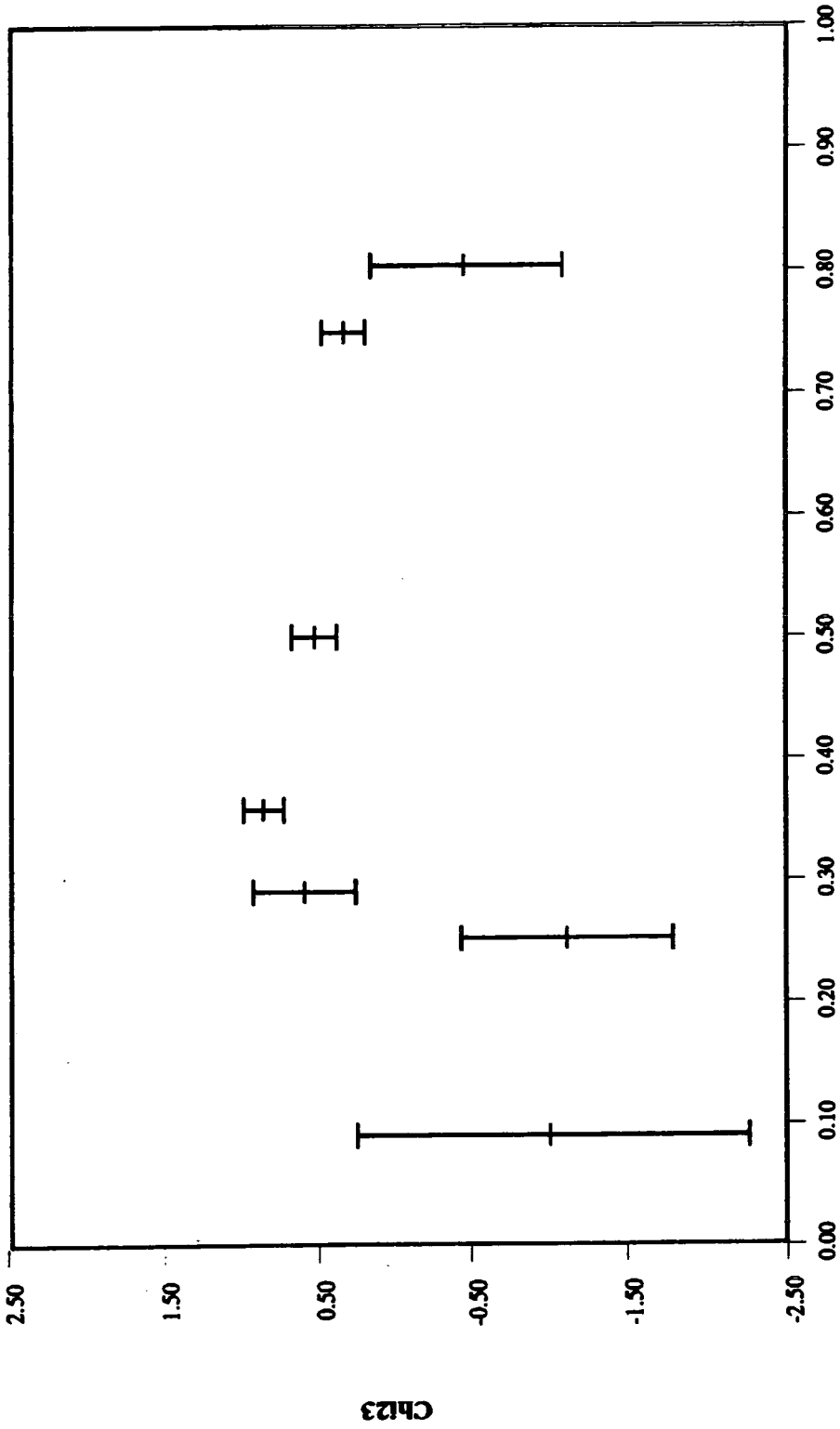
Mean values of $\bar{\chi}'_{23}$ vs composition at 353, 373 and 393K

Temperature / K	Wt. Fr. EVA in the mixture						
	0.0904	0.2516	0.2906	0.3589	0.5001	0.7497	0.8033
353	-0.9973	-1.1071	0.6001	0.8600	0.5351	0.3506	-0.4527
373	-0.1639	0.5269	0.4103	0.3004	0.8172	1.0369	-
393	0.4088	0.3236	0.5805	0.6653	0.8082	1.0014	-

4.6.2.1 353K : The means and standard deviations of these results are shown in Figure 4.3. At EVA weight fractions below 0.2906 the $\bar{\chi}'_{23}$ values are generally negative, suggesting that FVA rich blends interact favourably in these compositions, at this temperature, and consequently may be miscible. However, as the proportion of EVA is increased the interaction parameter becomes increasingly positive, reaching a maximum at about a weight fraction of 0.35 EVA.

The polymer-polymer interaction parameter

as a function of wt fraction EVA : 353K



Weight Fraction EVA

Figure 4.3

If the blend composition is re-expressed in mole fractions, the change from negative to positive occurs between 0.44 and 0.50 mol fraction EVA, reflecting that the maximum unfavourable interaction occurs when the concentration of each copolymer's repeat unit is approximately equal. The value of $\bar{\chi}'_{23}$ then decreases with increasing EVA concentration and ultimately, between 0.75 and 0.80 (wt/wt) EVA, becomes negative again. These results show that at 353K, mixtures of EVA and FVA are miscible at the extremes of composition. However, the standard deviation amongst the $\bar{\chi}'_{23}$ values is also largest at these compositions and this arises partially from the intrinsic error in measuring a small effect, but predominantly from the strong solvent dependence of the measured retention volume, *e.g.* isopropyl alcohol on the 0.0904 (wt/wt) EVA column. (This particular datum was not included in the calculation of either the arithmetic mean or the standard deviation since it bears no relation to any other value and was assumed to be erroneous). The hydrocarbons, methanol and methyl acetate all yield $\bar{\chi}'_{23}$ values which are particularly negative. This may indicate that the hydrocarbons are interacting with the pendant C₁₄ chains, while the methanol and methyl acetate are interacting with the vinyl acetate groups of the FVA. From the macrostructure of FVA, given in Figure 3.10, the hydrocarbon-alkyl interaction seems plausible. However the vinyl acetate groups are highly protected and the opportunity for hydrogen bonding with the solvent is severely hindered unless the FVA assumes a non-bulk orientation when it is deposited on the column. At low EVA concentrations the value of $\bar{\chi}'_{1(23)}$ would be expected to approximate to that for $\bar{\chi}_{12}$, *e.g.* for 0.0904 (wt/wt) EVA; these values are compared in Table 4.9.

Table 4.9

Comparison of polymer-solvent and (polymer-polymer)-solvent interaction parameters at 353K for low EVA concentrations

Solvent	$\bar{\chi}_{13}$	$\bar{\chi}_{12}$	$\bar{\chi}_{1(23)}$
Pentane	1.7156	1.8708	1.5023
Hexane	1.5361	1.7963	1.4587
Heptane	1.2541	1.5804	1.1519
Octane	1.3074	1.6320	1.2337
Methanol	3.4880	3.4908	3.2971
Isopropyl alcohol	2.5467	2.5287	2.3339
Acetone	2.2106	2.3111	2.0487
Methylethylketone	1.8528	1.9495	1.6874
Methyl Acetate	2.0115	2.1549	1.8444
Ethyl Acetate	2.5140	2.5817	2.2821
Dichloromethane	1.2237	1.2796	1.0919
Chloroform	0.7962	0.8461	0.6631
Carbon Tetrachloride	1.1198	1.3096	1.0081
Benzene	1.1927	1.2983	1.0432
Toluene	1.1038	1.2283	0.9568
Cyclohexane	1.2690	1.5692	1.1822

From the data shown above it is obvious that the value of $\bar{\chi}_{1(23)}$ does not approximate $\bar{\chi}_{13}$ at low EVA concentrations and thus it can be concluded that at a concentration of approximately 10% (wt/wt) EVA still has a significant effect. However, the values of $\bar{\chi}_{1(23)}$ do not appear to resemble either of the corresponding polymer-solvent results hence the small concentration of EVA must be assumed to be affecting either the morphology or the orientation of the major FVA phase. This conclusion is discussed more fully at the end of this chapter.

4.6.2.2 373K : The mean values and standard deviations of these results are shown in Figure 4.3

At 373K, small negative interaction parameters are still observed at very low EVA concentration, *i.e.* 0.0904 (wt/wt). However, their mean value at this composition is -0.1639 which is not sufficiently negative to guarantee miscibility. As the fraction of EVA in the mixture is increased the mean interaction value becomes more positive reaching its maximum value of 1.0369 at approximately 0.75 (wt/wt) EVA. The variation with composition is not as pronounced as that observed at 373K. These results show that blends of EVA and FVA of any composition are unlikely to be miscible at this temperature.

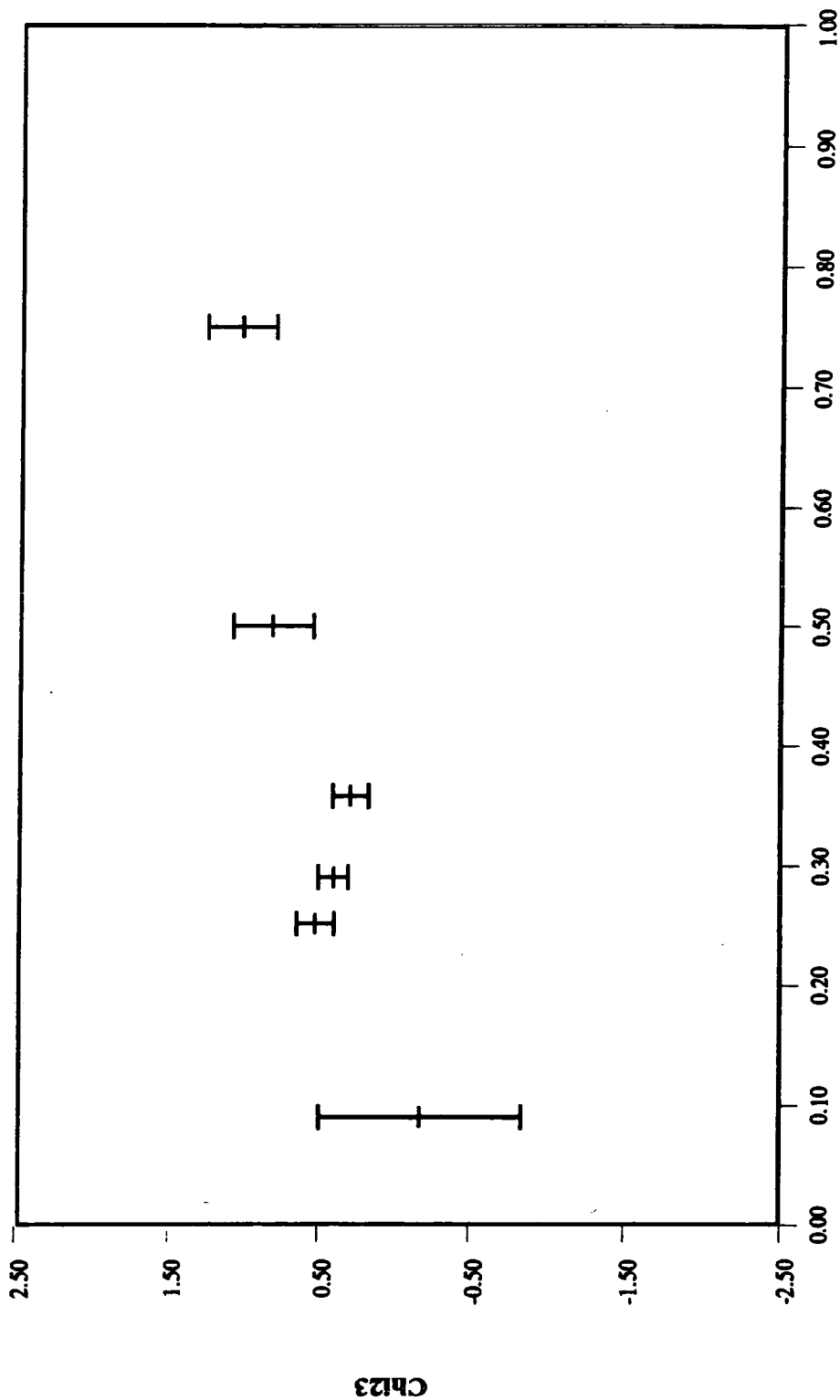
4.6.2.3 393K : The mean values and standard deviations of these results are shown in Figure 4.4

All the interaction parameters measured at 393K are positive and are generally larger than those at 353 and 373K. The values vary from 0.3260 to 0.9485 and show a general increase as the EVA fraction in the mixture increases. It should be noted that no results were obtained for methanol with mixtures containing less than 0.3589 (wt/wt) EVA because extremely asymmetric elution peaks were obtained and a reliable maximum could not be identified. The other methanol measurements give unlikely values of $\bar{\chi}'_{23}$, and as a consequence, have been removed from the calculations for the mean and standard deviation.

4.6.3 General Discussion

The polymer-solvent interaction parameters measured by IGC are generally small and positive, and decrease as temperature increases. The $\Delta\bar{\chi}$ effect is also small, *i.e.* the degree of interaction between each homopolymer and a specific solvent is approximately equal, and thus the apparent miscibility of this blend is unlikely to be controlled by the respective polymer-solvent interactions. The polymer-polymer interaction parameters were also found to be generally small and positive, showing that no strong interaction exists between the copolymers, and were observed generally to increase with temperature. Since $\bar{\chi}'_{23}$ is a measure of the change in free energy during mixing and becomes more unfavourable as the temperature is increased, it can be concluded that miscibility is more likely to occur at temperatures below 353K. However, at 353K, negative values of $\bar{\chi}'_{23}$ were obtained for FVA rich blends which suggests miscibility under these conditions.

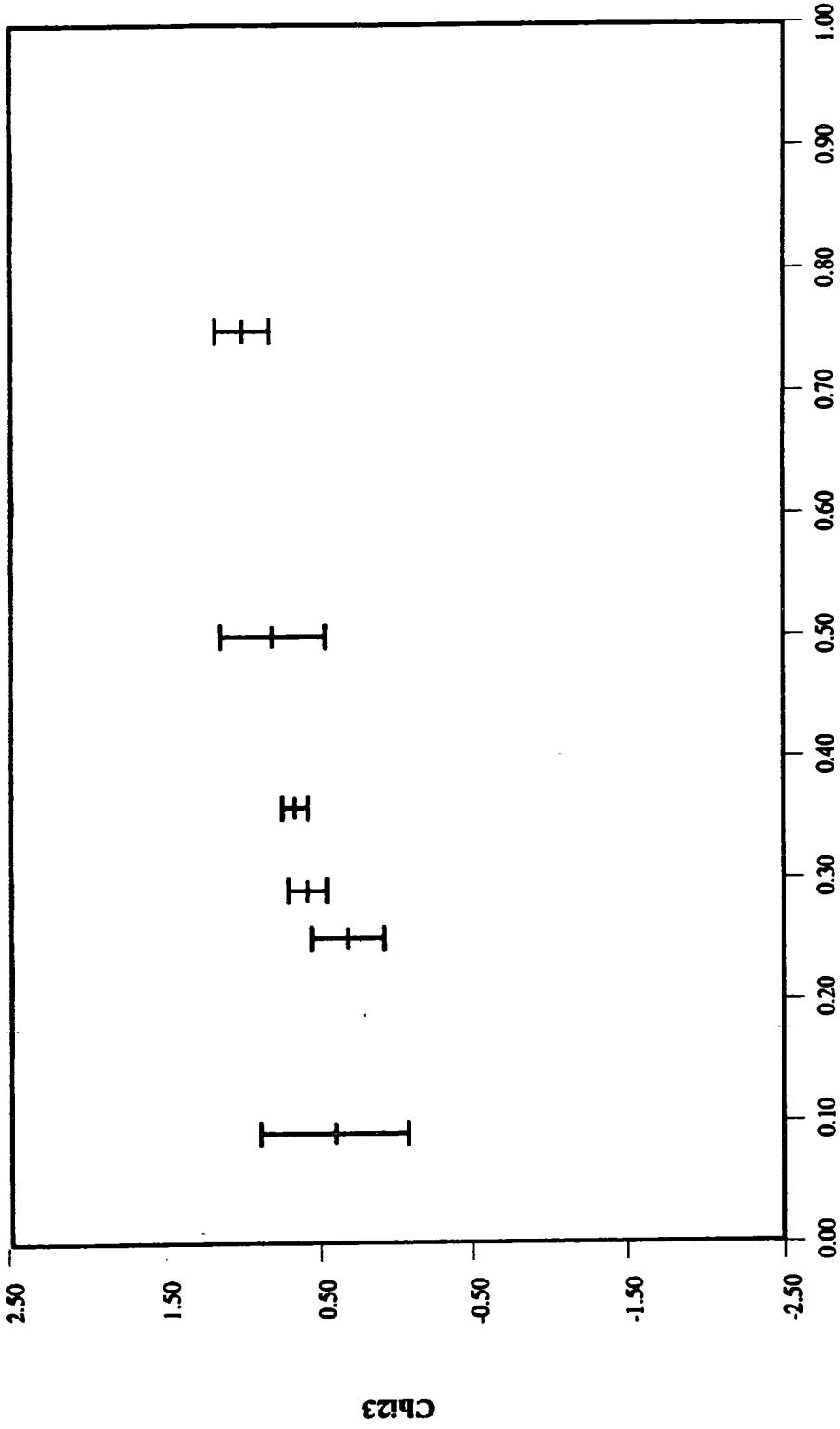
*The polymer-polymer interaction parameter
as a function of wt fraction EVA : 373K*



Weight Fraction EVA

Figure 4.4

*The polymer-polymer interaction parameter
as a function of wt fraction EVA : 393K*



*Weight Fraction EVA
Figure 4.5*

The microscopy experiments detailed in chapter 7 show that this predicted miscibility does not occur and the discrepancy has been assumed to be a consequence of the incompatibility of the mixture, and the respective domain sizes at these particular compositions and temperature. Equations 4.5a to 4.5c are rigorously applicable only to homogeneous systems and thus it can be argued that the results quoted earlier are of no relevance if the EVA/FVA mixture is immiscible. However, incompatible systems have been studied before using IGC^(21, 35,42-46), and extremely unrealistic values of $\bar{\chi}'_{23}$ were usually obtained when the experiment was unsuitable.

From these reports the question of IGC's applicability to any specific problem appears to be self-evident since Zhikaun and Walsh⁽⁴⁷⁾ stated, in a study of chlorinated poly(ethylene) / poly(butyl-acrylate), that the specific net retention volumes of immiscible blends, $V_{gc(23)}$, are merely the sum of the composition weighted values of the pure components, *i.e.*,

$$V_{gc(23)} = w_2 V_{gc,2} + w_3 V_{gc,3} \quad (4.21)$$

If these reports are correct then provisional experiments on any proposed, but unsuitable system, would yield results which would either satisfy equation 4.21 or be obviously incorrect. If the net retention volumes of the data used for the sample calculation in this work are considered, (*i.e.* chloroform at 373K on the 0.3589 (wt/wt) EVA column),

$$V_{gc(23) \text{ measured}} = 13.472 \text{ cm}^3 \text{ g}^{-1}$$

$$\text{and } V_{gc,2} = 12.380 \text{ cm}^3 \text{ g}^{-1} \text{ and } V_{gc,3} = 12.934 \text{ cm}^3 \text{ g}^{-1}$$

$$\text{hence, } V_{gc(23)} = (1.0 - 0.3589)(12.380) + (0.3589)(12.934)$$

$$V_{gc(23) \text{ calculated}} = 12.579 \text{ cm}^3 \text{ g}^{-1}$$

If this calculation is repeated across the composition range of the blend, for the same solvent at the same temperature, the following results are obtained,

Table 4.10

Comparison of experimental blend net retention volumes and those calculated from equation 4.21

$V_{gc(23)}$ $\text{cm}^3 \text{g}^{-1}$	Wt. Fr. EVA					
	0.0904	0.2516	0.2906	0.3589	0.5001	0.7497
measured	13.050	14.084	13.822	13.472	15.018	15.451
calculated	12.430	12.519	12.541	12.579	12.657	12.795

It is apparent from these data that although the EVA/FVA mixture is incompatible at 373K, the net specific volumes of the blend are not simply the sums of the weighted means of the pure components, as predicted by reference (47), but do reflect some attribute of the mixture. The composition dependence of the net specific retention volumes quoted above is unclear although Dipaola-Baranyi *et al* (25) reported a similarly inexplicable effect in a PS_(oligomeric)-PBMA system, particularly at PBMA rich compositions. Some understanding of the composition dependence of $\bar{\chi}'_{23}$, which has been found in some low molecular weight systems, may be obtained from the work of Galin *et al* (35). These workers confirmed the basic incompatibility of poly(styrene)/poly(dimethyl-siloxane) using IGC with low molecular weight block copolymers of varying composition, (for which small positive $\bar{\chi}'_{23}$ values were obtained), and then found that if the molecular weight of the samples was increased, a negative value of $\bar{\chi}'_{23}$ was finally obtained for this incompatible mixture. From these data Galin concluded that IGC was only suitable for either homogeneous or highly dispersed micro-phase separated block copolymers and not for incompatible blends which separate into macro domains. If the morphology of the EVA/FVA mixture is neither homogeneous nor micro-phase separated at low EVA concentrations around 353K, this hypothesis may explain the negative values of $\bar{\chi}'_{23}$ which were obtained.

4.7 REFERENCES

- (1) J.E.Guillet and O.Smidsrod, *Macromolecules*, 2, 272, (1969).
- (2) G.Dipaola-Barayni and J.E.Guillet, *Macromolecules*, 11, 228, (1977).
- (3) G.Dipaola-Barayni, *Macromolecules*, 14, 683, (1981).
- (4) D.J.Walsh, J.S.Higgins, S.Rostami and K.Weeraperuma, *Macromolecules*, 16, 391, (1983).
- (5) A.J.B.Cruickshank, M.L.Windsor and C.L.Young, *Proc. R. Soc. London, Ser. A*, 295, 259.
- (6) M.J.El-Hibri and P.Munk, *Macromolecules*, 21, 264, (1988).
- (7) T.W.Card, Z.Y.Al-Saigh and P.Munk, *Macromolecules*, 18, 1030, (1985).
- (8) M.J.El-Hibri, W.Cheng and P.Munk, *Macromolecules*, 21, 3458, (1988).
- (9) PYE Unicam instrument manual.
- (10) Supplied by Card Computers, c/o The Glasgow Computer Centre.
- (11) Z.Y.Al-Saigh and P.Munk, *Macromolecules*, 17, 803, (1984).
- (12) Supplied by Phase Separations Ltd.
- (13) Supplied by PYE Unicam Ltd.
- (14) R.C.Reid, J.M.Prausnitz and B.E.Polling, 'The Properties of Liquids and Gases', 4th Edition, McGraw-Hill, (1987).
- (15) C.F.Spencer and R.P.Danner, *J. Chem. and Eng. Data*, 17, No 2, (1972)
- (16) J.H.Dymond and E.B.Smith, 'The Virial Coefficients of Gases', Clarendon Press, Oxford, (1969).
- (17) B.B.MacDonald, private communication, to be published.
- (18) P.J Flory, 'Principles of Polymer Chemistry', Cornell University,(1954).
- (19) O.S.Tyagi, S.M.Sajjad and S.Husain, *Polymer*, 28, 2329, (1987).
- (20) J.R.Conder, *J.Chromatogr.*, 39, 273, (1969).

- (21) D.D.Deshpande, D.Patterson, H.P.Schreiber and C.S.Su, *Macromolecules*, 7, 530, (1974).
- (22) O.Olabisi, *Macromolecules*, 8, 316, (1975).
- (23) C.S.Su, D.Patterson and H.P.Schreiber, *J. Appl. Polym. Sci.*, 20, 1025, (1976).
- (24) C.S.Su and D.Patterson, *Macromolecules*, 10, 708, (1977).
- (25) G.Dipaola-Barayni and P.Degre, *Macromolecules*, 14, 1456, (1981).
- (26) D.J.Walsh and J.G.McKeown, *Polymer*, 21, 1335, (1980).
- (27) C.P.Doube and D.J.Walsh, *Eur. Poly. J.*, 17, 63, (1981).
- (28) K.Ito and J.E.Guillet, *Macromolecules*, 12, 1163, (1979).
- (29) G.J.Price, *Polym. Mater. Sci. and Eng.*, 58, 1009, (1988).
- (30) L.Zeman and D.Patterson, *Macromolecules*, 5, 513, (1972).
- (31) A.Robard, D.Patterson and G.Delmas, *Macromolecules*, 10,706, (1977).
- (32) C.C.Hsu and J.M.Prausnitz, *Macromolecules*, 7, 320, (1974).
- (33) D.D.Deshpande and O.S.Tyagi, *Macromolecules*, 11, 746, (1978).
- (34) D.D.Deshpande and O.S.Tyagi, *J. Appl. Polym. Sci.*, 33, 715, (1987).
- (35) M.Galin and M.C.Rapprecht, *Macromolecules*, 12, 506, (1979).
- (36) G.Dipaola-Barayni, *Polym.Mater. Sci. and Eng.*, 58, 735, (1988).
- (37) M.Prolongo, R.M.Masegosa and A.Horta, *Macromolecules*, 22, 4346, (1989).
- (38) C.Vidal-Madjor and G.Guiochon, *J. Chromatogr.*, 61, 142, (1977).
- (39) H.A.Boniface and D.M.Ruthven, *Chem. Eng. Sci.*, 40, 1401, (1985).
- (40) P.Hattam and P.Munk, *Macromolecules*, 21, 2083, (1988).
- (41) J.-Y. Wang and G.Charlet, *Macromolecules*, 22, 3781, (1989).
- (42) T.C.Ward, D.P.Sheehy, J.S.Riffle and J.E.McGrath, *Macromolecules*, 14, 1791, (1981)

- (43) J.Klein and H.Widdecke, *Chromatographia*, 147, 384 (1978).
- (44) J.Klein, H.Widdecke and G.Wolter,
 J. Polym. Sci., Polym. Symp., 68, 221, (1981)
- (45) K.Ito, N.Usami and Y.Yamashita, *Macromolecules*, 13, 216, (1980).
- (46) M.Galin and A.Mathias, *Macromolecules*, 14, 677, (1981).
- (47) C.Zhikaun and D.J.Walsh, *Eur Polym. J.*, 19:6, 519, (1983).

Chapter 5 Heats of Mixing

5.1 Introduction

The determination of the heat of mixing, ΔH_{mix} , of a binary system yields invaluable thermodynamic information since such data allow the general free energy of mixing term to be divided into enthalpic and entropic contributions. Unfortunately, the direct determination of this effect in polymer systems is often prohibited by the physical state and high viscosity of the materials or the restrictive operating temperatures of the calorimetric apparatus. Several attempts have been made to circumvent these problems, *e.g.* by determining the heats of mixing in the presence of a common solvent and extracting the polymer-polymer contribution using Hess's Law ⁽¹⁾, or by using low molecular weight analogues, *i.e.* unit structure models, or oligomers, and normalising the results with respect to the interacting segments of the actual polymers ^(2,3). Neither of these approaches has proven to be particularly reliable because significant errors have been reported and their origin is unclear. The heat of mixing measurements reported here are for the copolymers themselves, which was possible due to their low molecular weight and viscosity, and thus the use of the indirect methods described above was avoided.

5.2 Theoretical

5.2.1 Flory - Huggins Theory

Flory-Huggins theory relates the heat of mixing of two components to their interaction parameter with the following expression ⁽⁴⁾,

$$\Delta H_{mix} = kT \chi_{12} n_1 \phi_2 \quad (5.1a)$$

where,

χ_{12} = Flory-Huggins binary Interaction Parameter

n_1 = number of molecules of solvent

k = the Boltzmann constant, ($1.380662 \times 10^{-23} \text{ J K}^{-1}$)

T = absolute temperature, K

ϕ_2 = volume fraction of solute

This expression was originally derived for polymer solutions but it can be expressed for polymer blends as,

$$\Delta H_{mix} = kT \chi_{23} n_2 \phi_3 \quad (5.1b)$$

thus,

$$\chi_{23} = \Delta H_{mix} / kT n_2 \phi_3 \quad (5.1c)$$

Using this expression the enthalpic polymer-polymer interaction parameters were calculated for each value of ΔH_{mix} measured.

5.2.2 Flory's Equation of State

In the equation of state theory of Prigogine-Flory⁽⁵⁻⁹⁾, the residual free energy of mixing is given by,

$$G_M^R = \Delta H_M - T \Delta S_M^R - r N V^* Q_{23} \theta_3 \phi_2 \quad (5.2)$$

where,

$$\Delta H_M = r N V^* [\phi_2 P_2^* (\nu_2^{-1} - \nu^{-1}) + \phi_3 P_3^* (\nu_3^{-1} - \nu^{-1}) + \phi_2 \theta_3 X_{23} / \nu] \quad (5.3)$$

This interaction parameter, X_{23} , includes only the enthalpic contribution of the mixing process. Theoretically it represents the enthalpic interaction between the unit structures of the components being mixed. Consequently X_{23} should be constant for any polymer pair at a specific temperature and also independent of blend composition. It is commonly evaluated by fitting equation 5.3 to experimental heat of mixing data.

5.3 Materials

The EVA copolymer and C_{14} FVA copolymer were both annealed in a vacuum oven at 393K for 24 hours.

5.4 Apparatus

The heats of mixing were determined using a NBS batch-type calorimeter⁽¹⁰⁾, which measures the heat flux that occurs when two materials are mixed, using a series of thermo-electric cells. A significant period of time was spent modifying this apparatus from the description in reference⁽¹⁰⁾ because it was found that the original cell design, Figure 5.1, was inadequate in that it allowed leakage of both material and heat. It was apparent that the use of steel bolts with an aluminium press was unsuitable as continued usage

distorted and damaged the aluminium, thus causing the seal between the cell body and the PTFE end caps to fail, (points A & B). Additionally, after inversion, the mixing process occurred at A which aggravated the leakage. Another problem was the observed dependence of the baseline on the position of the sample cell, Figure 5.2. Although this effect was always present its magnitude varied thus preventing simple subtraction during data reduction. The variation in baseline was greatest when the loading channels of the inner and outer jackets were exactly aligned, *i.e.* at 0 degrees. It was concluded that the baseline drift was caused by heat loss through these channels owing to poor insulation and an excessive dead volume within the inner jacket arising from the design of the cell, region C in Figure 5.1. Consequently the cell was redesigned, Figure 5.3, to fill the inner jacket completely, and carefully machined steel and PTFE components were employed to ensure the seal. Additionally, by introducing the PTFE sample holder into the aluminium body horizontally, the mixing process now occurred in a less vulnerable section of the cell. PTFE blocks were introduced all round the cell body to improve insulation and ensure that any heat flux that occurred during mixing was directed through the walls which were in contact with the Peltier cells. Finally an aluminium block, machined to be a 'push-fit', was inserted behind the sample cell which effectively insulated the loading channel. Using this new system no material leakage was ever detected and the baseline was found to be independent of the position of the cell. Diagrams showing a cross-sectional view of the calorimeter together with a full schematic representation of the complete apparatus are given in Figures 5.4a and 5.4b respectively.

- 1: STEEL BOLTS
- 2: ALUMINIUM BRACES
- 3: PTFE END CAP
- 4: ALUMINIUM SHELL
- 5: BAFFLES
- 6: PTFE SAMPLE HOLDER

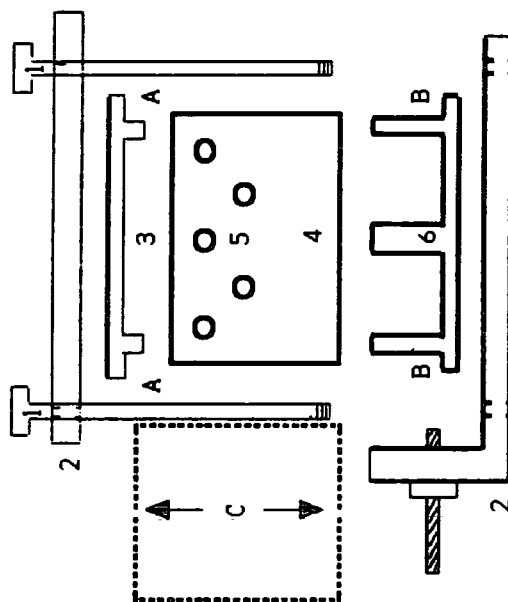


FIGURE 5.1: CHONGS ORIGINAL CELL DESIGN

5.5 Experimental Procedure

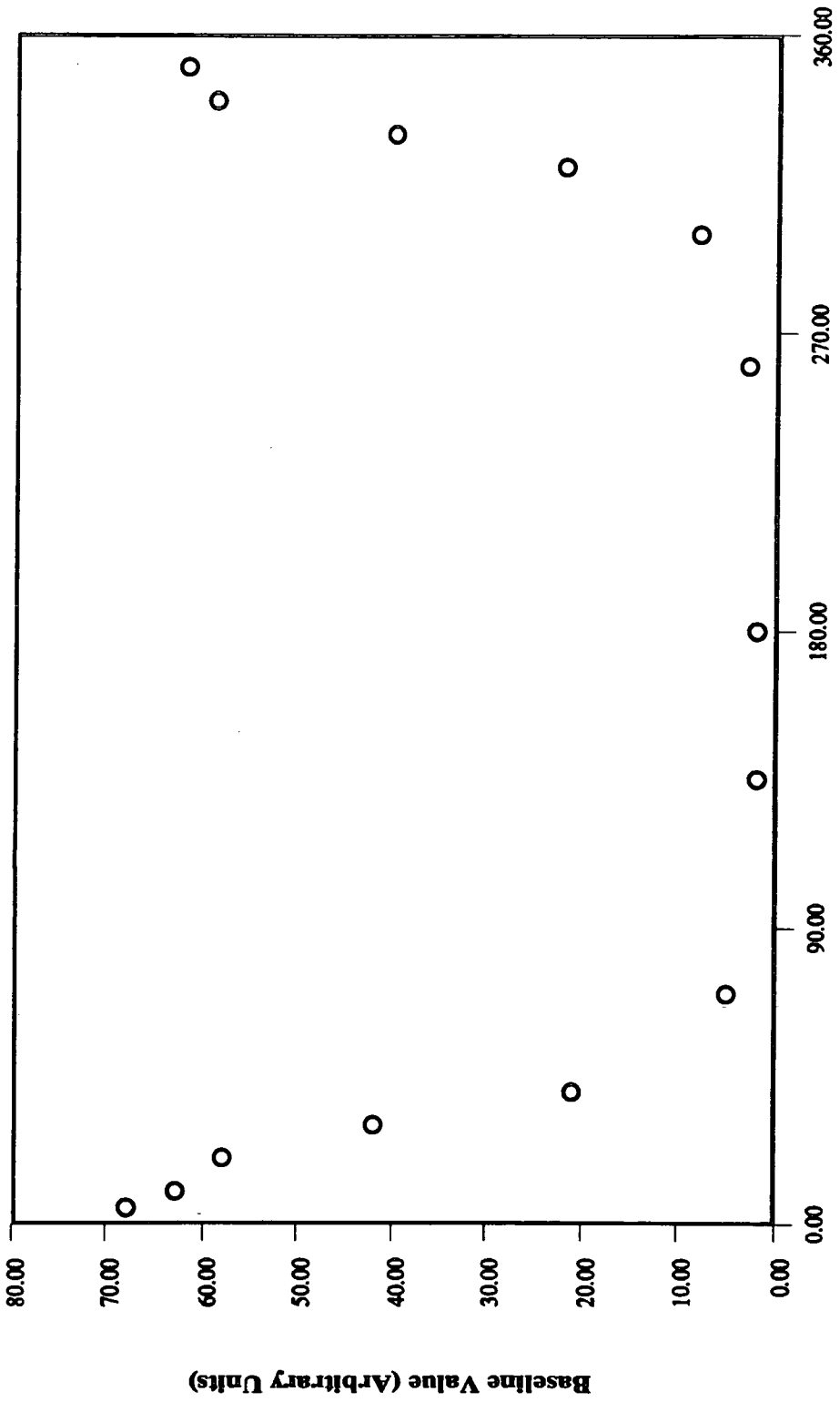
The temperature of the calorimeter was set using a potentiometer on the heating unit: the choice of setting being read from a calibration chart: the apparatus took approximately 48 hours to equilibrate at the selected temperature. Equilibrium was known to have been achieved when a constant reading was observed on the decade resistance bridge. The precise temperature of the instrument was then calculated from another calibration chart which correlated the settings of the resistance bridge with temperature.

Approximately 0.5 g of each component was then carefully weighed, to six significant figures, and charged to the individual compartments of the PTFE sample holder. This was placed inside the aluminium shell which then was sealed with the 2 machined PTFE end plates. Finally this was enclosed in the steel and PTFE bracing system and heated in an oven mounted on the front of the calorimeter, which was maintained at approximately the temperature of the instrument. After typically 1 hour the sample cell was inserted into the central block of the calorimeter followed by the aluminium block to seal the inner chamber of the apparatus. The temperature difference between these components and the calorimeter caused a heat flux which was detected by the thermo-electric cells which resulted in a deflection on the strip chart recorder. When this signal had stabilised the sample cell was considered to be in equilibrium with the calorimeter. The magnitude of the output from the thermo-electric modules was controlled by an amplifier on the integrator unit.

The detection of thermal equilibrium is essential for this type of measurement. Consequently the sensitivity of the amplifier was always increased beyond that normally required for the determination of the heat of mixing. When equilibrium had been attained, commonly 18-24 hours, and a steady baseline recorded, the amplifier was reset to the gain desired for the mixing measurement and the chart recorder and digital integrator reset to their zero values. The shaft of the central block was then rotated through 180 degrees, to mix the samples. The shaft was then attached to a motor-driven arm which moved slowly backwards and forwards through 90 degrees to agitate the mixture. Periodically the cell was inverted and this process repeated until the output returned to the baseline value.

The output from the Peltier cells was recorded on a digital integrator and converted to a heat of mixing value from the electrical calibration data.

***Dependency of Calorimeter Baseline
on Angle of Central Block Rotation***



***Degree of Rotation
Figure 5.2***

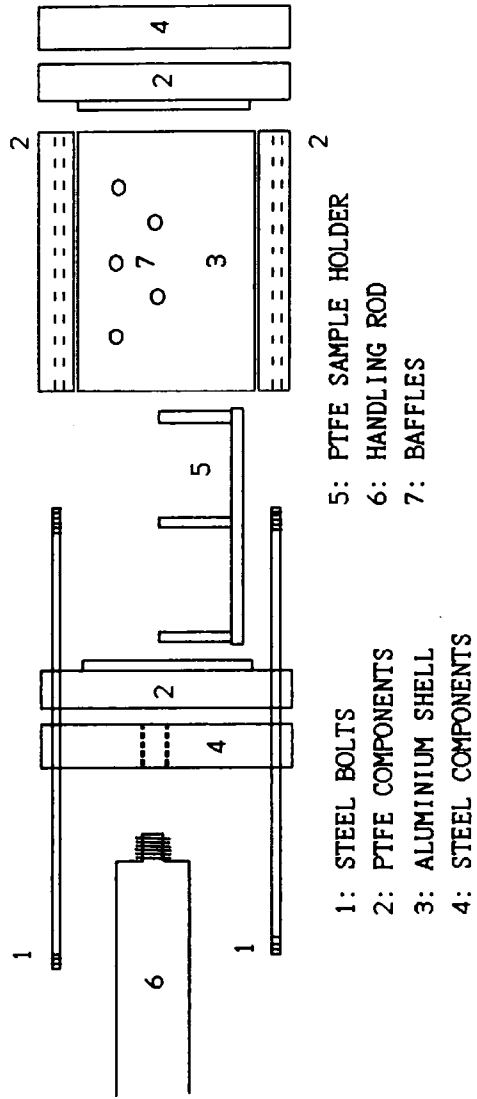


FIGURE 5.3: EXPLODED VIEW OF THE IMPROVED CELL DESIGN

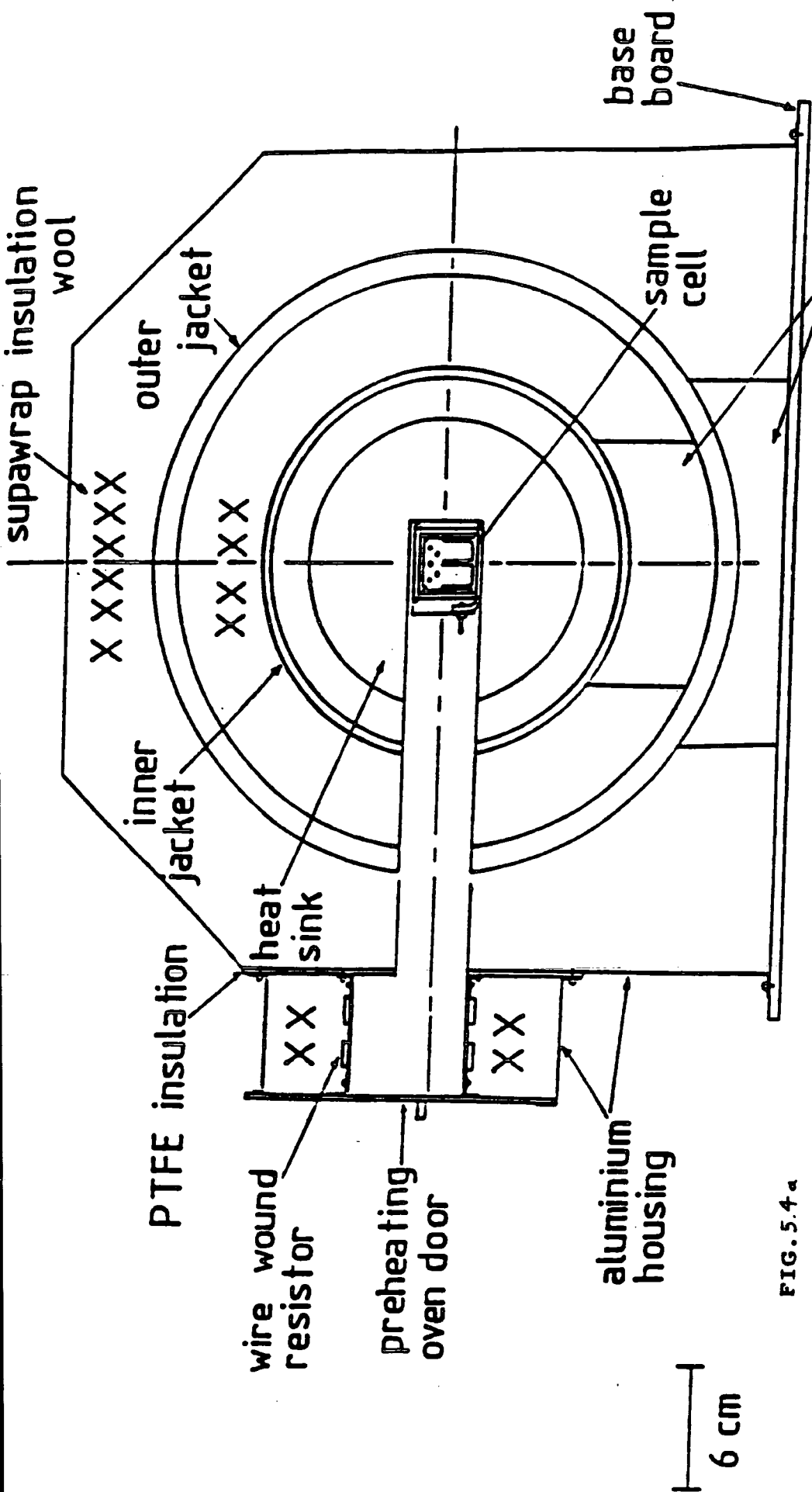


FIG. 5.4a

MICROCALORIMETER—END VIEW CROSS SECTION

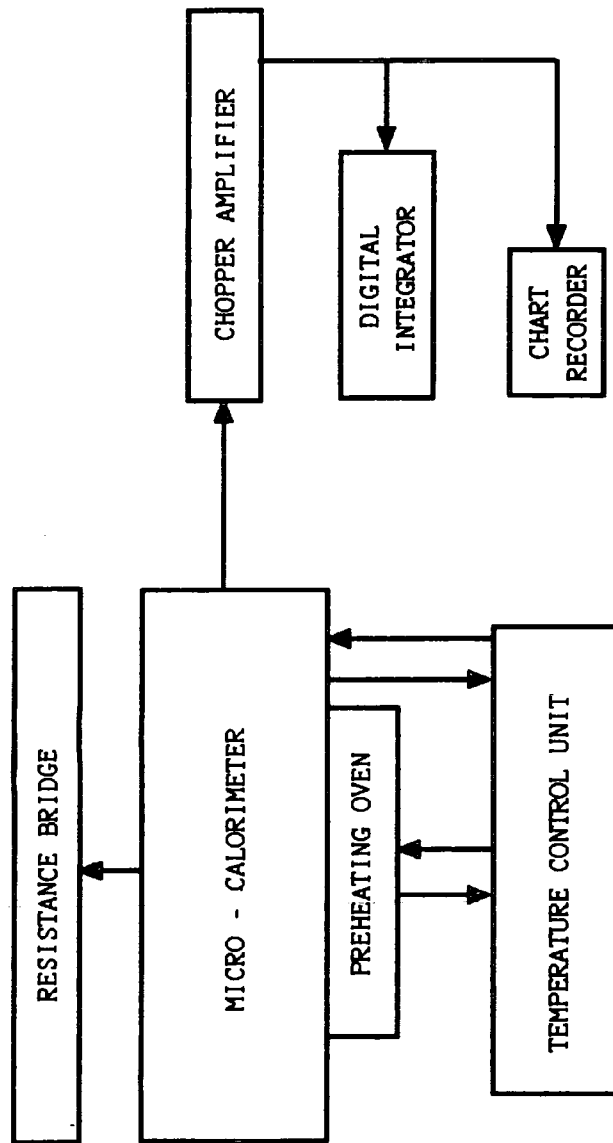


FIGURE 5.4b : SCHEMATIC DIAGRAM OF THE CALORIMETER APPARATUS

5.6 Results

Heats of mixing measurements and electrical calibrations were obtained at 348.7 and 359.3K for the EVA/C₁₄FVA blend.

Estimation of Errors

A full analysis of the accuracy and sensitivity of the calorimeter was not possible due to the limited time available on the instrument. However, since the apparatus was rebuilt to a standard higher than that quoted by Chong, it was assumed that the performance would be at least comparable. Chong and Rostami⁽¹¹⁾ both quote the thermal stability as $\pm 0.001\text{K}$ over a 3 hour period, and the accuracy as $\pm 0.002\text{J g}^{-1}$ as determined by an acid-base reaction. The reproducibility of the results was investigated by running approximately duplicate samples 48 hours apart. The results were as follows,

Sample No	Wt Fr EVA	$\Delta H_{mix} / 10^{-2}\text{J g}^{-1}$
1	0.4752	10.077
2	0.4786	10.047

These data show that the reproducibility was very high and that the error associated with each reading was less than 0.0001 J g^{-1}

Electrical Calibration

The sample cell used to calibrate the calorimeter was similar to the cell described earlier, except that it contained a $147.4\ \Omega$ ($\pm 0.02\%$) Muirhead wire-wound resistor immersed in a 50% (wt/wt) mixture of the system being studied. Since the calibration cell is not inverted, a small hole was created at the top of the PTFE seal through which the contacts of the resistor were fed. These were connected to a 0.02% Current Calibrator. It was found that the mains switch on this unit caused a detectable spike in the response of the thermo-electric cells and was consequently fitted with an additional switch across the output terminals. A variable current was applied to the resistor over a range of time periods, measured by stop watch, and the response recorded.

From this information it was possible to evaluate a calibration function as follows;

$$E = I^2 R t \quad (5.4)$$

where

$$E = \text{energy, J}$$

$$I = \text{current, A}$$

$$R = \text{resistance, } \Omega$$

$$t = \text{time, s}$$

When the analogue output of the cell, as determined by the integrator, is plotted against the calculated electrical energy supplied, a linear relationship is obtained. From this function the relative response of the calorimeter can be converted into an absolute measure of the enthalpy change within the system. Theoretically, the total heat of mixing, q , is proportional to the area A (cm^2) bounded by the peak and the baseline,

$$q = F A \quad (5.5)$$

where, $F = \text{calibration constant, J cm}^{-2}$.

A plot of q *versus* A should be linear and pass through the origin. The slope, F , is a function of the thermal conductivity and heat capacity of the material being examined and must be determined for every mixture at every temperature of interest.

Table 5.1
Electrical Calibration at 348.7K

Run	$E/J \times 10^{-2}$	Integrator Counts/10
1	3.65	4226
2	5.41	6772
3	7.22	10833
4	9.53	15047
5	12.30	19934
6	14.89	26339
7	15.76	27769

The intercept (a) and slope (b) were obtained by least-squares techniques.

$$a = -3511.5 \quad b = 1970 \quad r = 0.9986$$

Table 5.2
Electrical Calibration at 359.3K

Run	$E/J \times 10^{-2}$	Integrator Counts/10
1	3.69	4481
2	7.44	11260
3	9.43	15400
4	10.65	18201
5	12.18	21278

Again, from least-squares,

$$a = -3118.4 \quad b = 1987 \quad r = 0.9990$$

These calibration data are shown graphically in Figure 5.5

The slopes of these relationships correspond to the calibration constants of the calorimeter for this blend at these temperatures. These data show that the minimum energy detection limit of the apparatus is approximately 1.6 to 1.8×10^{-2} J for this temperature range and an amplifier gain equivalent to $300 \mu\text{V}$.

Least-squares techniques were applied to some of Chong's data and the following limits found,

- (a) polystyrene (1010) - polybutadiene (960) at $70.1 \text{ }^\circ\text{C}$ ^(10,p87),
 fsd = $100 \mu\text{V}$ minimum detection limit = 2.3×10^{-3} J
- (b) distilled water at $30.0 \text{ }^\circ\text{C}$ ^(10,p83),
 fsd = 1 mV minimum detection limit = 4.6×10^{-2} J

It is apparent that the minimum detection limit of the apparatus was not changed significantly by either the new design of sample cell or the replacement of the original thermo-electric modules. However, Chong recommends that the following equilibrium times be used for the respective amplifier settings,

Amplifier Setting	Equivalent FSD / mV	Equil. Time / h
E	1.0	0.5
G	0.1	1.5
H	0.03	> 12.0

The time required to reach equilibrium with the rebuilt calorimeter at setting G was always more than 12 hours. This order of magnitude increase was attributed to poor temperature control of the pre-heating oven, and the increased heat capacity of the sample cell and aluminium insulating block. It is unknown whether this also reflected an increase in the sensitivity of the instrument as the limited time available for experiment prohibited calibration with standard acid-base neutralisations.

Electrical Calibration Data

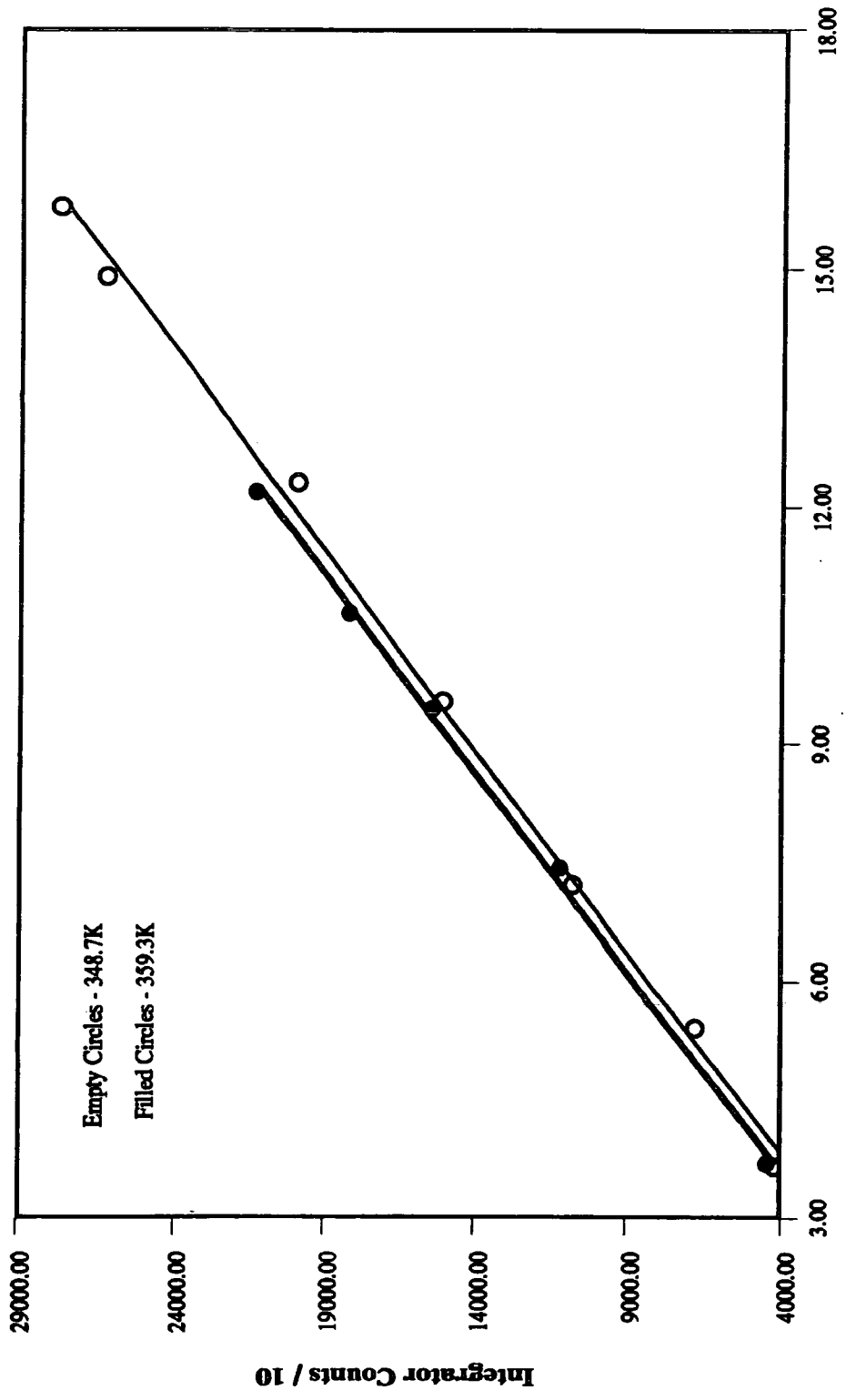


Figure 5.5

Table 5.3

Heat of Mixing data at 348.7K

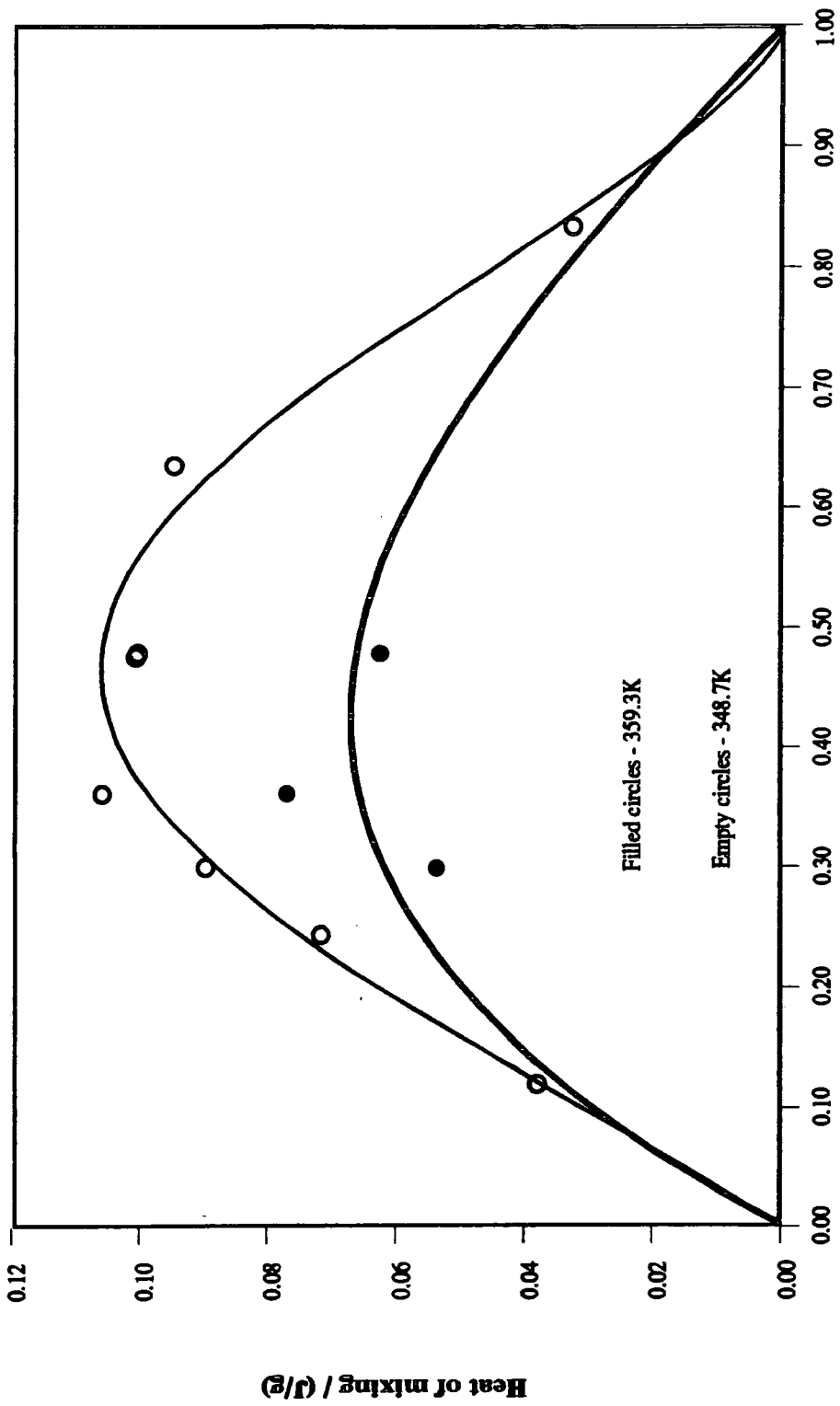
Run	Wt.Fr. EVA	Int /10	Total Mass/g	Int /10 g	$\Delta H_{mix} / 10^{-2} \text{J g}^{-1}$
1	0.1193	5973	1.4991	3984	3.804
2	0.2432	15616	1.4728	10603	7.162
3	0.2987	21360	1.5006	14234	9.005
4	0.3610	26085	1.5018	17369	10.596
5	0.4752	24534	1.5014	16341	10.077
6	0.4786	24477	1.5029	16287	10.047
7	0.6353	23263	1.5303	15202	9.496
8	0.8333	4358	1.5003	2905	3.257

Table 5.4

Heat of Mixing data at 359.3K

Run	Wt.Fr. EVA	Int /10	Total Mass/g	Int / 10 g	$\Delta H_{mix} / 10^{-2} \text{J g}^{-1}$
1	0.2991	13956	1.4977	9318	5.390
2	0.3613	18295	1.5011	12188	7.703
3	0.4786	13956	1.4977	9318	6.259

These results are shown in Figure 5.6

HEAT OF MIXING DATA FOR EVA/FVA MIXTURE**AT 348.7K AND 359.3K***Weight Fraction EVA***Figure 5.6**

Flory-Huggins Analysis

Definition: subscript 2 = C₁₄FVA, 3 = EVA

From Equation (5.1c) the polymer-polymer interaction parameters were evaluated at both 348.7K, Table 5.5, and 359.3K, Table 5.6,

Table 5.5

Run	Wt Fr EVA	$\Delta H_m / 10^{-2} \text{ J g}^{-1}$	ϕ_3	Π_2	χ_{23}
1	0.1193	3.804	0.1206	5.100	1.285
2	0.2432	7.162	0.2454	4.382	1.384
3	0.2987	9.005	0.2987	4.061	1.529
4	0.3610	10.596	0.3610	3.700	1.635
5	0.4752	10.077	0.4752	3.039	1.369
6	0.4786	10.047	0.4786	3.019	1.374
7	0.6353	9.496	0.6353	2.112	1.464
8	0.8333	3.257	0.8333	9.653	0.084

Taking the density values at 348.7K as,

$$\rho_{EVA} = 0.90836 \text{ g cm}^{-3} \quad \rho_{FVA} = 0.91947 \text{ g cm}^{-3} \text{ (Chapter 3.3)}$$

Table 5.6

Run	Wt Fr EVA	$\Delta H_m / 10^{-2} \text{ J g}^{-1}$	ϕ_3	Π_2	χ_{23}
1	0.2991	5.390	0.3020	4.059	0.866
2	0.3613	7.703	0.3644	3.698	1.152
3	0.4786	6.259	0.4820	3.019	0.867

Taking the density values at 359.3K as

$$\rho_{EVA} = 0.90000 \text{ g cm}^{-3} \quad \rho_{FVA} = 0.91235 \text{ g cm}^{-3} \quad (\text{Section 3.3})$$

These results are shown in Figure 5.7,

The free energy of mixing was calculated from the classical Flory - Huggins relation,

$$\Delta G_{mix} = RT (n_2 \text{Ln } \phi_2 + n_3 \text{Ln } \phi_3 + n_2 \phi_3 \chi_{23}) \quad (5.6)$$

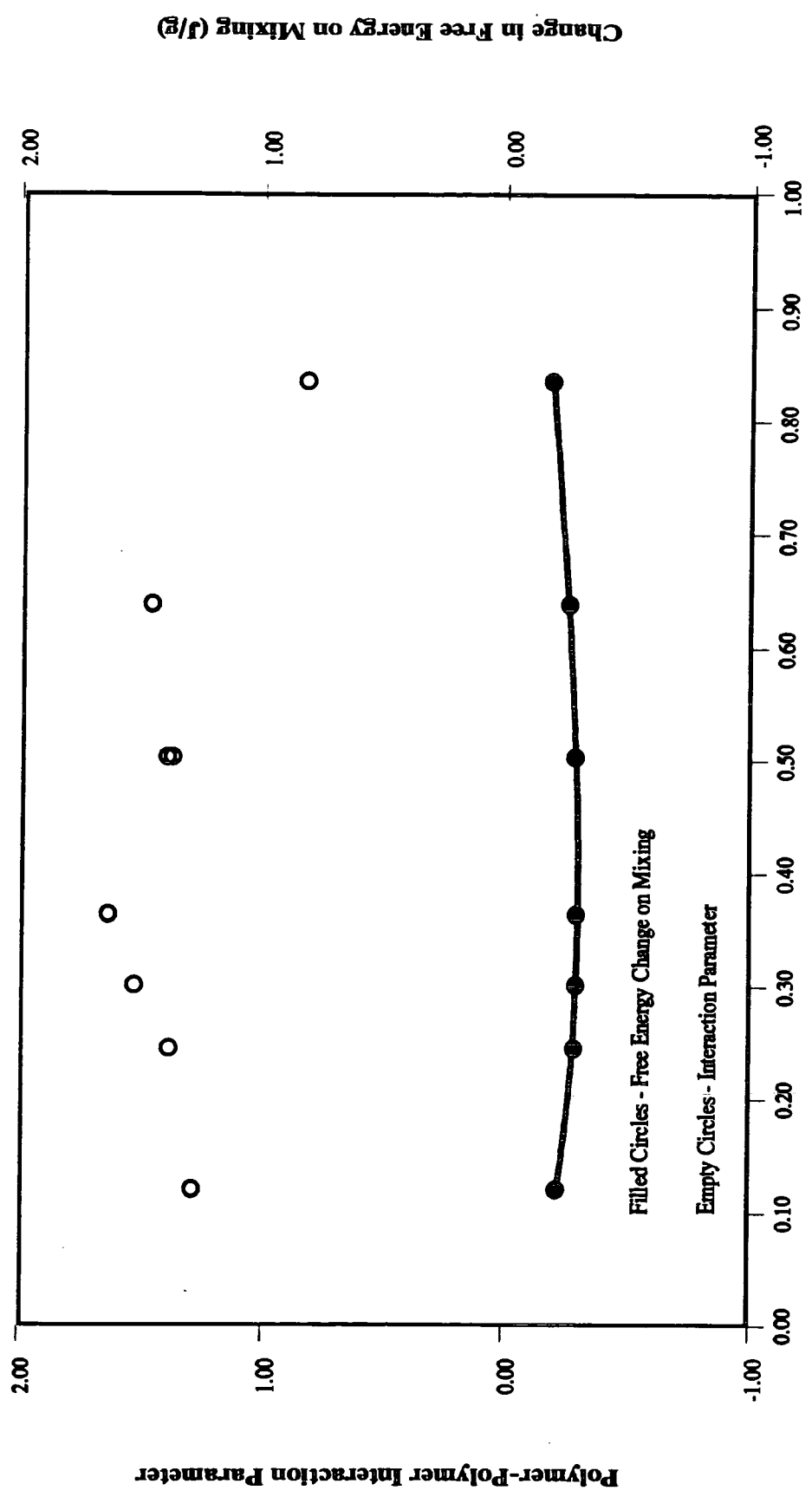
The many refinements which have been made to this expression have not been included here because it is intended to demonstrate the difference in the results obtained from a simple lattice theory and those from a simple partition theory, *i.e.* from the Flory - Huggins and the Equation of State theories respectively.

Table 5.7

Free Energy of Mixing at 348.7K

Run	$n_2 / 10^{19}$	ϕ_2	$n_3 / 10^{19}$	ϕ_3	χ_{23}	ΔG_{mix}
1	5.100	0.8794	2.184	0.1206	1.285	-0.216
2	4.382	0.7546	4.452	0.2454	1.384	-0.289
3	4.061	0.6988	5.467	0.3012	1.529	-0.296
4	3.700	0.6362	6.608	0.3638	1.635	-0.296
5	3.039	0.4970	8.698	0.5030	1.396	-0.287
6	3.019	0.4969	8.760	0.5031	1.374	-0.291
7	2.112	0.3619	11.629	0.6381	1.464	-0.260
8	0.965	0.1650	15.253	0.8350	0.840	-0.184

**ENTHALPIC POLYMER-POLYMER INTERACTION PARAMETER
AND CHANGE IN FREE ENERGY ON MIXING AT 348.7K**



Mole Fraction EVA
Figure 5.7

Table 5.8
Free Energy of Mixing at 359.3K

Run	$n_2 / 10^{19}$	ϕ_2	$n_3 / 10^{19}$	ϕ_3	χ_{23}	ΔG_{mix}
1	4.059	0.6980	5.475	0.3020	0.866	-0.345
2	3.698	0.6356	6.613	0.3644	1.152	-0.337
3	3.019	0.5180	8.760	0.4820	0.087	-0.353

These results form the lower section of Figure 5.7.

5.7 Discussion

Lattice theory assumes that configurational entropy, S_{conf} , is the only contribution to the entropy change on mixing and thus S_{conf} equals ΔS_{mix} . This term is often small for long chain molecules because the number of possible configurations that the chains can adopt on the lattice is small. Consequently, the miscibility of the majority of polymer blends, which do not show specific interactions, is controlled by the enthalpic contribution.

All the heat of mixing values obtained for EVA / C₁₄FVA were small and endothermic, ranging from approximately 3.3×10^{-2} to $10.6 \times 10^{-2} \text{ J g}^{-1}$. Although a positive ΔH_{mix} is unfavourable to the mixing process it does not preclude it, and it is the change in free energy that occurs during this process that must be considered.

The Flory - Huggins interaction parameters, which are derived on a purely enthalpic basis, are all positive and unfavourable, suggesting that the blend, if miscible at all, is likely to exhibit upper critical solution temperature behaviour. The calculated free energy of mixing values are however all negative, and consequently favourable, suggesting that this blend is miscible in all compositions in this temperature range. The discrepancy between these results can be attributed to the influence of the combinatorial entropy term. This is not unreasonable since both EVA and C₁₄FVA are of low molecular weight and the value of S_{conf} is likely to be relatively large since the chains can

adopt a greater number of lattice configurations. Interpretation of the results obtained from Flory-Huggins theory suggests that this blend is likely to have undergone UCST type behaviour somewhere below 348.7K while it remains miscible between this temperature and 359.3K, *i.e.* as shown in Figure 5.8. Additionally, it has been found that the thermodynamics of this blend are dominated by the entropic contribution.

The interaction parameters obtained from the EOS model are also small and positive but again they represent only the enthalpic component. A more extensive analysis of these results is presented in Chapter 8.

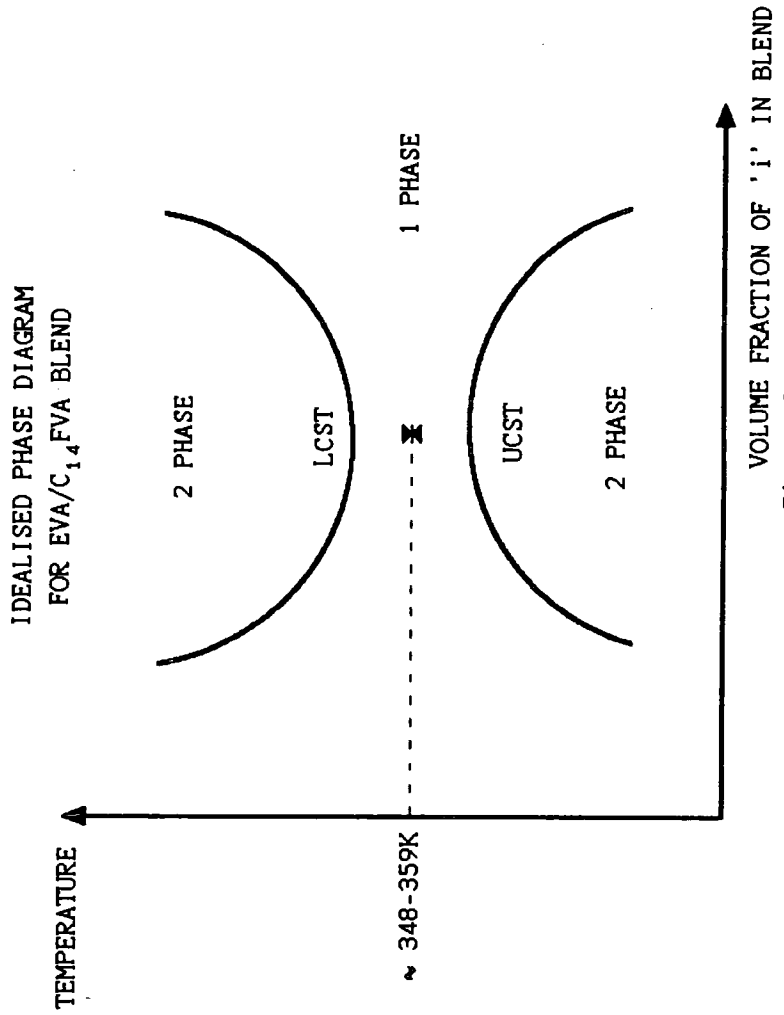


Figure 5.8

5.8 REFERENCES

- (1) A.A.Tager, T.T.Scholokhovich and Yu.S.Bessanov, Eur. Polym. J., 11, 321, (1975).
- (2) Z.Chai, S.Rouna, D.J.Walsh and J.S.Higgins, Polymer, 24, 263, (1983).
- (3) S.Rostami, D.J.Walsh, Macromolecules, 17, 315, (1984).
- (4) P.J.Flory, 'Principles of Polymer Chemistry', Cornell University Press, Ithaca, NY, (1953).
- (5) I.Prigogine, 'The Molecular Theory of Solutions', North-Holland, Amsterdam, (1957).
- (6) P.J.Flory, R.A.Orwell and A.Vrij, J. Am. Chem. Soc., 86, 3507, (1964).
- (7) P.J.Flory, R.A.Orwell and A.Vrij, J. Am. Chem. Soc., 86, 3515, (1964).
- (8) P.J.Flory, J.Am.Chem.Soc., 87:9, 1833, (1965).
- (9) B.E.Eichinger and P.J.Flory, Trans. Faraday Soc. 64, 2035, (1968).
- (10) C.L.Chong, PhD Thesis, Imperial College, (1981).
- (11) S.Rostami, PhD Thesis, Imperial College, (1983)

Chapter 6 Solvent Vapour Sorption

6.1 Introduction

Solvent vapour sorption, SVS, has been used for some decades to study the interactions of polymer mixtures. It involves exposing a polymeric sample under high vacuum to solvent vapour and measuring the equilibrium adsorption in terms of increased sample mass and respective solvent vapour pressure. In the context of polymer blends this technique shares a theoretical basis with IGC as it uses another species to quantify indirectly the interactions of interest. However, SVS has the advantage of being a static technique, and once equilibrium has been attained, in principle, it should be free of the surface adsorption and diffusion limitations inherent in IGC. Another advantage of SVS is that it comprises a true ternary system and provides information at a variety of solvent concentrations, as opposed to IGC which normally assumes the probe species to be at infinite dilution. The main disadvantage of the technique is the length of time required to achieve vapour adsorption equilibrium as each measurement can take up to a week. SVS and IGC have often been assumed to be synergistic and several workers have applied both techniques to the same system⁽¹⁻⁶⁾ with mixed conclusions. It was intended in this work to duplicate the IGC experiments to provide additional information about the EVA-C₁₄FVA interaction, and to consider both the relative merits and the agreement between the methods, but as a consequence of both technical and time constraints this was not possible. Instead a limited range of experiments was carried out and these results and those of their IGC analogues are reported and discussed.

6.2 Theoretical

The thermodynamic parameter which is commonly evaluated from SVS measurements is the activity of the solvent, a_1 .

In a binary system, *i.e.* solvent-homopolymer, this parameter is defined as,

$$\ln(a_1) = \ln(P/P^\circ) + [B_{11}(P - P^\circ)/RT] \quad (6.1)$$

where, P = measured vapour pressure of the solvent, atm.

P° = saturated vapour pressure of the solvent at T , atm.

B_{11} = second virial coefficient of the solvent at T , cm³ mol⁻¹

T = operating temperature, K

The activity coefficient can be related to the Flory-Huggins-Miller-Chang, (FHMC), interaction parameter, χ_{ij} , by,

$$\text{Ln}(a_1) = \text{Ln}(\phi_1) + (1 - r_1/r_2)\phi_2 + \chi_{12}\phi_2^2 \quad (6.2)$$

ϕ_i = volume fraction of component i

χ_{12} = solvent - polymer interaction parameter

r_i = the number of segments per molecule

Subscript 1 refers to the solvent, subscript 2 to the polymer. In the case of the solvent molecule, r is normally assumed to be unity as the solvent molecule is often approximately equal in size to a single segment unit.

If this approach is now extended to a ternary system consisting of solvent '1', and polymers '2' and '3', equation 6.2 becomes,

$$\begin{aligned} \text{Ln}(a_1) = & \text{Ln}(\phi_1) + (1 - r_1/r_2)\phi_2 + (1 - r_1/r_3)\phi_3 \\ & + (\chi_{12}\phi_2 + \chi_{13}\phi_3)(1-\phi_1) - \chi'_{23}\phi_2\phi_1 \end{aligned} \quad (6.3)$$

$$\text{where,} \quad \chi'_{23} = \chi_{23}(r_1/r_2) \quad (6.4)$$

However, equation 6.3 can only be used in the limiting case of $\phi_1 \rightarrow 0$, since both the homopolymer - solvent interaction parameters depend on the composition of the polymer blend which usually is unknown. To overcome this, the activity of the solvent in a ternary system is redefined as,

$$\text{Ln}(a_1) = \text{Ln}(\phi_1) + (1 - r_1/r_{23})\phi_{23} + \chi'_{1,23}\phi_{23}^2 \quad (6.5)$$

where,

$$\begin{aligned} \text{Ln}(a_1) = & \text{Ln}(\phi_1) + (1 - r_1/r_2)\phi_2 + \chi_{12}\phi_2^2 \\ \chi'_{1,23} = & [(\chi_{12}\phi_{12} + \chi_{13}\phi_{13})(1-\phi_1) - \chi'_{23}\phi_{12}\phi_{13}/\phi_{23}^2] \end{aligned} \quad (6.6)$$

By considering the polymer phase as a single entity, this definition avoids the need to calculate the individual homopolymer-solvent interaction values and reduces the ternary system to a binary, equation 6.5 becoming analogous to equation 6.2. The combined mixture parameters, *i.e.* r_{23} and ϕ_{23} , are calculated from the weighted averages of the individual contributions at zero solvent concentration,

$$r_{23} = X_{p2}r_2 + X_{p3}r_3 \quad (6.7)$$

and,

$$\phi_{23} = \phi_2 + \phi_3 = 1 - \phi_1 \quad (6.8)$$

where,

x_{pi} = mole fraction of polymer component i at zero solvent concentration

The volume fraction is most representative when the components have similar molar volumes and thus the polymer chain is subdivided into a number of segments which are approximately equivalent in size to a solvent molecule,

$$\begin{aligned} \text{i.e.} \quad \phi_i &= m_i v_{spi}^* / \sum m_i v_{spi}^* \\ &= x_i r_i / \sum x_i r_i \end{aligned} \quad (6.9)$$

where,

v_{spi}^* = characteristic specific volume of component 'i', $\text{cm}^3 \text{g}^{-1}$
(i.e. the specific volume of the defined segment)

x_i = mole fraction of component 'i' in the ternary mixture

If (6.5) is now equated to the measured experimental quantities, *via* (6.2), and rearranged for $\chi'_{1,23}$,

$$\chi'_{1,23} = 1/(\phi_{23})^2 \left\{ \text{Ln}(P/P^0) + B_{11}(P - P^0)/RT - \text{Ln}(\phi_1) - (1 - r_1/r_{23})\phi_{23} \right\}$$

from equations 6.7 and 6.8 and substituting $r_1 = 1$ gives,

$$\begin{aligned} \chi'_{1,23} &= 1/(\phi_{23})^2 \left\{ \text{Ln}(P/P^0) + B_{11}(P - P^0)/RT - \text{Ln}(\phi_1) \right. \\ &\quad \left. + \{1/(x_{p2}r_2 + x_{p3}r_3) - 1\}(\phi_2 + \phi_3) \right\} \end{aligned} \quad (6.10)$$

Thus, this approach simplifies the ternary by treating it as a pair of binary systems, *i.e.* the polymer-polymer system and the combined polymer-solvent system, and assumes volume additivity.

The true polymer-polymer interaction parameter, χ'_{23} , is calculated from the polymer-polymer-solvent interaction parameters at zero solvent content, $\chi^{\infty}_{1,23}$, using equation 6.11⁽⁷⁾,

$$\chi'_{23} = (\chi^{\infty}_{12}\phi_2^{\infty} + \chi^{\infty}_{13}\phi_3^{\infty} - \chi^{\infty}_{1,23})/(\phi_2^{\infty}\phi_3^{\infty}) \quad (6.11)$$

where,

ϕ_i^{∞} = volume fraction of component 'i' in the polymer blend

The values of χ^∞ are obtained by linear extrapolation of the χ'_{1j} vs. ϕ_j relationship to $\phi_j = 1$. This procedure introduces the possibility of a significant error since the results may not be linear and the selection of data for this fitting procedure is arbitrary.

6.3 Materials

Samples of both the EVA copolymer and the C_{14} FVA copolymer were stored at 393K under vacuum for the duration of these experiments. As the blends were prepared in the open atmosphere at ambient temperature, they were returned to a vacuum oven for 2 hours before being left under vacuum in the SVS rig overnight. This process served to remove excess air/moisture and to evenly distribute the molten sample within the glass holder.

6.4 Apparatus

The apparatus which was used in these experiments was designed and constructed as part of this experimental programme and is represented schematically in Figure 6.1. The components are listed below:-

6.4.1 The Isothermal Envelope

The apparatus was enclosed in a wooden box, (dimensions 2m x 1m x 1m), which was constructed of plywood of 3 cm thickness. The front of the box was hinged to allow access, and double glazed with 4mm MAKROLON to permit optical measurements. The interior was insulated with 16cm thick pads of fire retardant material.

6.4.2 The Vacuum System

The pump system comprised an Edwards E2M2 two-stage rotary pump and an Edwards (Type 53) diffusion pump. The latter was connected to the glassware *via* a flange joint with a neoprene 'O' ring. The glassware was fabricated from 12mm o.d. tubing and Young's greaseless taps were employed throughout. Another neoprene 'O' ring was used as a seal between the glass stopper and hook, (from which the quartz spring and sample basket were suspended), and the remaining glassware.

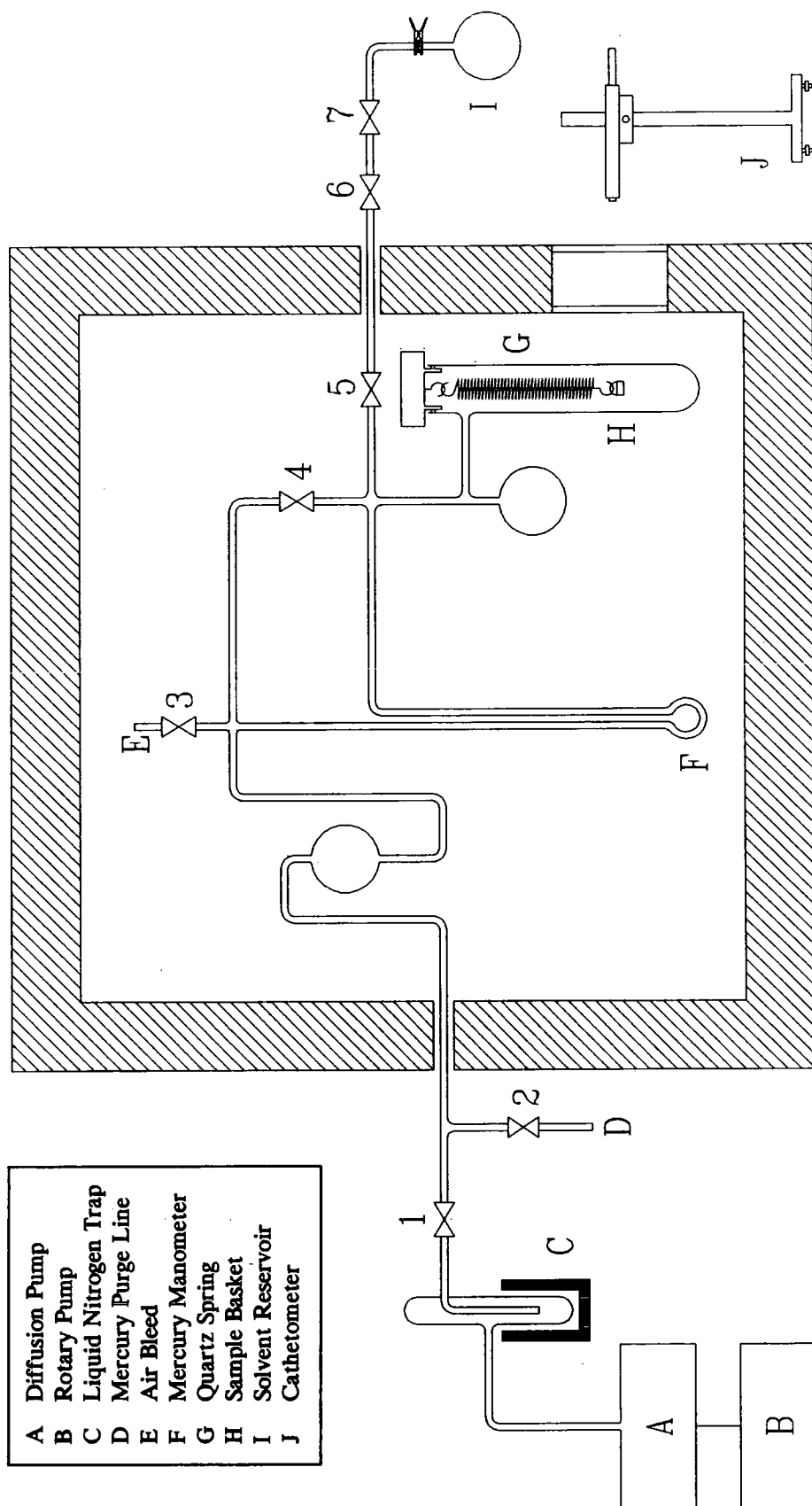


Figure 6.1 Schematic Representation of the SVS Rig

6.4.3 The Heating System and Temperature Control

A pair of platinum resistance thermometers were mounted on either side of the sample holder in the vacuum line, one of which served as the probe for a Digitron 3754 thermometer unit, while the other acted as the sensor for a CAL 9000 temperature control unit. This unit controlled a pair of 300W infrared lamps, mounted on the roof of the box, which provided the control energy. The bulk of the heat was supplied by a Bibby halogen hotplate, which was situated at the bottom of the box, and a 400W Electrothermal heating tape which was loosely wrapped around the internal support framework. The air was circulated by a 7cm, 240V a.c. fan. This arrangement controlled the temperature of the box to $\pm 0.05\text{K}$.

6.4.4 The Optical Measurements

The mercury levels in the manometer and the displacement of the sample basket were monitored using a cathetometer (The Precision Tool & Instrument Co., Model 2005). This instrument was mounted on a stand whose height was 1.5m with a 1m Vernier scale giving an accuracy of $\pm 5 \times 10^{-3}$ mm.

6.5 Experimental Procedure

Before absorption experiments could be performed the relationship between the extension of the quartz spring and the suspended mass had to be determined for each operating temperature. This involved the careful weighing of a series of aluminium foil weights, (typically from 140 to 180 mg), inserting each into the evacuated apparatus and recording the resulting extension. These results were then fitted by linear least-squares procedure to give calibration data for that particular spring at that temperature. Each polymer sample was placed in a glass basket and roughly weighed to ensure that it was within the calibration range. The basket was then suspended from the silica spring and the assembly inserted into the apparatus which was then evacuated by rotary pump for approximately 2 hours followed by overnight evacuation by a diffusion pump. Once the system had equilibrated the resulting spring extension was recorded relative to a reference rod, which hung in the middle of the spring coil, and the equivalent mass evaluated from the calibration function. This mass was then used as the initial mass in the subsequent calculations. The apparatus was then separated into the vapour pressure measurement section and the absorption section by closing tap 4, and left for approximately 4 hours until thermal stability was regained. The solvent reservoir was then opened at tap 7 and the rate of addition was monitored from the increase in vapour pressure on the manometer. After the required

volume of solvent had been added, the vapour pressure and the displacement of the sample basket were noted every 2 hours until no change in their positions were detected and it was assumed that equilibrium had been established. Using the same polymer mixture, this procedure was repeated with a range of solvent concentrations.

6.6 Results

A sample calculation has been included to demonstrate explicitly how the SVS data were analysed, and to show the sensitivity of the final results to the precision of the original measurements. The sample data are for Blend 2, *i.e.* with 41.3% (wt/wt) EVA in the EVA/C₁₄FVA mixture, at 313K.

6.6.1 Sample Calculation

(a) Saturated Vapour Pressure, P^0

As described in section 4.5.1, P^0 was calculated from the Wagner equation⁽⁸⁾,

$$P_1^0 = \text{Exp} \{ (w_1 t + w_2 t^{1.5} + w_3 t^3 + w_4 t^6 / T_r) \} \quad (6.11)$$

where,

$$t = 1.0 - T_r \quad \text{and}$$

$$w_i = \text{Wagner coefficients from Reid, Prausnitz and Polling}^{(8)}$$

and the Antoine equation⁽⁸⁾,

$$P_1^0 = \text{Exp} \{ A_0 - A_1 / (T + A_2) \} \quad (6.12)$$

where,

$$A_i = \text{Antoine coefficients from reference (8)}$$

A selection of the P_1^0 values at the SVS operating temperatures, which have been estimated by both of these methods is included in Table 6.1 for reference.

Table 6.1

The saturated vapour pressures of Hexane, P_1°

T/K	P_1° / mmHg (Antoine)	P_1° / mmHg (Wagner)
312.8	273.3	274.7
312.9	276.4	275.8
313.0	277.4	276.8
313.1	278.5	277.9
313.2	279.6	279.0
352.7	1053.2	1050.7
352.8	1056.3	1053.8
352.9	1059.4	1056.9
353.0	1062.4	1059.9
353.1	1065.5	1063.0
353.2	1068.7	1066.1
353.3	1071.8	1069.2
353.4	1074.9	1072.4
353.5	1078.0	1075.5
353.6	1081.2	1078.6
353.7	1084.3	1081.7
353.8	1087.5	1084.9
353.9	1090.6	1088.0

From the Wagner expression the saturated vapour pressure of hexane at 313K is estimated as 276.8 mmHg. The relative error in this value is considered to be insignificant.

(b)

Table 6.2

Reproducibility of extension measurements

Run	Reference Point /cm	Basket /cm	Extension / cm
1	13.839	9.640	4.199
2	13.849	9.654	4.195
3	13.852	9.644	4.208
4	13.852	9.634	4.218
5	13.849	9.647	4.202
Mean	13.848	9.644	4.204

Standard Deviation of extension = 8.02×10^{-3}

hence, mean extension = 4.204 ± 0.008 cm

The total range of extension values is 8.108 cm to 3.982 cm for this experiment, thus the standard deviation of the measurement when expressed as a percentage of the total range is,

$$\text{Error} = 0.008 / (8.108 - 3.982) = 0.2\%$$

From equation 6.1 the activity of the hexane is given by,

$$\begin{aligned} \ln(a_1) &= \ln(P/P^0) + [B_{11}(P - P^0)/RT] & (6.1) \\ &= \ln(4.278/27.68) \\ &\quad + (-1619.8)(4.278 - 27.68)/(82.057.313) \\ &= -1.867 + 1.476 \\ &= -0.391 \end{aligned}$$

Substituting this value into (6.10) gives,

$$\begin{aligned} x'_{1,23} = & 1/(\phi_{23})^2 \left\{ \text{Ln}(P/P^0) + B_{11}(P - P^0)/RT - \text{Ln}(\phi_1) \right. \\ & \left. + \{1/(x_{p2}r_2 + x_{p3}r_3) - 1\}(\phi_2 + \phi_3) \right\} \quad (6.10) \end{aligned}$$

The values of r are constant for each polymer sample and are calculated from the number average molecular weight of the polymer, as determined by GPC, divided by the unit structure molecular weight,

$$r_i = M_n / \text{Unit Structure Molecular Weight}$$

hence,

$$r_2(\text{EVA}) = 3290 / 254.4 = 12.9 \text{ segments}$$

$$r_3(\text{C}_{14}\text{FVA}) = 10400 / 594.8 = 17.5 \text{ segments}$$

If the binary system of polymers is considered, the mole fractions, (x_{pi}), of the components are,

$$\text{mass EVA} = 59.5 \text{ mg}$$

$$\text{hence moles of EVA} = 59.5 / 3290 \times 10^3 = 1.81 \times 10^{-5} \text{ moles}$$

$$\text{mass of C}_{14}\text{FVA} = 84.7 \text{ mg}$$

$$\text{hence moles of C}_{14}\text{FVA} = 84.7 / 10400 \times 10^3$$

$$= 8.14 \times 10^{-6} \text{ moles}$$

$$\text{hence, } x_{p2} = 1.81 \times 10^{-5} / (1.81 \times 10^{-5} + 8.14 \times 10^{-6})$$

$$= 0.690$$

and

$$x_{p3} = 1 - x_{p2} = 0.310$$

In the ternary system, the mass of the solvent is given by the extension of the spring converted to mass *via* the calibration function, the details are given below.

6.6.2 Microbalance calibration

A series of 5 weights, made from aluminium foil, was used to calibrate the quartz spring; aluminium was chosen because it is inert with respect to hexane.

Table 6.3
Quartz spring calibration

Reference No	mass / mg	Extension	
		mean / cm	s devn / cm
1	143.8	3.948	0.0145
2	150.5	4.081	0.0054
3	157.9	4.209	0.0138
4	169.8	4.465	0.0079
5	183.5	4.691	0.0134

Least-squares techniques were used to obtain the following values for the intercept (a) and slope (b) where,

$$\text{Extension} = a + b(\text{Mass})$$

$$a = 1.2326 \quad b = 0.0189 \quad r = 0.9990$$

These results are shown graphically in Figure 6.2

unexposed initial mass equivalent = 3.985 cm = 145.63 mg

final position mass equivalent = 4.030 cm = 148.01 mg

hence, increase in mass = 148.01 - 145.63 = 2.38 mg

number of moles of hexane = 2.38 / (mol wt of hexane)

$$= 2.38 / 86.17 \times 10^3$$

$$= 2.76 \times 10^{-5} \text{ moles}$$

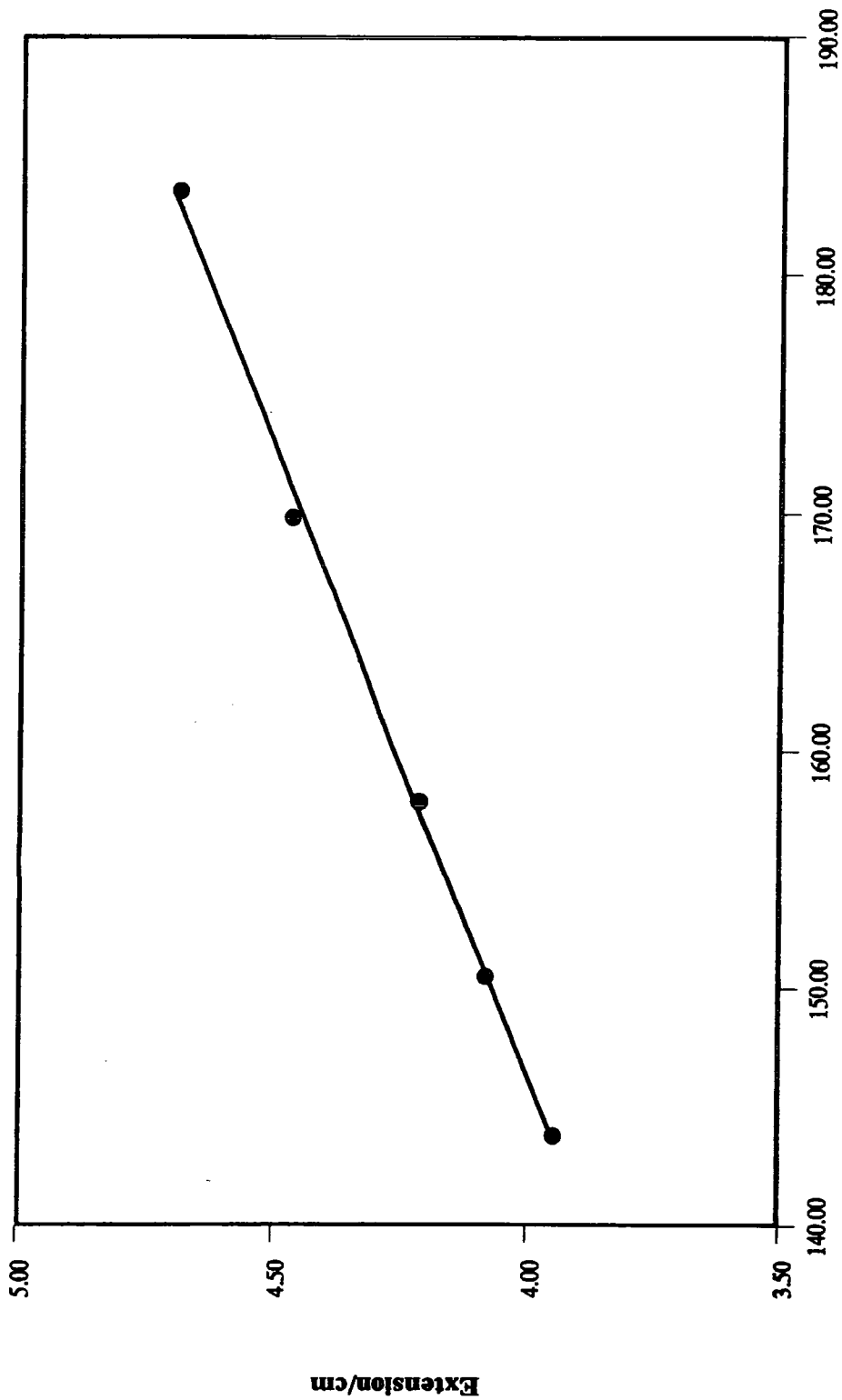
hence, the ternary mole fractions are,

$$x_1 = 2.76 / (2.76 + 1.81 + 0.81) = 0.513$$

$$x_2 = 1.81 / (2.76 + 1.81 + 0.81) = 0.336$$

$$x_3 = 1 - (x_2 + x_1) = 0.151$$

Linear Calibration of Quartz Spring
Extension vs. Mass



Mass/mg
Figure 6.2

and the volume fractions are,

$$\begin{aligned}\phi_1 &= (x_1 r_1) / (x_1 r_1 + x_2 r_2 + x_3 r_3) \\ &= (0.513 * 1) / (0.513 + 12.9 \times 0.336 + 17.5 \times 0.151) \\ &= 0.068\end{aligned}$$

$$\phi_2 = 3.8304 / 7.5001 = 0.511$$

$$\phi_3 = 1 - (0.068 + 0.511) = 0.421$$

and thus, $\phi_{23} = 0.511 + 0.421 = 0.932$

substitution of these values into (6.10) yields,

$$\begin{aligned}x_{1,23} &= 1/(0.932)^2 \{ (-0.391) - (-2.617) \\ &\quad + [1/(7.866 + 5.425) - 1](0.932) \} = 1.646\end{aligned}$$

6.6.3 The 313K Experiments

6.6.3.1 C₁₄FVA

Table 6.4

Initial Mass = 147.04 mg : P^o = 276.8 mmHg

Ref. No	M _{solv} / M _{polymer}	P / P ^o	φ ₂₃	χ ₁₍₂₃₎
1	0.0294	0.240	0.832	-0.6193
2	0.0302	0.240	0.828	-0.6510
3	0.0550	0.355	0.726	-0.7832
4	0.0536	0.355	0.731	-0.7452
5	0.0834	0.471	0.636	-0.8710
6	0.0860	0.471	0.629	-0.8661
7	0.1122	0.541	0.565	-0.9522
8	0.1111	0.541	0.567	-0.9336
9	0.1460	0.625	0.499	-0.9656
10	0.1457	0.625	0.500	-0.9593

A least-squares on all points gives

$$\chi_{13}^{\infty} = -0.4162$$

**Table 6.4: Interaction Parameter vs Volume Fraction
FVA at 313K**

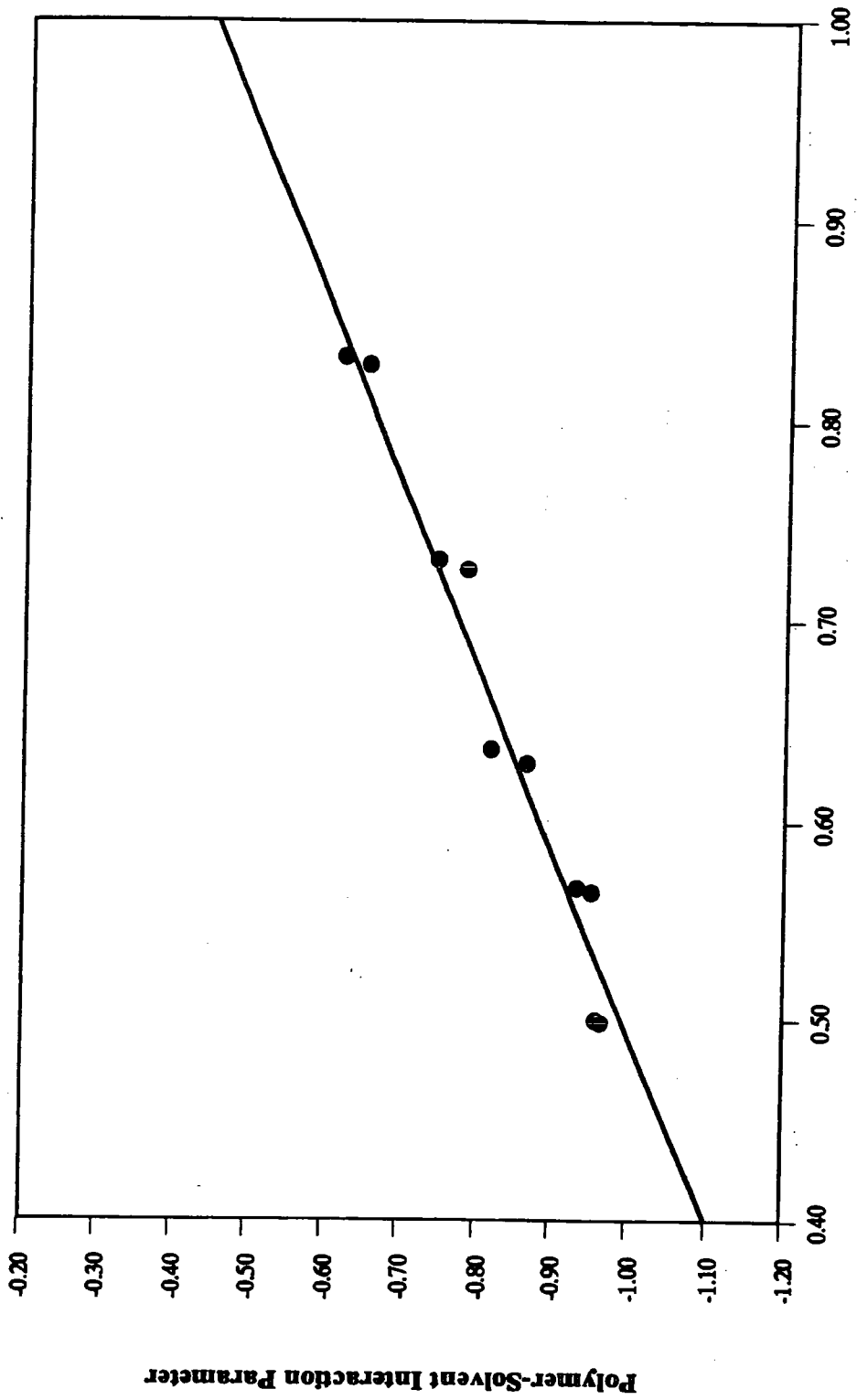


Figure 6.3

6.6.3.2 EVA

Table 6.5

Initial Mass = 146.30 mg : $P^0 = 276.8$ mmHg, [$\phi_{23} = \phi_2$]

Ref.No	$M_{\text{solv}} / M_{\text{polymer}}$	P / P^0	ϕ_{23}	$\chi_{1(23)}$
1	0.012	0.017	0.966	+ 0.117
2	0.010	0.017	0.971	+ 0.283
3	0.030	0.202	0.726	+ 1.728
4	0.033	0.202	0.911	+ 1.655
5	0.114	0.514	0.748	- 0.018
6	0.064	0.415	0.841	+ 0.222*
7	0.065	0.415	0.838	+ 0.201*
8	0.144	0.618	0.702	+ 0.088
9	0.140	0.618	0.707	+ 0.111
10	0.067	0.232	0.834	- 0.649*
11	0.065	0.232	0.839	- 0.599*

A least-squares on all the absorption points gives

$$\chi_{1,23}^{\infty} = +0.186$$

(desorption points are marked with an asterisk)

**Table 6.5: Interaction Parameter vs Volume Fraction
EVA at 313K**

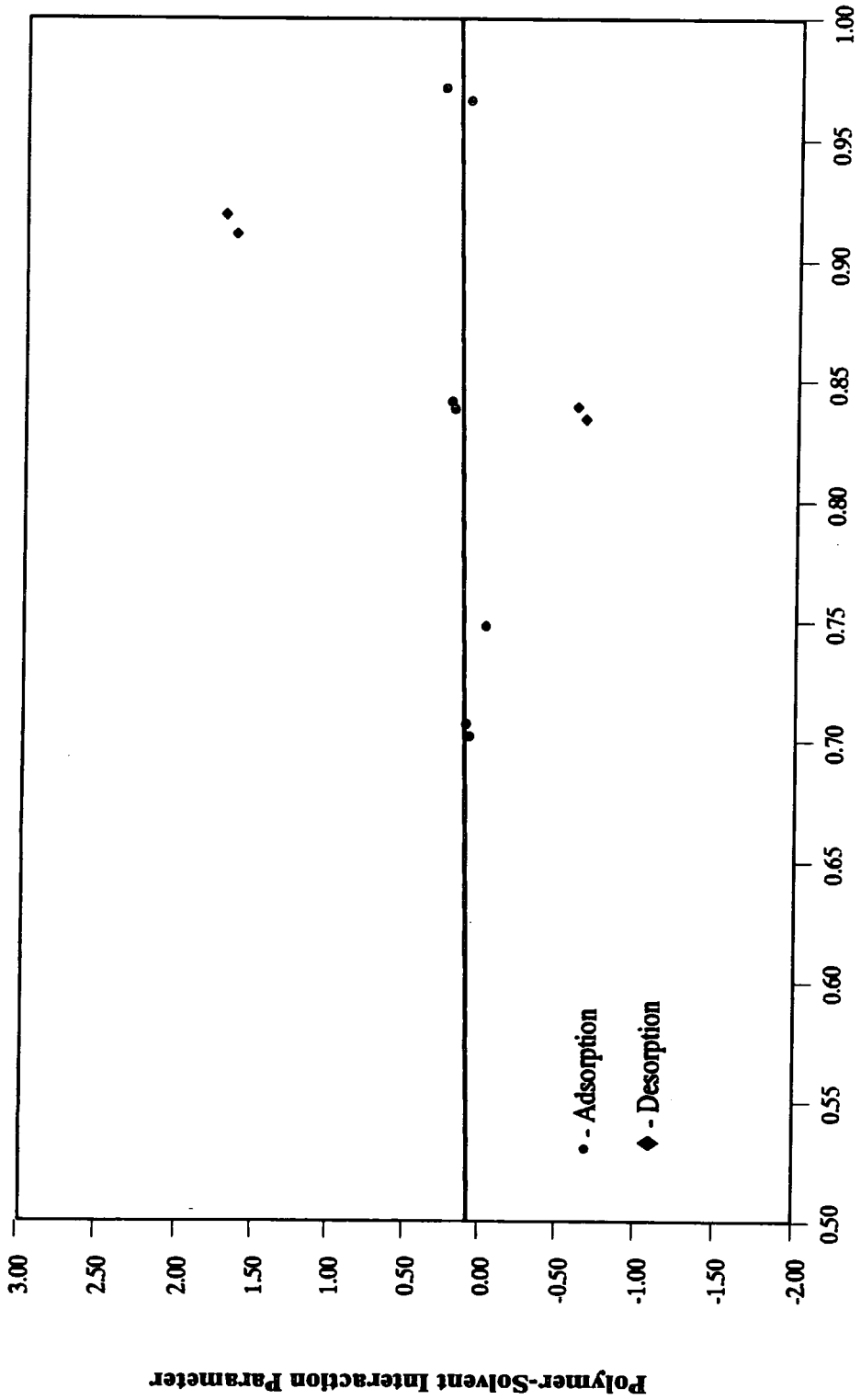


Figure 6.4

Table 6.6

Blend 1: (20% EVA, at 313 K)

Initial Mass = 140.0 mg : $P^0 = 276.8$ mmHg

Ref. No	$M_{\text{solv}} / M_{\text{polymer}}$	P / P^0	ϕ_{23}	ϕ_2	$\chi_{1(23)}$
2	0.040	0.213	0.837	0.279	+ 1.225
3	0.042	0.213	0.828	0.278	+ 1.187
4	0.079	0.398	0.721	0.235	+ 1.407
5	0.083	0.398	0.713	0.236	+ 1.398
6	0.122	0.517	0.627	0.208	+ 1.284
7	0.121	0.517	0.629	0.212	+ 1.483
8	0.145	0.585	0.586	0.198	+ 1.518
9	0.147	0.585	0.583	0.193	+ 1.521
10	0.047	0.213	0.812	0.273	+ 1.120*
11	0.050	0.213	0.803	0.269	+ 1.085*

A least-squares on all the absorption points gives

$$\chi_{1,23}^{\infty} = +1.014$$

(desorption points are marked with an asterisk)

Table 6.6: Interaction Parameter vs Volume Fraction
BLEND 1: 20% EVA (w/w), 313K

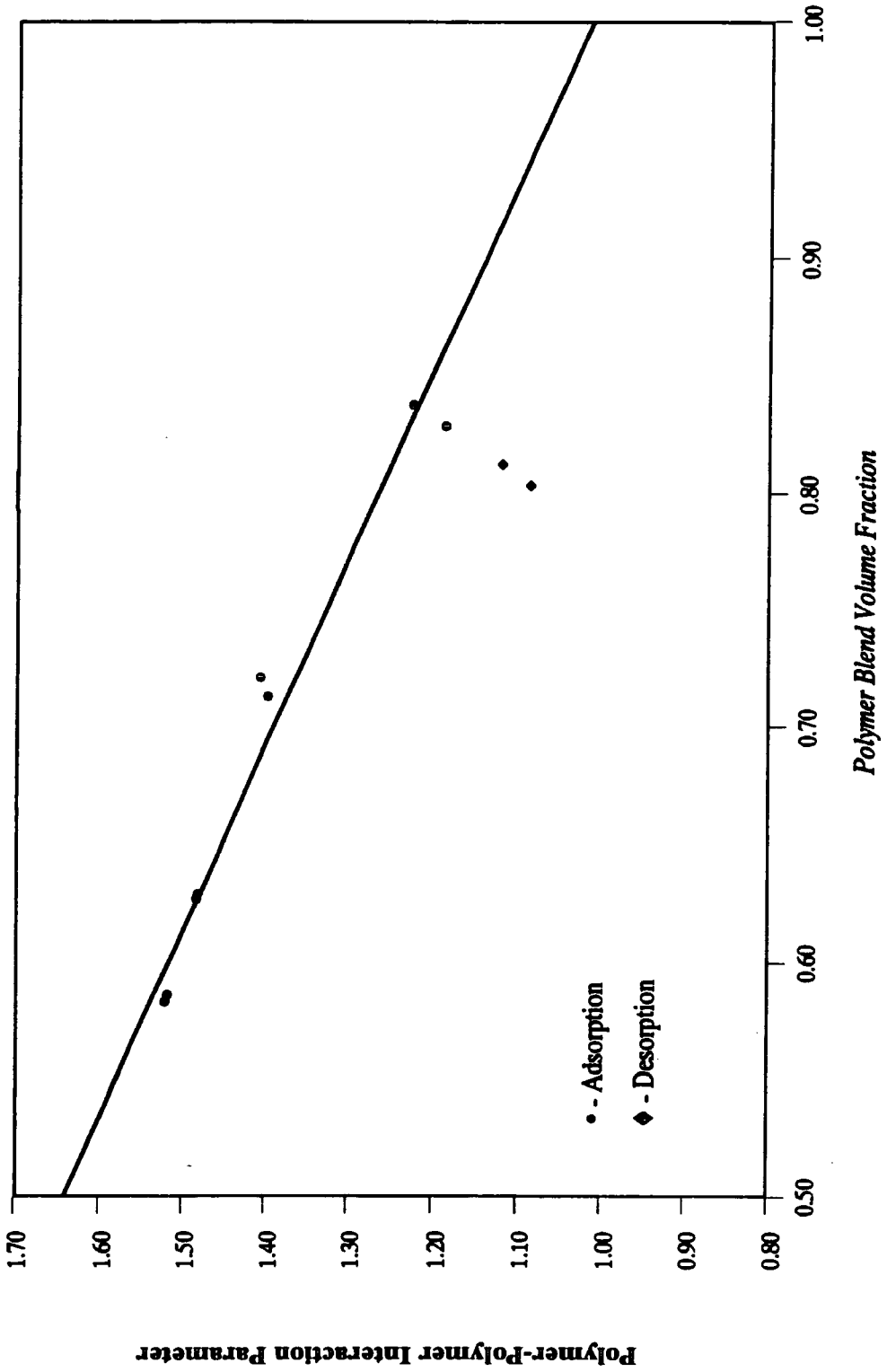


Figure 6.5

Table 6.7:

Blend 2: (40%EVA) - 313K

Initial Mass = 145.6 mg : $P^{\circ} = 276.8$ mmHg

Ref.No	$M_{\text{solv}} / M_{\text{polymer}}$	P / P°	ϕ_{23}	ϕ_2	$\chi_{1(23)}$
1	0.016	0.155	0.932	0.511	+ 1.647
2	0.020	0.154	0.919	0.572	+ 1.420
3	1.498	0.317	0.591	0.373	+ 1.109
4	1.494	0.317	0.591	0.373	+ 1.122

A least-squares calculation on all points gave $\chi_{1,23}^{\circ} = +1.631$

6.6.4 The 353K Experiments

6.6.4.1 C_{14} FVA

Table 6.8

Initial Mass = 146.68 mg : $P^{\circ} = 1081.7$ mmHg : [$\phi_{23} = \phi_3$]

Ref.No	$M_{\text{solv}} / M_{\text{polymer}}$	P / P°	ϕ_{23}	$\chi_{1(23)}$
1	0.006	0.427	0.962	-0.4687
2	0.006	0.739	0.962	+0.1224
3	0.016	0.932	0.901	-0.6817
4	0.014	0.930	0.910	-0.1987

A least-squares calculation on all points gives $\chi_{12}^{\circ} = +0.563$

Table 6.5: Interaction Parameter vs Volume Fraction
BLEND 2: 40% EVA (w/w), 313K

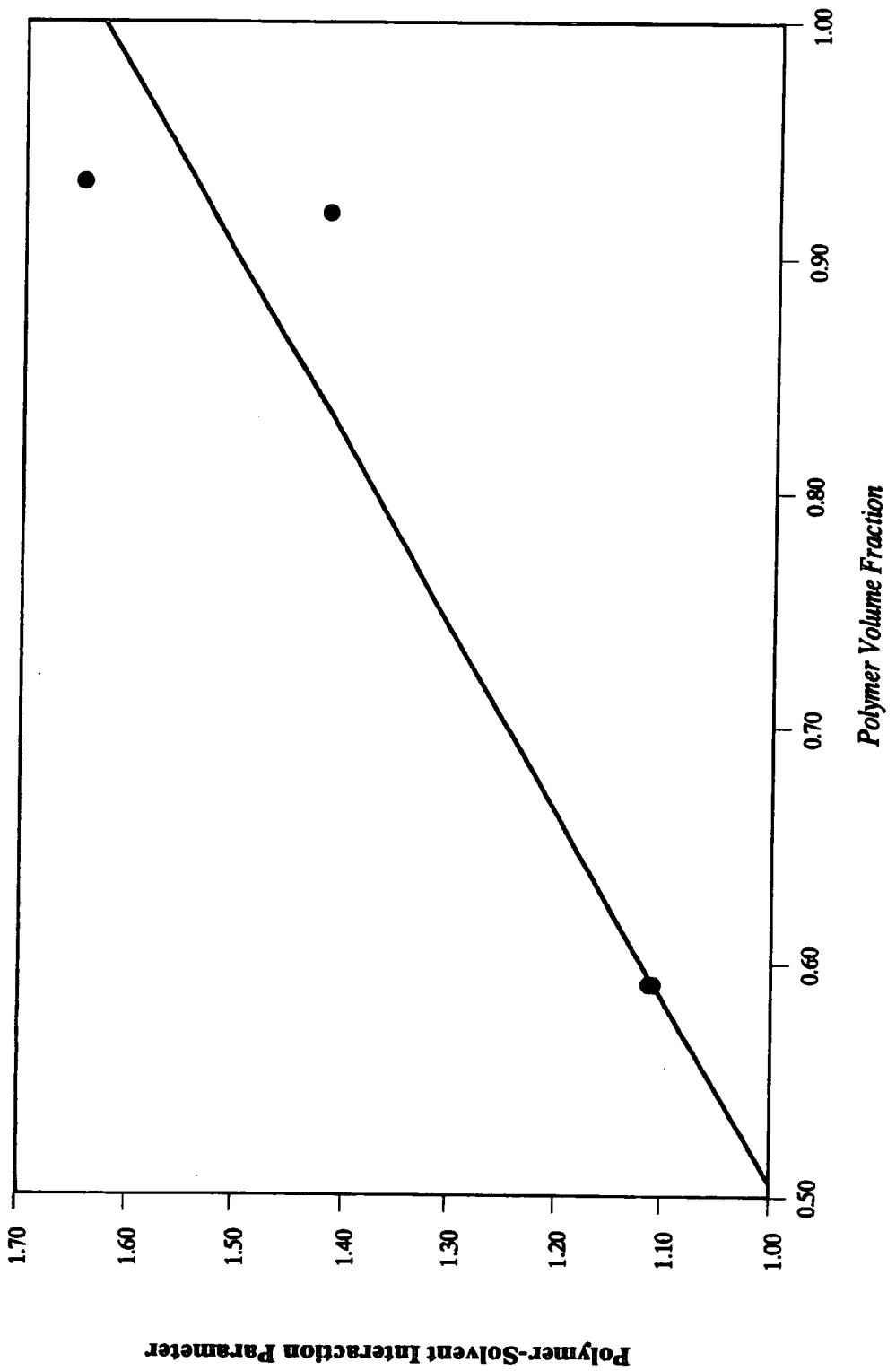


Figure 6.6

**Table 6.8: Interaction Parameter vs Volume Fraction
FVA at 353K**

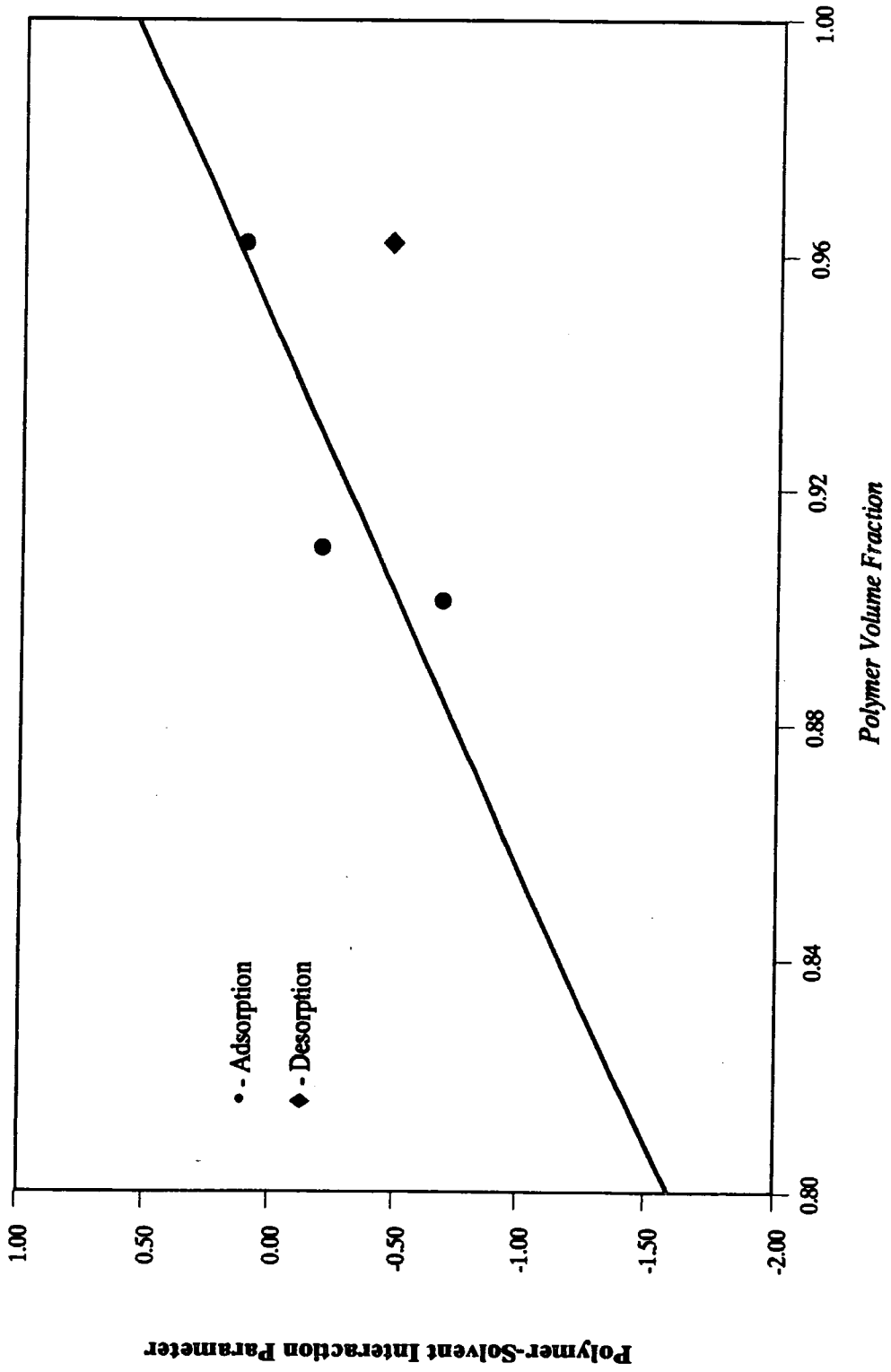


Figure 6.7

6.6.4.2 EVA

Table 6.9

Initial Mass = 134.31 mg : P^o = 1081.7 mmHg

Ref.No	M _{solv} / M _{polymer}	P / P ^o	ϕ_{23}	$\chi_{1(23)}$
1	0.024	0.066	0.925	-1.0676
2	0.041	0.130	0.880	-0.8727
3	0.028	0.083	0.915	-0.9615

A least-squares calculation on all points gave $\chi_{13}^{\infty} = -1.328$

6.7 Discussion

The design and construction of this apparatus required substantial effort and the limited number of experimental results reflects the prolonged commissioning period and the equilibrium time required per measurement. One major disadvantage of the original design was that the glass suspension hook and the sample chamber were connected by a greased ground-glass joint. After a new sample was inserted and the system evacuated, this joint leaked causing pressure surge into the RHS of the glassware with mercury being sprayed from the manometer into the LHS glassware. It is believed that often this seal failed because of a redistribution of the vacuum grease as the apparatus was heated to the operational temperature. This problem was eventually solved by replacing the grease with a neoprene 'O' ring. To ensure that mercury spillage could be removed readily, the glassware was modified to retain the spillage within an external purge line. This was the reason that a low temperature of 313K was chosen for the first experiments since it was initially unclear whether the mercury spillage was occurring as a result of a pressure leak or by condensation of the mercury vapour outside the thermal envelope of the rig. In view of the high density of the mercury, which prevented a large bore manometer being used owing to fear of fracture with its associated toxicological hazards, it might have been more prudent to have used an alternative medium, for example a high boiling silicone oil. The original

**Table 6.9: Interaction Parameter vs Volume Fraction
EVA at 353K**

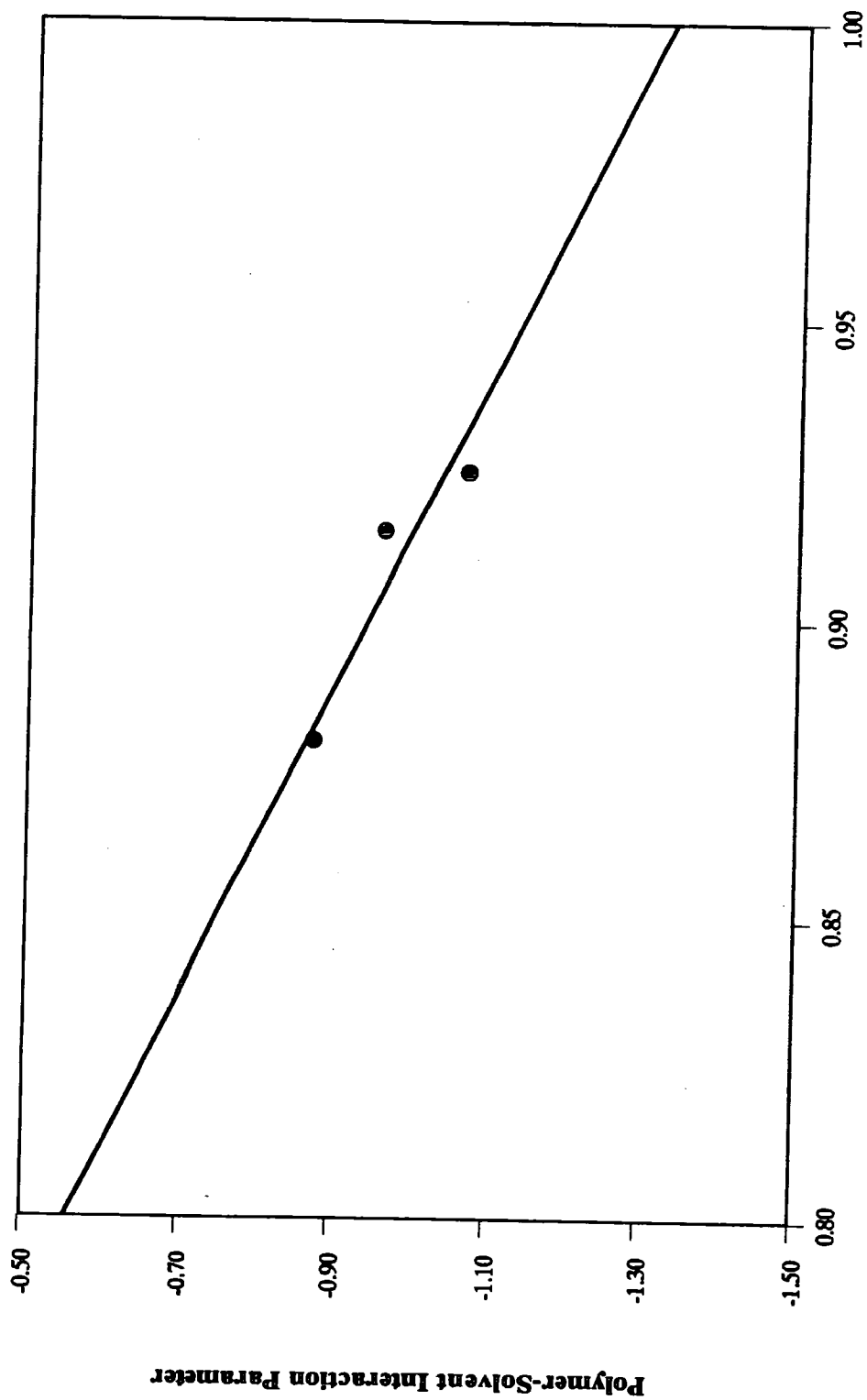


Figure 6.8

design was also found to have a significant temperature gradient between the top and bottom of the box which was overcome by remounting the infrared lamps on the roof and re-positioning the circulation fan.

Another factor which reduced the number of successful experiments was the time required to achieve equilibrium. This period was found to vary between 8 and 36 hours for absorption but the experimental results suggested that desorption equilibrium was not achieved even after as long as 100 hours.

Although the primary measurements were found to be reproducible, the linear extrapolation of the interaction parameters to the condition of infinite dilution of the solvent introduced significant errors for a number of reasons. Firstly, generally there were insufficient data at low solvent concentrations to apply statistical techniques to obtain a fit for the function, and secondly, there is no reason to assume, that even at low solvent concentrations, the interaction parameter is a linear function of ϕ_{23} . For example, if all the absorption data for EVA-Hexane at 313K are fitted as a series of polynomials of increasing order, the intercept value changes significantly as shown in Table 6.10, (it should also be noted that the assignment of data to any potential fit is arbitrary).

Table 6.10

Coefficients for polynomial fits of EVA-Hexane data at 313K

Order	a_0	a_1	a_2	a_3	a_4	Intercept at $\phi_{23} = 1$
1	-0.0305	0.2162	-	-	-	0.186
2	-0.0015	-0.1769	0.4211	-	-	0.242
3	0.0002	-2.5202	6.0515	-3.3324	-	0.199
4	0.0000	105.7400	-388.3998	471.9492	-189.3873	-0.098

These data show a significant variation in their extrapolated χ_{13}^{∞} values.

Values of the EVA-hexane interaction parameter change from small and positive to significantly negative over the temperature range 313 to 353K, Table 6.11, suggesting that hexane becomes a more effective solvent for EVA

which change from small and negative to small and positive.

Table 6.11

Polymer - Hexane Interaction Parameters

Method	Temp/K	χ_{12}^{∞}	χ_{13}^{∞}
SVS	313	0.1855	-0.4162
SVS	353	-1.3278	0.5625
IGC	353	1.7963	1.5361
IGC	373	2.0567	1.6421
IGC	393	2.2782	1.8190

The agreement between the SVS and IGC results at 353K for both systems is very poor with no obvious explanation for this difference. The variations in both the calculated values of the SVS homopolymer - hexane interaction parameters between 313 and 353K are an order of magnitude greater than those seen in the IGC results between 353 and 393K. The accuracy and reliability of the SVS results should be better than those derived from the IGC experiments since there are no unpredictable dynamic effects involved and there is no other material present which could affect the measurements, *e.g.* the PTFE support, but this reproducibility could not be verified owing to the limited data from the SVS experiments. Several workers have reported good agreement between IGC and SVS experiments^(1,3,9) and concluded that both techniques were equally valid. However, there have also been reports of noticeable discrepancies being observed between results obtained from IGC and those from SVS⁽⁴⁾ and even an inter-laboratory collaboration⁽¹⁰⁾ failed to resolve these differences. These discrepancies are more fully discussed in Chapter 9.

The polymer-polymer interaction parameters which were calculated at 313K for mixtures of 20 and 40%(wt/wt) EVA and C₁₄ FVA are both very large and negative, Table 6.12.

Table 6.12:

Polymer-Polymer Interaction Parameters for EVA/C₁₄ FVA
from Hexane Probes

% EVA (wt/wt)	T / K	χ_{12}^{∞}	ϕ_2	χ_{13}^{∞}	ϕ_3	$\chi_{1,23}^{\infty}$	χ'_{23}
20 SVS	313	+0.1857	0.355	-0.4162	0.665	+1.014	-5.515
40 SVS	313	+0.1857	0.621	-0.4162	0.379	+1.014	-7.110
25 IGC	353	+1.7963		+1.5361			-2.105
36 SVS	353	+1.7963		+1.5361			+0.743

These values predict that any mixture of less than 40%EVA (wt/wt) and C₁₄ FVA would be highly miscible at this temperature. The normal range of χ values is ± 1 , and thus these figures display major differences from those expected. Some doubt was felt as to the magnitude of these values and as a consequence it was decided to examine the sensitivity of the calculation.

If the 20%EVA data are taken, for example, from equation 6.11

$$\chi'_{23} = (\chi_{12}^{\infty} \phi_2^{\infty} + \chi_{13}^{\infty} \phi_3^{\infty} - \chi_{1,23}^{\infty}) / (\phi_2^{\infty} \phi_3^{\infty}) \quad (6.11)$$

$$\chi_{12}^{\infty} \phi_2^{\infty} = 0.062$$

$$\chi_{13}^{\infty} \phi_3^{\infty} = -0.277$$

$$\chi_{1,23}^{\infty} = 1.014$$

$$\phi_2^{\infty} \phi_3^{\infty} = 0.223$$

From these values it is apparent that $\chi_{1,23}^{\infty}$ dominates the calculation, and the net effect is multiplied by a factor of $(1.0/0.223)$, or approximately 5, from the product of the polymer mixture volume fractions. Since the value of $\chi_{1,23}^{\infty}$ is obtained by fitting a straight line to eight data points and extrapolating this function to $\phi_{23} = 1$, the potential error is significant, *i.e.* if a polynomial fit is used the extrapolated intercept varies considerably, Table 6.13,

Table 6.13

Coefficients for polynomial fits of Hexane-EVA data at 353K

Order	a ₀	a ₁	a ₂	a ₃	Intercept at $\phi_{23} = 1$
1	-2.2700	-1.2557	-	-	1.014
2	0.8076	2.9379	-2.9504	-	0.795
3	1.9813	-2.1328	4.2839	-3.4080	0.724

(The quadratic and cubic functions are shown in Figures 6.9 and 6.10)

If the quadratic fit intercept value is now inserted into the calculation of χ'_{23} ,

$$\chi'_{23} = (0.062 - 0.277 - 0.795)/(0.228) = -4.430$$

This represents a 20% difference in the estimated polymer-polymer interaction parameter. This difference could be greatly increased if the same procedure was applied to the extrapolated values of the homopolymer-solvent interaction parameters. The significance of this effect is not unique to the SVS data presented here: a similar analysis was performed on the data reported by Panayiotou and Vera⁽⁷⁾ for the system benzene-polystyrene-poly(vinyl methyl ether) with the following results.

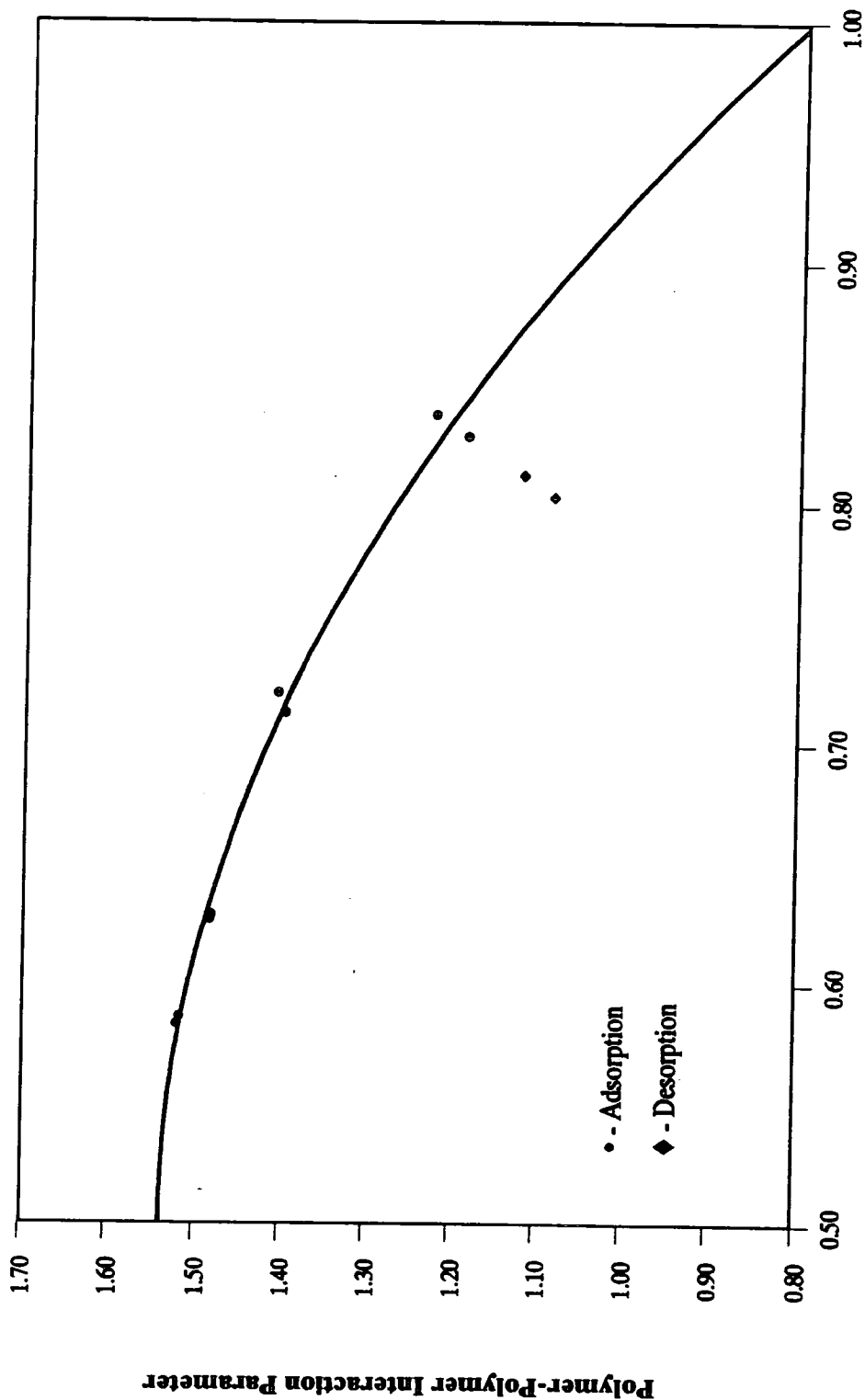
Table 6.14

Coefficients for polynomial fits of Benzene-PS-PVME data at 298K

(PS Wt.Fr. = 0.3337)

Order	a ₀	a ₁	a ₂	a ₃	Intercept at $\phi_{23} = 1$
1	0.2529	-0.0002	-	-	0.252
2	0.2628	-0.0316	0.0238	-	0.255
3	-0.4536	4.5564	-10.7404	10.9795	0.262

Table 6.6: Interaction Parameter vs Volume Fraction
BLEND 1: 20% EVA (w/w), 313K



Polymer Blend Volume Fraction
Figure 6.9

Table 6.6: Interaction Parameter vs Volume Fraction
BLEND 1: 20% EVA (w/w), 313K

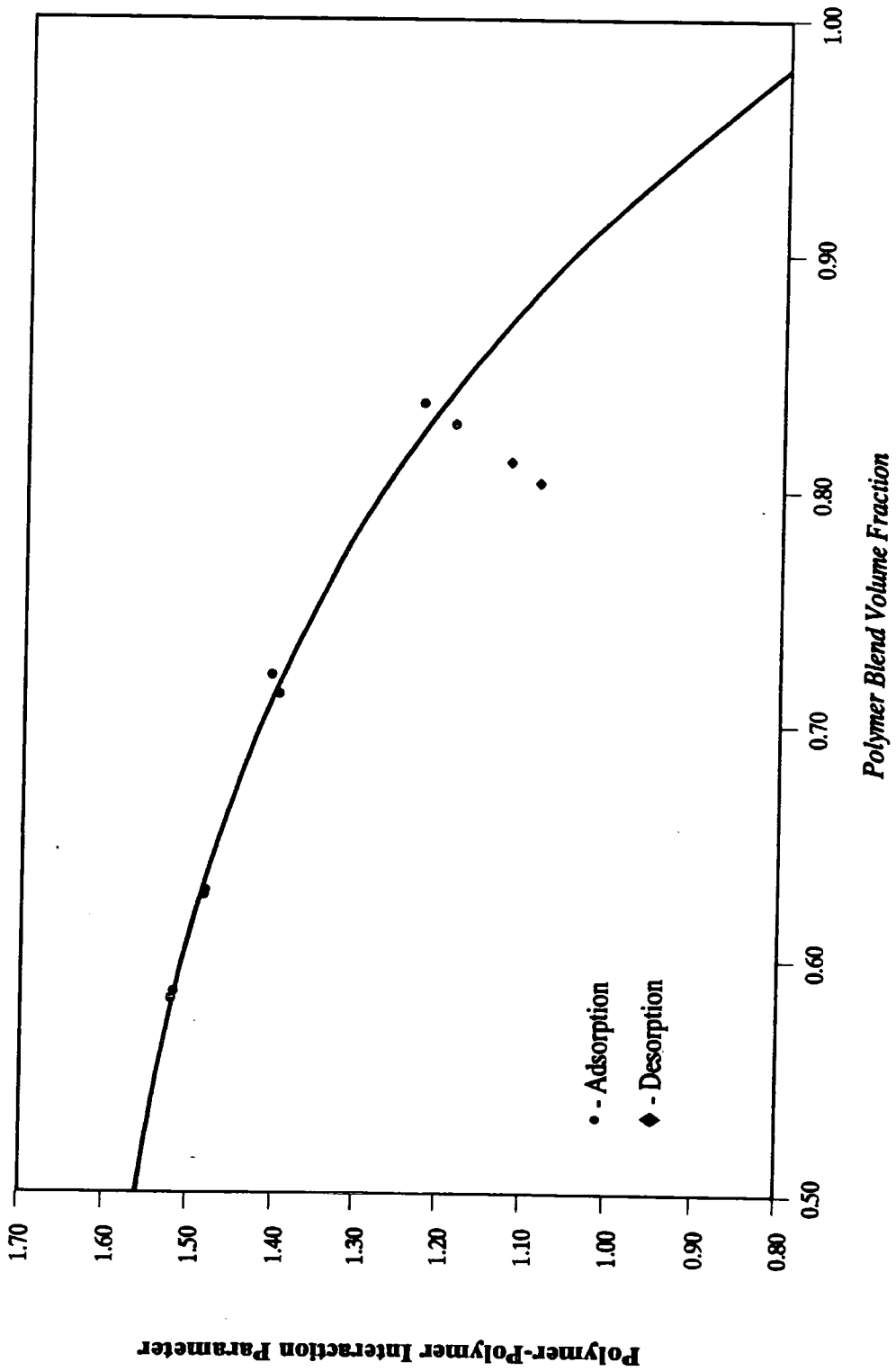


Figure 6.10

Reference (7) quotes $\chi_{1,23}^{\infty} = 0.252$ at $\phi_{23} = 1$, from a linear extrapolation, but fails to record that a correlation coefficient, r_{cc} , of 0.007 is obtained with this fit. This situation can be improved if the order of the polynomial is increased, *i.e.* $r_{cc} = 0.130$ for the quadratic and $r_{cc} = 0.210$ for the cubic. If some of the carbon tetrachloride-poly(vinyl chloride)-poly(ϵ -caprolactone) data at 338K from the same paper are considered,

Table 6.15

Polynomial fits of carbon tetrachloride-poly(vinyl chloride)-poly(ϵ -caprolactone) data at 338K (PVC Wt.Fr. = 0.7653)

Order	A	B	C	D	Intercept at $\phi_{23} = 1$
1	0.5451	0.5197	-	-	1.065
2	2.4150	-3.9755	2.6724	-	1.112
3	-13.4083	53.0946	-65.5265	27.0049	1.160

The correlation coefficients for the fits above are 0.8977, 0.9544 and 0.9830 respectively. These data, shown graphically in figure 6.11, demonstrate a major problem with the linear extrapolation technique. Essentially all of the points, except the last, lie on a straight line which if extrapolated to $\phi_{23} = 1$ would give $\chi_{1,23}^{\infty} = 1.029$, an 11% difference from the cubic fit. Panayiotou and Vera quote $\chi_{1,23}^{\infty} = 1.025$ which suggests that they have not included the last point in the fit, although this is not discussed in the text. These data clearly demonstrate the dilemma which arises when non-linear results are obtained, *i.e.* to decide whether this is truly a non-linear relationship or if the last point is erroneous, and without more information this cannot be resolved. The cubic fit gives the best correlation coefficient but the point of inflection at approximately $\phi_{23} = 0.76$ cannot be readily justified. This entire fitting procedure is without doubt a major source of error which will greatly affect the accuracy of any SVS data which are non-linear.

The only reliable conclusion that can be reached from the χ'_{23} values obtained in this work is that for mixture compositions of up to 40% EVA, the polymer-polymer interaction parameters of the EVA/C₁₄FVA system are likely to be significantly negative and thus favourable. This conclusion is in broad agreement with the IGC results for 353K.

Reference (7) quotes $\chi_{1,23}^{\circ} = 0.252$ at $\phi_{23} = 1$, from a linear extrapolation, but fails to record that a correlation coefficient, r_{cc} , of 0.007 is obtained with this fit. This situation can be improved if the order of the polynomial is increased, *i.e.* $r_{cc} = 0.130$ for the quadratic and $r_{cc} = 0.210$ for the cubic. If some of the carbon tetrachloride-poly(vinyl chloride)-poly(ϵ -caprolactone) data at 338K from the same paper are considered, the results are as in Table 6.15

Table 6.15
Polynomial fits of carbon tetrachloride-poly(vinyl chloride)-
poly(ϵ -caprolactone) data at 338K (PVC Wt.Fr. = 0.7653)

Order	a_0	a_1	a_2	a_3	Intercept at $\phi_{23} = 1$
1	0.5451	0.5197	-	-	1.065
2	2.4150	-3.9755	2.6724	-	1.112
3	-13.4083	53.0946	-65.5265	27.0049	1.160

The correlation coefficients for the fits above are 0.8977, 0.9544 and 0.9830 respectively. These data, shown graphically in figure 6.11, demonstrate a major problem with the linear extrapolation technique. Essentially all of the points, except the last, lie on a straight line which if extrapolated to $\phi_{23} = 1$ would give $\chi_{1,23}^{\circ} = 1.029$, an 11% difference from the cubic fit. Panayiotou and Vera⁽⁷⁾ quote $\chi_{1,23}^{\circ} = 1.025$ which suggests that they have not included the last point in the fit, although this is not discussed in the text. These data clearly demonstrate the dilemma which arises when non-linear results are obtained, *i.e.* to decide whether this is truly a non-linear relationship or if the last point is erroneous, and without more information this cannot be resolved. The cubic fit gives the best correlation coefficient but the point of inflection at approximately $\phi_{23} = 0.76$ cannot be readily justified. This entire fitting procedure is without doubt a major source of error which will greatly affect the accuracy of any SVS data which are non-linear.

The only reliable conclusion that can be reached from the χ_{23}' values obtained in this work is that for mixture compositions of up to 40% EVA, the polymer-polymer interaction parameters of the EVA/C₁₄FVA system are likely to be significantly negative and thus favourable. This conclusion is in broad agreement with the IGC results for 353K.

6.8 REFERENCES

- (1) P.J.T.Tait and M.A.Abushihada, *Polymer*, 18, 810, (1977).
- (2) A.J.Ashworth and G.J.Price, *Macromolecules*, 19, 358, (1986).
- (3) W.R.Summers, Y.B.Tewari and H.P.Schreiber, *Macromolecules*, 5, 12, 1972.
- (4) R.N.Lichtenthaler, R.D.Newman and J.M.Prausnitz, *Macromolecules*, 6, 650, 1973.
- (5) A.J.Ashworth and G.J.Price, *Macromolecules*, 19, 362, (1986).
- (6) J.-M.Braun, M.Cutajar, J.E.Guillet, H.P.Schreiber and D.Patterson, *Macromolecules*, 10, 864, (1977).
- (7) C.Panayiotou and J.H.Vera, *Polymer J.*, 16:2, 89, (1984).
- (8) R.C.Reid, J.M.Prausnitz and B.E.Polling, *'The Properties of Liquids and Gases'*, 4th Edition, McGraw Hill (1987)
- (9) A.J.Ashworth, C.-F.Chien, D.L.Furio, D.M.Hooker, M.M.Kopečni, R.J.Laub and G.J.Price, *Macromolecules*, 17, 1090, (1984).
- (10) R.N.Lichtenthaler, J.M.Prausnitz, C.S.Su, H.P.Schreiber, and D.Patterson, *Macromolecules*, 7, 136, (1974).

Chapter 7 Optical Microscopy

7.1 Introduction

The main attraction of optical microscopy as a characterisation technique is that a direct image of the sample is obtained without a demanding sample preparation. When this instrument is coupled to a hot stage, it is possible to observe many of the thermally induced transitions that macromolecules undergo and obtain an accurate estimation of the temperatures at which they occur. The main disadvantage of the technique is poor resolution, typically 200-600 nm, which is determined by the wavelength of light being used. For many applications in polymer science this is inadequate as the effects being studied are not physically large enough.

Optical microscopy is particularly useful in the study of polymer blends since optical clarity is usually the first indication of the conditions under which two polymers are miscible. However its application is restricted because of poor resolution in systems which have similar refractive indices; this resolution can be improved by a phase contrast facility which utilises a prism to split the transmitted beam. After passing through the sample both beams are recombined in an interferometer which shears the beams vertically against each other. The presence of a phase difference is shown by interference. Caution should be used when interpreting microphotographs as deceptive results can be obtained if the blend either separates into two distinct layers, or forms a two-phase structure which has domains that are smaller than the wavelength of the incident beam.

7.2 Apparatus and Materials

This study was carried out using an Olympus BH2 microscope fitted with a phase contrast condenser and a CK20 objective. The temperature of the sample was varied by a Linkam THM 600 hot stage. The image from the microscope was monitored by a JVC KYF-30 video camera and relayed as a SVHS signal, *via* a Linkam VTO 232 text overlayer, to a Sony UP-5000P mavigraph printer. The polymers were annealed at 373K under vacuum for 12 hours and then left in a desiccator containing silica for another 12 hours before being analysed. The samples were prepared by depositing a small amount of bulk polymer (typically 2mg), at ambient temperature, on a glass cover slip and compressing the polymer with another slip.

7.3 Refractive Index Calculations

As a preliminary to the phase contrast experiments, the refractive indices of the copolymers were calculated using the expression proposed by Gladstone and Dale ,

$$R_{GD} = (n-1)M/\rho = (n-1)V \quad (7.1a)$$

or,

$$n = 1 + R_{GD}/V \quad (7.1b)$$

where,

R_{GD} = Gladstone - Dale Molar Refraction index

n = refractive index

M = molecular weight of monomer unit

V = molar volume, $\text{cm}^3 \text{mol}^{-1}$

Using Goedhart's data ⁽¹⁾, the following refractive indices were calculated,

Table 7.1

Sample	R_{GD}	Mol Wt	n_D at 25°C
EVA	128.29	254.4	1.482
C_{14} FVA	290.11	594.8	1.461

The similarity in the refractive indices calculated above suggested that there was very little contrast between these two materials and consequently it might be difficult to resolve any morphological changes that occurred. This view was supported by some unsuccessful experiments using a polarising microscope. However, a phase contrast microscope was found to have adequate resolution.

7.4 Results

These experiments were undertaken in an attempt to resolve some of the discrepancies between the results of the other techniques. The first interest was the EVA sample itself which was already known to show some type of morphological change when heated. This material was heated at 2K min^{-1} from 313.2 to 343.2 K and the results are shown in Figure 7.1. This clearly shows crystalline structure at 313.2 K which accounts for the turbidity seen in the bulk. As the sample is heated this structure starts to disappear until 343.2 K when it either melts completely or is no longer large enough to be resolved. The turbidimetry work, chapter 3.5, showed that EVA became significantly clearer at approximately 326.2 K, yet this micrograph shows that some structure is still present at 333.2 K. C_{14} FVA was found to be optically transparent between 303.2 and 373.2 K. Two blends of differing composition were prepared by mixing the two copolymers from the bulk at room temperature and the results are described below,

Figures 7.2 a & b: Blend 1 - {49.4% EVA (w/w)}

These two figures show the behaviour of the blend as it was heated from 313.2 to 373.2 K at 5K min^{-1} . The mottled structure of EVA is easily seen against the formless FVA. As the temperature is increased both materials begin to expand although they remain discrete and the structure of EVA is still apparent up to 353.9 K. If the two final frames, at 363.2 and 373.3 K respectively, are studied carefully it can be seen that the phase boundary is still present. These micrographs show that at this composition of blend these materials are not miscible at temperatures between 313.2 and 373.2 K.

Figure 7.2 c : Blend 1 - Annealed at 373.2 K.

These micrographs feature Blend 1 after being annealed at 373.2 K for 10 minutes. It was thought that this apparent immiscibility may not have been a thermodynamic effect but may have arisen from poor dispersion of the polymers during the mixing process and the low mobility of these materials in the melt. To investigate this possibility another sample of Blend 1 was pretreated thermally and then heated at 5K min^{-1} from 303.2 to 373.3 K. The first image shows that after being annealed the polymers are considerably more disperse and that the EVA existed both as large mottled aggregates and small, dark circular areas. When this sample was heated it retained this general structure to 373.2 K, suggesting that these polymers are immiscible.

Figure 7.3 : Blend 2 - {16.7% EVA (w/w)}

The IGC results at 353.2 K produced negative polymer-polymer interaction parameters for both blend compositions below 44% EVA thus suggesting that the polymers were miscible under these conditions. Consequently a FVA rich blend was prepared to investigate this predicted miscibility. This blend was prepared directly from the bulk with neither polymer having any thermal history. The EVA is the dark crystalline material. As the sample was heated the EVA began to melt forming discrete circular structures. These micrographs clearly show again that these materials are immiscible under these conditions, contrary to the IGC findings.

Figure 7.4 : Blend 2 - Solution cast from chloroform

This experiment was the final attempt to observe the miscibility predicted by the IGC data. As the polymers were dissolved in chloroform before being used in the IGC experiments it was thought that this may have influenced the blend morphology. Another sample of Blend 2 was dissolved in the minimum volume of CHCl_3 and cast onto a glass cover slip. The solvent was left to evaporate naturally. From examination of the first image it is apparent that the polymers exist as a highly disperse two-phase structure after being cast from solution. The remaining micrographs show that these materials are still immiscible after being heated to 364.3 K.

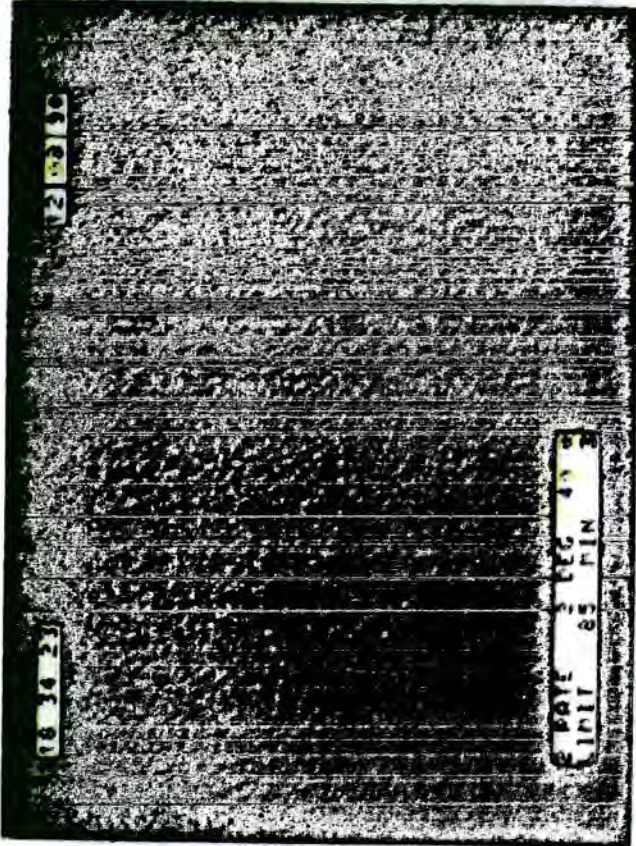
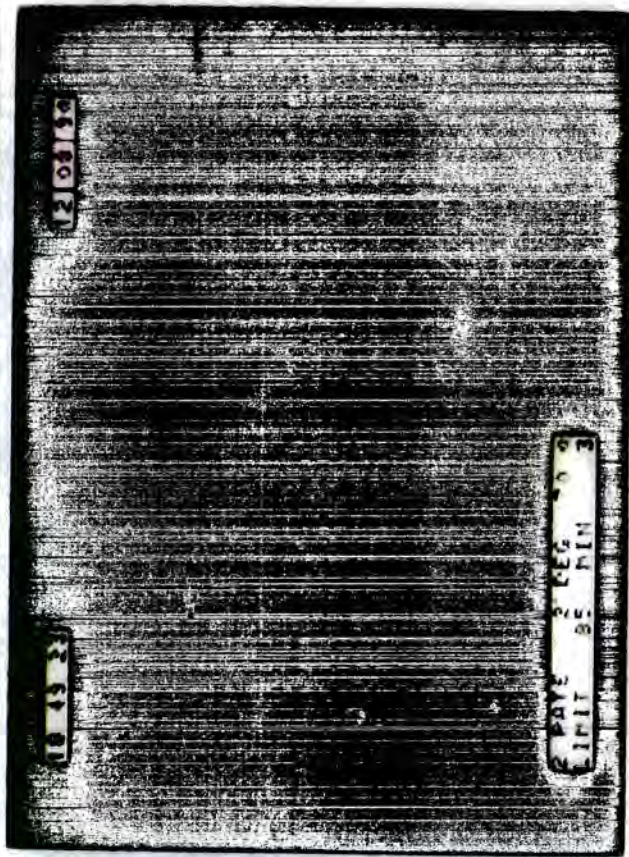


Figure 7.1

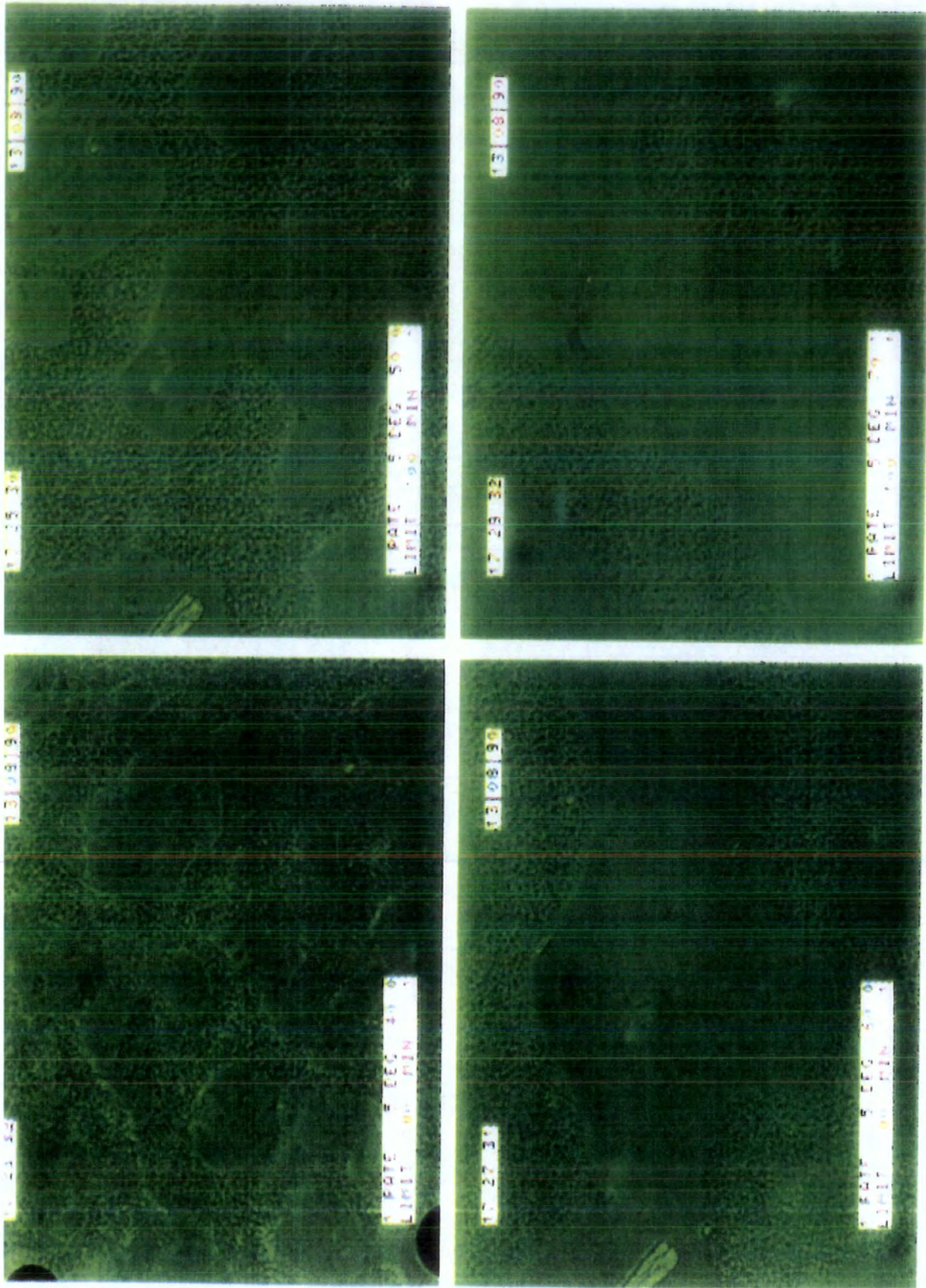


Figure 7.2(a)

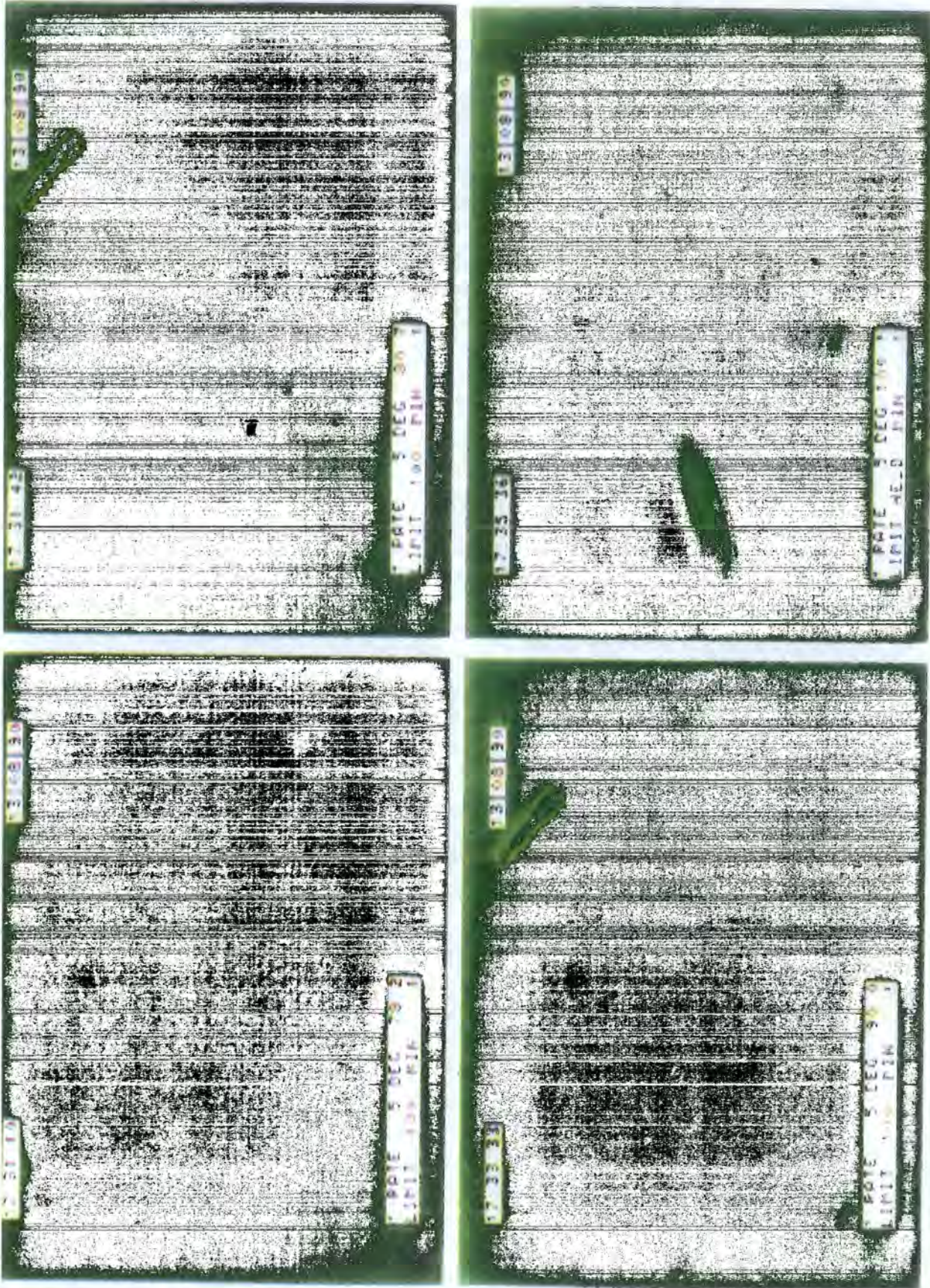


Figure 7.2(b)

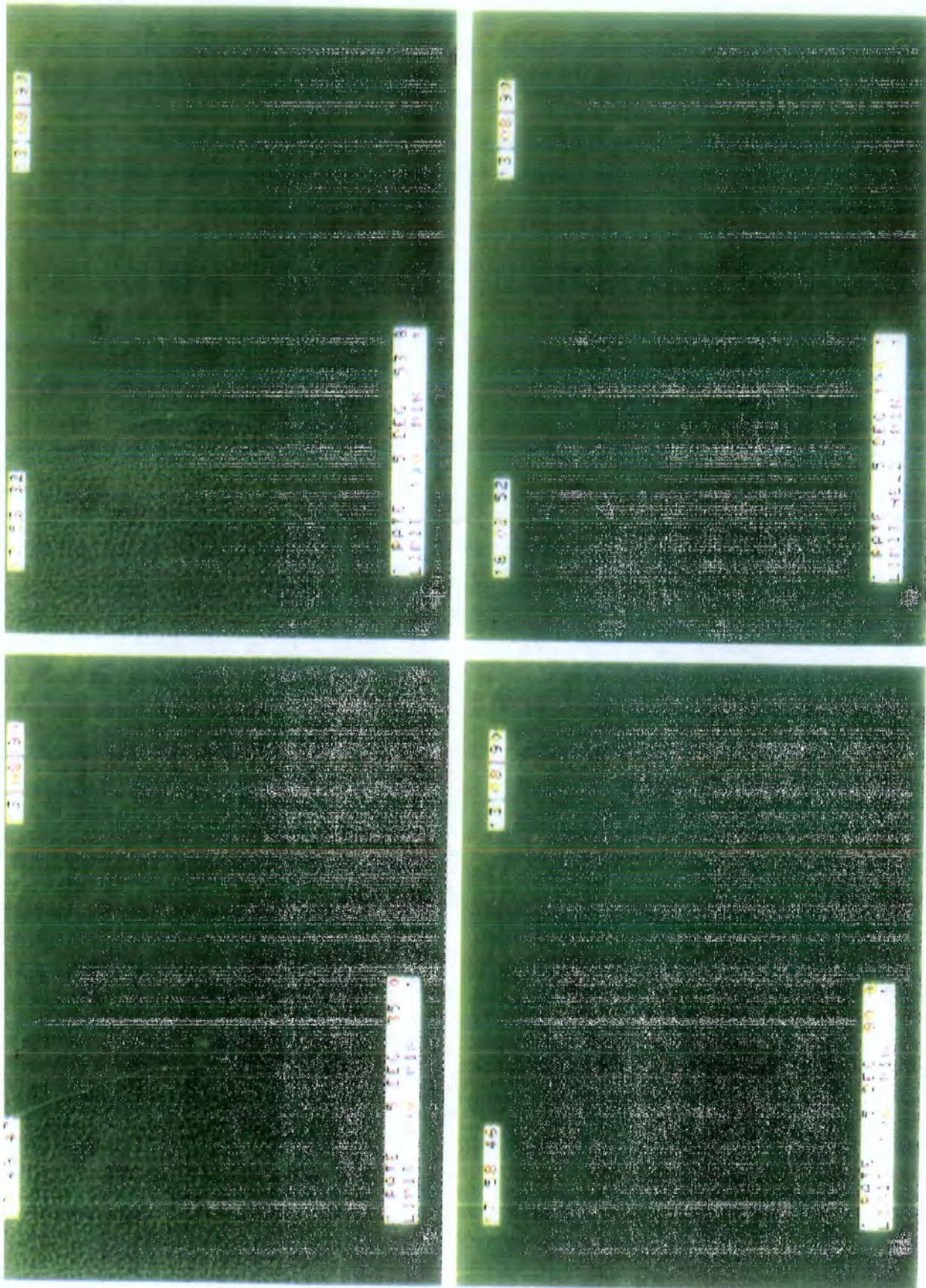


Figure 7.2(c)

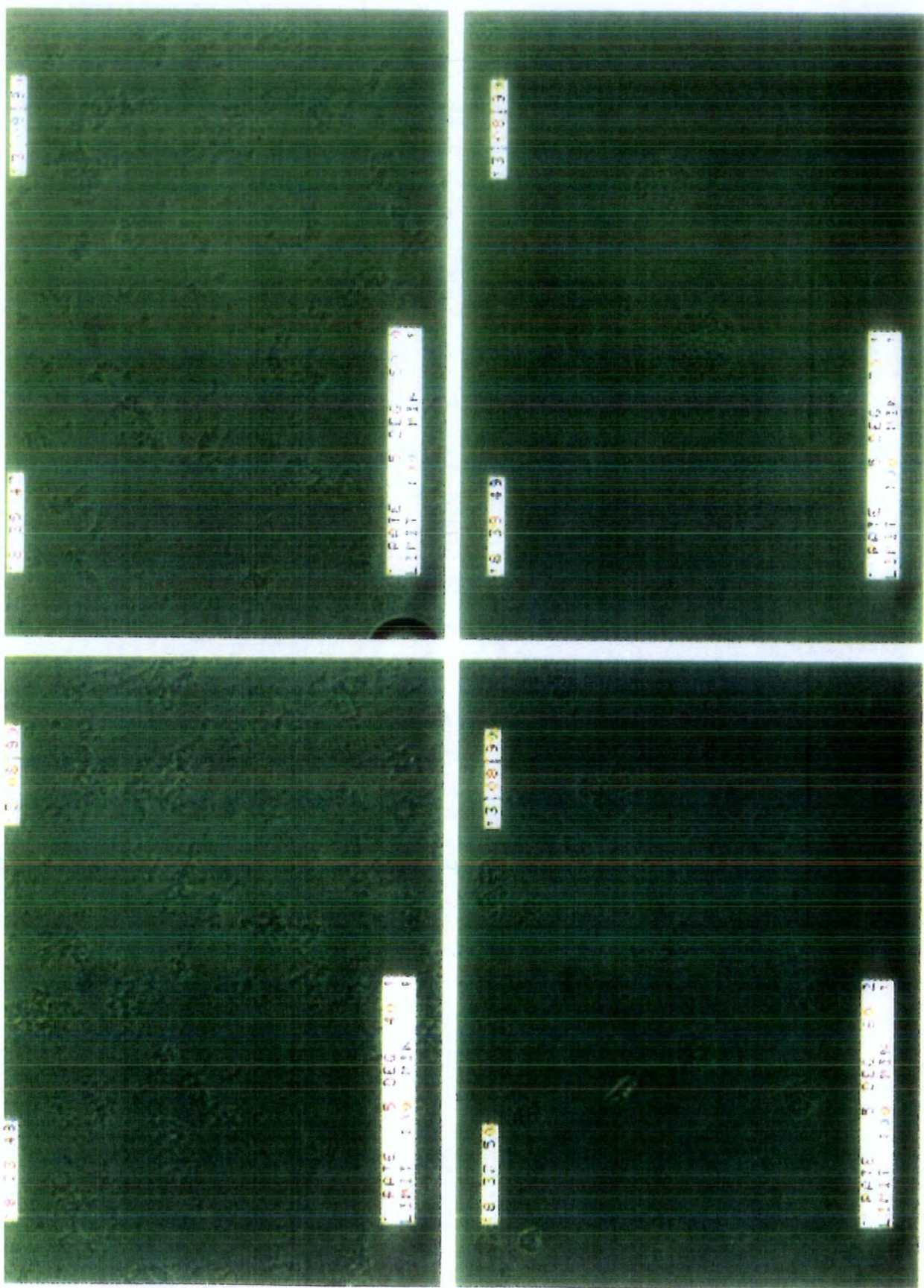


Figure 7.3

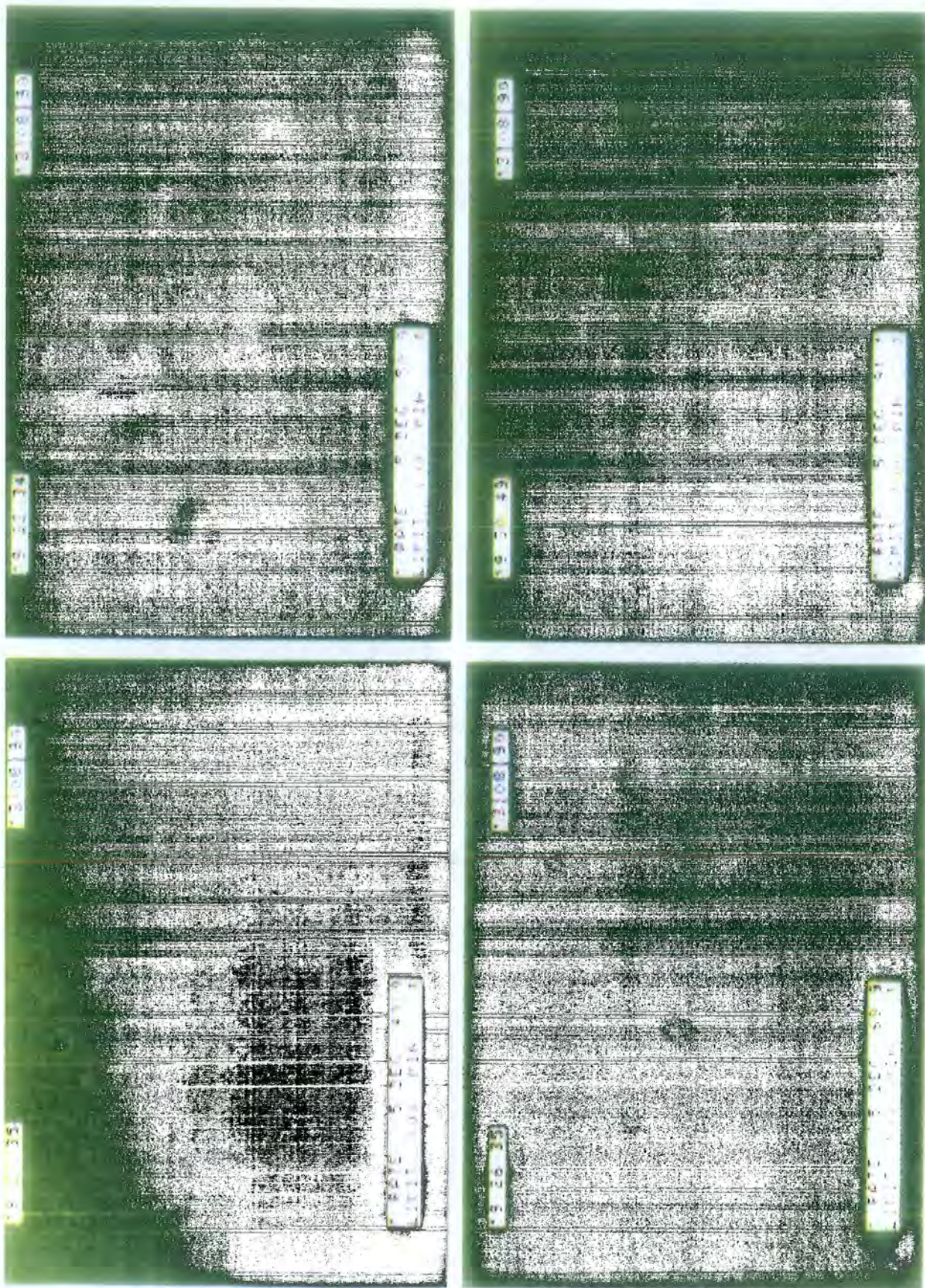


Figure 7.4

7.5 Discussion

From the micrographs on the previous pages it is apparent that these material were immiscible under the conditions pertaining to this work. These results are considered reliable because the polymers neither formed two discrete layers on the microscope slide, (since both could be seen simultaneously), nor did there appear to be any change in the macroscopic surface area of each component which would have occurred had a small two-phase structure been formed. The significance of these experiments is discussed in Chapter 9.

7.6 REFERENCE

- (1) D. W. Van Krevelen, "Properties of Polymers", Elsevier, (1972).

Chapter 8 Simulation of the Phase Boundary

8.1 Introduction

Many authors have tried to simulate theoretically the experimentally observed miscibility limits of various polymer mixtures using either a modified lattice model⁽¹⁻⁴⁾ or Prigogine - Flory's equation of state⁽⁵⁻⁸⁾. The latter approach obtains a polymer-polymer interaction parameter, X_{23} , by fitting to heat of mixing data. The equation of state for the spinodal condition also contains a corresponding entropic interaction parameter, defined as Q_{23} . These enthalpic and entropic interaction parameters can be related *via* a free energy parameter, \bar{X}_{23} , in an expression which is analogous to the classical expansion for the Gibbs free energy,

$$\bar{X}_{23} = X_{23} - T\tilde{V}Q_{23} \quad (8.1)$$

$$\text{and, } \Delta G = \Delta H - T\Delta S \quad (8.2)$$

In the majority of references cited above the spinodal boundary has been simulated by evaluating X_{23} from heat of mixing measurements and then fitting the experimentally determined spinodal to the theoretical spinodal by adjusting the value of Q_{23} . Since Q_{23} has no defined physical significance, *i.e.* it was not part of the original equation of state concept but was introduced subsequently to allow for excess entropic effects which had been observed experimentally, and through its continued use as a fitting parameter, it is now generally considered as nothing more than a 'fudge factor'. However, it is also generally accepted that spinodal boundaries which are obtained from the original equation of state, *i.e.* with $Q_{23} = 0$, commonly show very poor agreement with experimental cloud point curves, from which it can be concluded that the original model of the entropic contribution to the partition function is inadequate. Since any experiment, with the exception of calorimetry, which can be used to calculate a polymer-polymer interaction parameter, is following a free energy change the resulting interaction parameter is \bar{X}_{23} . Thus by using calorimetry in conjunction with another technique, for example IGC or vapour sorption, both X_{23} and \bar{X}_{23} can be evaluated, and, from equation 8.1, Q_{23} can be calculated directly.

8.2 Procedure

The best results are obtained from Prigogine - Flory's equation of state when PVT data for pure components are available. However, an analysis is still

possible if other physical information is known about both the pure components and the binary mixture. These parameters are outlined below.

Pure Component Parameters

- (1) Specific volume, v
- (2) Surface area to unit core volume ratio, s_3/s_2
- (3) Thermal expansion coefficient, α
- (4) Thermal pressure coefficient, γ

Mixture Parameters

- (5) Reduced volume, \tilde{v}
- (6) Enthalpic interaction term, X_{23}
- (7) Free energy interaction parameter, \bar{X}_{23}

There are a variety of routes available to obtain these parameters, *e.g.*,

- (1) Specific volume, v

Specific volumes are usually obtained from reciprocal density values, $v = 1/\rho$, measured either by equal density titration or pycnometry, and some values are available in the literature^(9,10). In this work, a digital densitometer, (described in section 3.3), was used to determine the density of both pure components and seven mixtures of varying composition for temperatures in the range 303 to 333K.

- (2) Surface area to unit core volume ratio, s_3/s_2

This ratio has a significant effect only when X_{23} or Q_{23} are also large, in which cases it acts to skew the spinodal boundary, and it is generally accepted that a rough approximation of its value is adequate under most circumstances⁽²¹⁾. There are a selection of methods available to estimate this ratio, *e.g.*

- (2.1) The tabulated results of Bondi⁽¹¹⁾.

Reference (11) defines the van der Waals volume of a molecule as that which is impenetrable to other species with normal thermal energies, and quotes the corresponding surface area.

These data are tabulated as group contributions and by dissecting the defined segment of the polymer of interest into its constituent parts, a total value of the surface area to volume ratio can be obtained. It should be noted that these values were originally intended to enable the van der Waals volumes and radii of small molecules to be estimated and were not intended for application to polymeric structures. It should also be noted that it is the s_3/s_2 ratio of the segment which is calculated and not that of an entire chain, thus no chain or steric effects are considered in the estimation.

(2.2) Casting shadows^(12-17,19).

This technique involves postulating a geometrical model of the molecule of interest, *e.g.* right cylinders for *n*-alkanes and a right cylinder with hemispherical caps for diphenyl⁽¹⁹⁾, and casting the shadow of this model, in a variety of orientations, and determining an average projected area. By assuming that small molecules are essentially spherical and polymer molecules are cylindrical the ratio s_3/s_2 can be determined.

(2.3) The equation of Abe and Flory^(18,19)

$$s_3/s_2 = (r_3/r_2)^{-1/3} = (v_3^*/v_2^*)^{-1/3} \quad (8.3)$$

This relation is based on the assumption that the number of contact sites per molecule is proportional to the surface area of a sphere of the same hard core volume. Although this equation was originally intended to describe small, non-polar molecules, it does serve as an approximate basis for macromolecular analyses.

Results from these traditional methods, 2.1, 2.2 and 2.3 usually show poor agreement and the majority of previous workers have used some type of mean value. This work used the commercially available molecular modelling software COSMIC to estimate the value of s_3/s_2 . This involved entering the structure of each polymeric segment into the program and obtaining the most favourable conformation of this unit by minimising the energetic effects. The software then calculated the surface area and volume of this optimal conformation. The results obtained from this approach are compared with those from the more traditional routes overleaf,

Comparable estimations of ratio of surface area to volume for the EVA/FVA mixture

Method	s_3/s_2
Bondi	0.997
Abe - Flory	1.473
Cosmic	1.105

Since the value of s_3/s_2 determined by COSMIC lies in between the other estimations it was assumed to be at least as reliable. The value of this ratio is significant in both the determination of mixture miscibility and the shape of the resulting phase boundary.

(3) Thermal Expansion Coefficient, α

The thermal expansion coefficient is defined as,

$$\alpha \equiv \frac{1}{v} \left(\frac{\partial v}{\partial T} \right)_P \quad (2.37)$$

and thus differentiation of the specific volume as a function of temperature data will yield α . Specific volume was found to be substantially linear with respect to both composition and temperature for both the pure components and the EVA/FVA mixtures and the following expression was developed in section 3.3, to characterise these functions,

$$v = (b_0 + b_1T) + (c_0 + c_1T + c_2T^2)w \quad (3.3)$$

where the numerical values of the coefficients and the units are as given on page 51.

By differentiating equation 3.3 with respect to temperature,

$$\alpha = \{b_1 + (c_1 + 2c_2 T)w\}/v \quad (8.4)$$

Using this relationship the thermal expansion coefficient was calculated for each composition, at each temperature, as required.

(4) Thermal Pressure Coefficient, γ

The thermal pressure coefficient is defined as,

$$\gamma \equiv \left(\frac{\partial P}{\partial T} \right)_v \quad (2.39)$$

Although direct measurements of γ have been carried out on polymeric materials^(20,21) the experiments are difficult and generally avoided since the term is only weakly influential in the equation of state⁽³⁰⁾.

The most common route used to evaluate γ is *via* the Hildebrand solubility parameter, δ . The cohesive energy density, (CED), of a material is a measure of its molecular cohesion and this is related algebraically to the solubility parameter and thermal pressure coefficient as follows,

$$P_i = T(\alpha/\beta_T) = T\gamma \quad (8.5)$$

$$\text{and } P_i = m(\text{CED}) \quad (8.6)$$

$$\text{but } \delta^2 = (\text{CED}) \quad (8.7)$$

hence

$$m\delta^2 = T\gamma \quad (8.8)$$

i.e.,

$$\gamma = \alpha/\beta_T \quad (8.9)$$

where,

α = thermal expansion coefficient, K^{-1}

β_T = isothermal compressibility, atm^{-1}

T = temperature, K

m = proportionality coefficient which is unity for polymers

P_i = pressure, atm

The solubility parameter of a polymer can be calculated from the sum of its group contributions in accordance with the theory of Small⁽²²⁾. This theory assumes that the solubility parameter is a linear function of an additive structural constant, f_i , defined as the 'molar attraction constant',

$$\delta = \rho \sum f_i / M \quad (8.10)$$

where,

M = molecular weight of a repeat unit, g

ρ = density, g cm⁻³

Small evaluated the molar attraction constants for a selection of common functional groups and chemical sequences from vapour pressure and heat of vaporisation data. These original data have subsequently been improved by Hoy⁽²³⁾ and Van Krevelen⁽²⁴⁾.

The solubility parameters and thermal pressure coefficients of EVA and FVA were evaluated at 353K as,

Table 8.1

Polymer	$\delta / (\text{cal cm}^{-3})^{0.5}$	$\gamma / \text{atm K}^{-1}$
EVA	8.05	0.1835
FVA	8.07	0.1844

The temperature dependence of γ is given by,

$$\gamma = \gamma_0 - \gamma_0(1+2\alpha_0 T) \Delta T / T \quad (8.11)$$

or it can be calculated directly from density data if they are available.

Mixture Parameters

(5) Reduced volume, \tilde{v}

The reduced volume is a measure of the volume change that occurs on mixing two materials and is related to the hard core volume by,

$$\tilde{v} = v/v^* \quad (2.33)$$

It is commonly obtained by measuring the density of a number of blends of differing compositions and fitting these data to provide a continuous function with respect to composition. The density data obtained in this work were substantially linear with respect to composition, (Table 3.3 and Figure 3.3)

(6) Enthalpic Interaction Parameter, X_{23}

This parameter represents the difference in energies between homogeneous and heterogeneous contacts in the mixture and thus should be independent of both temperature and composition. It is evaluated by fitting equation 2.52c to experimental heat of mixing data using a non-linear least squares procedure,

$$\Delta H_{mix} = n_2 V_1^* \left\{ \theta_3 X_{23} / \tilde{v}_2 + P_1^* (1/\tilde{v} - 1/\tilde{v}_2) - (\phi_2^* / \phi_1^*) P_2^* (1/\tilde{v} - 1/\tilde{v}_3) \right\} \quad (2.52c)$$

where X_{23} is the adjustable parameter. This has been carried out on the heat of mixing data obtained at 348.7K, described in chapter 5, and the results are quoted in Table 8.2. The recalculated values of ΔH_{mix} were obtained by re-inserting the value of X_{23} , obtained from the fit, into equation 2.52c and solving for ΔH_{mix} .

Table 8.2

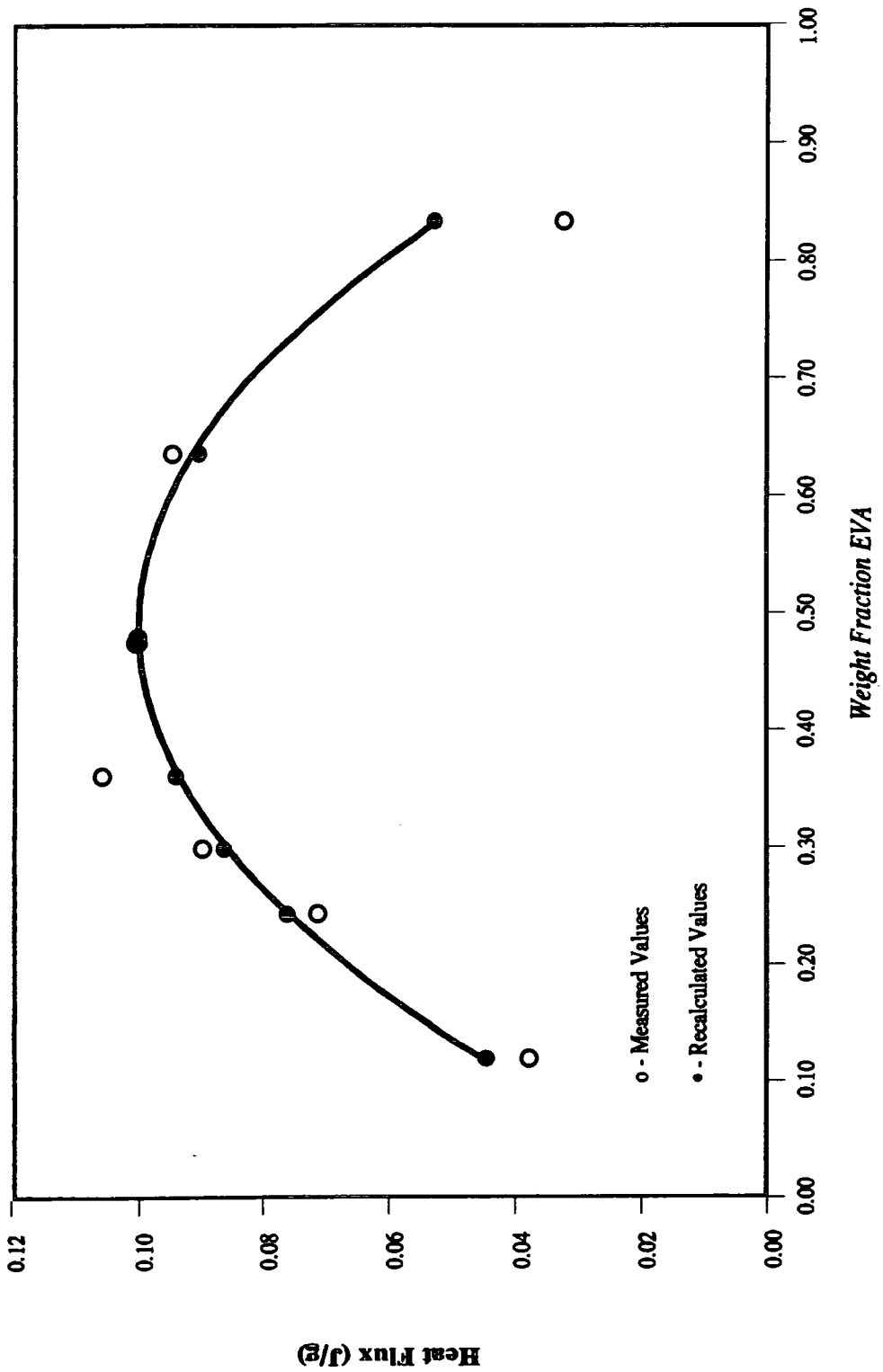
Measured and recalculated heat of mixing values at 348.7K

Run	Wt.Fr. EVA	Measured $\Delta H_{mix} / 10^{-2} \text{J g}^{-1}$	Recalculated $\Delta H_{mix} / 10^{-2} \text{J g}^{-1}$	Difference 10^{-2}J g^{-1}
1	0.119	3.804	4.468	0.664
2	0.243	7.162	7.647	0.512
3	0.299	9.005	8.657	0.348
4	0.361	10.596	9.440	- 1.156
5	0.475	10.077	10.025	- 0.052
6	0.479	10.047	10.026	- 0.021
7	0.635	9.496	9.068	- 0.410
8	0.833	3.257	5.286	2.029

Fitted value of $X_{23} = 5.667$ bar

These data are displayed in Figure 8.1. Although heat of mixing measurements were also performed at 359.3K these data have not been used in the simulation of the phase boundary for two reasons. Firstly, by definition, X_{23} should be independent of temperature and consequently the two sets of data should yield the same value of X_{23} , and secondly, owing to time constraints, only three experimental points were recorded at 359.3K and this was felt to be insufficient to justify the fitting procedure. The X_{23} value obtained at 348.7K, converted to J cm^{-3} , is compared to some literature values in Table 8.3.

Heat of Mixing for EVA/FVA Mixture at 348.7K
Measured and Recalculated Values



Weight Fraction EVA

Figure 8.1

Table 8.3

Comparison of interaction parameter values obtained from heat of mixing measurements

Polymer Mixture	$\Delta X_{23} / \text{J cm}^{-3}$	Reference
EVA / FVA	0.567 (348.7 K)	this work
(tetraglyme) - (4-phenoxy phenyl phenyl sulphone)	-40.00 (363.2 K)	25
(Cereclor 52) - (2-ethylhexyl acetate)	-2.63 (363.2 K)	7

where,

tetraglyme - model compound for poly(ethylene oxide), PEO: 4-phenoxy phenyl phenylsulphone - model compound for poly(ether sulphone), PES: Cereclor 52 - model compound for chlorinated poly(ethylene), CPE: 2-ethylhexyl acetate - model compound for poly(ethylene - vinyl acetate) copolymer, EVA.

It should be noted that both PEO/PES and CPE/EVA mixtures are known to be miscible, and undergo lower critical solution type phase separation, and that the heats of mixing values quoted above are those of low molecular weight analogues, and not the polymers themselves.

When allowances for these differences are made, the X_{23} value obtained for this immiscible, polymeric system appears to have the correct sign and order of magnitude.

(6) Free Energy Interaction Parameter, \bar{X}_{23}

The free energy interaction parameter can be obtained from a variety of experiments, *e.g.* melting point depression⁽²⁵⁾, solvent vapour sorption⁽²⁶⁾ or

inverse phase gas chromatography^(1,27). This work has used the data from the IGC experiments detailed in chapter 4 because of the volume of this information.

The Flory - Huggins - Chang - Miller theory polymer-polymer interaction parameter, $\bar{\chi}_{23}'$, is given by equation 4.7,

$$\bar{\chi}_{23}' = \frac{V_2}{V_1} \left\{ \frac{1}{\phi_2 \phi_3} \text{Ln} \left(\frac{V_{gc,23}}{w_2 V_2 + w_3 V_3} \right) - \phi_2 \text{Ln} (V_{gc,2}/V_2) - \phi_3 \text{Ln} (V_{gc,2}/V_2) \right\} \quad (4.7)$$

where,

$\bar{\chi}_{23}'$ = true polymer-polymer interaction parameter.

V_1 = molar volume of solvent, $\text{cm}^3 \text{mol}^{-1}$

V_2 = molar volume of polymer, $\text{cm}^3 \text{mol}^{-1}$

ϕ_i = volume fraction of component 'i'

v_i = specific volume of component 'i', $\text{cm}^3 \text{g}^{-1}$

w_i = weight fraction of component 'i' in blend

To convert equation 4.7 into the corresponding equation of state expression it is necessary to firstly replace the lattice theory volume fraction with the EOS hard core volume fractions, ϕ_i^* ,

$$\phi_1^* \equiv 1 - \phi_2^* \equiv N_1 r_1 / (N_1 r_1 + N_2 r_2) \quad (2.45a)$$

or,

$$\phi_1^* \equiv w_1 V_1^* / (w_1 V_1^* + w_2 V_2^*) \quad (2.45b)$$

where,

w_i = weight fraction of component 'i'

V_i^* = molar hard core volume of component 'i'

r_i = number of segments per molecule

N_i = number of molecules

As mentioned in chapter 2, the hard core volume fraction is defined as the volume which a segment of polymer would occupy at 0 K, and is more useful than a normal volume fraction because it is independent of temperature and pressure.

Since the characteristic dimension in EOS theory is an arbitrary segment of a polymer chain and the enthalpic contribution is based on the relative surface areas, it is convenient to introduce the surface fraction, θ ,

$$\theta_2 \equiv 1 - \theta_3 \equiv N_2 r_2 s_2 / (N_2 r_2 s_2 + N_3 r_3 s_3) \quad (2.46a)$$

or,

$$\theta_2 \equiv \frac{(s_3/s_2) \phi_2^*}{(s_3/s_2) \phi_2^* + \phi_3^*} \quad (2.46b)$$

where, $s_3/s_2 =$ surface area per unit volume ratio

The non-combinatorial contribution to mixing is described by the parameter χ^* and this can be easily calculated by reformulating equations 4.5a, 4.5b and 4.5c in terms of the hard core parameters, *i.e.*,

$$\bar{\chi}_{12} = \text{Ln} \left\{ \frac{RTv_2^*}{V_{gc} V_1 P_1^o} \right\} - \left\{ 1 - \frac{V_1}{(\bar{Mn})_2 v_2^*} \right\} - \frac{P_1^o}{RT} \{ B_{11} - V_1 \} \quad (8.11)$$

$$\bar{\chi}_{13} = \text{Ln} \left\{ \frac{RTv_3^*}{V_{gc} V_1 P_1^o} \right\} - \left\{ 1 - \frac{V_1}{(\bar{Mn})_3 v_3^*} \right\} - \frac{P_1^o}{RT} \{ B_{11} - V_1 \} \quad (8.12)$$

$$\begin{aligned} \bar{\chi}_{1,23} = \text{Ln} \left\{ \frac{RT(w_2 v_2^* + w_3 v_3^*)}{V_{gc,23} V_1 P_1^o} \right\} - \left\{ 1 - \frac{V_1}{(\bar{Mn})_2 v_2^*} \right\} \theta_2 \\ - \left\{ 1 - \frac{V_1}{(\bar{Mn})_3 v_3^*} \right\} \theta_3 - \frac{P_1^o}{RT} \{ B_{11} - V_1 \} \quad (8.13) \end{aligned}$$

\bar{X}_{23} and the free volume on mixing contribution can be related explicitly to χ^* by the corresponding states^(28,29) form of the the EOS theory,

$$RT \chi_{12}^* = \frac{v_1^* \bar{X}_{12}}{\tilde{v}_2} + P_1^* v_1^* \left(\frac{1}{\tilde{v}_1} - \frac{1}{\tilde{v}_2} + 3 \hat{T}_1 \text{Ln} \frac{\tilde{v}_1^{1/3} - 1}{\tilde{v}_2^{1/3} - 1} \right) \quad (8.14)$$

Similarly, for a ternary system with a mixed stationary phase, equation 8.14 becomes,

$$RT \chi_{1(23)}^* = \frac{s_1 v_1^*}{\tilde{v}} \left(\frac{\bar{X}_{12}}{s_1} \theta_2 + \frac{\bar{X}_{13}}{s_1} \theta_3 - \frac{\bar{X}_{13}}{s_2} \theta_2 \theta_3 \right) + P_1^* v_1^* \left(\frac{1}{\tilde{v}_1} - \frac{1}{\tilde{v}} + 3 \hat{T}_1 \text{Ln} \frac{\tilde{v}_1^{1/3} - 1}{\tilde{v}^{1/3} - 1} \right) \quad (8.15)$$

where,

subscript 1 refers to the IGC probe species, with 2 and 3 referring to EVA and FVA respectively in the polymer mixture.

R = Universal gas constant, (82.057 cm³ atm K⁻¹ mol⁻¹)

T = absolute temperature, K

s_i = surface area to volume ratio of component 'i', m⁻¹

θ_i = surface fraction of component 'i' in the stationary phase

The polymer solvent interaction parameters, \bar{X}_{12} and \bar{X}_{13} , are evaluated from the appropriate versions of equation 8.14. The value of s₁, i.e. the surface to volume ratio for each solvent probe was also obtained from the COSMIC molecular modelling package described above and the results are quoted in Table 8.4.

Table 8.4

Values of the surface area to volume ratio for the solvents used in the IGC experiments

Solvent	$s_1 / \text{\AA}$
Pentane	2.294
Hexane	2.233
Heptane	2.057
Octane	2.200
Methanol	2.391
Isopropyl alcohol	2.447
Acetone	2.295
Methylethylketone	2.324
Methyl Acetate	2.346
Ethyl Acetate	2.406
Dichloromethane	1.986
Chloroform	1.878
Carbon Tetrachloride	1.829
Benzene	2.398
Toluene	2.589
Cyclohexane	2.451

Once all of this information has been obtained, equation 8.15 can be solved for \bar{X}_{23} .

8.2 Evaluation of equation of state parameters

The EOS parameters of both the pure components and the mixture can now be derived from the physical information detailed above. The following is a brief outline of these calculations and the interdependence of these parameters.

8.2.1 The reduced volume, \tilde{v} , and hard core volume, v^*

The reduced volumes of the pure components and the mixture were calculated from equation 2.38, *via* the thermal expansion coefficients,

$$\tilde{v} = \left\{ 1 + \frac{\alpha T}{3(1 + \alpha T)} \right\} \quad (2.38)$$

thus, \tilde{v}_2 , \tilde{v}_3 and \tilde{v}_{23} were obtained. Equation 2.33 relates the hard core volume of the pure components and the mixture to the reduced parameters.

$$\tilde{v} = v/v^* \quad (2.33)$$

$$\text{or } v^* = v/\tilde{v}$$

8.2.2 Hard core pressure, P^*

Equation 2.40 was used to calculate the hard core pressures of the pure components from thermal pressure coefficients and the reduced volumes.

$$P^* = \gamma T \tilde{v}^2 \quad (2.40)$$

The hard core pressure of the mixture is related to the pure component values by equation 2.47,

$$P^* = \phi_2 P_2^* + \phi_3 P_3^* - \phi_2 \phi_3 X_{23} \quad (2.47)$$

8.2.3 Hard core temperature, T^*

The hard core temperature was obtained by solving the equation of state, equation 2.36, assuming the pressure to be substantially zero for the reduced temperatures,

$$\tilde{T} = (\tilde{v}^{1/3} - 1)/\tilde{v}^{4/3} \quad (2.36)$$

and substituting these values into equation 2.34,

$$\tilde{T} = T/T^* \quad (2.34)$$

The hard core temperature of the mixture is related to the pure component values by equation 2.48,

$$T^* = \frac{\phi_2 P_1^* + \phi_3 P_2^* - \phi_2 \theta_3 X_{23}}{\phi_2 P_1^* / T_1^* + \phi_3 P_2^* / T_2^*} \quad (2.48)$$

Once all of these parameters were evaluated the equation of state was used to predict the mixtures thermodynamic properties and behaviour.

8.3 Results

Tables 8.5 and 8.6 list the characteristic parameters of EVA and FVA respectively which have been calculated using the information and procedures outlined above.

Table 8.5: EOS parameters for EVA - $s_2 = 2.3251 \text{ \AA}$

Temperature / K	$v / \text{cm}^3 \text{ g}^{-1}$	$v^* / \text{cm}^3 \text{ g}^{-1}$	T^* / K	P^* / bar
353	1.10456	0.88932	6293.3	4106.5
373	1.12269	0.89820	6508.4	3927.7
393	1.14083	0.90722	6723.8	3719.4

Table 8.6: EOS parameters for FVA - $s_3 = 2.0633 \text{ \AA}$

Temperature / K	$v / \text{cm}^3 \text{ g}^{-1}$	$v^* / \text{cm}^3 \text{ g}^{-1}$	T^* / K	P^* / bar
353	1.09042	0.90087	6031.6	3909.5
373	1.10559	0.90775	7145.3	3776.8
393	1.12075	0.91477	7359.2	3621.0

To judge the reliability of these values the EVA results were compared with those in the literature for an EVA copolymer (EVA 45) and an EVA model compound OC-AC⁽⁷⁾. However, the materials used in reference (7) had the following physical characteristics,

$$\text{EVA copolymer: } \bar{M}_n = 37,700 \quad \bar{M}_w = 256,000 \quad \bar{M}_w / \bar{M}_n = 6.79$$

Model Compound: 1-methyl heptyl acetate, molecular weight = 172.3 g mol^{-1}

Since the EVA sample used in this work had a number average molecular weight one order of magnitude lower than that for the EVA sample described above, it was expected that its EOS properties would lie somewhere between those of the copolymer and the model compound. The comparison is shown in Table 8.7.

Table 8.7

Comparison of EOS parameters for EVA45, OC-AC and EVA

Material	T / K	v / cm ³ g ⁻¹	v* / cm ³ g ⁻¹	T* / K	P* / bar
EVA45	356.7	1.0636	0.9288	9250.3	3761.8
OC-AC	356.7	1.2442	0.9877	6067.2	2769.3
EVA	353	1.1046	0.8893	6293.3	4106.5

As anticipated, the specific volume and hard core characteristic temperature of the EVA fall between those of the EVA45 and the OC-AC. However the hard core characteristic volume and pressure do not. This discrepancy arises from the dependence of these terms on the reduced volume, \tilde{v} , and hence on the thermal expansion coefficient. The thermal expansion coefficient of the EVA was estimated, from the density-temperature measurements, to be an order of magnitude greater than that for either EVA45 or OC-AC,

$$i.e. \quad \alpha_{(EVA, 353K)} = 7.52 \times 10^{-3} \text{ K}^{-1}$$

$$\alpha_{(EVA45, 367.7K)} = 4.51 \times 10^{-4} \text{ K}^{-1}$$

$$\alpha_{(OC-AC, 367.7K)} = 8.85 \times 10^{-4} \text{ K}^{-1}$$

The α values of EVA45 and OC-AC were determined by dilatometry at a single temperature. It was concluded that this discrepancy in magnitude must have arisen from the method of estimation although this could not be verified as no reference experiments were employed.

Equation of state theory gives the chemical potential of component 2 as,

$$\frac{\partial}{\partial \phi_2} \left(\frac{\Delta \mu_1}{RT} \right)_{T,P} = 0 \quad (8.16)$$

This equation is then used to derive the phase boundary from the spinodal condition defined as,

$$\begin{aligned}
 & -\frac{1}{\phi_1} + 1 - \frac{r_1}{r_2} - \frac{P_1^* V_1^*}{RT_1^*} \frac{\partial \bar{v}}{\partial \phi_2} \frac{1}{\bar{v}^{2/3} (\bar{v}^{1/3} - 1)} + \frac{P_1^* V_1^*}{RT_{sp}} \frac{\partial \bar{v}}{\partial \phi_2} \left(\frac{1}{\bar{v}^2} - \tilde{P}_1 \right) \\
 & + \frac{V_1^* X_{12}}{RT_{sp}} \left(\frac{2\theta_1 \theta_2^2}{\bar{v} \phi_1 \phi_2} - \frac{\theta_2^2}{\bar{v}^2} \frac{\partial \bar{v}}{\partial \phi_2} \right) - \frac{V_1^* Q_{12}}{R} \frac{2\theta_1 \theta_2^2}{\bar{v} \phi_1 \phi_2} = 0
 \end{aligned}
 \tag{8.17}$$

where the partial derivatives are given in the equations below

$$\begin{aligned}
 \frac{\partial \bar{v}}{\partial \phi_2} &= \left\{ \frac{\partial \tilde{P}}{\partial \phi_2} - \frac{1}{T} \left(\tilde{P} + \frac{1}{\bar{v}^2} \right) \frac{\partial \tilde{T}}{\partial \phi_2} \right\} / \\
 & \left\{ \frac{2}{\bar{v}^3} - \tilde{T} \left(\bar{v}^{1/3} - \frac{2}{3} \frac{1}{\bar{v}^{5/3} (\bar{v}^{1/3} - 1)} \right) \right\} \\
 \frac{\partial \tilde{P}}{\partial \phi_2} &= \frac{P}{P^*} \left\{ P_1^* - P_2^* + X_{12} \theta_2 (\theta_1 / \phi_2 - 1) \right\} \\
 \frac{\partial \tilde{T}}{\partial \phi_2} &= \frac{T}{P^*} \left\{ \frac{P_2^*}{T_2^*} - \frac{P_1^*}{T_1^*} \right\} + \frac{\tilde{T}}{P^*} \left\{ P_1^* - P_2^* + X_{12} \theta_2 (\theta_1 / \phi_2 - 1) \right\}
 \end{aligned}$$

This equation was solved iteratively using the technique known as inverse parabolic interpolation in which a root of an equation is first bracketed and thereafter a parabola is fitted to successive error terms for the three 'best' trial values until the absolute value of the error is either minimised or becomes less than some preset value. The routine used was a Modula 2 version of the Pascal procedure known as Brent's method and which is fully described in Chapter 10, pp 318-322 of 'Numerical Recipes in Pascal'⁽³¹⁾. In this particular

case a mixture composition was chosen, for which X_{23} and Q_{23} were known and the reduced parameters and composition variables at successive trial temperatures were evaluated; when the error term had been reduced to a suitable value the corresponding trial temperature was taken as T_{sp} . This process was repeated for the mixture compositions for which data were available. Collectively these solutions represent the spinodal boundary. The results are listed in Tables 8.8, 8.9 and 8.10. In the interests of brevity and clarity the X_{23} , Q_{23} and spinodal temperatures calculated for each solvent have been combined as arithmetic means for each composition at each temperature: a full listing of the individual results is given in Appendix 1. The standard deviation in interaction parameter values from different solvents has been calculated, and is displayed in figures 8.2, 8.3 and 8.4 as an error bar. It should be noted that a spinodal temperature is not quoted for the mixture of weight fraction 0.2515 EVA at 353K, because equation 8.18 would not converge between limits of 0 and 5000K for the X_{23} and Q_{23} values obtained.

Table 8.8

Mean values of \bar{X}_{23} , Q_{23} and Spinodal temperature
for mixtures at 353K

Wt Fraction	\bar{X}_{23}/bar	$Q_{23}/\text{bar K}^{-1}$	T_{spin}/K
0.0904	-8.25	-0.1292	6.32
0.2515	-500.13	1.1750	-
0.2905	324.56	-0.7404	7.33
0.3588	446.40	-1.0214	5.88
0.5000	306.49	-0.6947	8.79
0.7496	212.31	-0.4742	11.52
0.8033	-299.59	0.6991	51.37

Table 8.9

Mean \bar{X}_{23} , Q_{23} and Spinodal temperatures for the
EVA/FVA mixture at 373K

Wt Fraction	\bar{X}_{23} /bar	Q_{23} / bar K ⁻¹	T_{spin} /K
0.0904	- 35.07	0.0892	15.20
0.2515	300.10	-0.6436	9.62
0.2905	235.68	-0.5023	11.40
0.3588	183.84	-0.3884	16.24
0.5000	448.80	-0.9622	6.81
0.7496	606.83	-1.2971	4.87

Table 8.10

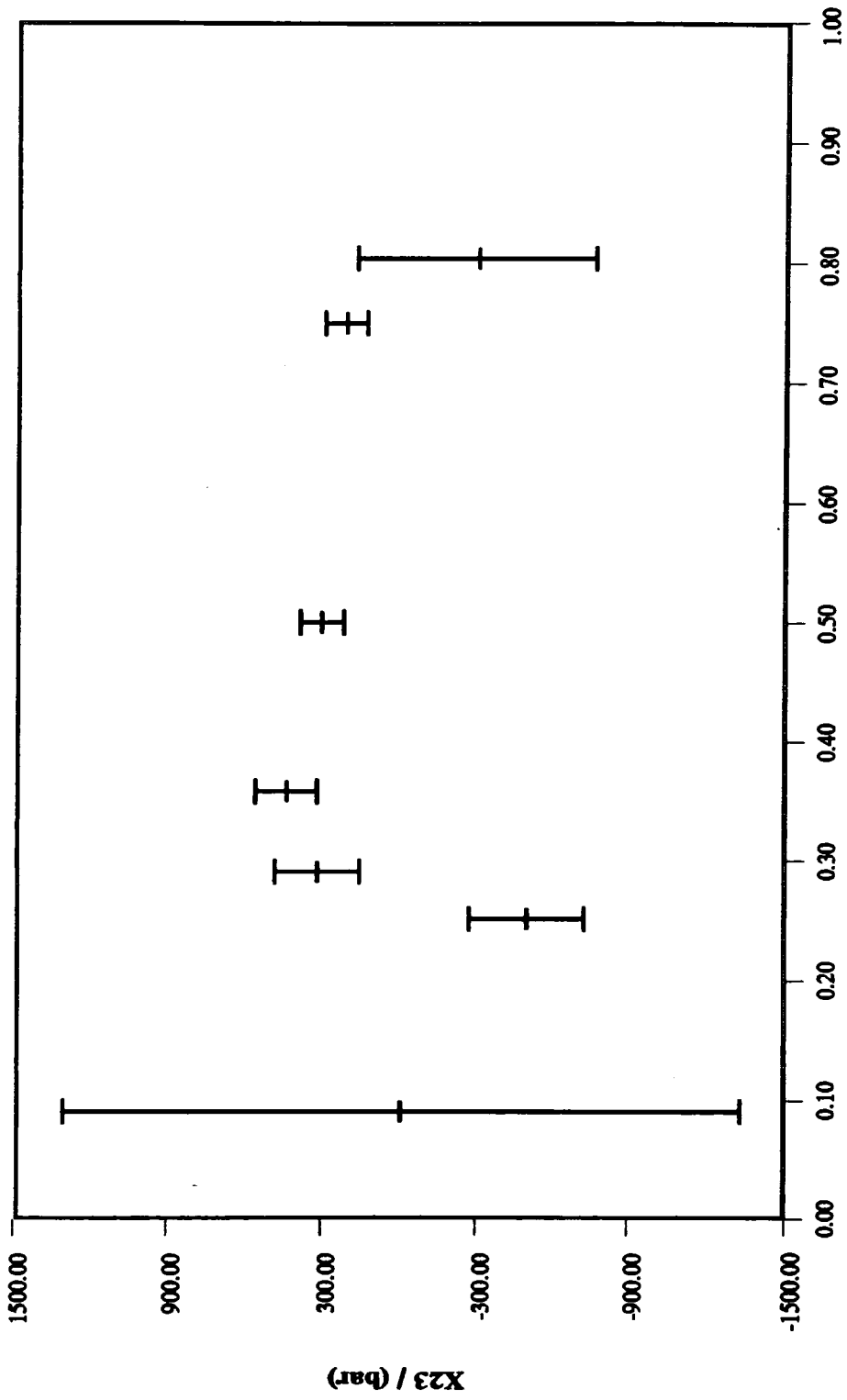
Mean values of \bar{X}_{23} , Q_{23} and Spinodal
temperature for mixture at 393K

Wt Fraction	\bar{X}_{23} /bar	Q_{23} / bar K ⁻¹	T_{spin} /K
0.0904	164.56	-0.3292	11.45
0.2515	186.54	-0.3731	18.12
0.2905	338.31	-0.6853	8.35
0.3588	417.18	-1.1233	7.21
0.5000	574.88	-1.1661	6.81
0.7496	691.91	-1.3969	4.25

The \bar{X}_{23} data at 353, 373 and 393K are displayed as functions of EVA weight fraction in Figures 8.2, 8.3 and 8.4 respectively, and the simulated spinodals are shown in Figures 8.5, 8.6 and 8.7.

Mean values of X23 for EVA/FVA mixture at 353K

Equation of state analysis of IGC results

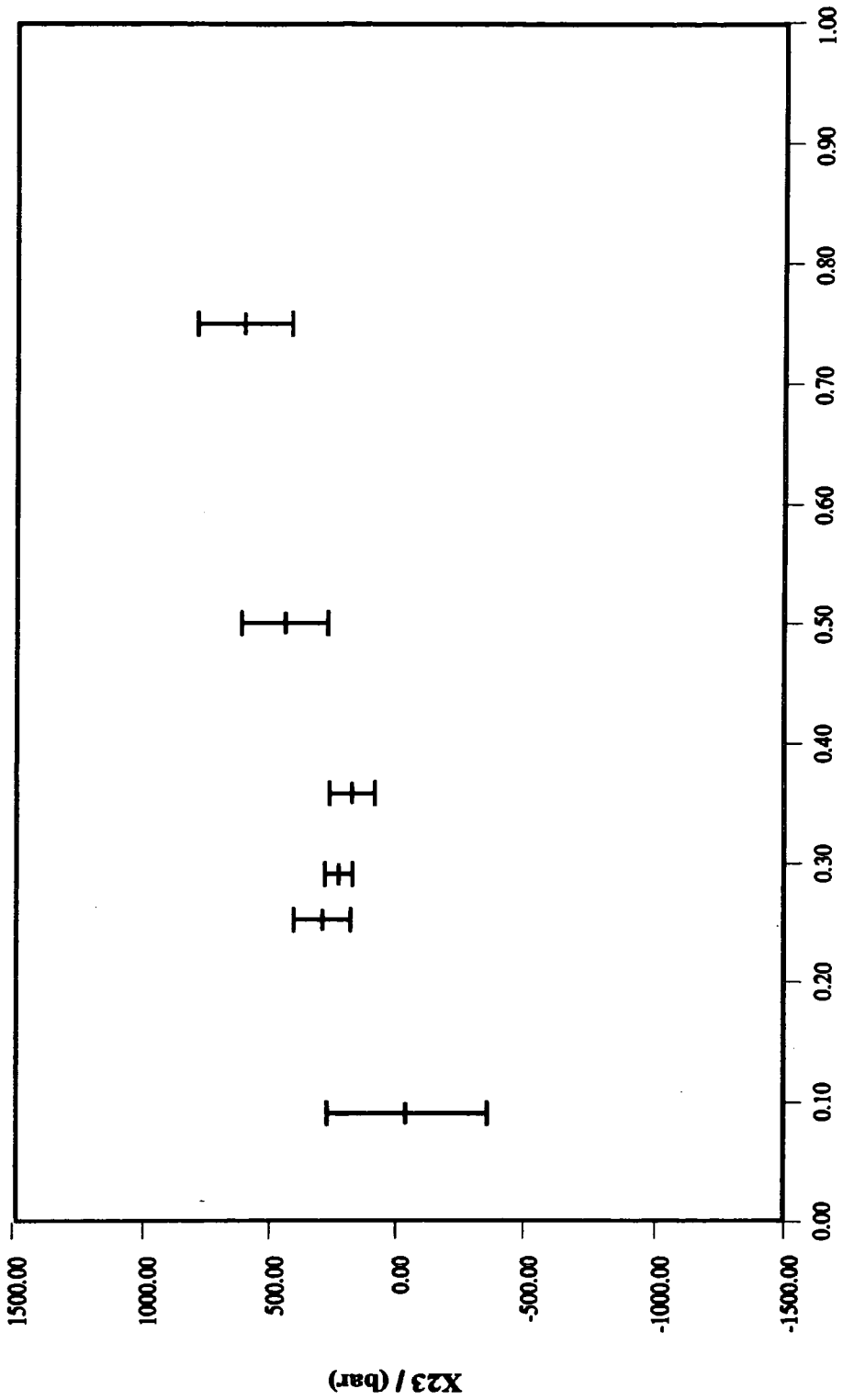


Weight Fraction EVA

Figure 8.2

Mean values of X23 for EVA/FVA mixture at 373K

Equation of state analysis of IGC results

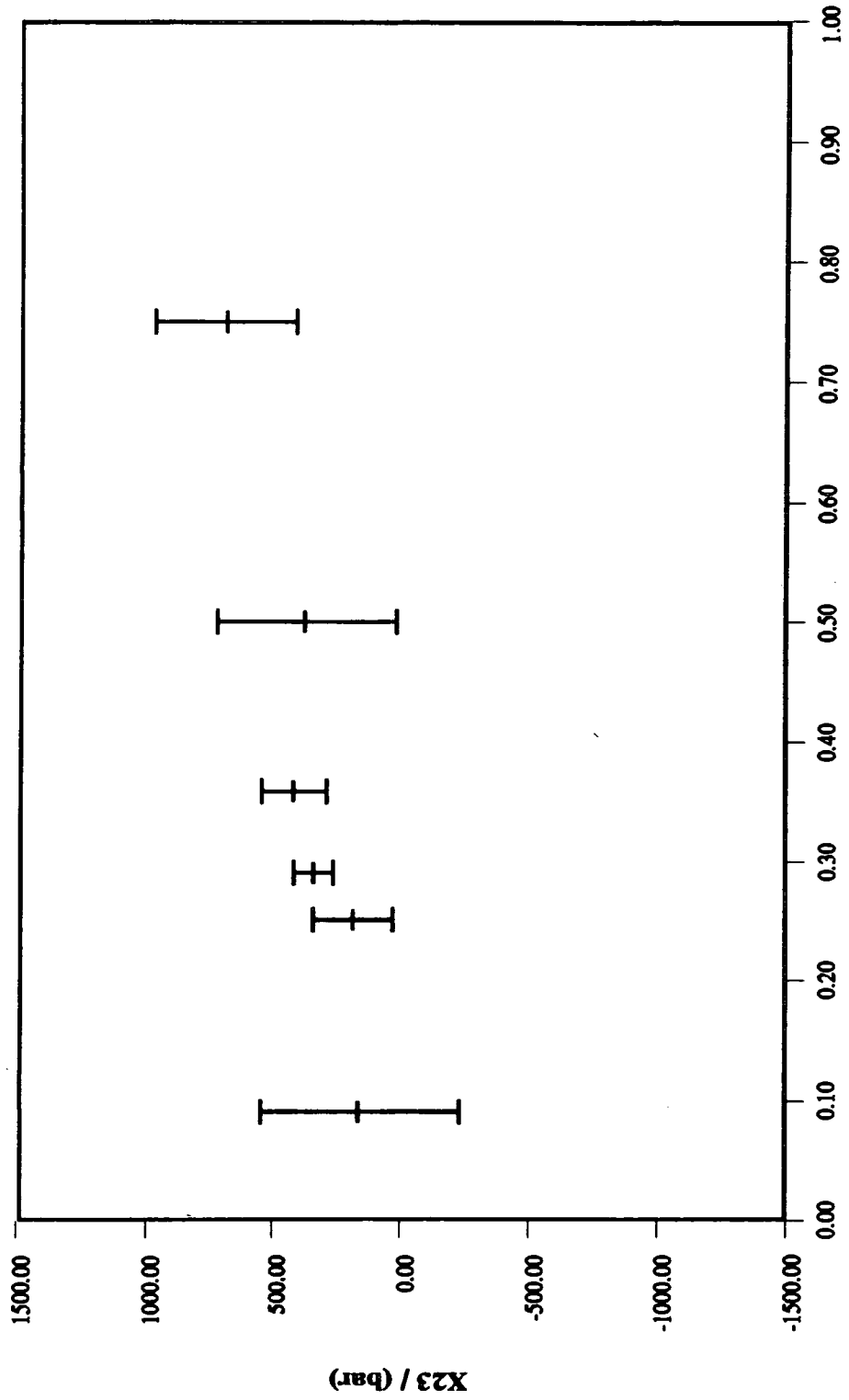


Weight Fraction EVA

Figure 8.3

Mean values of X23 for EVA/FVA mixture at 393K

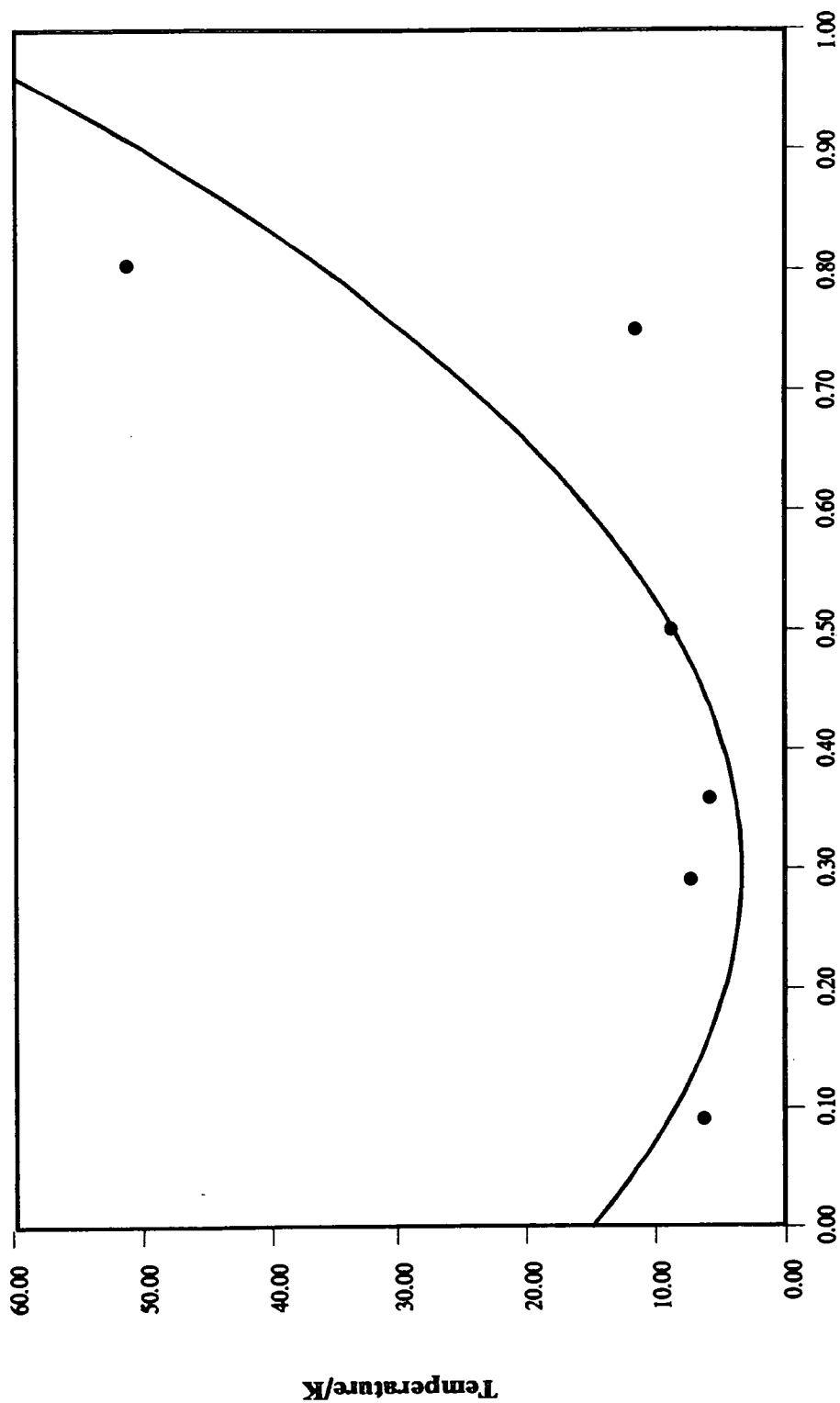
Equation of state analysis of IGC results



Weight Fraction EVA

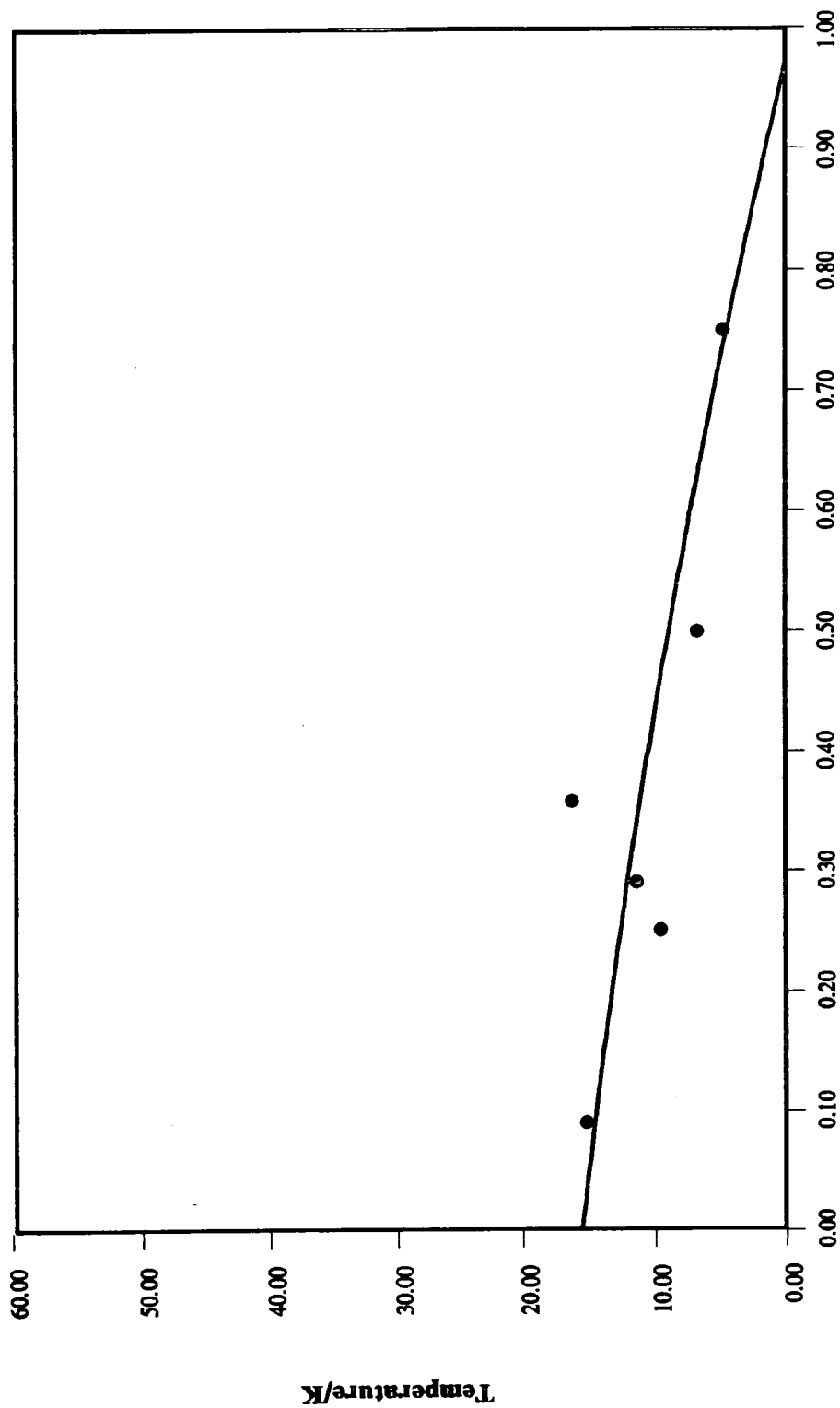
Figure 8.4

*Simulated Spinodal from 353K Data
(Quadratic Fit)*



*Mass Fraction EVA
Figure 8.5*

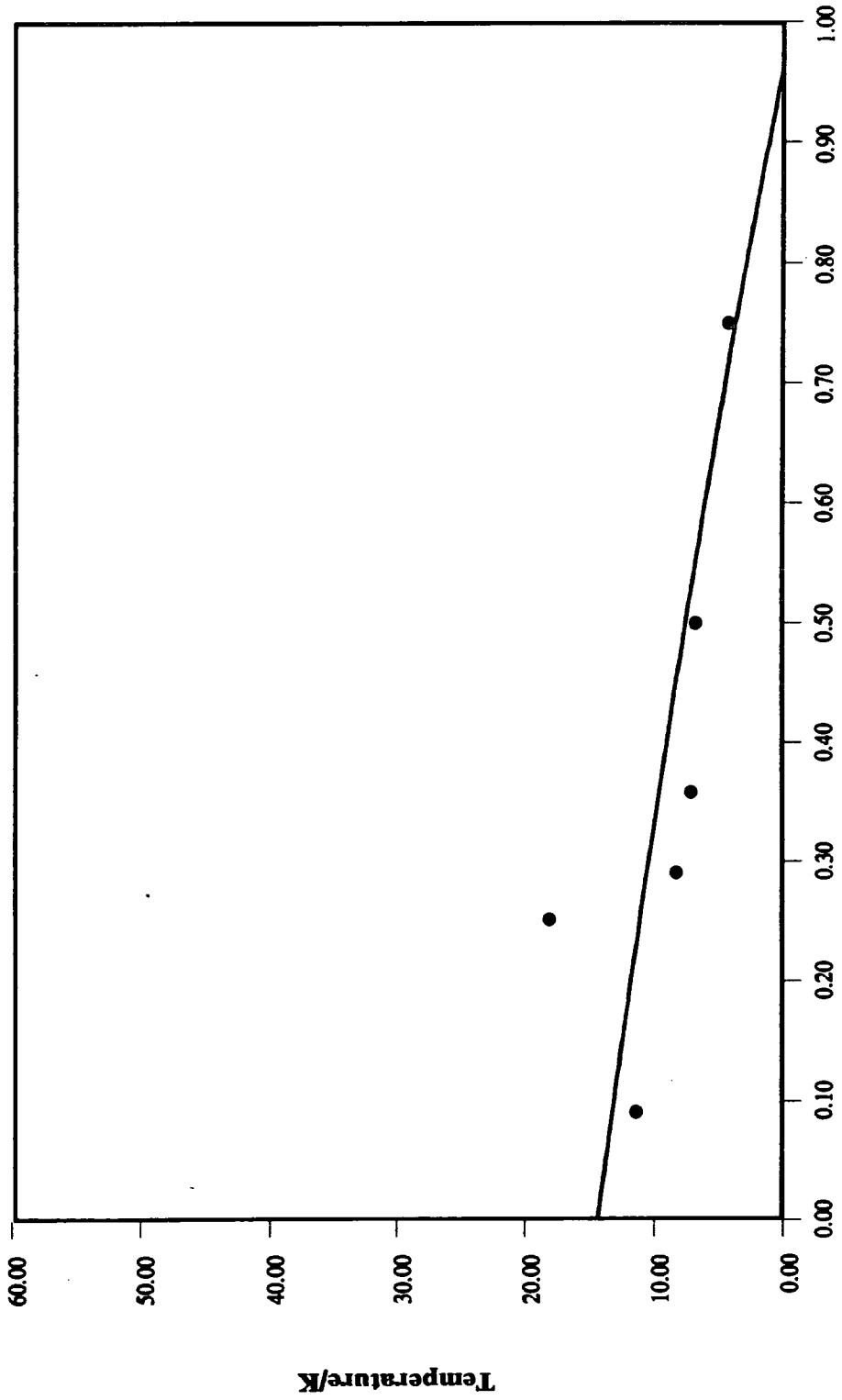
*Simulated Spinodal from 373K Data
(Quadratic Fit)*



Mass Fraction EVA

Figure 8.6

*Simulated Spinodal from 393K Data
(Quadratic Fit)*



Mass Fraction EVA

Figure 8.7

8.4 Discussion

The previous results have shown that the EOS can be used to predict the thermodynamics and miscibility limits of a polymer mixture and this discussion has been subdivided into an analysis of the dominant parameters in this mathematical model, the context and validity of the predictions that have been made and the reliability of the data upon which these predictions were based.

McMaster⁽³⁰⁾ demonstrated that a general form of Flory's EOS was capable of predicting both LCST and UCST behaviour, either independently or simultaneously, in theoretical polymer blends and that the simulated phase boundary could be radically altered by varying some state parameters.

Olabisi⁽¹⁾ verified some of McMaster's conclusions from studies of a blend of poly(ϵ -caprolactone) and poly(vinyl chloride) and thus some alterations to the state parameter values were performed in this work to find out whether this model responded in a similar manner. It should be stressed that the envelope of the model was not fully characterised owing to its inherent limitations and the unlikely predictions which were obtained from the experimental data.

8.4.1 The Sensitivity of the Model

In order to understand the relative influence of some of the physical terms in this model, a series of variations was performed and the net effect on the predicted spinodal temperature recorded.

8.4.1.1 Number average molecular weight, M_n

The number average molecular weights of the components do not feature directly in the spinodal equation. Instead their influence is exerted *via* the interaction parameters. Three scenarios were considered,

- | | | |
|-----|-------------------|-------------------|
| (a) | $M_{EVA} = 10400$ | $M_{FVA} = 10400$ |
| (b) | $M_{EVA} = 10000$ | $M_{FVA} = 20000$ |
| (c) | $M_{EVA} = 20000$ | $M_{FVA} = 10000$ |

The recalculated data are listed in Tables 8.11, 8.12 and 8.13 respectively and are shown graphically in Figure 8.8.

Table 8.11: Scenario (a)

Wt Fraction	\bar{X}_{23}/bar	$Q_{23}/\text{bar K}^{-1}$	T_{spin}/K
0.2390	202.9	-0.4314	14.43
0.5151	303.3	-0.6461	9.41
0.5642	302.6	-0.6438	9.42
0.6389	310.1	-0.6588	9.13
0.7597	622.4	-1.3304	4.34
0.9044	1401.8	-3.095	1.86

Table 8.12: Scenario (b)

Wt Fraction	\bar{X}_{23}/bar	$Q_{23}/\text{bar K}^{-1}$	T_{spin}/K
0.1357	231.25	-0.4947	12.02
0.3469	261.4	-0.5577	11.01
0.3930	242.4	-0.5156	11.99
0.4694	288.9	-0.4724	13.17
0.6125	415.8	-0.8881	6.67
0.8236	786.8	-1.6821	3.38

*Effect of Varying the Molecular Weight
Cyclohexane data at 373K*

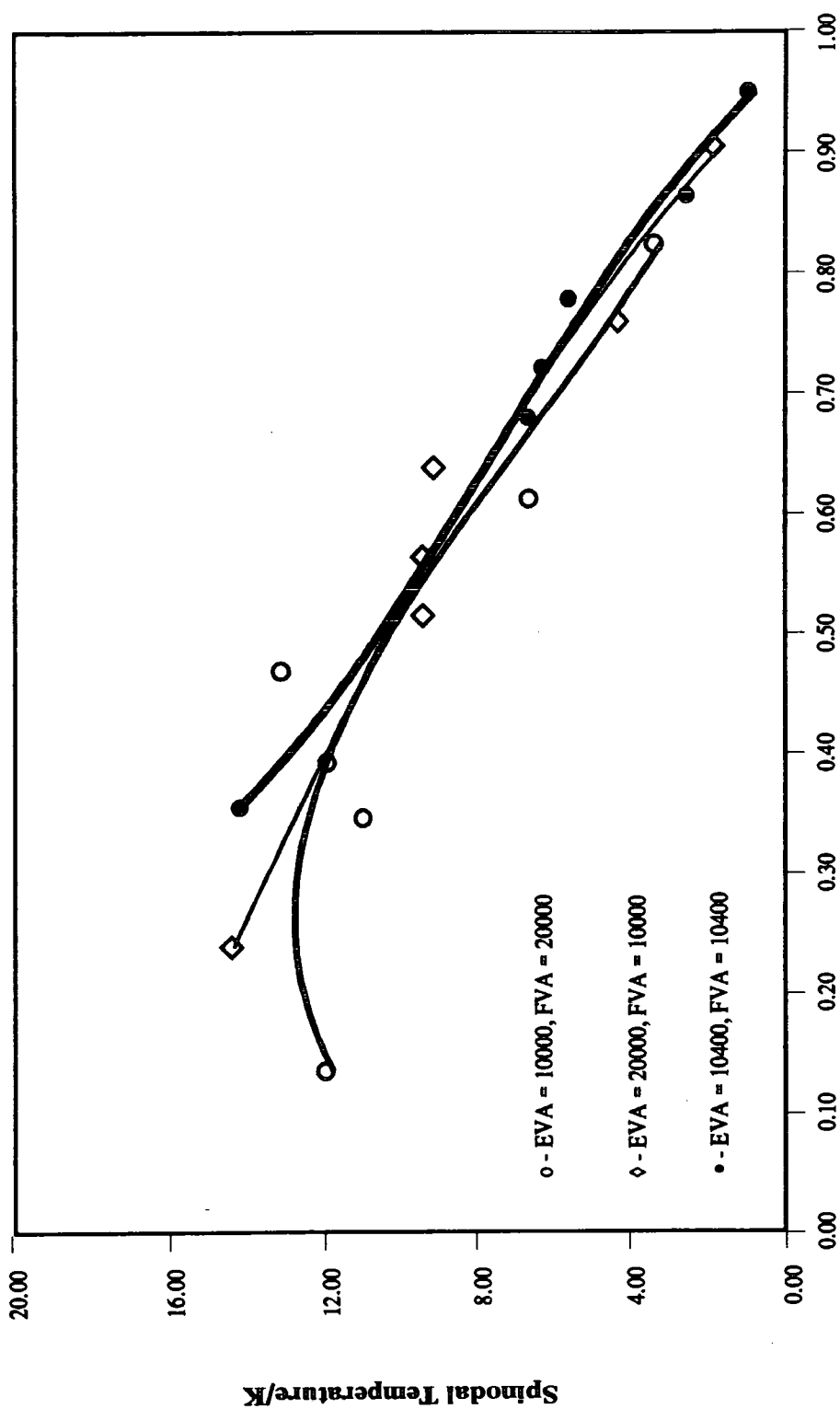


Figure 8.8

Table 8.13: Scenario (c)

Wt Fraction	\bar{X}_{23}/bar	$Q_{23}/\text{bar K}^{-1}$	T_{spin}/K
0.3558	214.7	-0.4553	14.23
0.6800	422.6	-0.9013	6.69
0.7216	445.9	-0.9505	6.31
0.7786	493.7	-1.0522	5.64
0.8634	1052.8	-2.2527	2.55
0.9498	2636.6	-5.6478	0.99

McMaster's⁽³⁰⁾ EOS model predicted that increasing the molecular weight of one component of the blend would reduce the mutual solubility, manifested in the corresponding spinodal temperature, and skew the phase boundary to the side of increased mass. The results obtained here also exhibit this skewing effect as the molecular weight of each component was increased but very little change was observed in the overall temperature of phase separation.

8.4.1.2 The Surface Area to Volume ratio (s_2/s_3) of the blend components.

Three scenarios were considered,

- (a) $s_2 = 2.0 \times 10^{-10}$; $s_3 = 2.0 \times 10^{-10}$; $s_2/s_3 = 1$
- (b) $s_2 = 1.0 \times 10^{-10}$; $s_3 = 2.0 \times 10^{-10}$; $s_2/s_3 = 0.5$
- (c) $s_2 = 2.0 \times 10^{-10}$; $s_3 = 1.0 \times 10^{-10}$; $s_2/s_3 = 2$

The recalculated data are listed in Tables 8.14, 8.15 and 8.16 respectively and are shown graphically in Figure 8.9.

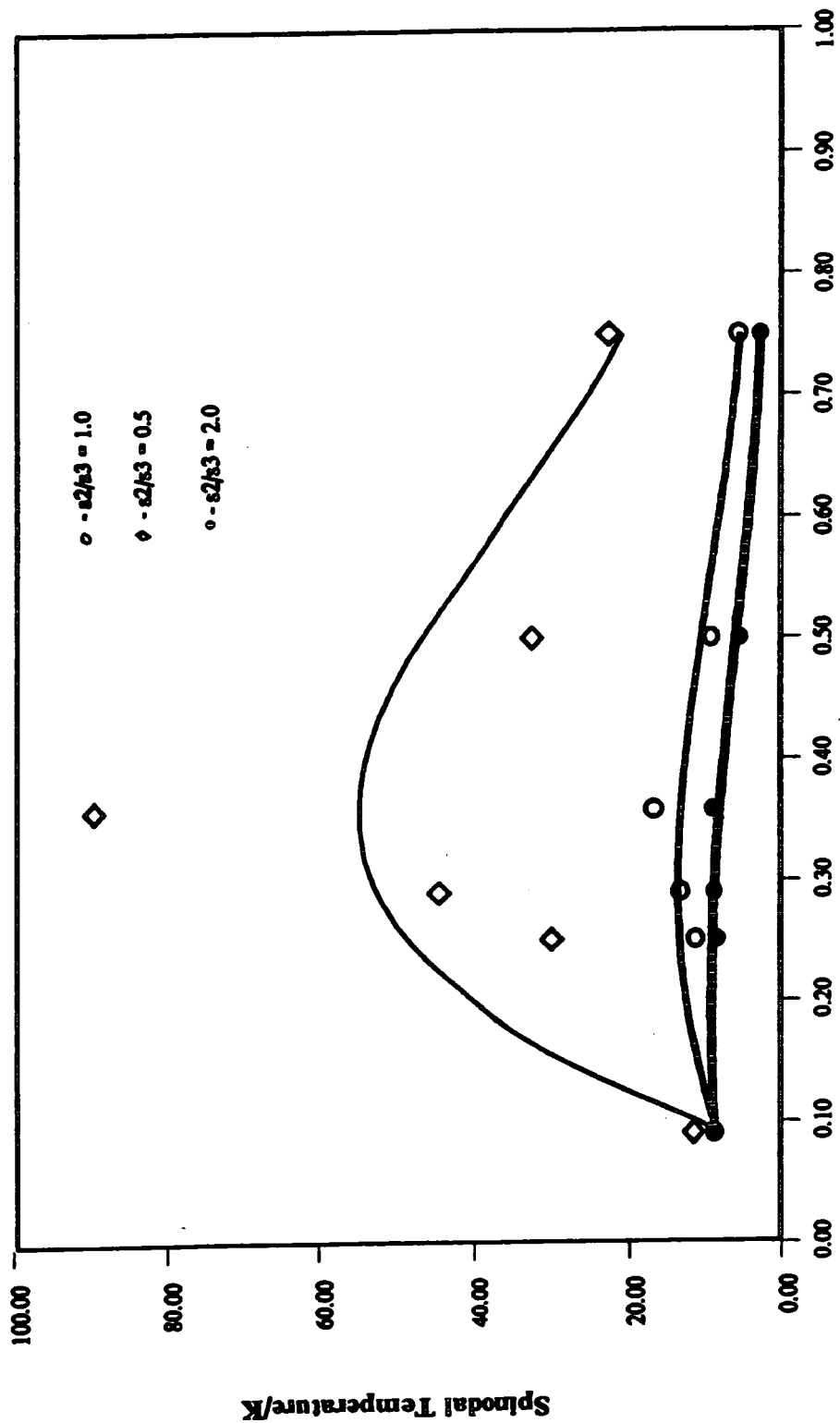
Table 8.14: Scenario (a)

Wt Fraction	\bar{X}_{23}/bar	$Q_{23}/\text{bar K}^{-1}$	T_{spin}/K
0.0904	115.0	-0.2402	11.83
0.2515	72.3	-0.1457	29.42
0.2905	44.1	-0.0840	44.62
0.3588	13.2	-0.0165	89.85
0.5000	75.2	-0.1512	32.17
0.7496	102.8	-0.2096	22.67

Table 8.15: Scenario (b)

Wt Fraction	\bar{X}_{23}/bar	$Q_{23}/\text{bar K}^{-1}$	T_{spin}/K
0.0904	236.8	-0.5075	8.78
0.2515	215.2	-0.4582	11.61
0.2905	183.8	-0.3891	13.69
0.3588	148.2	-0.3108	17.09
0.5000	274.1	-1.5830	9.39
0.7496	431.0	-0.9178	5.74

**Effect of Varying the Surface Area to Volume Ratio
Cyclohexane data at 373K**



Weight Fraction EVA
Figure 8.9

Table 8.16: Scenario (c)

Wt Fraction	\bar{X}_{23}/bar	$Q_{23}/\text{bar K}^{-1}$	T_{spin}/K
0.0904	255.8	-0.5492	8.86
0.2515	300.2	-0.6439	8.43
0.2905	288.9	-0.6184	8.82
0.3588	279.8	-0.5977	9.16
0.5000	465.7	-1.0000	5.51
0.7496	843.2	-1.8070	2.86

Reference (30) reported that the relative magnitude of the surface area to volume ratio affects the symmetry of the phase boundary but only affects the spinodal temperature when the system also possesses a large enthalpic interaction parameter and Rostami⁽⁸⁾ stated that an increasing s_2/s_3 ratio in conjunction with a constant negative value of X_{23} introduced bimodality in the phase boundary. Increasing the surface area to volume ratio in this work caused suppression of the UCST behaviour in the phase boundary. These changes did not cause the position of the maximum to move.

8.4.1.3 The Thermal Expansion Coefficient

The spinodal condition is known to be extremely sensitive to the numerical value of the thermal expansion coefficient and this is confirmed by the results given by the current model. A slight variation of the thermal expansion coefficient can be seen to have a massive effect on the predicted spinodal temperature. This is most apparent in the majority of cases where convergence to a spinodal condition is not reached throughout the range of blend compositions.

To enlarge the model envelope, five scenarios, using a range of values for the thermal expansion coefficients, were examined:-

- (a) $a_2 = 1.0 \times 10^{-3}$; $a_3 = 1.0 \times 10^{-3}$; $a_{23} = 1.0 \times 10^{-3}$;
 (b) $a_2 = 0.5 \times 10^{-4}$; $a_3 = 0.5 \times 10^{-4}$; $a_{23} = 0.5 \times 10^{-4}$;
 (c) $a_2 = 1.0 \times 10^{-3}$; $a_3 = 1.0 \times 10^{-3}$; $a_{23} = 0.75 \times 10^{-3}$;
 (d) $a_2 = 7.272 \times 10^{-4}$; $a_3 = 8.080 \times 10^{-4}$; $a_{23} = 7.676 \times 10^{-4}$;
 (e) $a_2 = 5.656 \times 10^{-4}$; $a_3 = 8.080 \times 10^{-4}$; $a_{23} = 6.868 \times 10^{-4}$;

The recalculated data are listed in Tables 8.17 to 8.22 respectively and are shown graphically in Figure 8.10.

Table 8.17: Scenario (a)

Wt Fraction	\bar{X}_{23}/bar	$Q_{23}/\text{bar K}^{-1}$	T_{spin}/K
0.0904	943.7	-2.0591	2.57
0.2515	656.8	-1.4231	3.70
0.2905	627.8	-1.3577	3.86
0.3588	603.6	-1.3055	3.98
0.5000	804.7	-1.7349	2.99
0.7496	1394.1	-2.9955	1.68

Table 8.18: Scenario (b)

Wt Fraction	\bar{X}_{23}/bar	$Q_{23}/\text{bar K}^{-1}$	T_{spin}/K
0.0904	-745.0	1.6474	-
0.2515	-340.8	9.7569	-
0.2905	-346.3	0.7681	-
0.3588	-371.2	0.8211	-
0.5000	-303.5	0.6710	-
0.7496	-647.0	1.4077	-

Table 8.19: Scenario (c)

Wt Fraction	\bar{X}_{23}/bar	$Q_{23}/\text{bar K}^{-1}$	T_{spin}/K
0.0904	579.3	-1.2592	4.85
0.2515	208.2	-0.4428	61.8
0.2905	143.8	-0.3018	1.6×10^4
0.3588	44.5	-0.0849	-
0.5000	20.8	-0.0330	-
0.7496	-435.9	0.9523	-

Table 8.20: Scenario (d)

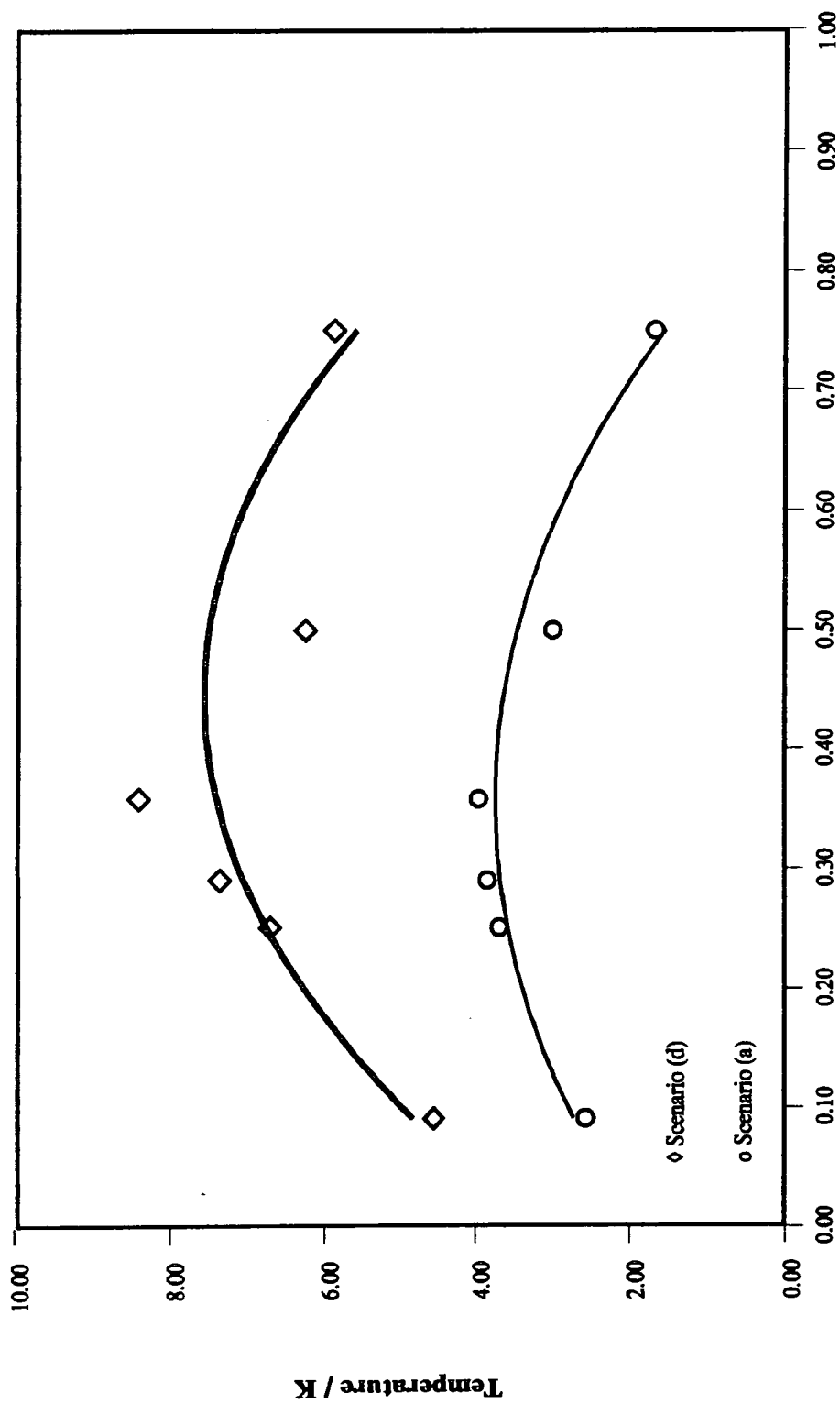
Wt Fraction	\bar{X}_{23}/bar	$Q_{23}/\text{bar K}^{-1}$	T_{spin}/K
0.0904	516.6	-1.1203	4.57
0.2515	369.4	-0.7950	6.72
0.2905	340.3	-0.7308	7.37
0.3588	305.6	-0.6538	8.43
0.5000	445.3	-0.9546	6.26
0.7496	680.8	-1.4566	5.89

Table 8.21: Scenario (e)

Wt Fraction	\bar{X}_{23}/bar	$Q_{23}/\text{bar K}^{-1}$	T_{spin}/K
0.0904	383.1	-0.8287	624.3
0.2515	195.0	-0.4140	25.9
0.2905	151.6	-0.3187	55.4
0.3588	86.2	-0.1755	-
0.5000	136.1	-0.2835	-
0.7496	-41.9	0.1025	-

Of the five thermal expansion coefficient scenarios examined only two produced interaction parameters permitting the spinodal equation to converge. This statistic alone demonstrates the influence of this variable in the EOS. McMaster⁽³⁰⁾ reported that a 6% increase in an α value of a model blend caused a 4.6% decrease in T^* , 2.0% increase in P^* and a 1.0% decrease in v^* at 300K. Scenarios (a) and (d) produce the most consistent results and are plotted in figure 8.10. However, it should be noted that both of these scenarios produced an UCST type phase boundary, whereas the experimental phase boundaries were all LCST. Scenario (b) represents the situation when the α values were an order of magnitude smaller than those measured, which produced a significantly negative \bar{X}_{23} , correspondingly positive Q_{23} values and the combination of these data produced exponentially large spinodal solutions which have not been recorded. Both (c) and (e) produced spinodal temperatures at low EVA concentrations although these functions became exponential as the FVA concentration was increased. A clearer representation of the influence of α was not obtained because by fixing the values of α , X_{23} and \bar{X}_{23} , the only remaining variable was Q whose value became unrealistic and prevented the spinodal equation from converging.

*Effect of varying the Thermal Expansion
Cyclohexane data at 3734K*



Mass Fraction EVA

Figure 8.10

8.4.1.4 The Q parameter

Various values of Q were used to predict the spinodal temperature while keeping the other parameters at their original values.

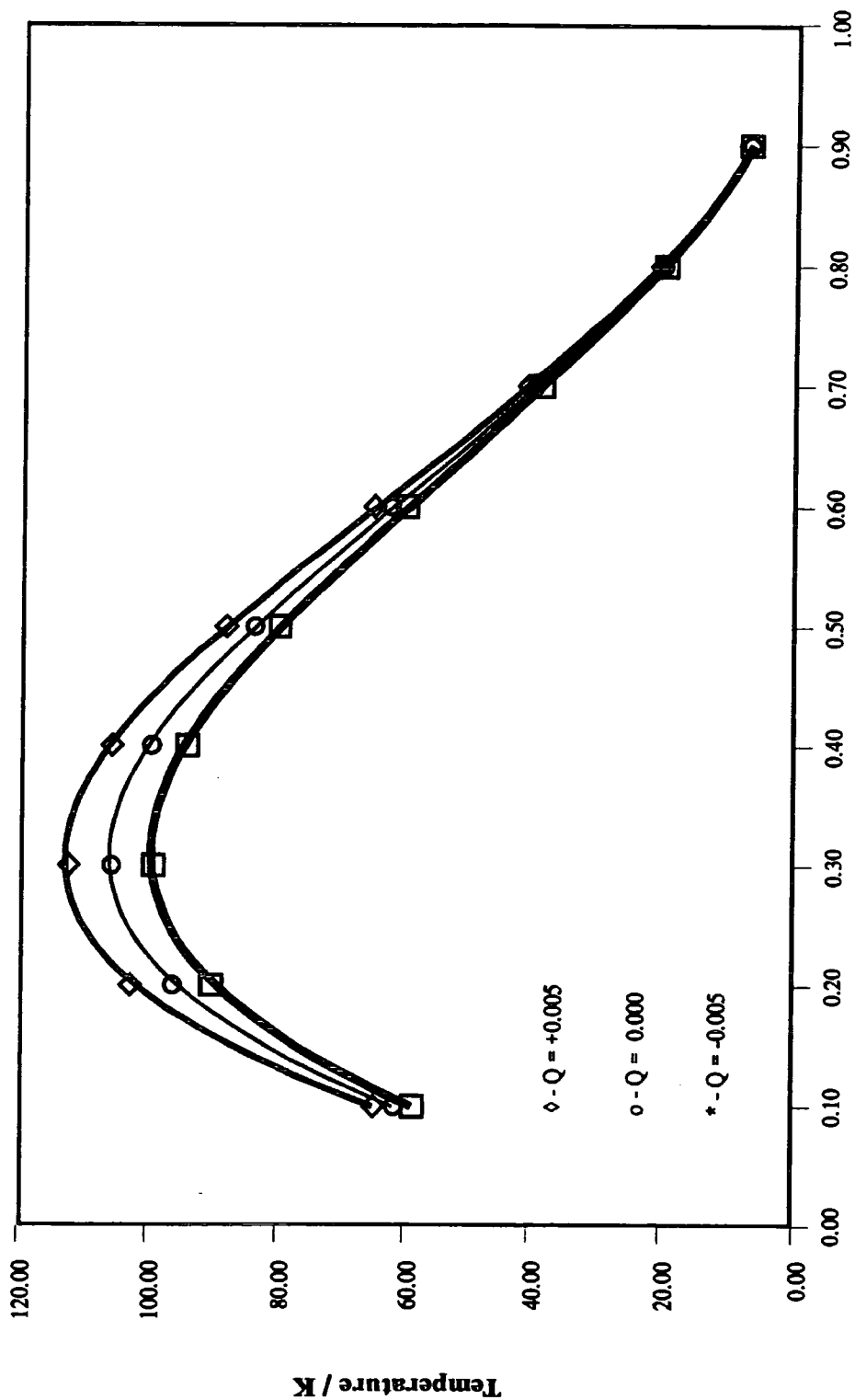
(a) For a temperature of 373K

Table 8.22:

Wt. Fr	T_{spin} / K (Q = 0.0)	T_{spin} / K (Q = 0.005)	T_{spin} / K (Q = -0.005)
0.1	61.7	64.8	58.8
0.2	96.2	102.8	90.3
0.3	105.7	112.4	99.3
0.4	99.6	105.7	94.1
0.5	83.9	88.3	79.9
0.6	62.5	65.2	60.1
0.7	39.6	40.8	38.5
0.8	20.1	20.4	19.8
0.9	7.2	7.2	7.1

These results are shown in figure 8.11. As Q_{23} is increased the spinodal temperature also increases, the effect being most dramatic at the larger values of T_{spin} . However it was found that T_{spin} increased exponentially as Q_{23} approached a specific value and this was studied by increasing its value gradually. These results are given in Table 8.23 and shown in figure 8.12.

**Effect of Varying the Q Parameter
Cyclohexane data at 373K**



Mass Fraction EVA
Figure 8.11

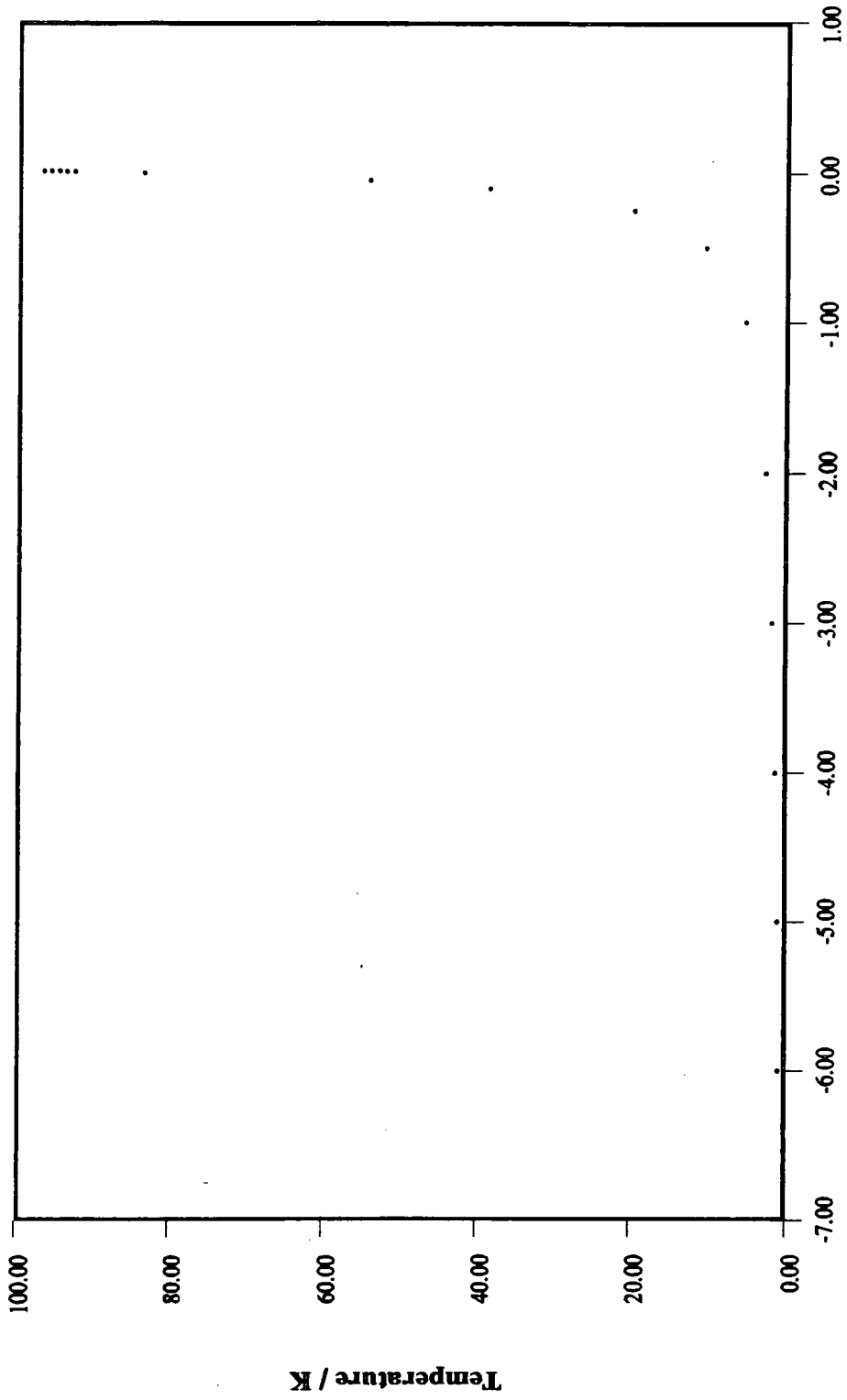
Table 8.23

Q	T_{spin} / K	Q	T_{spin} / K
-1.0	5.5	0.015	-
-2.0	2.8	0.011	93.9
-3.0	1.9	0.012	94.9
-4.0	1.4	0.013	95.9
-5.0	1.1	0.014	-
-6.0	0.9	0.0135	96.46
-0.5	10.7	0.0138	96.77
-0.25	19.8	0.0139	96.87
-0.10	38.6	0.01391	96.85
-0.05	54.1	0.013915	96.88
0.10	92.9	0.139152	96.88

8.5 General discussion

The temperatures which satisfy the spinodal equation for the EVA/FVA mixtures quoted in Tables 8.8 - 8.10 are all below 52 K and of little practical use, because although they may reflect the physics of the system, under these conditions both polymers are significantly below their glass transition temperatures and miscibility would be prohibited by their physical state. This prediction partially supports the results of the phase contrast microscopy experiments which showed no evidence of miscibility between 303 and 523 K. It can thus be concluded, both on experimental and theoretical grounds, that these two polymers are never miscible in the bulk state. However, several features of this calculation should be noted and the results considered in context. Firstly, since the reduced parameters of the pure components and the mixture require to be evaluated at each spinodal temperature during the iterative calculation, in this case they have been linearly extrapolated over approximately 250K. This is without doubt invalid. It was also felt that it was worth reconsidering the sources of these data, and the fundamental assumptions of the calculation.

*Relationship between the Spinodal Temperature
and the Q Parameter*



*Q Parameter
Figure 8.12*

Possibly the greatest flaw in the basis of this estimation was that X_{23} is defined as being constant, and independent of temperature. This definition assumes that any density, steric or end group effects which contribute to the heat of mixing will either be incorporated in the other parameters in equation 2.52c,

$$\Delta H_{mix} = n_2 V_1^* \left\{ \theta_3 X_{23} / \tilde{v}_2 + P_1^* (1/\tilde{v} - 1/\tilde{v}_2) - (\phi_2^* / \phi_1^*) P_2^* (1/\tilde{v} - 1/\tilde{v}_3) \right\} \quad (2.52c)$$

which they are not, or they are insignificant in relation to the contributions from the respective exchange enthalpies. Since other experiments in this current work have shown that there is very little energetic difference in the homopolymers intermolecular contacts, and no strong specific interaction between heterogeneous contacts, the enthalpy of mixing in this system may be dominated by the unaccounted physical effects. This scenario would not affect the reproducibility of the measurements since they could be precise but inaccurate. However, these alternative effects are more likely to be temperature dependent and in view of this possibility, some additional heats of mixing experiments were carried out at 359.3K and the results are given in Table 8.24.

Table 8.24

Measured and recalculated heat of mixing values for 359.3K

Run	Measured $\Delta H_{mix} / 10^{-2} \text{J g}^{-1}$	Recalculated $\Delta H_{mix} / 10^{-2} \text{J g}^{-1}$	Difference 10^{-2}J g^{-1}
1	5.390	5.957	0.567
2	7.162	6.497	- 1.206
3	6.259	6.905	0.646

By fitting the data in Table 8.24 with a non-linear least squares function X_{23} , at 359.3K, was estimated as 3.315bar. The recalculated values given above represent the corresponding data values from the fitted function. The difference between the X_{23} values at 348.7 and 359.3K represents a

change of about 40% over a 10.6 K range. Owing to insufficient experimental time and calorimetry data, this effect could not be studied fully and thus the influence of a heavily temperature dependent enthalpic contribution on the phase boundary was not quantitatively examined. If it is assumed that the value of X_{23} would continue to decrease with increasing temperature, *i.e.* that heterogeneous contacts would begin to become more favourable than the homogeneous, the critical point of the predicted phase boundary would be elevated⁽³⁰⁾. However, this should also be considered in context. The moduli of the mean values of \bar{X}_{23} at 353K, quoted in Table 8.8, are *circa* two orders of magnitude greater than those of X_{23} and thus although the enthalpic value used in this simulation may be a crude approximation, it is insignificant in relation to the entropic contribution. This contribution is manifested in the value of Q_{23} which itself is insignificant for the majority of values but entirely dominant over a very short range, *i.e.* Table 8.24 and Figure 8.12. In view of this dominance, it was apparent that a reliable estimation of Q_{23} was imperative to produce a realistic simulation of the phase boundary. It is unsurprising that this term has generally been used as the fitting parameter for experimental and theoretical phase boundaries since it has the potential to alter the predicted spinodal temperature by orders of magnitude. However, the entire EOS approach to predicting the thermodynamics of mixtures will be fundamentally weakened unless a more representative partition function is adopted which accounts for the influence of physical effects on the heat of mixing and a clear model of the effects which contribute to excess entropy.

8.6 REFERENCES

- (1) O. Olabisi, *Macromolecules*, 8, 316, (1975).
- (2) G. ten Brinke, A. Eshuis, E. Roerdrink and G. Challa, *Macromolecules*, 14, 867, (1981).
- (3) R. Koningsveld, L. A. Kleintjens and H. M Schaffelers, *Pure Appl. Chem.*, 39, 1, (1974).
- (4) R. Koningsveld, W. H. Stockmayer, J. A. Kennedy and L. A. Kleintjens, *Macromolecules*, 7, 73, (1974).
- (5) Z. Chai, S. Rouna, D. J. Walsh and J. S. Higgins, *Polymer*, 24, 263, (1983).
- (6) D. J. Walsh and S. Rostami, *Polymer*, 26, 418, (1985).
- (7) S. Rostami and D. J. Walsh, *Macromolecules*, 17, 315, (1984).
- (8) S. Rostami, PhD thesis, Imperial College, University of London, (1983).
- (9) D. W. van Krevelen, 'Properties of Polymers', Elsevier, (1972).
- (10) J. Brandrup and E. J. Immergut, 'Polymer Handbook', Wiley, (1975).
- (11) A. Bondi, *J. Phys. Chem.*, 68:3, 441, (1964).
- (12) B. E. Eichinger and P. J. Flory, *Trans. Faraday Soc.*, 64, 2035, (1968).
- (13) B. E. Eichinger and P. J. Flory, *Trans. Faraday Soc.*, 64, 2053, (1968).
- (14) B. E. Eichinger and P. J. Flory, *Trans. Faraday Soc.*, 64, 2061, (1968).
- (15) B. E. Eichinger and P. J. Flory, *Trans. Faraday Soc.*, 64, 2065, (1968).
- (16) H. Shih and P.J. Flory, *Macromolecules*, 5, 758, (1972).
- (17) H. Shih and P.J. Flory, *Macromolecules*, 5, 761, (1972).
- (18) P. J. Flory and A. Abe, *J. Amer. Chem. Soc.*, 86, 3563, (1964).
- (19) A. Abe and P. J. Flory, *J. Amer. Chem. Soc.*, 87:9, 1838, (1965).
- (20) G. Allen, G. Gee, D. Mangaraj, D. Sims and G.J. Wilson, *Polymer*, 1, 467, (1960).
- (21) R. A. Orwoll and P. J. Flory, *J. Amer. Chem. Soc.*, 89:26, 6814, (1967).

- (22) P. A. Small, *J. Appl. Chem.*, 3, 71, (1953).
- (23) K. L. Hoy, *J. Paint Technol.*, 42, 76, (1970).
- (24) D. W. van Krevelen, 'Properties of Polymers', Elsevier, (1972).
- (25) D. J. Walsh, S. Rostami and V. B. Singh,
Makromol. Chem., 186, 145, (1895).
- (26) C. Panayiotou and J. H. Vera, *Polymer Journal*, 16:2, 103, (1984).
- (27) B. M. Mandal, C. Bhattacharya and S. N. Bhattacharya,
J. Makromol. Sci-Chem., A26(1), 175, (1989).
- (28) D. Patterson and G. Delmas, *Discuss. Faraday Soc.*, 49, 98, (1970).
- (29) D. Patterson, *Pure Appl. Chem.*, 31, 133, (1972).
- (30) L. P. McMaster, *Macromolecules*, 6, 760, (1973).
- (31) W.H. Press, B.P. Flannery, S.A. Teukolsky and W.T. Vetterling,
'Numerical Recipes in Pascal', Cambridge University Press 1989.

Chapter 9 Final Conclusions

The objectives of this work were to examine experimentally and characterise the thermodynamics and miscibility limits of a mixture of two copolymers, EVA and C_{14} FVA, and to review the applicability of the experimental techniques which were employed to obtain the thermodynamic data.

The density measurements, (Chapter 3), showed that mixtures of all compositions were volume additive between 303 and 333K, and the thermal expansion coefficients of both the homopolymers and of each blend, which were required for an equation of state analysis, were calculated from these data. By definition, materials which are volume additive when mixed do not strongly or specifically interact and in these systems the intermolecular forces between homo-contacts must be approximately equal to those between hetero-contacts. Alternatively, volume additivity can arise in cases where the component materials do not mix on a truly molecular level and consequently the system is effectively a micro-dispersion rather than a mixture. The EVA and C_{14} FVA copolymers are chemically very similar and it is likely therefore that the intermolecular forces between the homo-species would be very similar to those in the blend. On this basis, and in the absence of contrary information and for the application of an equation of state analysis, it was assumed that molecular mixing did occur. However, the ultimate conclusion from both the majority of the experimental results and the theoretical predictions is that the copolymers are immiscible in all proportions between 303 and 393K. This suggests that the density measurements, together with the thermal expansivities and reduced mixture volumes calculated from them, actually refer to dispersions of EVA and C_{14} FVA rather than to mixtures. Similarly, the heats of mixing calculated in Chapter 5 would then refer to the enthalpic changes which occur when the surfaces of these materials are contacted. However the magnitude of such an enthalpic effect would be highly dependent on the interfacial area of the hetero-contact which can be assumed to be variable. The consistency of the heats of mixing data in Chapter 5 show that this is not the case. These factors all cast doubt on the validity of the unusual phase boundaries predicted in Chapter 8. In view of the importance of accurate determinations of the specific volumes and thermal expansion coefficients of component materials to an EOS treatment, it is suggested that future workers should obtain as much information as possible about the density-temperature-composition relationships of these species, preferably using more than one technique.

Differential scanning calorimetry, (Chapter 3), was used to characterise the temperature-heat capacity responses of the polymers and consequently identify any thermal transitions which they had undergone. EVA was found to have $T_g \approx 140\text{K}$ and no identifiable melt: C_{14} FVA $T_g \approx 160\text{K}$ and $T_m \approx 300\text{K}$. A polymer-polymer interaction parameter can be obtained from DSC if one of the components of a binary mixture is crystalline and the other amorphous. For this purpose the C_{14} FVA was defined as being crystalline and the depression in its melting point was measured as a function of EVA concentration. This experimental programme was abandoned because the observed depression of the C_{14} FVA melting point was insignificant from which it was concluded that the copolymers did not co-crystallise and thus the presence of the EVA had no effect on the chemical potential of the C_{14} FVA. DSC can also be used to examine the phase boundary of a mixture as the T_g value of each component is replaced by a single transition in a miscible blend. The movements of the T_g values of EVA and C_{14} FVA were followed after the samples had been annealed at a range of temperatures and the predicted phase boundary was of the LCST type, occurring at between 340 and 315K across the composition range. However, some doubt arose over the validity of this prediction owing to the weak and non-reproducible nature of the salient features of the thermograms of both materials, and it was concluded that DSC was inappropriate for exploring the thermodynamics of this particular mixture. A complicating factor was the observation that EVA went from opaque to translucent when heated to about 325K and this effect was quantitatively characterised using laser turbidimetry, (Chapter 3). No reflection of this change was observed in either the density or the DSC experiments, *i.e.* it did not cause a change in either unit volume or heat capacity. This was most probably caused by the solubilisation of the extreme elements of either the molecular weight or the compositional distributions. As a consequence, it was decided that subsequent experiments should be performed above 325K to ensure that any manifestations of this effect were not included unwittingly in the results.

Inverse phase gas chromatography, (Chapter 4), was used to evaluate polymer-solvent and polymer-polymer interaction parameters at 353, 373 and 393K and from these data it was observed that the polymer-polymer interaction varied significantly with both composition and temperature. In general, the interaction parameters were found to be small and positive with values from EVA rich mixtures being more favourable to miscibility. The probability of mutual solubility decreased as the FVA concentration and the temperature increased. The experimental data were highly consistent and

reproducible although the polymer-polymer interaction parameters did exhibit a significant solvent dependence. Several attempts were made to correlate this dependence with either a physical characteristic of the solvent, or with the empirical functions which have been quoted in the literature, but without success. It is apparent that IGC as a technique would benefit enormously from a greater theoretical analysis, preferably from a chromatographic viewpoint, which had the object of understanding and quantifying the various processes which can occur on the column, as the elution peak appeared to contain considerably more information than that utilised by the current method of analysis. It was intended that the accuracy of the dynamic IGC results would be verified by a series of static solvent vapour sorption, SVS, experiments but owing to technical and time constraints this was not achieved. However, the normal SVS procedure of linearly extrapolating the interaction parameter vs. mixture mass fraction relationship to zero solvent concentration was found to introduce significant uncertainty in both the interaction parameters obtained in this work and those obtained by others, (Chapter 6). It was concluded that since this linear fitting procedure had no theoretical or practical basis it should be replaced by fitting the highest justifiable polynomial. It is also suggested that previously published SVS data be re-analysed using more appropriate extrapolation procedures which may affect the magnitude of the reported discrepancies between equivalent SVS and IGC data.

Heat of mixing experiments were carried out to separate the free energy of mixing into its enthalpic and entropic components (Chapter 5). The enthalpy of mixing was found to be small and positive, *i.e.* unfavourable to mixing, but a Flory-Huggins-Chang-Miller analysis estimated the Gibbs free energy of mixing to be negative and favourable. This suggested that the free energy change on mixing was dominated by the entropic contribution. Since gel permeation chromatography had shown that both EVA and C₁₄FVA were low molecular weight materials, this entropic dominance was quite possible and thus a more advanced theoretical analysis should be used to predict the thermodynamics of the mixture since the simple FHCM model only considers configurational contributions whereas the equation of state theories also take account of contributions from the external degrees of freedom of the polymer chains. The equation of state approach of Flory and Prigogine was adopted on the basis that it provided a general partition function and because it was the most studied of all the EOS theories. The theoretical LCST spinodal boundaries, which predicted that these copolymers would always be miscible above about 50K, are of little practical value (Chapter 8). It is believed that

this is the first work to calculate directly the entropic correction factor, Q , and thus produce spinodal functions which do not contain a 'fudge factor'.

However, in the absence of an experimental phase boundary, it is impossible to conclude whether these calculations, and thus the theory, produce realistic solutions for this mixture. It was clear from altering some of the state parameters, for both homopolymers and mixtures, that the solution of the spinodal condition was dominated by the magnitude of the Q parameter, which in turn arose from the two orders of magnitude difference between the enthalpic and free energy interaction parameters, calculated from heats of mixing and IGC respectively. It was concluded, from the two sets of heats of mixing data obtained at different temperatures, that the EOS assumption of a constant enthalpic interaction parameter for any polymer pair is dubious. However the greatest cause for doubt lay in the incompatibility of the heats of mixing results with those obtained for IGC. It should be noted that the six parameter copolymer theory of Cowie *et al* ⁽¹⁾ was not employed in this work because it requires investigation of the homopolymers of each monomer unit in each copolymer, *i.e.* in this case polyethylene, polyvinylacetate and a polymer of the di-substituted C_{14} fumaric ester.

Finally, optical microscopy, (Chapter 7), was employed to observe the behaviour of a selection of mixtures as they were heated from 313 to 373K, and the resulting micrographs demonstrated that EVA and C_{14} FVA were not miscible in this temperature range, which supported the results from IGC, heats of mixing and the EOS predictions.

It is concluded that the *ad hoc* addition of the Q parameter will always reduce the potency of the EOS, particularly when the mixing is dominated by the entropic contribution. It is suggested that a new partition function, which directly incorporates an entropic contribution with a clear physical significance, should be considered.

The true value of this work can only be estimated if it is repeated with a low viscosity blend for which an experimental phase boundary can be determined.

REFERENCE

- (1) J.M.G. Cowie, V.M.C.Reid and I.J.McEwen, *Polymer*, 31, 486, (1990)

Values of the Chi functions for Benzene at 80°C						
Wt Fr	χ_{23}	χ_{23}	S and P	Star	123	123*
0.0000	1.1927	1.1927	1.4307	1.4307	1.1927	1.4307
0.0904	0.7244	27.4707	-1.6035	-5.1447	1.1422	1.3922
0.2516	-0.5800	-21.9942	-1.6238	-5.2098	1.3294	1.6010
0.2906	0.7489	28.3995	-0.2105	-0.6755	1.0685	1.3453
0.3589	0.8128	30.8243	-0.0561	-0.1800	1.0432	1.3293
0.5001	0.6958	26.3866	-0.1216	-0.3900	1.0719	1.3771
0.7497	0.3919	14.8630	-0.7379	-2.3674	1.1991	1.5386
0.8033	-0.0586	- 2.2241	-1.4107	-4.5263	1.2870	1.6339
1.0000	1.2983	1.2983	1.6727	1.6727	1.2983	1.6727

Values of the Chi functions for Dichloromethane at 80°C						
Wt Fr	χ_{23}	χ_{23}	S and P	Star	123	123*
0.0000	1.2238	1.2238	1.4710	1.4710	1.2238	1.4710
0.0904	-0.2539	- 13.1558	- 2.5806	- 11.8734	1.2500	1.5048
0.2516	-0.8378	- 43.4080	- 1.8804	- 8.6518	1.3967	1.6651
0.2906	0.6189	32.0695	- 0.3393	- 1.5612	1.1119	1.3836
0.3589	0.6585	34.1177	- 0.2093	- 0.9630	1.0919	1.3695
0.5001	0.4964	25.7208	- 0.3198	- 1.4714	1.1278	1.4176
0.7497	0.1303	6.7493	- 0.9984	- 4.5935	1.2415	1.5531
0.8033	-0.5464	- 28.3104	- 1.8973	- 8.7294	1.3544	1.6708
1.0000	1.2797	1.2797	1.6136	1.6136	1.2797	1.6136

Values of the Chi functions for Carbon Tetrachloride at 80°C						
Wt Fr	χ_{23}	χ_{23}	S and P	Star	123	123*
0.0000	1.1199	-1.1199	1.3669	1.3669	1.1199	1.3669
0.0904	- 0.4439	- 15.5346	- 2.7739	- 8.2031	1.1741	1.4344
0.2516	- 0.7360	- 25.7592	- 1.7819	- 5.2697	1.3075	1.5916
0.2906	0.6625	23.1868	- 0.2990	- 0.8843	1.0382	1.3280
0.3589	0.7813	27.3441	- 0.0898	- 0.2655	1.0081	1.3081
0.5001	0.6493	22.7250	- 0.1702	- 0.5033	1.0531	1.3742
0.7497	0.4718	16.5135	- 0.6601	- 1.9522	1.1746	1.5335
0.8033	- 0.1999	- 6.9956	- 1.5541	- 4.5960	1.3040	1.6710
1.0000	1.3096	1.3096	1.7068	1.7068	1.3096	1.7068

Values of the Chi functions for Cyclohexane at 80°C						
Wt Fr	χ_{23}	χ_{23}	S and P	Star	123	123*
0.0000	1.2691	1.2691	1.5378	1.5378	1.2691	1.5378
0.0904	- 0.2564	- 7.9918	- 2.5891	- 6.8624	1.3179	1.6016
0.2516	- 0.7426	- 23.1483	- 1.7914	- 4.7479	1.4861	1.7968
0.2906	0.6580	20.5088	- 0.3063	- 0.8119	1.2207	1.5381
0.3589	0.8464	26.3826	- 0.0274	- 0.0727	1.1823	1.5111
0.5001	0.7062	22.0128	- 0.1161	- 0.3076	1.2436	1.5965
0.7497	0.6699	20.8814	- 0.4648	- 1.2320	1.3699	1.7656
0.8033	- 0.0991	- 3.0894	- 1.4562	- 3.8595	1.5264	1.9313
1.0000	1.5692	1.5692	2.0084	2.0084	1.5692	2.0084

Values of the Chi functions for Pentane at 80°C						
Wt Fr	χ_{23}	χ_{23}	S and P	Star	123	123*
0.0000	1.7157	1.7157	2.0731	2.0731	1.7157	2.0731
0.0904	- 2.0050	- 56.5768	- 4.3339	- 11.4128	1.8965	2.2688
0.2516	- 2.7918	- 78.7808	- 3.8368	- 10.1035	2.2842	2.6834
0.2906	0.6587	18.5889	- 0.3018	- 0.7947	1.6247	2.0304
0.3589	1.1672	32.9362	0.2971	0.7825	1.5023	1.9195
0.5001	0.5124	14.4592	- 0.3061	- 0.8060	1.6657	2.1068
0.7497	0.2421	6.8313	- 0.8889	- 2.3407	1.7873	2.2709
0.8033	- 0.4681	- 13.2083	- 1.8213	- 4.7961	1.9141	2.4070
1.0000	1.8709	1.8709	2.3978	2.3978	1.8709	2.3978

Values of the Chi functions for Hexane at 80°C						
Wt Fr	χ_{23}	χ_{23}	S and P	Star	123	123*
0.0000	1.5361	1.5361	1.8773	1.8773	1.5361	1.8773
0.0904	- 2.1632	- 54.8625	- 4.4948	- 10.1769	1.7397	2.0988
0.2516	- 2.1052	- 53.3894	- 3.1527	- 7.1381	2.0012	2.3924
0.2906	0.6679	16.9389	- 0.2952	- 0.6685	1.4740	1.8731
0.3589	0.7427	18.8361	- 0.1300	- 0.2942	1.4588	1.8716
0.5001	0.4917	12.4699	- 0.3294	- 0.7459	1.5442	1.9855
0.7497	0.3706	9.3992	- 0.7630	- 1.7275	1.6627	2.1549
0.8033	0.2780	7.0502	- 1.0779	- 2.4405	1.7021	2.2053
1.0000	1.7963	1.7963	2.3402	2.3402	1.7963	2.3402

Values of the Chi functions for Heptane at 80°C						
Wt Fr	χ_{23}	χ_{23}	S and P	Star	123	123*
0.0000	1.2541	1.2541	1.5916	1.5916	1.2541	1.5916
0.0904	- 2.4872	- 56.8075	- 4.8204	- 9.5334	1.4907	1.8490
0.2516	- 1.9846	- 45.3282	- 3.0338	- 6.0000	1.7131	2.1090
0.2906	- 0.6169	- 14.0903	- 1.5817	- 3.1281	1.4777	1.8827
0.3589	0.9537	21.7819	0.0794	0.1570	1.1520	1.5731
0.5001	0.4165	9.5121	- 0.4063	- 0.8035	1.3142	1.7686
0.7497	0.4037	9.2205	- 0.7315	- 1.4468	1.4243	1.9380
0.8033	0.1478	3.3753	- 1.2097	- 2.3925	1.4937	2.0204
1.0000	1.5804	1.5804	2.1545	2.1545	1.5804	2.1545

Values of the Chi functions for Octane at 80°C						
Wt Fr	χ_{23}	χ_{23}	S and P	Star	123	123*
0.0000	1.3074	1.3074	1.6496	1.6496	1.3074	1.6496
0.0904	- 2.6732	- 55.4319	- 5.0063	- 8.8017	1.5593	1.9254
0.2516	- 1.9864	- 41.1915	- 3.0355	- 5.3368	1.7663	2.1753
0.2906	0.4816	9.9868	- 0.4830	- 0.8492	1.3028	1.7223
0.3589	0.8277	17.1627	- 0.0465	- 0.0818	1.2338	1.6715
0.5001	0.3776	7.8308	- 0.4450	- 0.7823	1.3764	1.8522
0.7497	0.2589	5.3696	- 0.8762	- 1.5404	1.5033	2.0469
0.8033	- 0.1386	- 2.8738	- 1.4960	- 2.6302	1.5906	2.1488
1.0000	1.6321	1.6321	2.2444	2.2444	1.6321	2.2444

Values of the Chi functions for Toluene at 80°C						
Wt Fr	χ_{23}	χ_{23}	S and P	Star	123	123*
0.0000	1.1039	1.1039	1.3499	1.3499	1.1039	1.3499
0.0904	0.6617	21.1387	- 1.6666	- 4.4220	1.0603	1.3213
0.2516	- 0.6151	- 19.6512	- 1.6594	- 4.4028	1.2521	1.5402
0.2906	0.7545	24.1033	- 0.2053	- 0.5447	0.9840	1.2787
0.3589	0.8318	26.5739	- 0.0375	- 0.0995	0.9569	1.2631
0.5001	0.7001	22.3659	- 0.1176	- 0.3121	0.9915	1.3218
0.7497	0.3989	12.7437	- 0.7313	- 1.9404	1.1232	1.4963
0.8033	- 0.2943	- 9.4029	- 1.6468	- 4.3696	1.2503	1.6327
1.0000	1.2284	1.2284	1.6451	1.6451	1.2284	1.6451

Values of the Chi functions for 2-Butanone at 80°C						
Wt Fr	χ_{23}	χ_{23}	S and P	Star	123	123*
0.0000	1.8529	1.8529	2.1146	2.1146	1.8529	2.1146
0.0904	-0.1581	-5.9064	-2.4857	-8.0590	1.8749	2.1484
0.2516	-0.7953	-29.7148	-1.8389	-5.9619	2.0282	2.3229
0.2906	0.6595	24.6427	-0.2996	-0.9714	1.7445	2.0445
0.3589	0.8680	32.4318	-0.0007	-0.0022	1.6874	1.9964
0.5001	0.5560	20.7722	-0.2612	-0.8467	1.7626	2.0905
0.7497	0.2981	11.1395	-0.8314	-2.6956	1.8700	2.2317
0.8033	-0.2637	-9.8510	-1.6155	-5.2377	1.9721	2.3411
1.0000	1.9496	1.9496	2.3456	2.3456	1.9496	2.3456

Values of the Chi functions for Trichloromethane at 80°C						
Wt Fr	χ_{23}	χ_{23}	S and P	Star	123	123*
0.0000	0.7963	0.7963	1.0388	1.0388	0.7963	1.0388
0.0904	-0.5704	-23.7700	-2.8969	-10.4045	0.8482	1.1012
0.2516	-1.0257	-42.7452	-2.0681	-7.4279	1.0033	1.2751
0.2906	0.5825	24.2769	-0.3755	-1.3487	0.6902	0.9665
0.3589	0.6548	27.2901	-0.2127	-0.7640	0.6631	0.9475
0.5001	0.5450	22.7127	-0.2710	-0.9733	0.6851	0.9862
0.7497	0.3919	16.3321	-0.7365	-2.6453	0.7607	1.0917
0.8033	-0.0256	-1.0674	-1.3763	-4.9432	0.8404	1.1779
1.0000	0.8461	0.8461	1.2075	1.2075	0.8461	1.2075

Values of the Chi functions for Methanol at 80°C						
Wt Fr	χ_{23}	χ_{23}	S and P	Star	123	123*
0.0000	2.0116	2.0116	2.1470	2.1470	2.0116	2.1470
0.0904	-2.7010	-118.574	-5.0299	-16.9518	2.2491	2.3960
0.2516	-0.8607	-37.7863	-1.9056	-6.4222	2.2111	2.3785
0.2906	0.6985	30.6653	-0.2619	-0.8827	1.9088	2.0813
0.3589	0.9485	41.6392	0.0785	0.2647	1.8444	2.0257
0.5001	0.6034	26.4901	-0.2150	-0.7245	1.9329	2.1325
0.7497	0.4454	19.5524	-0.6855	-2.3101	2.0364	2.2687
0.8033	-1.6322	-71.6523	-2.9853	-10.0611	2.3829	2.6223
1.0000	2.1550	2.1550	2.4206	2.4206	2.1550	2.4206

Values of the Chi functions for Methyl Acetate at 80°C						
Wt Fr	χ_{23}	χ_{23}	S and P	Star	123	123*
0.0000	2.0116	2.0116	2.1470	2.1470	2.0116	2.1470
0.0904	- 2.7010	- 118.5744	- 5.0299	- 16.9518	2.2491	2.3960
0.2516	- 0.8607	- 37.7863	- 1.9056	- 6.4222	2.2111	2.3785
0.2906	0.6985	30.6653	- 0.2619	- 0.8827	1.9088	2.0813
0.3589	0.9485	41.6392	0.0785	0.2647	1.8444	2.0257
0.5001	0.6034	26.4901	- 0.2150	- 0.7245	1.9329	2.1325
0.7497	0.4454	19.5524	- 0.6855	- 2.3101	2.0364	2.2687
0.8033	- 1.6322	- 71.6523	- 2.9853	- 10.0611	2.3829	2.6223
1.0000	2.1550	2.1550	2.4206	2.4206	2.1550	2.4206

Values of the Chi functions for 2-Propanone at 80°C						
Wt Fr	χ_{23}	χ_{23}	S and P	Star	123	123*
0.0000	2.2107	2.2107	2.4861	2.4861	2.2107	2.4861
0.0904	- 0.2195	- 9.8335	- 2.5473	- 10.2965	2.2381	2.5224
0.2516	- 0.9680	- 43.3707	- 2.0117	- 8.1317	2.4196	2.7200
0.2906	0.6394	28.6510	- 0.3199	- 1.2931	2.1076	2.4119
0.3589	0.8586	38.4690	- 0.0103	- 0.0416	2.0488	2.3600
0.5001	0.4758	21.3175	- 0.3415	- 1.3805	2.1423	2.4679
0.7497	0.1955	8.7611	- 0.9342	- 3.7762	2.2498	2.6010
0.8033	- 2.0501	- 91.8553	- 3.4021	- 13.7517	2.6130	2.9698
1.0000	2.3111	2.3111	2.6885	2.6885	2.3111	2.6885

Values of the Chi functions for Isopropanol 80°C						
Wt Fr	χ_{23}	χ_{23}	S and P	Star	123	123*
0.0000	2.5468	2.5468	2.8238	2.8238	2.5468	2.8238
0.0904	7.0080	302.411	4.6832	18.1673	1.9627	2.2492
0.2516	- 0.5396	- 23.2856	- 1.5803	- 6.1305	2.6444	2.9478
0.2906	0.7554	32.5992	- 0.2008	- 0.7791	2.3849	2.6924
0.3589	0.8934	38.5527	0.0276	0.1071	2.3339	2.6487
0.5001	0.4389	18.9415	- 0.3753	- 1.4558	2.4280	2.7578
0.7497	0.2769	11.9479	- 0.8498	- 3.2965	2.4816	2.8385
0.8033	- 0.4335	- 18.7051	- 1.7824	- 6.9144	2.6002	2.9630
1.0000	2.5288	2.5288	2.9132	2.9132	2.5288	2.9132

Values of the Chi functions for Ethyl Acetate at 80°C						
Wt Fr	χ_{23}	χ_{23}	S and P	Star	123	123*
0.0000	2.5141	2.5141	2.8037	2.8037	2.5141	2.8037
0.0904	0.3554	12.0758	- 1.9714	- 5.9167	2.4907	2.7932
0.2516	- 0.5495	- 18.6695	- 1.5923	- 4.7789	2.6354	2.9611
0.2906	0.9276	31.5159	- 0.0308	- 0.0923	2.3417	2.6731
0.3589	1.0843	36.8394	0.2164	0.6495	2.2882	2.6295
0.5001	0.7322	24.8771	- 0.0841	- 0.2524	2.3651	2.7271
0.7497	0.5380	18.2775	- 0.5908	- 1.7731	2.4647	2.8635
0.8033	- 1.2722	- 43.2235	- 2.6233	- 7.8730	2.7681	3.1749
1.0000	2.5818	2.5818	3.0181	3.0181	2.5818	3.0181

Values of the Chi functions for Benzene at 100°C						
Wt Fr	χ_{23}	χ_{23}	S and P	Star	123	123*
0.0000	1.3145	1.3145	1.5703	1.5703	1.3145	1.5703
0.0904	0.1107	4.1507	- 2.2884	- 7.3970	1.3195	1.5871
0.2516	0.4726	17.7129	- 0.6042	- 1.9531	1.2644	1.5532
0.2906	0.4640	17.3932	- 0.5258	- 1.6997	1.2638	1.5579
0.3589	0.2928	10.9759	- 0.6039	- 1.9521	1.3031	1.6063
0.5001	0.7006	26.2599	- 0.1432	- 0.4630	1.2176	1.5397
0.7497	1.1338	42.4964	- 0.0327	- 0.1057	1.2202	1.5760
1.0000	1.4697	1.4697	1.8599	1.8599	1.4697	1.8599

Values of the Chi functions for Dichloromethane at 100°C						
Wt Fr	χ_{23}	χ_{23}	S and P	Star	123	123*
0.0000	1.5225	1.5225	1.7933	1.7933	1.5225	1.7933
0.0904	- 0.7294	- 37.0565	- 3.1254	- 14.4691	1.5859	1.8642
0.2516	0.4932	25.0578	- 0.5805	- 2.6872	1.4363	1.7281
0.2906	0.3593	18.2532	- 0.6275	- 2.9048	1.4565	1.7515
0.3589	0.2748	13.9589	- 0.6189	- 2.8650	1.4696	1.7703
0.5001	0.7493	38.0663	- 0.0914	- 0.4233	1.3499	1.6626
0.7497	0.9320	47.3493	- 0.2313	- 1.0710	1.3708	1.7051
1.0000	1.5516	1.5516	1.9077	1.9077	1.5516	1.9077

Values of the Chi functions for Carbon Tetrachloride at 100°C						
Wt Fr	χ_{23}	χ_{23}	S and P	Star	123	123*
0.0000	1.3166	1.3166	1.5815	1.5815	1.3166	1.5815
0.0904	0.5773	- 19.9720	- 1.8212	- 1.8212	1.2805	1.5584
0.2516	0.5705	19.7384	- 0.5056	- 0.5056	1.2415	1.5430
0.2906	0.4984	17.2428	- 0.4908	- 0.4908	1.2515	1.5586
0.3589	0.3064	10.6016	- 0.5896	- 0.5896	1.2931	1.6102
0.5001	0.5588	19.3344	- 0.2843	- 0.2843	1.2427	1.5806
0.7497	0.9756	33.7513	- 0.1902	- 0.1902	1.2332	1.6083
1.0000	1.4471	1.4471	1.8600	1.8600	1.4471	1.8600

Values of the Chi functions for Cyclohexane at 100°C						
Wt Fr	χ_{23}	χ_{23}	S and P	Star	123	123*
0.0000	1.4484	1.4484	1.7354	1.7354	1.4484	1.7354
0.0904	0.6358	19.5728	- 1.7649	- 4.7129	1.4155	1.7173
0.2516	0.5818	17.9092	- 0.4965	- 1.3258	1.3935	1.7220
0.2906	0.5006	15.4096	- 0.4908	- 1.3107	1.4086	1.7436
0.3589	0.4086	12.5788	- 0.4897	- 1.3076	1.4330	1.7794
0.5001	0.7380	22.7187	- 0.1074	- 0.2867	1.3738	1.7438
0.7497	1.1540	35.5254	- 0.0104	- 0.0374	1.3975	1.8097
1.0000	1.6664	1.6664	2.1214	2.1214	1.6664	2.1214

Values of the Chi functions for Pentane at 100°C						
Wt Fr	χ_{23}	χ_{23}	S and P	Star	123	123*
0.0000	2.0068	2.0068	2.3941	2.3941	2.0068	2.3941
0.0904	- 1.8814	- 51.5235	- 4.2896	- 11.3468	2.2104	2.6126
0.2516	0.2443	6.6901	- 0.8415	- 2.2260	2.0909	2.5196
0.2906	0.4549	12.4569	- 0.5441	- 1.4391	2.0631	2.4982
0.3589	0.3652	10.0024	- 0.5406	- 1.4299	2.1082	2.5547
0.5001	1.1919	32.6400	0.3389	0.8966	1.9673	2.4373
0.7497	1.3503	36.9798	0.1747	0.4621	2.1413	2.6534
1.0000	2.5196	2.5196	3.0744	3.0744	2.5196	3.0744

Values of the Chi functions for Hexane at 100°C						
Wt Fr	χ_{23}	χ_{23}	S and P	Star	123	123*
0.0000	1.6422	1.6422	2.0072	2.0072	1.6422	2.0072
0.0904	- 0.7364	- 18.2936	- 3.1419	- 7.1544	1.7415	2.1242
0.2516	0.4395	10.9182	- 0.6438	- 1.4659	1.6643	2.0788
0.2906	0.4831	12.0014	- 0.5132	- 1.1687	1.6637	2.0860
0.3589	0.2445	6.0740	- 0.6587	- 1.5000	1.7359	2.1717
0.5001	0.7136	17.7295	- 0.1367	- 0.3112	1.6727	2.1367
0.7497	1.1802	29.3200	0.0072	0.0163	1.7344	2.2486
1.0000	2.0568	2.0568	2.6219	2.6219	2.0568	2.6219

Values of the Chi functions for Heptane at 100°C						
Wt Fr	χ_{23}	χ_{23}	S and P	Star	123	123*
0.0000	1.4121	1.4121	1.7694	1.7694	1.4121	1.7694
0.0904	-0.2245	-5.0490	-2.6271	-5.2290	1.4584	1.8364
0.2516	0.5647	12.7021	-0.5155	-1.0262	1.3816	1.7967
0.2906	0.4136	9.3027	-0.5798	-1.1540	1.4148	1.8389
0.3589	0.1866	4.1971	-0.7136	-1.4204	1.4781	1.9181
0.5001	0.5928	13.3336	-0.2545	-0.5066	1.4157	1.8885
0.7497	1.0156	22.8439	-0.1544	-0.3073	1.4496	1.9811
1.0000	1.7132	1.7132	2.3041	2.3041	1.7132	2.3041

Values of the Chi functions for Octane at 100°C						
Wt Fr	χ_{23}	χ_{23}	S and P	Star	123	123*
0.0000	1.3889	1.3889	1.7483	1.7483	1.3889	1.7483
0.0904	-0.4871	-9.9812	-2.8912	-5.1175	1.4625	1.8455
0.2516	0.4343	8.8982	-0.6474	-1.1459	1.3981	1.8236
0.2906	0.3488	7.1477	-0.6459	-1.1433	1.4223	1.8581
0.3589	0.2004	4.1051	-0.7013	-1.2413	1.4730	1.9269
0.5001	0.4350	8.9123	-0.4138	-0.7324	1.4615	1.9530
0.7497	1.1075	22.6930	-0.0639	-0.1131	1.4535	2.0119
1.0000	1.7487	1.7487	2.3749	2.3749	1.7487	2.3749

Values of the Chi functions for Toluene at 100°C						
Wt Fr	χ_{23}	χ_{23}	S and P	Star	123	123*
0.0000	1.2189	1.2189	1.4803	1.4803	1.2189	1.4803
0.0904	0.6656	21.0703	-1.7331	-4.6335	1.1764	1.4527
0.2516	0.5415	17.1420	-0.5349	-1.4299	1.1520	1.4550
0.2906	0.5283	16.7251	-0.4611	-1.2328	1.1506	1.4601
0.3589	0.3098	9.8079	-0.5865	-1.5679	1.1983	1.5192
0.5001	0.5962	18.8755	-0.2471	-0.6607	1.1407	1.4854
0.7497	0.2825	8.9437	-0.8835	-2.3620	1.2721	1.6591
1.0000	1.3595	1.3595	1.7894	1.7894	1.3595	1.7894

Values of the Chi functions for 2-Butanone at 100°C						
Wt Fr	χ_{23}	χ_{23}	S and P	Star	123	123*
0.0000	2.0512	2.0512	2.3336	2.3336	2.0512	2.3336
0.0904	0.2023	7.4426	- 2.1947	- 7.1615	2.0409	2.3350
0.2516	0.7129	26.2240	- 0.3617	- 1.1803	1.9341	2.2492
0.2906	0.5089	18.7213	- 0.4788	- 1.5622	1.9666	2.2868
0.3589	0.4078	15.0017	- 0.4867	- 1.5883	1.9829	2.3120
0.5001	0.8752	32.1922	0.0335	0.1094	1.8684	2.2162
0.7497	1.1313	41.6128	- 0.0330	- 0.1077	1.8943	2.2753
1.0000	2.1227	2.1227	2.5375	2.5375	2.1227	2.5375

Values of the Chi functions for Trichloromethane at 100°C						
Wt Fr	χ_{23}	χ_{23}	S and P	Star	123	123*
0.0000	1.0687	1.0687	1.3314	1.3314	1.0687	1.3314
0.0904	0.5849	24.0236	- 1.8100	- 6.5490	1.0189	1.2919
0.2516	0.6211	25.5099	- 0.4514	- 1.6334	0.9478	1.2394
0.2906	0.4692	19.2713	- 0.5164	- 1.8685	0.9679	1.2639
0.3589	0.2973	12.2098	- 0.5952	- 2.1536	0.9957	1.2996
0.5001	0.6846	28.1182	- 0.1550	- 0.5606	0.8916	1.2120
0.7497	1.0132	41.6154	- 0.1490	- 0.5390	0.8711	1.2209
1.0000	1.0568	1.0568	1.4365	1.4365	1.0568	1.4365

Values of the Chi functions for Methyl Acetate at 100°C						
Wt Fr	χ_{23}	χ_{23}	S and P	Star	123	123*
0.0000	2.3643	2.3643	2.5159	2.5159	2.3643	2.5159
0.0904	- 0.3208	- 14.0806	- 2.7161	- 9.3285	2.3911	2.5539
0.2516	0.4689	20.5815	- 0.6040	- 2.0743	2.2756	2.4584
0.2906	0.2451	10.7587	- 0.7408	- 2.5445	2.3137	2.5014
0.3589	0.1512	6.6384	- 0.7416	- 2.5470	2.3297	2.5260
0.5001	0.9275	40.7094	0.0876	0.3009	2.1329	2.3470
0.7497	0.8316	36.4986	- 0.3310	- 1.1367	2.2102	2.4561
1.0000	2.3653	2.3653	2.6435	2.6435	2.3653	2.6435

Values of the Chi functions for 2-Propanone at 100°C						
Wt Fr	χ_{23}	χ_{23}	S and P	Star	123	123*
0.0000	2.5520	2.5520	2.8521	2.8521	2.5520	2.8521
0.0904	- 0.6545	-28.6749	- 3.0517	-12.3836	2.6133	2.9222
0.2516	0.4933	21.6110	- 0.5815	- 2.3595	2.4772	2.8020
0.2906	0.3184	13.9485	- 0.6695	- 2.7166	2.5076	2.8363
0.3589	0.2155	9.4393	- 0.6793	- 2.7564	2.5290	2.8645
0.5001	0.9730	42.6248	0.1312	0.5323	2.3460	2.6956
0.7497	1.0240	44.8591	- 0.1405	- 0.5700	2.4169	2.7919
1.0000	2.6258	2.6258	3.0267	3.0267	2.6258	3.0267

Values of the Chi functions for Isopropanol at 100°C						
Wt Fr	χ_{23}	χ_{23}	S and P	Star	123	123*
0.0000	2.7016	2.7016	3.0036	3.0036	2.7016	3.0036
0.0904	0.3000	12.6649	- 2.0938	- 8.1581	2.6713	2.9826
0.2516	0.8048	33.9765	- 0.2666	- 1.0387	2.5341	2.8622
0.2906	0.4040	17.0577	- 0.5804	- 2.2615	2.6007	2.9329
0.3589	0.6600	27.8646	- 0.2313	- 0.9013	2.5281	2.8674
0.5001	0.8903	37.5884	0.0520	0.2024	2.4498	2.8040
0.7497	1.0823	45.6937	- 0.0787	- 0.3066	2.4565	2.8374
1.0000	2.6437	2.6437	3.0517	3.0517	2.6437	3.0517

Values of the Chi functions for Ethyl Acetate at 100°C						
Wt Fr	χ_{23}	χ_{23}	S and P	Star	123	123*
0.0000	2.5088	2.5088	2.8212	2.8212	2.5088	2.8212
0.0904	- 0.0238	- 0.7926	- 2.4204	- 7.3032	2.5160	2.8412
0.2516	0.5296	17.6606	- 0.5446	- 1.6433	2.4229	2.7710
0.2906	0.3844	12.8192	- 0.6029	- 1.8191	2.4459	2.7996
0.3589	0.2828	9.4305	- 0.6114	- 1.8447	2.4642	2.8277
0.5001	0.8469	28.2433	0.0057	0.0172	2.3259	2.7099
0.7497	1.0268	34.2414	- 0.1371	- 0.4136	2.3607	2.7810
1.0000	2.5661	2.5661	3.0234	3.0234	2.5661	3.0234

Values of the Chi functions for Benzene at 120°C						
Wt Fr	χ_{23}	χ_{23}	S and P	Star	123	123*
0.0000	1.3979	1.3979	1.6731	1.6731	1.3979	1.6731
0.0904	0.7156	26.4455	- 1.7502	- 5.6977	1.3529	1.6398
0.2516	0.5709	21.0978	- 0.5361	- 1.7454	1.3304	1.6383
0.2906	0.6141	22.6943	- 0.4037	- 1.3141	1.3176	1.6306
0.3589	0.6944	25.6612	- 0.2278	- 0.7415	1.2956	1.6176
0.5001	0.5316	19.6458	- 0.3363	- 1.0950	1.3460	1.6866
0.7497	1.1581	42.7992	- 0.0422	- 0.1375	1.3034	1.6773
1.0000	1.5584	1.5584	1.9661	1.9661	1.5584	1.9661

Values of the Chi functions for Dichloromethane at 120°C						
Wt Fr	χ_{23}	χ_{23}	S and P	Star	123	123*
0.0000	1.7301	1.7301	2.0270	2.0270	1.7301	2.0270
0.0904	0.5154	25.5684	- 1.9482	- 9.0685	1.6936	1.9979
0.2516	0.3907	19.3828	-0.7141	- 3.3242	1.6740	1.9916
0.2906	0.4555	22.5953	-0.5601	- 2.6071	1.6564	1.9772
0.3589	0.4909	24.3502	-0.4291	- 1.9973	1.6424	1.9689
0.5001	0.8442	41.8757	-0.0216	- 0.1005	1.5550	1.8933
0.7497	0.8907	44.1853	-0.3074	- 1.4311	1.6180	1.9775
1.0000	1.8013	1.8013	2.1823	2.1823	1.8013	2.1823

Values of the Chi functions for Carbon Tetrachloride at 120°C						
Wt Fr	χ_{23}	χ_{23}	S and P	Star	123	123*
0.0000	1.4032	1.4032	1.6878	1.6878	1.4032	1.6878
0.0904	0.8033	27.4034	- 1.6628	- 4.9952	1.3520	1.6495
0.2516	0.4883	16.6591	- 0.6190	- 1.8595	1.3544	1.6750
0.2906	0.6724	22.9374	-0.3457	- 1.0384	1.3143	1.6405
0.3589	0.7017	23.9375	-0.2207	- 0.6631	1.3035	1.6396
0.5001	0.5138	17.5281	-0.3544	- 1.0647	1.3617	1.7183
0.7497	1.1447	39.0510	-0.0559	- 0.1680	1.3200	1.7132
1.0000	1.5755	1.5755	2.0058	2.0058	1.5755	2.0058

Values of the Chi functions for Cyclohexane at 120°C						
Wt Fr	χ_{23}	χ_{23}	S and P	Star	123	123*
0.0000	1.5094	1.5094	1.8164	1.8164	1.5094	1.8164
0.0904	0.8444	25.6041	-1.6241	-4.3682	1.4636	1.7853
0.2516	0.5144	15.5975	-0.5953	-1.6013	1.4800	1.8280
0.2906	0.7054	21.3888	-0.3151	-0.8475	1.4418	1.7962
0.3589	0.7944	24.0880	-0.1304	-0.3508	1.4230	1.7887
0.5001	0.4726	14.3309	-0.3980	-1.0706	1.5265	1.9155
0.7497	1.2639	38.3260	0.0609	0.1637	1.4761	1.9067
1.0000	1.7774	1.7774	2.2501	2.2501	1.7774	2.2501

Values of the Chi functions for Pentane at 120°C						
Wt Fr	χ_{23}	χ_{23}	S and P	Star	123	123*
0.0000	2.3689	2.3689	2.7903	2.7903	2.3689	2.7903
0.0904	-2.4972	-65.8571	-4.9864	-13.2278	2.6761	3.1121
0.2516	0.3264	8.6087	-0.8041	-2.1331	2.5812	3.0435
0.2906	0.8498	22.4123	-0.1914	-0.5079	2.5090	2.9776
0.3589	1.3514	35.6386	0.4057	1.0761	2.4469	2.9268
0.5001	2.3402	61.7169	1.4486	3.8428	2.3266	2.8298
0.7497	3.1209	82.3063	1.8968	5.0317	2.5985	3.1431
1.0000	3.4446	3.4446	4.0313	4.0313	3.4446	4.0313

Values of the Chi functions for Hexane at 120°C						
Wt Fr	χ_{23}	χ_{23}	S and P	Star	123	123*
0.0000	1.8190	1.8190	2.2105	2.2105	1.8190	2.2105
0.0904	-0.9706	-23.5173	-3.4439	-7.8802	1.9422	2.3512
0.2516	0.2245	5.4400	-0.8900	-2.0365	1.8934	2.3338
0.2906	0.6738	16.3257	-0.3514	-0.8042	1.8142	2.2623
0.3589	0.6964	16.8731	-0.2332	-0.5337	1.8247	2.2861
0.5001	0.8005	19.3959	-0.0750	-0.1715	1.8506	2.3399
0.7497	1.3244	32.0878	0.1164	0.2664	1.9185	2.4574
1.0000	2.2782	2.2782	2.8673	2.8673	2.2782	2.8673

Values of the Chi functions for Heptane at 120°C						
Wt Fr	χ'_{23}	χ_{23}	S and P	Star	123	123*
0.0000	1.5400	1.5400	1.9190	1.9190	1.5400	1.9190
0.0904	- 0.0049	- 0.1081	- 2.4741	- 4.9538	1.5686	1.9682
0.2516	0.3665	8.0949	- 0.7440	- 1.4896	1.5486	1.9850
0.2906	0.6483	14.3184	- 0.3729	- 0.7466	1.4957	1.9410
0.3589	0.6189	13.6686	- 0.3067	- 0.6141	1.5084	1.9693
0.5001	0.5520	12.1896	- 0.3195	- 0.6397	1.5570	2.0504
0.7497	1.0070	22.2386	- 0.1969	- 0.3943	1.5840	2.1353
1.0000	1.8472	1.8472	2.4571	2.4571	1.8472	2.4571

Values of the Chi functions for Octane at 120°C						
Wt Fr	χ'_{23}	χ_{23}	S and P	Star	123	123*
0.0000	1.4889	1.4889	1.8672	1.8672	1.4889	1.8672
0.0904	0.2780	5.6147	- 2.1905	- 3.9021	1.4916	1.8933
0.2516	0.3404	6.8742	- 0.7694	- 1.3706	1.4962	1.9399
0.2906	0.7247	14.6372	- 0.2958	- 0.5269	1.4214	1.8753
0.3589	0.6631	13.3927	- 0.2618	- 0.4664	1.4380	1.9098
0.5001	0.4963	10.0242	- 0.3744	- 0.6669	1.5071	2.0161
0.7497	0.9843	19.8805	- 0.2188	- 0.3898	1.5182	2.0933
1.0000	1.7709	1.7709	2.4129	2.4129	1.7709	2.4129

Values of the Chi functions for Toluene at 120°C						
Wt Fr	χ'_{23}	χ_{23}	S and P	Star	123	123*
0.0000	1.2557	1.2557	1.5340	1.5340	1.2557	1.5340
0.0904	0.8327	26.0721	- 1.6328	- 4.3974	1.2003	1.4933
0.2516	0.5416	16.9582	- 0.5652	- 1.5221	1.1919	1.5114
0.2906	0.6577	20.5933	- 0.3598	- 0.9690	1.1643	1.4901
0.3589	0.6212	19.4501	- 0.3007	- 0.8098	1.1678	1.5049
0.5001	0.4758	14.8968	- 0.3919	- 1.0555	1.2142	1.5747
0.7497	1.0450	32.7201	- 0.1551	- 0.4177	1.1769	1.5791
1.0000	1.4092	1.4092	1.8537	1.8537	1.4092	1.8537

Values of the Chi functions for 2-Butanone at 120°C						
Wt Fr	χ_{23}	χ_{23}	S and P	Star	123	123*
0.0000	2.1646	2.1646	2.4698	2.4698	2.1646	2.4698
0.0904	0.7449	26.8893	- 1.7182	-5.6399	2.1074	2.4241
0.2516	0.2654	9.5811	- 0.8389	-2.7536	2.1280	2.4654
0.2906	0.5593	20.1901	- 0.4557	- 1.4959	2.0643	2.4068
0.3589	0.6012	21.7027	- 0.3182	- 1.0444	2.0452	2.3965
0.5001	0.9382	33.8667	0.0730	0.2396	1.9573	2.3270
0.7497	0.9056	32.6922	- 0.2919	-0.9583	2.0368	2.4393
1.0000	2.2186	2.2186	2.6544	2.6544	2.2186	2.6544

Values of the Chi functions for Trichloromethane at 120°C						
Wt Fr	χ_{23}	χ_{23}	S and P	Star	123	123*
0.0000	1.2209	1.2209	1.5058	1.5058	1.2209	1.5058
0.0904	0.8402	33.9054	- 1.6217	-5.9088	1.1515	1.4466
0.2516	0.7395	29.8418	- 0.3637	- 1.3250	1.0825	1.3958
0.2906	0.6513	26.2843	- 0.3625	- 1.3209	1.0880	1.4057
0.3589	0.6389	25.7815	- 0.2794	- 1.0179	1.0761	1.4017
0.5001	0.6718	27.1080	- 0.1923	-0.7006	1.0571	1.3988
0.7497	1.0843	43.7559	- 0.1121	-0.4086	1.0254	1.3961
1.0000	1.2291	1.2291	1.6292	1.6292	1.2291	1.6292

Values of the Chi functions for Methyl Acetate at 120°C						
Wt Fr	χ_{23}	χ_{23}	S and P	Star	123	123*
0.0000	2.6963	2.6963	2.8679	2.8679	2.6963	2.8679
0.0904	0.2900	12.6970	- 2.1732	-7.6256	2.6774	2.8597
0.2516	- 0.0552	- 2.4185	- 1.1597	-4.0691	2.7214	2.9232
0.2906	0.4883	21.3825	- 0.5269	- 1.8487	2.6118	2.8182
0.3589	0.7873	34.4750	- 0.1322	-0.4640	2.5350	2.7498
0.5001	1.2463	54.5756	0.3810	1.3368	2.4136	2.6457
0.7497	0.6947	30.4208	- 0.5030	- 1.7650	2.6102	2.8730
1.0000	2.7535	2.7535	3.0476	3.0476	2.7535	3.0476

Values of the Chi functions for 2-Propanone at 120°C						
Wt Fr	χ_{23}	χ_{23}	S and P	Star	123	123*
0.0000	2.9219	2.9219	3.2492	3.2492	2.9219	3.2492
0.0904	0.1485	6.3309	-2.3143	-9.4170	2.9132	3.2493
0.2516	-0.1253	-5.3434	-1.2293	-5.0023	2.9561	3.3079
0.2906	0.3514	14.9825	-0.6633	-2.6992	2.8609	3.2166
0.3589	0.7614	32.4630	-0.1577	-0.6419	2.7607	3.1231
0.5001	1.5514	66.1468	0.6865	2.7933	2.5547	2.9311
0.7497	0.7701	32.8331	-0.4273	-1.7385	2.8095	3.2109
1.0000	2.9628	2.9628	3.3897	3.3897	2.9628	3.3897

Values of the Chi functions for Isopropanol at 120°C						
Wt Fr	χ_{23}	χ_{23}	S and P	Star	123	123*
0.0000	2.8419	2.8419	3.1715	3.1715	2.8419	3.1715
0.0904	0.0850	3.4955	-2.3750	-9.2848	2.8286	3.1674
0.2516	0.0354	1.4550	-1.0658	-4.1668	2.8181	3.1735
0.2906	0.3315	13.6297	-0.6805	-2.6603	2.7533	3.1128
0.3589	0.5691	23.4037	-0.3472	-1.3572	2.6860	3.0525
0.5001	1.3033	53.5932	0.4412	1.7249	2.4823	2.8635
0.7497	0.8045	33.0824	-0.3899	-1.5245	2.6419	3.0494
1.0000	2.7750	2.7750	3.2093	3.2093	2.7750	3.2093

Values of the Chi functions for Ethyl Acetate at 120°C						
Wt Fr	χ_{23}	χ_{23}	S and P	Star	123	123*
0.0000	2.4985	2.4985	2.8361	2.8361	2.4985	2.8361
0.0904	0.6008	19.5908	-1.8628	-5.6466	2.4555	2.8057
0.2516	0.2335	7.6143	-0.8713	-2.6412	2.4738	2.8467
0.2906	0.5942	19.3769	-0.4213	-1.2771	2.3977	2.7762
0.3589	0.6766	22.0643	-0.2433	-0.7374	2.3700	2.7581
0.5001	0.9182	29.9419	0.0525	0.1591	2.3078	2.7161
0.7497	0.9429	30.7475	-0.2552	-0.7736	2.3810	2.8253
1.0000	2.5754	2.5754	3.0561	3.0561	2.5754	3.0561

Probe - Benzene at 80°C

Wt Fr	X_{23}	Q_{23}	T_{sp}
0.0000	584.4	0.0000	-
0.0904	339.6	-0.7795	6.26
0.2515	-262.0	0.6216	-
0.2905	366.5	-0.8379	6.59
0.3588	402.8	-0.9204	6.04
0.5000	357.1	-0.8114	6.81
0.7496	217.2	-0.4854	10.00
0.8033	-18.8	0.0559	69.11
1.0000	781.7	0.0000	-

Probe - Dichloromethane at 80°C

Wt Fr	X_{23}	Q_{23}	T_{sp}
0.0000	752.2	0.0000	-
0.0904	-126.7	0.3087	-
0.2515	-447.8	1.0534	-
0.2905	344.8	-0.7873	7.00
0.3588	371.9	-0.8488	6.54
0.5000	290.7	-0.6582	8.34
0.7496	85.7	-0.1837	21.14
0.8033	-325.7	0.7590	-
1.0000	978.0	0.0000	-

Probe - Cyclohexane at 80°C

Wt Fr	X_{23}	Q_{23}	T_{sp}
0.0000	521.3	0.0000	-
0.0904	78.1	0.1952	-
0.2515	-275.3	0.6526	-
0.2905	286.2	-0.6515	8.40
0.3588	367.4	-0.8384	6.62
0.5000	319.5	-0.7247	7.60
0.7496	320.2	-0.7217	73.57
0.8033	-21.5	0.0620	-
1.0000	783.7	0.0000	-

Probe - Carbon tetrachloride at 80°C

Wt Fr	X_{23}	Q_{23}	T_{sp}
0.0000	513.3	0.0000	-
0.0904	-223.5	0.3087	-
0.2515	-397.9	1.0534	-
0.2905	400.9	-0.7873	6.03
0.3588	475.9	-0.8488	5.12
0.5000	411.2	-0.6582	5.92
0.7496	320.8	-0.1837	21.14
0.8033	-105.2	0.7590	7.05
1.0000	738.1	0.0000	-

Probe - Pentane at 80°C

Wt Fr	X_{23}	Q_{23}	T_{sp}
0.0000	598.1	0.0000	-
0.0904	766.3	1.8012	-
0.2515	-1112.1	2.5969	-
0.2905	283.9	0.6460	8.47
0.3588	498.3	1.1416	4.89
0.5000	234.4	0.5283	10.30
0.7496	125.4	0.2749	15.80
0.8033	-195.7	0.4610	-
1.0000	820.8	0.0000	-

Probe - Hexane at 80°C

Wt Fr	X_{23}	Q_{23}	T_{sp}
0.0000	494.0	0.0000	-
0.0904	-725.8	1.7067	-
0.2515	-731.7	1.7131	-
0.2905	259.7	0.5898	9.25
0.3588	290.8	0.6608	8.35
0.5000	205.1	0.4605	11.73
0.7496	167.7	0.3720	12.47
0.8033	132.4	0.2905	13.81
1.0000	731.9	0.0000	-

Probe - Heptane at 80°C

Wt Fr	X_{23}	Q_{23}	T_{sp}
0.0000	370.3	0.0000	-
0.0904	-790.6	1.8579	-
0.2515	-649.5	1.5211	-
0.2905	-188.5	0.4504	-
0.3588	352.5	-0.8038	6.90
0.5000	171.4	-0.3827	13.96
0.7496	175.4	-0.3895	12.01
0.8033	79.9	-0.1703	19.35
1.0000	605.9	0.0000	-

Probe - Octane at 80°C

Wt Fr	X_{23}	Q_{23}	T_{sp}
0.0000	364.8	0.0000	-
0.0904	-707.0	1.6627	-
0.2515	-539.7	1.2670	-
0.2905	155.7	-0.3484	15.17
0.3588	257.6	-0.5839	9.41
0.5000	131.8	-0.2913	17.93
0.7496	101.4	-0.2198	76.69
0.8033	-23.2	0.0659	-
1.0000	582.5	0.0000	-

Probe - 2-Butanone at 80°C

Wt Fr	X_{23}	Q_{23}	T_{sp}
0.0000	882.8	0.0000	—
0.0904	- 63.8	0.1619	—
0.2515	- 378.8	0.8932	—
0.2905	337.8	- 0.7712	7.14
0.3588	447.6	- 1.0241	5.44
0.5000	299.8	- 0.6791	6.13
0.7496	175.2	- 0.3890	7.41
0.8033	-132.8	0.3170	55.65
1.0000	1096.8	0.0000	—

Probe - Toluene at 80°C

Wt Fr	X_{23}	Q_{23}	T_{sp}
0.0000	471.7	0.0000	—
0.0904	240.3	- 0.5478	8.40
0.2515	- 211.4	0.5040	—
0.2905	284.9	- 0.6483	8.44
0.3588	317.7	- 0.7231	7.65
0.5000	277.3	- 0.6273	8.74
0.7496	171.4	- 0.3803	12.25
0.8033	- 107.8	0.2596	—
1.0000	654.0	0.0000	—

Probe - Chloroform at 80°C

Wt Fr	X_{23}	Q_{23}	T_{sp}
0.0000	398.2	0.0000	—
0.0904	- 361.2	0.8559	—
0.2515	- 680.7	1.5945	—
0.2905	404.9	- 0.9268	5.97
0.3588	460.7	- 1.0546	5.29
0.5000	397.0	- 0.9036	6.13
0.7496	303.8	- 0.6842	55.65
0.8033	- 8.6	0.0324	—
1.0000	575.4	0.0000	—

Probe - Methyl Acetate at 80°C

Wt Fr	X_{23}	Q_{23}	T_{sp}
0.0000	364.8	0.0000	—
0.0904	- 707.0	1.6627	—
0.2515	- 539.7	1.2670	5.50
0.2905	155.7	- 0.3484	4.07
0.3588	257.6	- 0.5839	6.07
0.5000	131.8	- 0.2913	7.12
0.7496	101.4	- 0.2198	21.14
0.8033	- 23.2	0.0659	—
1.0000	582.5	0.0000	—

Probe - 2-Propanone at 80°C

Wt Fr	X_{23}	Q_{23}	T_{sp}
0.0000	1221.6	0.0000	—
0.0904	- 137.0	0.3327	—
0.2515	- 674.2	1.5794	—
0.2905	472.6	- 1.0842	5.12
0.3588	639.2	- 1.4681	3.81
0.5000	371.7	- 0.8451	6.54
0.7496	170.1	- 0.3773	12.33
0.8033	- 1623.0	3.7308	—
1.0000	1493.7	0.0000	—

Probe - Isopropanol at 80°C

Wt Fr	X_{23}	Q_{23}	T_{sp}
0.0000	1088.7	0.0000	—
0.0904	4607.3	-10.7388	0.52
0.2515	- 374.5	0.8830	—
0.2905	513.7	-1.1793	4.72
0.3588	617.9	- 1.4188	3.94
0.5000	310.2	- 0.7032	7.83
0.7496	204.7	- 0.4567	10.53
0.8033	- 337.8	0.7866	—
1.0000	1387.8	0.0000	—

Probe - Ethyl Acetate at 80°C

Wt Fr	X_{23}	Q_{23}	T_{sp}
0.0000	1097.3	0.0000	—
0.0904	191.8	-0.4347	10.09
0.2515	- 278.9	0.6609	—
0.2905	505.1	- 1.1596	4.79
0.3588	597.4	- 1.3712	4.08
0.5000	419.6	- 0.9559	5.80
0.7496	328.2	- 0.7400	6.91
0.8033	- 742.5	1.7137	—
1.0000	1310.7	0.0000	—

Probe - Benzene at 100°C

Wt Fr	X_{23}	Q_{23}	T_{sp}
0.0000	657.5	0.0000	—
0.0904	68.0	-0.1371	21.17
0.2515	251.0	-0.5364	10.03
0.2905	248.9	-0.5311	10.22
0.3588	165.1	-0.3475	15.42
0.5000	384.9	-0.8234	6.71
0.7496	645.8	-1.3812	3.88
1.0000	900.4	0.0000	—

Probe - Dichloromethane at 100°C

Wt Fr	X_{23}	Q_{23}	T_{sp}
0.0000	969.1	0.0000	—
0.0904	-399.1	0.8881	—
0.2515	288.6	-0.6185	8.08
0.2905	213.5	-0.4540	11.88
0.3588	167.5	-0.3519	15.22
0.5000	459.8	-0.9861	5.63
0.7496	601.2	-1.2850	4.15
1.0000	978.0	0.0000	—

Probe - Cyclohexane at 100°C

Wt Fr	X_{23}	Q_{23}	T_{sp}
0.0000	608.3	0.0000	—
0.0904	277.9	-0.5977	7.82
0.2515	264.9	-0.5668	9.52
0.2905	232.5	-0.4953	10.92
0.3588	196.0	-0.4149	13.04
0.5000	349.1	-0.7457	7.39
0.7496	563.4	-1.2034	4.41
1.0000	855.3	0.0000	—

Probe - Carbon tetrachloride at 100°C

Wt Fr	X_{23}	Q_{23}	T_{sp}
0.0000	615.4	0.0000	—
0.0904	353.8	-0.7643	6.76
0.2515	362.5	-0.7800	7.01
0.2905	321.6	-0.6900	7.95
0.3588	207.8	-0.4406	5.12
0.5000	374.8	-0.8017	5.92
0.7496	674.4	-1.4430	3.72
1.0000	830.8	0.0000	—

Probe - Pentane at 100°C

Wt Fr	X_{23}	Q_{23}	T_{sp}
0.0000	710.2	0.0000	-
0.0904	-740.7	1.6380	-
0.2515	139.8	-0.2933	17.46
0.2905	231.6	-0.4934	10.96
0.3588	195.7	-0.4143	13.06
0.5000	573.8	-1.2338	4.52
0.7496	679.2	-1.4531	3.69
1.0000	1115.2	0.0000	-

Probe - Hexane at 100°C

Wt Fr	X_{23}	Q_{23}	T_{sp}
0.0000	530.4	0.0000	-
0.0904	-241.2	0.5416	-
0.2515	193.8	-0.4113	12.85
0.2905	212.0	-0.4506	11.94
0.3588	122.7	-0.2553	20.42
0.5000	313.2	-0.6679	8.22
0.7496	525.4	-1.1214	4.72
1.0000	731.9	0.0000	-

Probe - Heptane at 100°C

Wt Fr	X_{23}	Q_{23}	T_{sp}
0.0000	420.7	0.0000	-
0.0904	-55.9	0.1348	-
0.2515	224.8	-0.4790	11.15
0.2905	172.0	-0.3633	14.60
0.3588	91.2	-0.1865	26.86
0.5000	247.4	-0.5250	10.36
0.7496	428.8	-0.9130	5.71
1.0000	666.5	0.0000	-

Probe - Octane at 100°C

Wt Fr	X_{23}	Q_{23}	T_{sp}
0.0000	392.7	0.0000	-
0.0904	-119.0	0.2734	-
0.2515	151.1	-0.3180	16.24
0.2905	126.7	-0.2643	19.48
0.3588	83.1	-0.1690	29.17
0.5000	159.3	-0.3337	15.84
0.7496	390.4	-0.8301	6.22
1.0000	582.5	0.0000	-

Probe - 2-Butanone at 100°C

Wt Fr	X_{23}	Q_{23}	T_{sp}
0.0000	1006.3	0.0000	—
0.0904	112.1	- 0.2337	15.63
0.2515	381.6	- 0.8217	6.67
0.2905	277.9	- 0.5945	9.18
0.3588	228.2	- 0.4851	11.24
0.5000	491.7	- 1.0552	5.27
0.7496	666.0	- 1.4248	3.76
1.0000	1227.3	0.0000	—

Probe - Toluene at 100°C

Wt Fr	X_{23}	Q_{23}	T_{sp}
0.0000	532.7	0.0000	—
0.0904	257.5	- 0.5529	8.34
0.2515	219.3	- 0.4671	11.42
0.2905	216.1	- 0.4595	11.72
0.3588	133.7	- 0.2792	18.84
0.5000	253.4	- 0.5380	10.12
0.7496	133.4	- 0.2758	15.76
1.0000	654.0	0.0000	—

Probe - Chloroform at 100°C

Wt Fr	X_{23}	Q_{23}	T_{sp}
0.0000	547.8	0.0000	—
0.0904	407.8	- 0.8828	5.62
0.2515	448.6	- 0.9681	5.69
0.2905	343.1	- 0.7369	7.46
0.3588	222.7	- 0.4731	11.51
0.5000	521.3	- 1.1198	4.97
0.7496	810.3	- 1.7360	3.12
1.0000	707.7	0.0000	—

Probe - Methyl Acetate at 100°C

Wt Fr	X_{23}	Q_{23}	T_{sp}
0.0000	1382.7	0.0000	—
0.0904	- 183.8	0.4155	—
0.2515	311.7	- 0.6690	8.13
0.2905	170.9	- 0.3606	14.70
0.3588	112.2	- 0.2322	22.22
0.5000	636.5	- 1.3697	4.07
0.7496	602.5	- 1.2879	4.14
1.0000	1498.2	0.0000	—

Probe - 2-Propanone at 100°C

Wt Fr	X_{23}	Q_{23}	T_{sp}
0.0000	1459.5	0.0000	—
0.0904	- 461.9	1.0260	—
0.2515	- 383.9	- 0.8267	6.63
0.2905	254.6	- 0.5436	10.00
0.3588	179.2	- 0.3784	14.22
0.5000	785.4	- 1.6931	3.30
0.7496	870.2	- 1.8652	2.91
1.0000	1742.6	0.0000	—

Probe - Isopropanol at 100°C

Wt Fr	X_{23}	Q_{23}	T_{sp}
0.0000	1162.2	0.0000	—
0.0904	200.3	- 0.4274	10.22
0.2515	572.4	- 1.2387	4.47
0.2905	285.8	- 0.6117	8.93
0.3588	479.4	- 1.0324	5.40
0.5000	669.9	- 1.4424	3.87
0.7496	860.8	- 1.8449	2.94
1.0000	1462.1	0.0000	—

Probe - Ethyl Acetate at 100°C

Wt Fr	X_{23}	Q_{23}	T_{sp}
0.0000	1128.0	0.0000	—
0.0904	- 1.77	0.0160	46.44
0.2515	307.4	- 0.6596	—
0.2905	228.2	- 0.4860	11.12
0.3588	173.5	- 0.3659	14.68
0.5000	511.5	- 1.0983	5.06
0.7496	650.6	- 1.3916	3.85
1.0000	1344.6	0.0000	—

Probe - Benzene at 120°C

Wt Fr	X_{23}	Q_{23}	T_{sp}
0.0000	706.9	0.0000	–
0.0904	317.9	-0.6440	8.43
0.2515	343.6	-0.6963	7.88
0.2905	392.1	-0.7947	6.98
0.3588	313.4	-0.6305	8.69
0.5000	384.9	-0.8234	6.71
0.7496	697.6	-1.4084	3.81
1.0000	973.1	0.0000	–

Probe - Dichloromethane at 100°C

Wt Fr	X_{23}	Q_{23}	T_{sp}
0.0000	1117.1	0.0000	–
0.0904	310.3	-0.6310	7.48
0.2515	246.0	-0.4958	10.80
0.2905	287.7	-0.5811	9.38
0.3588	314.0	-0.6351	8.69
0.5000	549.6	-1.1143	4.99
0.7496	610.4	-1.2310	4.32
1.0000	1410.7	0.0000	–

Probe - Cyclohexane at 120°C

Wt Fr	X_{23}	Q_{23}	T_{sp}
0.0000	641.1	0.0000	–
0.0904	386.8	-0.7894	6.19
0.2515	252.9	-0.5099	10.52
0.2905	341.2	-0.6913	7.94
0.3588	387.0	-0.7842	7.07
0.5000	246.7	-0.4939	10.98
0.7496	553.4	-1.3185	4.05
1.0000	931.2	0.0000	–

Probe - Carbon tetrachloride at 120°C

Wt Fr	X_{23}	Q_{23}	T_{sp}
0.0000	661.0	0.0000	–
0.0904	517.0	-1.0591	4.78
0.2515	334.6	-0.6783	8.02
0.2905	455.9	-0.9275	5.97
0.3588	481.8	-0.9761	5.69
0.5000	369.9	-0.7462	7.39
0.7496	837.2	-1.6926	3.19
1.0000	916.7	0.0000	–

Probe - Pentane at 120°C

Wt Fr	X_{23}	Q_{23}	T_{sp}
0.0000	848.8	0.0000	—
0.0904	1015.8	2.1150	—
0.2515	215.6	-0.4330	12.25
0.2905	454.5	-0.9246	5.98
0.3588	691.7	-1.4106	3.97
0.5000	1181.1	-2.4079	2.33
0.7496	1633.0	-3.3122	1.67
1.0000	1522.6	0.0000	—

Probe - Hexane at 120°C

Wt Fr	X_{23}	Q_{23}	T_{sp}
0.0000	587.8	0.0000	—
0.0904	342.1	0.7199	—
0.2515	121.1	-0.2383	20.92
0.2905	302.6	-0.6118	8.93
0.3588	316.2	-0.6385	8.63
0.5000	369.3	-0.7450	7.40
0.7496	620.4	-1.2514	4.25
1.0000	746.3	0.0000	—

Probe - Heptane at 120°C

Wt Fr	X_{23}	Q_{23}	T_{sp}
0.0000	458.8	0.0000	—
0.0904	21.7	-0.0334	33.76
0.2515	162.8	-0.3242	15.96
0.2905	271.7	-0.5481	9.92
0.3588	264.3	-0.5318	10.29
0.5000	245.4	-0.4912	11.04
0.7496	449.6	-0.9037	5.76
1.0000	725.2	0.0000	—

Probe - Octane at 120°C

Wt Fr	X_{23}	Q_{23}	T_{sp}
0.0000	423.1	0.0000	—
0.0904	104.0	-0.2038	17.01
0.2515	127.2	-0.2508	20.02
0.2905	250.3	-0.5041	10.74
0.3588	234.1	-0.4699	11.59
0.5000	185.7	-0.3690	14.44
0.7496	366.2	-0.7339	6.96
1.0000	660.8	0.0000	—

Probe - 2-Butanone at 120°C

Wt Fr	X_{23}	Q_{23}	T_{sp}
0.0000	1083.4	0.0000	—
0.0904	404.9	- 0.8286	5.95
0.2515	156.4	- 0.3109	16.57
0.2905	320.4	- 0.6485	8.44
0.3588	348.8	- 0.7056	7.83
0.5000	554.7	- 1.1247	4.95
0.7496	564.5	- 1.1376	4.65
1.0000	1314.3	0.0000	—

Probe - Toluene at 120°C

Wt Fr	X_{23}	Q_{23}	T_{sp}
0.0000	544.9	0.0000	—
0.0904	338.3	- 0.6890	6.95
0.2515	232.8	- 0.4685	11.38
0.2905	282.2	- 0.5696	9.56
0.3588	271.2	- 0.5461	10.04
0.5000	217.4	- 0.4339	12.41
0.7496	484.8	- 0.9754	5.37
1.0000	783.4	0.0000	—

Probe - Chloroform at 120°C

Wt Fr	X_{23}	Q_{23}	T_{sp}
0.0000	627.8	0.0000	—
0.0904	619.1	- 1.2705	4.06
0.2515	565.8	- 1.1551	4.79
0.2905	503.6	- 1.0258	5.41
0.3588	501.6	- 1.0197	5.46
0.5000	543.2	- 1.1013	5.05
0.7496	918.4	- 1.8579	2.92
1.0000	818.7	0.0000	—

Probe - Methyl Acetate at 120°C

Wt Fr	X_{23}	Q_{23}	T_{sp}
0.0000	1674.9	0.0000	—
0.0904	210.0	- 0.4233	10.29
0.2515	- 18.1	0.0487	231.87
0.2905	355.6	- 0.7209	7.62
0.3588	569.5	- 1.1594	4.81
0.5000	917.1	- 1.8672	3.00
0.7496	547.7	- 1.1033	4.79
1.0000	1839.7	0.0000	—

Probe - 2-Propanone at 120°C

Wt Fr	X_{23}	Q_{23}	T_{sp}
0.0000	1721.2	0.0000	—
0.0904	124.3	- 0.2458	15.13
0.2515	- 87.7	0.1922	—
0.2905	291.8	- 0.5896	9.25
0.3588	628.1	- 1.2799	4.37
0.5000	1306.7	- 2.6652	2.11
0.7496	689.9	- 1.3927	3.85
1.0000	2011.5	0.0000	—

Probe - Isopropanol at 120°C

Wt Fr	X_{23}	Q_{23}	T_{sp}
0.0000	1226.5	0.0000	—
0.0904	54.5	- 0.1012	24.34
0.2515	19.3	- 0.0283	73.98
0.2905	246.5	- 0.4962	10.90
0.3588	435.3	- 0.8834	6.29
0.5000	1037.7	- 2.1143	3.87
0.7496	672.8	- 1.3580	32.94
1.0000	1542.8	0.0000	—

Probe - Ethyl Acetate at 120°C

Wt Fr	X_{23}	Q_{23}	T_{sp}
0.0000	1119.4	0.0000	—
0.0904	354.8	- 0.7232	6.67
0.2515	151.3	- 0.3005	17.08
0.2905	366.9	- 0.7443	7.39
0.3588	422.1	- 0.8564	6.48
0.5000	585.3	- 1.1874	4.69
0.7496	632.8	- 1.2765	4.18
1.0000	1375.4	0.0000	—

University of Durham

Board of Studies in Chemistry

Colloquia, lectures and Seminars given by Invited Speakers

1st August 1989 to 31st July 1990

<u>ASHMAN</u>	Mr A (Durham Chemistry Teacher's Centre)	
	The National Curriculum - An Update	11th Oct 1989
<u>BADYAL</u>	Dr J P S (Durham University)	
	Breakthroughs on Heterogeneous Catalysis	1st Nov 1989
<u>BECHER</u>	Dr J (Odense University)	
	Synthesis of New Macrocyclic Systems using Heterocyclic Building Blocks	13th Nov 1989
<u>BERCAW</u>	Prof J E (California Institute of Technology)	
	Synthetic and Mechanistic Approaches to Ziegler-natta Polymerization of Olefins	10th Nov 1989
<u>BLEASDALE</u>	Dr C (Newcastle University)	
	The Mode of Action of some Anti-tumour Agents	21st Feb 1990
<u>BOLLEN</u>	Mr F (formerly Science Advisor, Newcastle LEA)	
	What's new in Satis, 16-19	27th Mar 1990
<u>BOWMAN</u>	Prof J M (Emory University)	
	Fitting Experiment with Theory in Ar-OH	23rd Mar 1990
<u>BUTLER</u>	Dr A (St Andrews University)	
	The Discovery of Penicillin: Facts and Fancies	7th Dec 1989
<u>CAMPBELL</u>	Mr W A (Durham Chemistry Teachers Centre)	
	Industrial Catalysis - Some Ideas for the National Curriculum	12th Sep 1989
<u>CHADWICK</u>	Dr P (Dept of Physics, Durham University)	
	Recent Theories of the Universe (with respect to National Curriculum Attainment Target 16)	24th Jan 1990
<u>CHEETHAM</u>	Dr A K (Oxford University)	
	Chemistry of Zeolite Cages	8th Mar 1990

- CLARK** Prof D T (ICI Wilton)
Spatially resolved Chemistry (using Nature's Paradigm in the Advanced Materials Arena) 22nd Feb 1990
- COLE-HAMILTON** Prof D J (St Andrews University)
New Polymers from Homogeneous Catalysis 29th Nov 1989
- CROMBIE** Prof L (Nottingham University)
The Chemistry of Cannabis and Khat 15th Feb 1990
- DYER** Dr U (Glaxo)
Synthesis and Conformation of C-Glycosides 31st Jan 1990
- FLORIANI** Prof C (University of Lausanne, Switzerland)
Molecular Aggregates - A Bridge between Homogeneous and Heterogeneous Systems 25th Oct 1989
- GERMAN** Prof L S (USSR Academy of Sciences, Moscow)
New Syntheses in Fluoroaliphatic Chemistry: Recent Advances in the Chemistry of Fluorinated Oxiranes 9th Jul 1990
- GRAHAM** Dr D (BP Research Centre)
How Proteins Absorb to Interfaces 4th Dec 1989
- GREENWOOD** Prof J H (University of Leeds)
Novel Cluster Geometries in Metalloborane Chemistry 9th Nov 1989
- HOLLOWAY** Prof J H (University of Leicester)
Noble Gas Chemistry 1st Feb 1990
- HUGHES** Dr M N (King's College, London)
A Bug's Eye View of the Periodic Table 30th Nov 1989
- HUISGEN** Prof R (Universitat Munchen)
Recent Mechanistic Studies of [2+2] Additions 15th Dec 1989
- IDDON** Dr B (University of Salford)
Schools' Christmas Lecture - The Magic of Chemistry 15th Dec 1989
- JONES** Dr M E (Durham Chemistry Teachers' Centre)
The Chemistry A Level 1990 3rd Jul 1989

<u>IONES</u>	Dr M E (Durham Chemistry Teachers' Centre)	21st Nov 1989
	GCSE and Dual Award Science as a starting point for A level Chemistry - how suitable are they ?	
<u>JOHNSON</u>	Dr G A L (Durham Teachers' Training Centre)	8th Feb 1990
	Some aspects of local Geology in the National Science Curriculum (attainment target 9)	
<u>KLINOWSKI</u>	Dr J (Cambridge University)	13th Dec 1989
	Solid State NMR Studies of Zeolite Catalysts	
<u>LANCASTER</u>	Rev R (Kimbolton Fireworks)	8th Feb 1990
	Fireworks - Principles and Practice	
<u>LUNAZZI</u>	Prof L (University of Bologna)	12th Feb 1990
	Application of Dynamic NMR to the Study of Conformational Enantiomerism	
<u>PALMER</u>	Dr F (Nottingham University)	17th Oct 1989
	Thunder and Lightning	
<u>PARKER</u>	Dr D (Durham University)	16th Nov 1989
	Macrocycles, Drugs and Rock 'n' Roll	
<u>PERUTZ</u>	Dr R N (York University)	24th Jan 1990
	Plotting the Course of C-H Activations with Organometallics	
<u>PLARINOV</u>	Prof V E (USSR Academy of Sciences, Novosibirsk)	9th Jul 1990
	Polyfluoroindanes: Synthesis and Transformation	
<u>POWELL</u>	Dr R L (ICI)	6th Dec 1989
	The Development of CFC Replacements	
<u>POWIS</u>	Dr I (Nottingham University)	21st Mar 1990
	Spinning off in a huff: Photodissociation of Methyl Iodide	
<u>RICHARDS</u>	Mr C (Health and Safety Executive, Newcastle)	28th Feb 1990
	Safety in School Science Laboratories and COSHH	

- ROZHKOVA Prof I N (USSR Academy of Sciences,
Moscow) 9th Jul 1990
Reactivity of Perfluoroalkyl Bromides
- STODDART Dr J F (Sheffield University) 1st Mar 1990
Molecular Lego
- SUTTON Prof D (Simon Fraser University,
Vancouver BC) 14th Feb 1990
Synthesis and Applications of Dinitrogen and
Diazo Compounds of Rhenium and Iridium
- 12*
THOMAS Dr R K (Oxford University) 28th Feb 1990
Neutron Reflectometry from Surfaces
- THOMPSON Dr D P (Newcastle University) 7th Feb 1990
The role of Nitrogen in Extending Silicate
Crystal Chemistry

```

REM      This is the final version of the GFA Basic program used for data collection
REM
DEFINT   "e,i-n"           ! 4 byte signed integers, i.e. up to 2147483648
DEFSTR   "s"               ! strings
DEFBIT   "o"               ! 1 byte Boolean variables
REM
DIM       exptl_pt(10000)
DIM       c(8),st_w(10),st_q(10),st_f(10),ok_q(10)
REM
          max_trys = 15000
          menu
REM
REM
PROCEDURE findadc
REM
REM      a procedure supplied with the ADC for channel allocation
REM
          rom = &HFB0000
          c(1) = rom+1           ! Channel 1
          c(2) = rom+3           ! Channel 2
          c(3) = rom+5           ! Channel 3
          c(4) = rom+7           ! Channel 4
          c(5) = rom+9           ! Channel 5
          c(6) = rom+11          ! Channel 6
          c(7) = rom+13          ! Channel 7
          c(8) = rom+15          ! Channel 8
          channel = c(1)         ! Set Channel to 1 as default
RETURN
REM
REM
PROCEDURE getadc
REM
REM      the procedure which obtains a reading from the ADC
REM
          rd% = PEEK(channel)    ! Puts address on ROM
          rd% = PEEK(channel)    ! Got to be read TWICE
RETURN
REM
REM
PROCEDURE dummy
RETURN
REM
REM      does nothing - used with a loop which monitors the keyboard
REM
PROCEDURE co_ordr(ncols,nlines,VAR nxpixels,nypixels)
          ncx = MUL(8,SUB(nx,1))
          ncy = MUL(16,SUB(ny,1))
RETURN
REM
REM
PROCEDURE off_set(st,VAR n_off,n_chars)
REM
REM      returns the offset, n_off, to centre a string and the number
REM      of characters, n_chars, in the string st
REM
LOCAL    n0,n1,n2
          n_chars = LEN(st)
          n1 = 80
          n_off = ADD(DIV(SUB(n1,n_chars),2),1)
RETURN
REM

```

```

REM
PROCEDURE clr_line(nx1,nx2,ny)
    PRINT AT(nx1,ny1);SPACE$(ADD(1,SUB(nx2,nx1)))
    RETURN
REM
REM
PROCEDURE screen_box(nx1,ny1,nx2,ny2,n0)
REM
REM      draws a box on the screen - if n0=0 the entire screen is cleared
REM      while if n0=1 then the area bounded by the lines ny1 and ny2
REM      is cleared otherwise the area bounded by nx1,ny1,nx2,ny2
REM
LOCAL    mx1,mx2,my1,my2
          co_ords(nx1,ny1,mx1,my1)
          co_ords(nx2,ny2,mx2,my2)
          IF n0=0
              CLS
          ELSE
              DEFFILL,0
              BOUNDARY 0

              IF n0= 1
                  PBOX 0,my1,640,my2
              ELSE PBOX mx1,my1,mx2,my2
              ENDIF
              BOUNDARY 1
          ENDIF
          BOX ADD(mx1,4),ADD(my1,8),ADD(mx2,4),ADD(my2,8)

RETURN
REM
REM
PROCEDURE message(st,nx1,ny1,nx2,ny2,nb,nc)
LOCAL    jx,jy
REM
REM      this procedure assumes the existance of a box which is specified
REM      by the global variables nbx1,nby1,nbx2 and nby2 - it is assumed
REM      that the message will be printed at nx1,ny1 and that the cursor will
REM      be located either, if nc=0, at nx2,ny2 or if nc>0, at 5 spaces past
REM      the last character in the string.
REM
          jx = ADD(nbx1,1)
          jy = ADD(nby1,1)
          IF nb > 0
              clr_line(jx,jy,ny1)
          ENDIF
          PRINT AT(nx1,ny1); st
          IF nc = 0
              jx = ADD(ADD(LEN(st),5), nx1)
              jy = ny1
          ELSE
              jx = nx2
              jy = ny2
          ENDIF
          LOCATE jx,jy

RETURN
REM

```

```

REM
PROCEDURE paws(st,ny,n0)
REM
REM      suspends program operation until next key press
REM
LOCAL    j0,j1,k1,k2,key1
          off_set(st,j0,j1)
          k1 = SUB(j0,2)
          k2 = ADD(j0,ADD(j1,2))
          screen_box(k1,SUB(ny,1),k2,ADD(ny,1),n0)
          PRINT AT(j0,ny); st
          key1 = INP(2)
          k1 = SUB(ny,1)
          FOR k2=k1 TO k1+2
              clr_line(1,80,k2)
          NEXT k2

RETURN
REM
REM
PROCEDURE yes_or_no(n)
LOCAL    st1,st2
          st1 = "YN"
          REPEAT
              st2 = UPPER$(INKEY$)
          UNTIL INSTR(st1,st2)
          ok_q(n) = st2 = "Y"

RETURN
REM
REM
PROCEDURE enter_data
REM
REM      Requests the necessary initial data for the experiment and tests dt_set
REM      to ensure that it is >= 0.01; values of dt_set are also rounded up to the
REM      the nearest 1/100 of a second. Also determines whether the run is
REM      a software test (ok_test) of the real thing (ok_real).
REM
LOCAL    jx1,jx2,jy1,jy2,nx1,nx2,ny1
          st_w(1) = "Enter the following information"
          st_w(2) = "The time delay in seconds (to nearest 1/100)"
          st_w(3) = "The total number of experimental points"
          st_w(4) = "The percentage difference to be used in START_UP"
          st_w(5) = "The number of successively increasing points"
          st_w(6) = "A zero for test data consisting of random numbers"
          st_w(4) = "The time interval must be at least 0.01 seconds - try again"

REM
          jx1 = 5                                !Determine coordinates of box
          jx2 = 75
          jy1 = 1
          jy2 = ADD(jy1,MUL(7,2))

REM
          nx1 = 10
          nx2 = ADD(LEN(st_w(6)),nx1+5)

```

```

REPEAT
  screen_box(jx1,jy1,jx2,jy2,1)
  ny1 = ADD(jy1,2)
  message(st_w(1),nx1,ny1,nx2,ny2,1)
  ADD ny1,2
  message(st_w(2),nx1,ny1,nx2,ny2,1)
  INPUT "",dt_set
  IF dt_set < 0.01 THEN
    ADD ny1,6
    message(st_w(7),nx1,ny1,nx2,ny2,1)
    DELAY 2
  ENDIF
UNTIL dt_set >= 0.01
dt_set = 0.01*CINT(100*dt_set)
ADD ny1,2
message(st_w(3),nx1,ny1,nx2,ny2,1)
INPUT "",n_max
ADD ny1,2
message(st_w(4),nx1,ny1,nx2,ny2,1)
INPUT "",pct
ADD ny1,2
message(st_w(5),nx1,ny1,nx2,ny2,1)
INPUT "",n_spec
ADD ny1,2
message(st_w(6),nx1,ny1,nx2,ny2,1)
INPUT "",n_test
ok_test = n_test=0
ok_run = NOT ok_test

REM
IF ok_run THEN
  st_w(1) = "Enter the following additional information"
  st_w(2) = "Carrier gas flow rate           (cm3 s-1)"
  st_w(3) = "Column inlet pressure          (mmHg)"
  st_w(4) = "Column outlet pressure         (mmHg)"
  st_w(5) = "Mass of polymer on the column      (g)"

  jy2 = ADD(jy1,MUL(6,2))
  screen_box(jx1,jy1,jx2,jy2,0)
  ny1 = ADD(jy1,2)
  message(st_w(1),nx1,ny1,nx2,ny2,1)
  ADD ny1,2
  age(st_w(2),nx1,ny1,nx2,ny2,1)
  INPUT "",gas_flow_rate
  ADD ny1,2
  age(st_w(3),nx1,ny1,nx2,ny2,1)
  INPUT "",inlet_pressure
  ADD ny1,2
  message(st_w(4),nx1,ny1,nx2,ny2,1)
  INPUT "",outlet_pressure
  ADD ny1,2
  age(st_w(5),nx1,ny1,nx2,ny2,1)
  INPUT "",wt_of_polymer

ELSE
ENDIF
RETURN

REM

```

```

REM
PROCEDURE time_check(dt_set)
REM
REM      This procedure determines when the next sample is to be taken.
REM
LOCAL   n_set,n0,n1
n_set = CINT(200*dt_set) ! expresses sample interval in 200ths of a second
n0 = TIMER                ! obtains starting time
REPEAT
    n1 = TIMER
    SUB n1,n0              ! calculates time interval in 200ths
UNTIL n1 >= n_set        ! compares the current interval with that desired
RETURN
REM
REM
PROCEDURE exptl_pt(n)
REM      Obtains either a random number or a measurement as appropriate
LOCAL   j
time_check(dt_set)
IF ok_test
    j = RANDOM(255) ! a random number between 0 and 255
    INC j           ! eliminates chance of zero, i.e. 1 to 256
ELSE
    GOSUB getadc
    j = rd%
ENDIF
exptl_pt(n) = j
RETURN
REM
REM
PROCEDURE compare(n,VAR ok_greater)
REM
REM      Tests whether the current result exceeds the previous value by
REM      the percentage specified in the data input procedure.
REM
LOCAL   fx,x_old,x_new,ok
x_new = exptl_pt(n)
ok_greater = x_new > 0          ! avoids chance of division by zero
IF ok_greater
    x_old = exptl_pt(n-1)      ! previous reading
    fx = 100*(1 - x_old/x_new)
    ok_greater = fx > pct      ! compare with specified %age
ELSE
ENDIF
RETURN
REM

```

```

REM
PROCEDURE start_up
REM      Monitors the specified number of successively increasing values which defines
REM      the beginning of the experiment

LOCAL   j,n_ok,ok,nx1,ny1
        j = 1
        n_ok = 0
        expt_tot = 0           ! to collect total for base line
        ADD n_trys,1
        exptl_pt(n_ok)
        WHILE (n_ok < n_ints) AND (max_trys >= n_trys)
            INC j
            INC n_trys
            exptl_pt(j)
            compare(j,ok)
            PRINT AT (nx,ny); n_trys
            IF ok
                INC n_ok
            ELSE
                exptl_pt(1) = exptl_pt(j)
                j = 1
                n_ok = 0
            ENDIF
        ENDIF

REM
        IF max_trys = n_trys
            st_w(1) = "The maximum permitted attempts has been
                reached"
            st_w(2) = "To continue enter Y else N which terminates
                program"
            nx1 = 10
            ny1 = 5
            message(st_w(1),nx1,ny1,nx1,ny1,0)
            ADD ny1,2
            message(st_w(2),nx1,ny1,nx1,ny1,1)
            REPEAT
                st_w(3) = INKEY$
                IF LEN(st_w(3)) = 1
                    st_w(3) = UPPER$(st_w(3))
                ENDIF
            UNTIL (st_w(3) = "Y") OR (st_w(3) = "N")
            IF st_w(3) = "N"
                END
            ELSE
                n_trys = 0
                expt_total = 0
                clr_line(6,74,5)
                clr_line(6,74,7)
                clr_line(nx-5,74,ny)
            ENDIF
        ENDIF
    WEND
    n_base = CINT(DIV(expt_total,n_trys))

RETURN
REM

```

```

REM
PROCEDURE capture
REM
REM      This procedure obtains the specified number of experimental values;
REM      locates the peak value together with the corresponding time and
REM      displays this information on the screen.
REM
LOCAL      jx1,jy1,jx2,jy2,nx1,nx2,ny1,nx,ny
           enter_data
           findadc

RENM
REM      The first step is to halt the program just prior to introducing
REM      the sample - do this by calling for the dummy procedure
REM
           st_w(1) = "Introduce the sample, then press any key"
           paws(st_w(1),23,1)

REM
REM      The next section compares successive readings until the specified
REM      number of points which have increased by at least the specified
REM      percentage difference have been detected.
REM
           jx1 = 5
           jx2 = 75
           jy1 = 2
           jy2 = 10
           screen_box(jx1,jy1,jx2,jy2,0)
           n_ints = n_spec - 1           ! no. intervals one less than no. points
           n_trys = 0
           st_w(2) = "Current number of trys"
           nx1 = 10                     ! x coordinate for writing to screen
           ny1 = ADD(jy1,1)             ! y coordinate for writing to screen
           message(st_w(2),nx1,ny1,nx1,ny1,0)
           n_start = TIMER
           nx = ADD(nx1,ADD(LEN(st_w(2)),5))
           ny = ny1
           start_up(nx,ny)
           n_end = TIMER
           dead_time = 0.005*(n_end - n_start)
           dt_start = dead_time/n_trys
           st_w(1) = "The following successive increasing values have been detected"
           ADD ny1,2
           ny = ny1
           message(st_w(1),nx1,ny,65,ny,0)
           ADD ny1,2
           ny = ny1
           nx = 25
           FOR j=1 TO n_spec
               PRINT AT(nx,ny); exptl_pt(j)
               ADD nx,8
           Next j
           st_w(1) = "The time interval between the initial points = "
           ADD ny1,2
           ny = ny1
           message(st_w(1),10,ny,10,ny,0)
           nx = ADD(nx1,LEN(st_w(1)))
           PRINT AT(nx,ny); USING "####.####", dt_start
           nx = ADD(nx,8)
           PRINT AT(nx,ny); "seconds"

REM

```

```

REM          Now collect either experimental data of random numbers in the range
REM          0 to 255 as a simulation of experimental data
REM

```

```

          jx1 = 5
          jx2 = 75
          jy1 = 12
          jy2 = 20
          screen_box(jx1,jy1,jx2,jy2)
          ny1 = ADD(jy1,1)
          st_w(1) = "Now beginning the storage of "
          st_w(2) = "experimental values"
          nx = ADD(LEN(st_w(1),ADD(5,LEN(st_w(2))))
          nx = SUB(jx2,jx1,ADD(nx,1))
          PRINT AT(nx,nxy); st_w(1); n_max; st_w(2)
          n_data = n_spec
          n_start = TIMER
          REPEAT
              INC n_data
              exptl_pt(n_data)
          UNTIL n_data = n_max
          n_end = TIMER
          dt_main = 0.005*(n_end-n_start)/(n_max - n_spec - 1)

```

```

REM          Now find the peak value and calculate the corresponding time
REM
REM

```

```

          n_data = 1;
          max_val = exptl_pt(1)
          REPEAT
              INC n_data
              m = exptl_pt(n_data)
              IF m > max_value
                  max_value = m
                  inc_val% = n_data
              ELSE
                  ENDIF
          UNTIL n_data = n_max

```

```

REM          peak_time = dt_start*(n_spec - 1) + dt_main*(inc_val% - n_spec)
REM          total_time = peak_time + dead_time

```

```

REM          ADD ny1,2
REM          st1 = "Time from injection to peak = "
REM          st0 = st1 + "####.####" + "seconds"
REM          off_set(st0,nx1,j0)
REM          PRINT AT(nx1,ny1); st1
REM          nx = ADD(nx1,LEN(st1))
REM          PRINT AT(nx,ny1); USING "####.####", total_time
REM          PRINT AT(nx+8,ny1); "seconds"

```

```

REM          ADD ny1,2
REM          st1 = "Time from detection to peak = "
REM          PRINT AT(nx1,ny1); st1
REM          nx = ADD(nx1,LEN(st1));
REM          PRINT AT(nx,ny1); USING "####.####", peak_time
REM          PRINT AT(nx+8,ny1); "seconds"

```

```

REM
REM

```

```

j0 = INSTR(st1, "=")           ! Find position of equals sign
nx1 = nx1 + j0 - LEN("Peak Value ") - 1 ! Align = sign with others
ADD ny1,2
st1 = "Peak Value = "
PRINT AT(nx1,ny1);st1
PRINT AT(nx1+LEN(st1),ny1); max_value;
st1 = "To continue, press any key"
Paws(st1,23,1)

RETURN

REM
REM
PROCEDURE filename(VAR file_title$)
REM
REM      Obtains appropriate drive (A: or B:) together with the name of the
REM      file in which the data are to be stored. Determines the type of
REM      experiment being carried out,i.e.(0, 1, 10, 11)
REM

st_w(1) = "The method used to store data presupposes the existance"
st_w(2) = "of at least four 'folders' to store data files; these are"
st_w(3) = "CH4_UC, CH4_C, SOLVT_UC and SOLVT_C respectively."
st_w(1) = "Data can be stored only on drives A: and B:"
st_w(1) = "Please supply the following data:"
screen_box(5,1,75,21,0)
st_q(1) = "Are the data to be stored on drive A: (y/n)?"
st_q(2) = "Is the solvent methane (y/n)?"
st_q(3) = "Is the column coated (y/n)?"
st_q(4) = "Supply the name of the data file."
st_q(5) = "Are the CH4_UC data stored on drive A: (y/n)?"
st_q(6) = "Supply the file name for the CH4_UC data."
st_q(7) = "Are the CH4_C data stored on drive A: (y/n)?"
st_q(8) = "Supply the file name for the CH4_C data."

REM

n = 3
k = ADD(LEN(st_w(5)),5)
FOR j = 1 TO 4
    PRINT AT(10,n); st_w(j)
    ADD n,2
NEXT j
INC n
PRINT AT(10,n); st_w(5)
FOR j = 1 TO 3
    ADD n,2
    message(st_q(j),10,n,k!,n,1)
    yes_or_no(j)
NEXT j
ADD n,2
message(st_q(4),10,n,k!,n,1)
INPUT st_f(4)

REM

IF ok_q(1)
    st_f(1) = "a:"
ELSE
    st_f(1) = "b:"
ENDIF
IF ok_q(2)
    st_f(2) = "\CH4_"
ELSE
    st_f(2) = "\SOLVT_"
ENDIF

```

```

IF ok_q(3)
  st_f(3) = "C\"
ELSE
  st_f(3) = "UC\"
file_title$ = st_f(1)+st_f(2)+st_f(3) + st_f(4) + ".LST"
ENDIF
IF ok_q(2)
  n2 = 0
ELSE
  n2 = 1
ENDIF
IF NOT ok_q(3)
  n3 = 0
ELSE
  n3 = 1
ENDIF
expt_type = n2 + 10*n3
OPEN "O", #1, file_1$

RETURN
REM
REM
PROCEDURE store_data
REM
REM      Arranges for the storage of the data; experimental results
REM      from the ADC are arranged in rows of 15
REM
OPEN "O", #1, file_title$                ! opens file for writing
PRINT #1, USING "####.####", total_time
PRINT #1, USING "####.####", peak_time
PRINT #1, USING "###", n_base
PRINT #1, dt_set, ""n_spec""n_max""pct
PRINT #1, gas_flow_rate, ""inlet_pressure""outlet_pressure""wt_of_polymer

REM
DIV n_max, 15                ! divides by 15 and truncates
MUL n_max, 15                ! ensures that final value is a multiple of 15
n_data = 0
REPEAT
  j = 0
  REPEAT
    INC j
    PRINT #1, USING "####", expt_pt(n_data+j);
  UNTIL j = 15
  ADD n_data, 15
UNTIL n_data = n_max
CLOSE #1

RETURN
REM
REM
PROCEDURE lose_arrow(VAR s)
LOCAL s0, n
n = LEN(s)
s0 = LEFT$(s, 3)
IF s0 = " ==>"
  s = RIGHT$(s, SUB(n, 3))
ENDIF

RETURN
REM

```

```

REM
PROCEDURE get_number(s0, VAR s1,real)
LOCAL
    j,k,s2
    s1 = TRIM$(s1)
    j = LEN(s1)
    k = INSTR(s1,s0)
    s2 = LEFT$(s1,k-1)
    s1 = RIGHT$(s1,j-k)
    real = VAL(s2)
    s1 = TRIM$(s1)

RETURN

REM
REM
PROCEDURE get_data(VAR n_pts, n_peak)
LOCAL
    j,k,s1,file_title$
    file_name(file_title$)           ! obtains the file name
    OPEN "I",#1,file_title$         ! opens file for reading
    INPUT #1,total_time              ! reads the first data item
    INPUT #1,pk_time                  ! reads the second data item
    INPUT #1,n_base                   ! reads the third data item
    INPUT #1,s1                       ! reads the fourth string
    lose_arrow(s1)
    get_number(" ",s1,dt_set)        ! obtains dt_set
    n_peak = ROUND(pk_time/dt_set)
    get_number(" ",s1,pts_spec)       ! obtains specified no. of points
    n_spec = ROUND(pts_spec)          ! round to integer
    get_number(" ",s1,pts_max)        ! obtains maximum no. of points
    n_spec = ROUND(pts_max)           ! round to integer
    pct = VAL(s1)                     ! %age difference for initial points

REM
    INPUT #1,s1                       ! reads third string
    lose_arrow(s1)
    get_number(" ",s1,gas_flow)        ! obtains gas flow rate
    get_number(" ",s1,p_inlet)         ! obtains column inlet pressure
    get_number(" ",s1,p_outlet)        ! obtains column outlet pressure
    polymer_wt = VAL(s1)               ! obtains weight of polymer

REM
    n_pts = 0
    CLS
    PRINT AT(20,8); "Current number of point being processed"
    DO UNTIL EOF(#1)
        LINE INPUT #1,s1
        lose_arrow(s1)
        DO WHILE LEN(s1) > 4
            n_pts = npts + 1
            PRINT AT(38,10); n_pts
            get_number(" ",s1,z)        ! proc. returns a real value
            exptl_pt(n_pts) = ROUND(z) ! round to integer
        LOOP
        n_pts = npts+1
        exptl_pt(n_n_pts) = ROUND(VAL(s1))
    LOOP
    CLOSE #1
    CLS
    PRINT AT(20,10); USING "Number of experimental points #####",n_pts
    PRINT AT(20,12); USING "Approximate point of maximum #####",n_peak
    st0 = "To show the experimental data, press any key"
    paws(st0,23,1)

RETURN

```

```

REM
PROCEDURE exptl
REM
REM      procedure for storing results for all systems
REM
LOCAL   file_title$
        capture
        file_name(file_title$)
        store_data(file_title$)
        CLOSE #1

RETURN

REM
REM
PROCEDURE pplot
CLS
IF (n_pts > 640) AND (n_peak > 320)
    n_finish = n_peak + 320
    IF n_finish > n_pts
        n_finish = n_pts
    ENDIF
    n_start = n_finish - 640
ELSE
    n_start = 1
    IF n_pts > 640
        n_finish = 640
    ELSE IF (n_pts < 640)
        n_finish = n_pts
    ENDIF
ENDIF
FOR n = n_start TO n_finish
    PLOT n - n_start, 300 - exptl_pt(n)
NEXT n
st0 = "To continue, press any key"
paws(st0,23,1)

RETURN

REM
REM
PROCEDURE partial_plot
REM
REM      Where the number of points is in excess of that which can be shown on
REM      the screen, it is convenient to be able to show the general shape of the
REM      curve by plotting only every nth point where n depends upon the total
REM      number of experimental points.
REM
LOCAL   n,n_th,n_count,ok,j,k
        CLS
        n_th = n_max DIV 640           ! to determine plotting interval
        INC n_th
        SELECT n_th
            CASE 1
                s = ""
            CASE 2
                s = STR$(n_th) + "nd"
            CASE 3
                s = STR$(n_th) + "rd"
            CASE 4,5,6,7,8,9
                s = STR$(n_th) + "th"
        ENDSELECT

```

```

REM
    s = "Plotting every " + s + " point"
    off_set(s,j,k)
    PRINT AT(j,1);s
    n_count = 0
    FOR n = 1 TO n_max
        ok = (n MOD n_th) = 0
        IF ok
            INC n_count                ! determine value for x-axis
            PLOT n_count,SUB(300,exptl_pt(n))
REM                                     ! plot every nth point
            ENDIF
        NEXT n
    st0 = "To continue, press any key"
    paws(st0,23,1)

RETURN
REM
REM
PROCEDURE plot_area
LOCAL delta_a,j,n,n_rem,n_sections,f0,f1
CLS
IF n_pts > 640
    n_rem = 640
ELSE
    n_rem = n_pts
ENDIF
n_begin = n_start
n_sections = 0
area = 0
f1 = 6/140
WHILE n_rem > 6
    delta_a = 0
    FOR j = 0 TO 6
        n = n_begin + j
        SELECT j                ! Newton-Cotes weight. factors for 6 strip
            CASE 0,6
                f0 = 41
            CASE 1,5
                f0 = 216
            CASE 2,4
                f0 = 27
            CASE 3
                f0 = 272
        ENDSELECT
        delta_a = delta_a + f0*SUB(exptl_pt(n),n_base)
    NEXT j
    delta_a = f1*dt_set*delta_a
REM
    IF delta_a > 0                ! only positive value are meaningful
        area = area + delta_a
    ENDIF

```

```

        ADD n_begin,6
        SUB n_rem,6
        INC n_sections
        PRINT AT(10,5);
        USING "Number of Integration Sections ###", n_sections
        PRINT AT(10,7);
        USING "Current value part area under curve ###.#####", delta_a
        PRINT AT(10,9);
        USING "Cumulative value of area under curve #####.##", delta_a
        PAUSE 2
    WEND

RETURN
REM
REM
PROCEDURE menu
LOCAL n_type,nx,my,n,j
    menustart:
        nbx1 = 5
        nby1 = 2
        nbx2 = 75
        nby2 = ADD(4,MUL(6,2))
        screen_box(nbx1,nby1,nbx2,nby2,0)
        st_w(1) = "There are five operations possible:"
        st_w(2) = "(1)- To obtain and store experimental results."
        st_w(3) = "(2)- To plot dat which includes the peak height."
        st_w(4) = "(3)- To plot selected data to show the entire curve."
        st_w(5) = "(4)- Numerical integration to get the area under the curve."
        st_w(6) = "(5)- To exit from the program."
        st_w(7) = "Make your selection - (1 to 5)."
        off_set(st_w(5),nx,j)
        ny = ADD(nby1,1)
REM
        FOR n = 1 TO 6 DO
            message(st_w(n),nx,ny,nx+j,ny,2,0)
            ADD ny,2
        NEXT n
        j = LEN(st_w(7))
        REPEAT
            PRINT AT(nx,ny); st_w(7)
            LOCAT nx+j+1,ny
            s = INKEY$
            k = ASC(s)
        UNTIL (48 < k) AND (k < 54)
        n_type = k - 48
REM
        SELECT n_type
        CASE 1
            exptl
            GOTO menu_start
        CASE 2, 3, 4
            screen_box(5,21,75,23,1)
            st = "Is it necessary to read the data from a file (y/n) ?"
            off_set(st,n,j)
            message(st,n,22,n+j,22,2,0)
            REPEAT
                s = INKEY$
                s = UPPER$(s)
                k = ASC(s)
            UNTIL (k = 78) OR (k = 89)

```

```
IF s = "Y"  
    get_data(n_pts,n_peak)  
ENDIF  
IF n_type = 2  
    pplot  
    GOTO menu_start  
ENDIF  
IF n_type = 3  
    partial_plot  
    GOTO menu_start  
ENDIF  
IF n_type = 4  
    plot_area  
    GOTO menu_start  
ENDIF  
CASE 5  
    END  
ENDSELECT  
paws("To continue, press any key",22,0)  
RETURN  
REM
```

DEFINITION MODULE bbmutils; (* 14th August 1990 *)

IMPORT Str,Window,IO;

TYPE

String = ARRAY[1..80] OF CHAR;
 Words = ARRAY[0..21] OF String;
 Data = ARRAY[1..20] OF LONGREAL;
 SigFigs = ARRAY[1..20] OF CARDINAL;

VAR

spaces : ARRAY[1..80] OF String;

PROCEDURE SpaceFill;

PROCEDURE SizeArray(w: Words; n1,n2: CARDINAL; VAR jchars,jrow: CARDINAL);

PROCEDURE NewWindow(w: Words; n1,n2: CARDINAL; m: Window.WinType;
 VAR xc1,yc1,xc2,yc2: Window.AbsCoord);

PROCEDURE OffSet(s: ARRAY OF CHAR; VAR nchars,nspaces: CARDINAL;
 xmin,xmax: CARDINAL);

PROCEDURE LocateStr(s: ARRAY OF CHAR; nxmin,nxmax,nLine: CARDINAL);

PROCEDURE WrArray(Ar: Words; ns,nf,xmin,xmax: CARDINAL; LastLine: BOOLEAN);

PROCEDURE Pause(VAR w: Words; nLines,nMessage: CARDINAL);

PROCEDURE Round(VAR n: CARDINAL; x: LONGREAL);

PROCEDURE CharDisplay;

PROCEDURE ShowData(VAR wh,wd: Words; d: Data; np: SigFigs; nh,nd: CARDINAL);

PROCEDURE bbmConcat(VAR s: String; w: Words; n1,n2: CARDINAL);

PROCEDURE AddSpaces(VAR wd: Words; nvalues: CARDINAL);

END bbmutils.

IMPLEMENTATION MODULE bbmutils;

(*# optimize(i386 => on) *)

(*# optimize(i387 => on) *)

(*# debug(vid => full) *)

(*# check(index => on) *)

(*# check(stack => on) *)

PROCEDURE SpaceFill;

VAR n : CARDINAL;

BEGIN

n := 1; spaces[1] := ' ';

FOR n := 2 TO 80 DO Str.Concat(spaces[n],spaces[n-1], ' '); END;

END SpaceFill;

```
PROCEDURE SizeArray(w:Words; n1,n2:CARDINAL; VAR jchars,jrow:CARDINAL);
```

```
(* This procedure determines the largest string in an array of String; beginning at n1
and ending at n2; jchars is the length and jrow is the index of the largest string *)
```

```
VAR   j,k                               :CARDINAL;
BEGIN
    jchars := 0;
    FOR k := n1 TO n2 DO
        j := Str.Length(w[k]);
        IF j > jchars THEN jchars := j; jrow := k END;
    END;
END   SizeArray;
```

```
PROCEDURE NewWindow(w:Words; n1,n2:CARDINAL; m:Window.WinType;
VAR xc1,yc1,xc2,yc2:Window.AbsCoord);
```

```
(* This procedure re-sizes the current window to accomodate an array w of String
6 spaces are added to each side of the largest string and 3 lines to each half of
the window *)
```

```
VAR   jmax,jrow,k,n                       :CARDINAL;
BEGIN
    SizeArray(w,n1,n2,jmax,jrow);

    (* determine width in terms of spaces *)
    jmax := jmax DIV 2; INC(jmax,6);
    IF jmax > 40 THEN jmax := 40 END;
    xc1 := 40 - jmax; xc2 := 40 + jmax;

    (* determine length in terms of lines *)
    k := n2 - n1 + 1;
    IF ODD(k) THEN INC(k,1) END;
    k := k DIV 2; INC(k,3);
    IF k > 11 THEN k := 11 END;
    yc1 := 12 - k; yc2 := 12 + k;
    Window.Change(m,xc1,yc1,xc2,yc2);
    Window.PutOnTop(m);
END   NewWindow;
```

```
PROCEDURE OffSet(s:ARRAY OF CHAR; VAR nchars,nspaces:CARDINAL;
xc1,xc2:CARDINAL);
```

```
BEGIN
    nchars := Str.Length(s);
    nspaces := xc2 - xc1;
    DEC(nspaces,nchars);
    nspaces := nspaces DIV 2;
    INC(nspaces);
END   OffSet;
```

```
PROCEDURE LocateStr(s:ARRAY OF CHAR; xc1,xc2,nLine:CARDINAL);
```

```

  VAR   j,k                               :CARDINAL;

  BEGIN
    OffSet(s,j,k,xc1,xc2);
    Window.DirectWrite(k,nLine,ADR(s),Str.Length(s));
  END   LocateStr;
```

```
PROCEDURE WrArray(Ar:Words; ns,nf,xc1,xc2:CARDINAL; LastLine:BOOLEAN);
```

```
(* This procedure writes the contents of an array to the current
   window which must be large enough to accommodate the text. *)
```

```

  VAR   i,j,k,nmax,klast,n,nrows         :CARDINAL;

  BEGIN
    SizeArray(Ar,ns,nf,j,nmax);
    OffSet(Ar[nmax],j,k,xc1,xc2);
    IF LastLine THEN OffSet(Ar[nf],j,klast,xc1,xc2) END;

    i := 2;
    FOR j := ns TO nf DO
      IF (j = nf) AND LastLine THEN n := klast ELSE n := k END;
      Window.DirectWrite(n,j+i,ADR(Ar[j]),Str.Length(Ar[j]))
    END;
    Window.GotoXY(n+Str.Length(Ar[nf])+1,nf-ns+i);
  END   WrArray;
```

```
PROCEDURE Pause(VAR w:Words; nRows,nMessage:CARDINAL);
```

```

  VAR   j,k,i,n,nl,nmax                 :CARDINAL;
        xc1,yc1,xc2,yc2                 :Window.AbsCoord;
        ch                               :CHAR;
        s                               :Words;
        wd1,wd2                          :Window.WinDef;
        w1,w2                            :Window.WinType;
```

```
BEGIN
```

```
(* The array containing the information to be displayed should not exceed
   5 lines of text - i.e. nRows = 4 the third line will consist of a message
   determined by the third parameter *)
```

```

  wd2 := Window.WinDef(0,0,79,24,Window.Red,Window.Black,
    TRUE,FALSE,TRUE,TRUE,Window.SingleFrame,
    Window.Yellow,Window.Black);
```

```
  w2 := Window.Open(wd2);
```

```
  IF nRows > 4 THEN
```

```

    s[0] := 'Pause has been called with too many lines of text';
    NewWindow(w,0,0,w2,xc1,yc1,xc2,yc2);
    LocateStr(s[0],xc1,xc2,3);
    HALT;
```

```
  END;
```

```

nl := nrows; INC(nl);
IF nMessage = 0 THEN w[nl] := 'press the space bar to continue.';
ELIF nMessage = 1 THEN w[nl] := 'Do you wish to continue (y/n) ?';
ELSE
END;

```

```

SizeArray(w,0,nl,j,nmax);
NewWindow(w,0,nl,w2,xc1,yc1,xc2,yc2);
WrArray(w,0,nl,xc1,xc2,TRUE);

```

```

REPEAT
    ch := CAP(IO.RdKey());
    IF ch = 'N' THEN HALT END;
UNTIL (ch = ' ') OR (ch = 'Y');

```

```

Window.Close(w2);
Window.CursorOn;

```

```

END Pause;

```

```

PROCEDURE Round(VAR n:CARDINAL; x:LONGREAL);

```

```

    VAR dx :LONGREAL;
        s :String;

```

```

BEGIN

```

```

    IF x > 65535.0 THEN
        s := 'Round called with a LongReal > Maximum permitted Cardinal';
        LocateStr(s,0,79,24);
        HALT;

```

```

    END;
    n := TRUNC(x);
    dx := x - VAL(LONGREAL,n);
    IF dx >= 0.5 THEN INC(n) END;

```

```

END Round;

```

```

PROCEDURE CharDisplay;

```

```

    VAR j,k,n,r,c,nchar,nrow,ncol :CARDINAL;
        m1 :Window.WinType;
        d1 :Window.WinDef;

```

```

BEGIN

```

```

    d1 := Window.WinDef(0,0,79,25,Window.LightBlue,Window.Black,
        FALSE,FALSE,FALSE,TRUE,Window.SingleFrame,
        Window.Yellow,Window.Black);

```

```

    m1 := Window.Open(d1);

```

```

    ncol := 1; nrow := 1;
    FOR nchar := 128 TO 255 DO
        Window.GotoXY(ncol,nrow); IO.WrCard(nchar,3);
        Window.GotoXY(ncol+1,nrow+1); IO.WrChar(CHR(nchar));
        INC(ncol,5);
        IF ncol > 77 THEN INC(nrow,3); ncol := 1; END;

```

```

    END;

```

```

END CharDisplay;

```

```

PROCEDURE ShowData(VAR wh,wd:Words; d:Data; np:SigFigs; nh,nd:CARDINAL);
  VAR
    j,k,n,nx,ny,xc1,xc2,yc1,yc2,nmin,k0,
    maxlines,maxchars           :CARDINAL;
    m0                           :Window.WinType;
    d0                           :Window.WinDef;
    ok                           :BOOLEAN;
    ch                           :CHAR;
    s                            :String;
    wtemp                        :Words;

  BEGIN
    (* This procedure is intended to display numerical data for debugging
    purposes;
    the arrays should contain the following information:
    wh - nh lines of text for a heading;
    wd - identifiers for the numerical data;
    d - nd items of numerical data;
    np - the number of figures after the point.
    nd should not exceed 20 though no protection is provided. *)

    nmin := 8;
    FOR n := 1 TO nd DO
      wtemp[n] := wd[n];

      (* determine number of places before decimal point*)
      k := TRUNC(ABS(d[n]));
      Str.CardToStr(VAL(LONGCARD,k),s,10,ok);
      k := nmin - Str.Length(s);
      IF d[n] < 0.0 THEN DEC(k) END;
      Str.Append(wtemp[n],spaces[k]);

      (* obtain a string representation of the LONGREALs in
      array d to the number of places stored in np *)

      Str.FixRealToStr(d[n],np[n],s,ok);
      Str.Append(wtemp[n],s);
    END;
    wtemp[nd+1] := 'Press any Key';

    (* Find the longest string *)
    maxchars := 0;
    FOR n := 0 TO nh-1 DO
      k := Str.Length(wh[n]);
      IF k > maxchars THEN maxchars := k END;
    END;

    FOR n := 1 TO nd DO
      k := Str.Length(wtemp[n]);
      IF k > maxchars THEN maxchars := k END;
    END;
    maxlines := nh + (nd+3) + 2;

    maxchars := maxchars DIV 2; INC(maxchars,6);
    IF maxchars > 39 THEN xc1 := 1; xc2 := 80
      ELSE xc1 := 40 - maxchars; xc2 := 40 + maxchars; END;
    maxlines := maxlines DIV 2; INC(k,3);

```

```

IF maxlines > 12 THEN yc1 := 1;          yc2 := 24
ELSE yc1 := 12 - maxlines; yc2 := 12 + maxlines; END;

```

```

d0 := Window.WinDef(0,0,79,24,Window.LightBlue,Window.Black,
FALSE,FALSE,FALSE,TRUE,Window.SingleFrame,
Window.Yellow,Window.Black);

```

```

m0 := Window.Open(d0);
Window.CursorOn;
Window.Change(m0,xc1,yc1,xc2,yc2);
Window.PutOnTop(m0);

```

```
(* Write heading *)
```

```

ny := 0;
FOR n := 0 TO nh-1 DO
  OffSet(wh[n],j,k,xc1,xc2);
  INC(ny);
  Window.DirectWrite(k,ny,ADR(wh[n]),j);
END;

```

```
(* Underline last line of input *)
```

```

k0 := Str.Length(wh[nh-1]);
s := wh[nh-1];
FOR n := 1 TO k0 DO s[n] := CHR(196) END;
INC(ny);
Window.DirectWrite(k,ny,ADR(s),k0);

```

```
(* Write numerical values to window *)
```

```

OffSet(wtemp[1],j,k,xc1,xc2);
FOR n := 1 TO nd DO
  INC(ny);
  Window.DirectWrite(k,ny,ADR(wtemp[n]),Str.Length(wtemp[n]));
END;

```

```
(* Pause to examine data *)
```

```

INC(ny,2);
s := wtemp[nd+1];
OffSet(s,j,k,xc1,xc2);
Window.DirectWrite(k,ny,ADR(s),j);
Window.GotoXY(j+k+2,ny);
ch := IO.RdKey();
Window.Close(m0);

```

```
END ShowData;
```

```
PROCEDURE bbmConcat(VAR s:String; w:Words; n1,n2:CARDINAL);
```

```
VAR k :CARDINAL;
```

```
BEGIN
```

```
s := "";
```

```
FOR k := n1 TO n2 DO Str.Append(s,w[k]) END;
```

```
END bbmConcat;
```

```
PROCEDURE AddSpaces(VAR wd:Words; nvalues:CARDINAL);
```

```
    (* This procedure will add spaces to the beginning of the string representation  
    of LONGREALs when used as identifiers in ShowData. *)
```

```
    VAR    n,nmax,j                                :CARDINAL;
```

```
    BEGIN
```

```
        (* Find longest string *)
```

```
        nmax := 0;
```

```
        FOR n:= 1 TO nvalues DO
```

```
            j := Str.Length(wd[n]);
```

```
            IF j > nmax THEN nmax := j END;
```

```
        END;
```

```
        (* Add extra spaces at the beginning of the string *)
```

```
        FOR n:= 1 TO nvalues DO
```

```
            j := nmax - Str.Length(wd[n]);
```

```
            IF j > 0 THEN Str.Concat(wd[n],spaces[j],wd[n]) END;
```

```
        END;
```

```
    END    AddSpaces;
```

```
BEGIN
```

```
    SpaceFill;
```

```
END    bbutils.
```

DEFINITION MODULE retvols;

```

TYPE
  VrtData = ARRAY[1..2] OF ARRAY[1..9] OF LONGREAL;
VAR
  SolventRefNo      :CARDINAL;
  Vret              :VrtData;

```

PROCEDURE RetentVols80(SolventRefNo: CARDINAL);

PROCEDURE RetentVols100(SolventRefNo: CARDINAL);

PROCEDURE RetentVols120(SolventRefNo: CARDINAL);

END retvols.

IMPLEMENTATION MODULE retvols;

```

(*# optimize( i386 => on ) *)
(*# optimize( i387 => on ) *)
(*# debug( vid => full ) *)
(*# check( index => on ) *)
(*# check( stack => on ) *)

```

(* Vret[1,n] represent mol fractions as recalculated from original wt fractions *)

PROCEDURE RetentVols80(SolventRefNo: CARDINAL);

BEGIN

```

  Vret[1,1] := 0.00000;  Vret[1,2] := 0.23906;
  Vret[1,3] := 0.51520;  Vret[1,4] := 0.56425;
  Vret[1,5] := 0.63894;  Vret[1,6] := 0.75975;
  Vret[1,7] := 0.90447;  Vret[1,8] := 0.92811;
  Vret[1,9] := 1.00000;

```

CASE SolventRefNo OF

```

| 1: (* Methanol, RPS 62, RPP 117 *)
  Vret[2,1] := 3.616;    Vret[2,2] := 2.899;
  Vret[2,3] := 3.245;    Vret[2,4] := 4.208;
  Vret[2,5] := 4.410;    Vret[2,6] := 3.803;
  Vret[2,7] := 3.796;    Vret[2,8] := 3.551;
  Vret[2,9] := 3.683;

```

```

| 2: (* Ethanol, RPS 102, RPP 170 *)

```

```

| 3: (* Benzene, RPS 242, RPP 343 *)
  Vret[2,1] := 29.894;   Vret[2,2] := 31.532;
  Vret[2,3] := 26.278;   Vret[2,4] := 34.155;
  Vret[2,5] := 35.102;   Vret[2,6] := 34.258;
  Vret[2,7] := 30.400;   Vret[2,8] := 27.888;
  Vret[2,9] := 27.739;

```

- 4: (* Dichloromethane, RPS 53, RPP 107 *)
Vret[2,1] := 11.842; Vret[2,2] := 11.563;
Vret[2,3] := 10.027; Vret[2,4] := 13.345;
Vret[2,5] := 13.638; Vret[2,6] := 13.206;
Vret[2,7] := 11.863; Vret[2,8] := 10.611;
Vret[2,9] := 11.493;
- 5: (* Carbon Tetrachloride, RPS 42, RPP 94 *)
Vret[2,1] := 26.920; Vret[2,2] := 25.574;
Vret[2,3] := 22.497; Vret[2,4] := 29.488;
Vret[2,5] := 30.456; Vret[2,6] := 29.251;
Vret[2,7] := 26.112; Vret[2,8] := 22.982;
Vret[2,9] := 22.998;
- 6: (* Cyclohexane, RPS 249, RPP 353 *)
Vret[2,1] := 23.289; Vret[2,2] := 22.251;
Vret[2,3] := 18.912; Vret[2,4] := 24.692;
Vret[2,5] := 25.722; Vret[2,6] := 24.310;
Vret[2,7] := 21.611; Vret[2,8] := 18.516;
Vret[2,9] := 17.859;
- 7: (* Pentane, RPS 223, RPP 311 *)
Vret[2,1] := 3.918; Vret[2,2] := 3.281;
Vret[2,3] := 2.240; Vret[2,4] := 4.338;
Vret[2,5] := 4.915; Vret[2,6] := 4.196;
Vret[2,7] := 3.750; Vret[2,8] := 3.310;
Vret[2,9] := 3.481;
- 8: (* Hexane, RPS 271, RPP 379 *)
Vret[2,1] := 10.363; Vret[2,2] := 8.485;
Vret[2,3] := 6.575; Vret[2,4] := 11.156;
Vret[2,5] := 11.358; Vret[2,6] := 10.487;
Vret[2,7] := 9.407; Vret[2,8] := 9.063;
Vret[2,9] := 8.312;
- 9: (* Heptane, RPS 308, RPP 429 *)
Vret[2,1] := 27.188; Vret[2,2] := 21.545;
Vret[2,3] := 17.368; Vret[2,4] := 22.015;
Vret[2,5] := 30.580; Vret[2,6] := 26.157;
Vret[2,7] := 23.682; Vret[2,8] := 22.143;
Vret[2,9] := 20.474;
- 10: (* Octane, RPS 354, RPP 483 *)
Vret[2,1] := 62.399; Vret[2,2] := 48.710;
Vret[2,3] := 39.894; Vret[2,4] := 63.531;
Vret[2,5] := 68.285; Vret[2,6] := 59.591;
Vret[2,7] := 53.089; Vret[2,8] := 48.770;
Vret[2,9] := 47.207;
- 11: (* Toluene, RPS 286, RPP 400 *)
Vret[2,1] := 70.841; Vret[2,2] := 74.229;
Vret[2,3] := 61.615; Vret[2,4] := 80.665;
Vret[2,5] := 83.081; Vret[2,6] := 80.638;
Vret[2,7] := 71.297; Vret[2,8] := 62.899;
Vret[2,9] := 64.722;

```
| 12: (* 2-Butanone, RPS 167, RPP 243 *)  
      Vret[2,1] := 15.240;   Vret[2,2] := 14.951;  
      Vret[2,3] := 12.891;   Vret[2,4] := 17.139;  
      Vret[2,5] := 18.185;   Vret[2,6] := 16.943;  
      Vret[2,7] := 15.335;   Vret[2,8] := 13.870;  
      Vret[2,9] := 14.272;  
  
| 13: (* Trichloromethane, RPS 50, RPP 103 *)  
      Vret[2,1] := 27.734;   Vret[2,2] := 26.400;  
      Vret[2,3] := 22.715;   Vret[2,4] := 31.103;  
      Vret[2,5] := 32.020;   Vret[2,6] := 31.452;  
      Vret[2,7] := 29.375;   Vret[2,8] := 27.166;  
      Vret[2,9] := 27.166;  
  
| 14: (* Tetrahydrofuran, RPS 168, RPP 244 *)  
      Vret[2,1] := 18.115;   Vret[2,2] := 19.510;  
      Vret[2,3] := 15.992;   Vret[2,4] := 20.892;  
      Vret[2,5] := 21.497;   Vret[2,6] := 20.563;  
      Vret[2,7] := 18.053;   Vret[2,8] := 16.554;  
      Vret[2,9] := 16.352;  
  
| 15: (* Methyl Acetate, RPS 129, RPP 203 *)  
      Vret[2,1] := 7.435;    Vret[2,2] := 5.878;  
      Vret[2,3] := 6.134;    Vret[2,4] := 8.308;  
      Vret[2,5] := 8.878;    Vret[2,6] := 8.159;  
      Vret[2,7] := 7.409;    Vret[2,8] := 5.247;  
      Vret[2,9] := 6.627;  
  
| 16: (* Acetone, RPS 122, RPP 196 *)  
      Vret[2,1] := 6.270;    Vret[2,2] := 6.116;  
      Vret[2,3] := 5.124;    Vret[2,4] := 7.008;  
      Vret[2,5] := 7.447;    Vret[2,6] := 6.809;  
      Vret[2,7] := 6.158;    Vret[2,8] := 4.289;  
      Vret[2,9] := 5.832;  
  
| 17: (* Isopropanol, RPS 134, RPP 208 *)  
      Vret[2,1] := 9.668;    Vret[2,2] := 17.382;  
      Vret[2,3] := 8.832;    Vret[2,4] := 11.462;  
      Vret[2,5] := 12.085;   Vret[2,6] := 11.045;  
      Vret[2,7] := 10.543;   Vret[2,8] := 9.378;  
      Vret[2,9] := 10.129;  
  
| 18: (* Ethyl Acetate, RPS 172, RPP 249 *)  
      Vret[2,1] := 13.524;   Vret[2,2] := 13.885;  
      Vret[2,3] := 12.079;   Vret[2,4] := 16.224;  
      Vret[2,5] := 17.154;   Vret[2,6] := 15.958;  
      Vret[2,7] := 14.564;   Vret[2,8] := 10.772;  
      Vret[2,9] := 13.061;
```

ELSE

END;

END

RetentVols80;

PROCEDURE Retent Vols100(SolVentRefNo:CARDINAL);

BEGIN

Vret[1,1] := 0.00000; Vret[1,2] := 0.23906;
 Vret[1,3] := 0.51520; Vret[1,4] := 0.56425;
 Vret[1,5] := 0.63894; Vret[1,6] := 0.75975;
 Vret[1,7] := 0.90447; Vret[1,8] := 1.00000;

CASE SolVentRefNo OF

- | 1: (* Methanol, RPS 62, RPP 117 *)
 - Vret[2,1] := 0.951; Vret[2,2] := 0.912;
 - Vret[2,3] := 1.071; Vret[2,4] := 1.025;
 - Vret[2,5] := 1.043; Vret[2,6] := 1.512;
 - Vret[2,7] := 1.344; Vret[2,8] := 1.078;

- | 2: (* Ethanol, RPS 102, RPP 170 *)

- | 3: (* Benzene, RPS 242, RPP 343 *)
 - Vret[2,1] := 14.913; Vret[2,2] := 14.884;
 - Vret[2,3] := 15.814; Vret[2,4] := 15.843;
 - Vret[2,5] := 15.268; Vret[2,6] := 16.710;
 - Vret[2,7] := 16.806; Vret[2,8] := 13.204;

- | 4: (* Dichloromethane, RPS 53, RPP 107 *)
 - Vret[2,1] := 5.308; Vret[2,2] := 4.995;
 - Vret[2,3] := 5.828; Vret[2,4] := 5.718;
 - Vret[2,5] := 5.655; Vret[2,6] := 6.400;
 - Vret[2,7] := 6.312; Vret[2,8] := 5.306;

- | 5: (* Carbon Tetrachloride, RPS 42, RPP 94 *)
 - Vret[2,1] := 12.776; Vret[2,2] := 13.288;
 - Vret[2,3] := 13.894; Vret[2,4] := 13.775;
 - Vret[2,5] := 13.246; Vret[2,6] := 14.000;
 - Vret[2,7] := 14.257; Vret[2,8] := 11.611;

- | 6: (* Cyclohexane, RPS 249, RPP 353 *)
 - Vret[2,1] := 11.092; Vret[2,2] := 11.503;
 - Vret[2,3] := 11.830; Vret[2,4] := 11.670;
 - Vret[2,5] := 11.418; Vret[2,6] := 12.179;
 - Vret[2,7] := 12.004; Vret[2,8] := 9.260;

- | 7: (* Pentane, RPS 223, RPP 311 *)
 - Vret[2,1] := 1.837; Vret[2,2] := 1.504;
 - Vret[2,3] := 1.706; Vret[2,4] := 1.757;
 - Vret[2,5] := 1.684; Vret[2,6] := 1.950;
 - Vret[2,7] := 1.655; Vret[2,8] := 1.145;

- | 8: (* Hexane, RPS 271, RPP 379 *)
 - Vret[2,1] := 5.428; Vret[2,2] := 4.934;
 - Vret[2,3] := 5.367; Vret[2,4] := 5.379;
 - Vret[2,5] := 5.019; Vret[2,6] := 5.379;
 - Vret[2,7] := 5.111; Vret[2,8] := 3.742;

- | 9: (* Heptane, RPS 308, RPP 429 *)
 - Vret[2,1] := 12.727; Vret[2,2] := 12.202;
 - Vret[2,3] := 13.274; Vret[2,4] := 12.864;
 - Vret[2,5] := 12.112; Vret[2,6] := 12.976;
 - Vret[2,7] := 12.686; Vret[2,8] := 9.857;

- | 10: (* Octane, RPS 354, RPP 483 *)
 Vret[2,1] := 28.632; Vret[2,2] := 26.720;
 Vret[2,3] := 28.722; Vret[2,4] := 28.090;
 Vret[2,5] := 26.788; Vret[2,6] := 27.285;
 Vret[2,7] := 27.839; Vret[2,8] := 20.972;
- | 11: (* Toluene, RPS 286, RPP 400 *)
 Vret[2,1] := 33.112; Vret[2,2] := 34.667;
 Vret[2,3] := 35.737; Vret[2,4] := 35.837;
 Vret[2,5] := 34.255; Vret[2,6] := 36.474;
 Vret[2,7] := 32.277; Vret[2,8] := 29.847;
- | 12: (* 2-Butanone, RPS 167, RPP 243 *)
 Vret[2,1] := 6.901; Vret[2,2] := 6.994;
 Vret[2,3] := 7.825; Vret[2,4] := 7.585;
 Vret[2,5] := 7.480; Vret[2,6] := 8.427;
 Vret[2,7] := 8.281; Vret[2,8] := 6.646;
- | 13: (* Trichloromethane, RPS 50, RPP 103 *)
 Vret[2,1] := 12.380; Vret[2,2] := 13.050;
 Vret[2,3] := 14.084; Vret[2,4] := 13.822;
 Vret[2,5] := 13.472; Vret[2,6] := 15.018;
 Vret[2,7] := 15.451; Vret[2,8] := 12.934;
- | 14: (* Tetrahydrofuran, RPS 168, RPP 244 *)
 Vret[2,1] := 8.834; Vret[2,2] := 9.354;
 Vret[2,3] := 9.506; Vret[2,4] := 9.572;
 Vret[2,5] := 9.557; Vret[2,6] := 10.450;
 Vret[2,7] := 10.164; Vret[2,8] := 8.309;
- | 15: (* Methyl Acetate, RPS 129, RPP 203 *)
 Vret[2,1] := 3.079; Vret[2,2] := 3.006;
 Vret[2,3] := 3.391; Vret[2,4] := 3.268;
 Vret[2,5] := 3.223; Vret[2,6] := 3.941;
 Vret[2,7] := 3.676; Vret[2,8] := 3.172;
- | 16: (* Acetone, RPS 122, RPP 196 *)
 Vret[2,1] := 2.589; Vret[2,2] := 2.442;
 Vret[2,3] := 2.812; Vret[2,4] := 2.731;
 Vret[2,5] := 2.679; Vret[2,6] := 3.231;
 Vret[2,7] := 3.033; Vret[2,8] := 2.480;
- | 17: (* Isopropanol, RPS 134, RPP 208 *)
 Vret[2,1] := 3.886; Vret[2,2] := 4.017;
 Vret[2,3] := 4.631; Vret[2,4] := 4.338;
 Vret[2,5] := 4.675; Vret[2,6] := 5.078;
 Vret[2,7] := 5.084; Vret[2,8] := 4.249;
- | 18: (* Ethyl Acetate, RPS 172, RPP 249 *)
 Vret[2,1] := 6.305; Vret[2,2] := 6.280;
 Vret[2,3] := 6.933; Vret[2,4] := 6.785;
 Vret[2,5] := 6.678; Vret[2,6] := 7.707;
 Vret[2,7] := 7.510; Vret[2,8] := 6.170;

ELSE

END;

END

RetentVols100;

PROCEDURE RetentVols120(SolVentRefNo:CARDINAL);

BEGIN

Vret[1,1] := 0.00000; Vret[1,2] := 0.23906;
 Vret[1,3] := 0.51520; Vret[1,4] := 0.56425;
 Vret[1,5] := 0.63894; Vret[1,6] := 0.75975;
 Vret[1,7] := 0.90447; Vret[1,8] := 1.00000;

CASE SolVentRefNo OF

| 1: (* Methanol, RPS 62, RPP 117 *)
 Vret[2,1] := 0.021; Vret[2,2] := -0.1030;
 Vret[2,3] := -0.1115; Vret[2,4] := -0.0393;
 Vret[2,5] := 0.091; Vret[2,6] := 0.372;
 Vret[2,7] := 0.035; Vret[2,8] := 0.035;

| 2: (* Ethanol, RPS 102, RPP 170 *)

| 3: (* Benzene, RPS 242, RPP 343 *)
 Vret[2,1] := 8.292; Vret[2,2] := 8.702;
 Vret[2,3] := 8.953; Vret[2,4] := 9.081;
 Vret[2,5] := 9.306; Vret[2,6] := 8.894;
 Vret[2,7] := 9.365; Vret[2,8] := 7.322;

| 4: (* Dichloromethane, RPS 53, RPP 107 *)
 Vret[2,1] := 2.767; Vret[2,2] := 2.878;
 Vret[2,3] := 2.950; Vret[2,4] := 3.006;
 Vret[2,5] := 3.055; Vret[2,6] := 3.349;
 Vret[2,7] := 3.169; Vret[2,8] := 2.659;

| 5: (* Carbon Tetrachloride, RPS 42, RPP 94 *)
 Vret[2,1] := 7.265; Vret[2,2] := 7.673;
 Vret[2,3] := 7.702; Vret[2,4] := 8.029;
 Vret[2,5] := 8.137; Vret[2,6] := 7.718;
 Vret[2,7] := 8.122; Vret[2,8] := 6.350;

| 6: (* Cyclohexane, RPS 249, RPP 353 *)
 Vret[2,1] := 6.365; Vret[2,2] := 6.688;
 Vret[2,3] := 6.622; Vret[2,4] := 6.891;
 Vret[2,5] := 7.041; Vret[2,6] := 6.385;
 Vret[2,7] := 6.782; Vret[2,8] := 5.068;

| 7: (* Pentane, RPS 223, RPP 311 *)
 Vret[2,1] := 0.845; Vret[2,2] := 0.624;
 Vret[2,3] := 0.691; Vret[2,4] := 0.744;
 Vret[2,5] := 0.794; Vret[2,6] := 0.901;
 Vret[2,7] := 0.694; Vret[2,8] := 0.301;

| 8: (* Hexane, RPS 271, RPP 379 *)
 Vret[2,1] := 2.826; Vret[2,2] := 2.509;
 Vret[2,3] := 2.654; Vret[2,4] := 2.878;
 Vret[2,5] := 2.857; Vret[2,6] := 2.802;
 Vret[2,7] := 2.648; Vret[2,8] := 1.869;

| 9: (* Heptane, RPS 308, RPP 429 *)
 Vret[2,1] := 6.610; Vret[2,2] := 6.452;
 Vret[2,3] := 6.634; Vret[2,4] := 7.008;
 Vret[2,5] := 6.943; Vret[2,6] := 6.659;
 Vret[2,7] := 6.560; Vret[2,8] := 5.103;

```

| 10: (* Octane, RPS 354, RPP 483 *)
      Vret[2,1] := 14.077;   Vret[2,2] := 14.105;
      Vret[2,3] := 14.159;   Vret[2,4] := 15.289;
      Vret[2,5] := 15.091;   Vret[2,6] := 14.185;
      Vret[2,7] := 14.209;   Vret[2,8] := 11.177;

| 11: (* Toluene, RPS 286, RPP 400 *)
      Vret[2,1] := 18.108;   Vret[2,2] := 19.208;
      Vret[2,3] := 19.494;   Vret[2,4] := 20.072;
      Vret[2,5] := 20.056;   Vret[2,6] := 19.253;
      Vret[2,7] := 20.181;   Vret[2,8] := 16.155;

| 12: (* 2-Butanone, RPS 167, RPP 243 *)
      Vret[2,1] := 3.638;    Vret[2,2] := 3.865;
      Vret[2,3] := 3.809;    Vret[2,4] := 4.065;
      Vret[2,5] := 4.154;    Vret[2,6] := 4.559;
      Vret[2,7] := 4.249;    Vret[2,8] := 3.575;

| 13: (* Trichloromethane, RPS 50, RPP 103 *)
      Vret[2,1] := 6.636;    Vret[2,2] := 7.135;
      Vret[2,3] := 7.688;    Vret[2,4] := 7.656;
      Vret[2,5] := 7.766;    Vret[2,6] := 7.954;
      Vret[2,7] := 8.281;    Vret[2,8] := 6.813;

| 14: (* Tetrahydrofuran, RPS 168, RPP 244 *)
      Vret[2,1] := 7.265;    Vret[2,2] := 7.673;
      Vret[2,3] := 7.702;    Vret[2,4] := 8.029;
      Vret[2,5] := 8.137;    Vret[2,6] := 7.718;
      Vret[2,7] := 8.122;    Vret[2,8] := 6.350;

| 15: (* Methyl Acetate, RPS 129, RPP 203 *)
      Vret[2,1] := 1.395;    Vret[2,2] := 1.426;
      Vret[2,3] := 1.372;    Vret[2,4] := 1.533;
      Vret[2,5] := 1.659;    Vret[2,6] := 1.882;
      Vret[2,7] := 1.559;    Vret[2,8] := 1.362;

| 16: (* Acetone, RPS 122, RPP 196 *)
      Vret[2,1] := 1.104;    Vret[2,2] := 1.117;
      Vret[2,3] := 1.076;    Vret[2,4] := 1.185;
      Vret[2,5] := 1.313;    Vret[2,6] := 1.621;
      Vret[2,7] := 1.267;    Vret[2,8] := 1.096;

| 17: (* Isopropanol, RPS 134, RPP 208 *)
      Vret[2,1] := 1.757;    Vret[2,2] := 1.786;
      Vret[2,3] := 1.815;    Vret[2,4] := 1.939;
      Vret[2,5] := 2.079;    Vret[2,6] := 2.561;
      Vret[2,7] := 2.202;    Vret[2,8] := 1.944;

| 18: (* Ethyl Acetate, RPS 172, RPP 249 *)
      Vret[2,1] := 3.271;    Vret[2,2] := 3.427;
      Vret[2,3] := 3.386;    Vret[2,4] := 3.659;
      Vret[2,5] := 3.772;    Vret[2,6] := 4.036;
      Vret[2,7] := 3.787;    Vret[2,8] := 3.148;

```

ELSE

END;

RetentVols120;

END

BEGIN

END retvols.

DEFINITION MODULE rjmutils;

IMPORT Window,Str,bbmutils,IO,FIO,Graph;
 FROM bbmutils IMPORT Words,String,spaces,Data,SigFigs;
 FROM MATHLIB IMPORT Exp,Log,Sqrt;

TYPE CharSet = SET OF CHAR;
 CardSet = SET OF CARDINAL;
 VrtData = ARRAY[1..2] OF ARRAY[1..9] OF LONGREAL;

CONST

CtoK = 273.16; GasConst = 8.3144; (* J/(mol K) *)

(* Constants for the effect of temperature on the calculation
 of the specific volume of polymer blends. *)

a0b0 = 1.02976406; a0b1 = 7.58275052E-4;
 a1b0 = 2.25513866E-3; a1b1 = 1.48485124E-4; a1b2 = 3.29117195E-11;

(* Constants for the physical properties of the polymers *)

SegMolWt2 = 254.4; sigmaG2 = 3147.3; NoAvMolWt2 = 3290.0;
 SegMolWt3 = 594.89; sigmaG3 = 4982.4; NoAvMolWt3 = 10400.0;

VAR

(* Global *)

MolWt,Tcrit,Pcrit,ZRa,Omega,Rho20,OmegaSRK,
 VpA,VpB,VpC,VpD,b0,b1,b2,VP,TdegC,Vast,
 SolubilityParameter,
 v1,vred1,vstar1,Pstar1,Pred1,Tred1,Tstar1,
 v2,vred2,vstar2,v3,vred3,vstar3,Pstar2,Pstar3,
 Pred2,Pred3,Tred2,Tred3,Tstar2,Tstar3,
 v23,vred23,vstar23,vrbarN,
 P,Pstar23,Pred23,TdegK,Tstar23,Tred23,phi2,phi3,
 phistar2,phistar3,theta2,theta3,
 StoVRatio1,StoVRatio2,StoVRatio3,
 WtFr,dPred,dTred,dvred

:LONGREAL;

SolventRefNo :CARDINAL;

SolventName :String;

Vret :VrtData;

Debug :ARRAY[1..20] OF BOOLEAN;

PROCEDURE CubeRoot(x:LONGREAL):LONGREAL;

PROCEDURE SetDebugParams(nLines: CARDINAL);

PROCEDURE CancelDebug;

PROCEDURE SolventChoice(VAR SolventRefNo: CARDINAL;
 DisplayMenu: BOOLEAN; VAR SolventName: String);

PROCEDURE ProbePhysProps(SolventRefNo: CARDINAL);

PROCEDURE VPmmHg(VAR VP: LONGREAL; TdegC: LONGREAL;
 SolventRefNo: CARDINAL);

PROCEDURE HBT(VAR Vsat,Kval: LONGREAL; TdegC,Psystm: LONGREAL);

PROCEDURE RackettSD(VAR Vsat: LONGREAL; TdegC: LONGREAL);

```

PROCEDURE AlphaCalc(VAR alpha:LONGREAL; TdegC: LONGREAL);
PROCEDURE RSD(VAR vt,alpha,kval:LONGREAL; TdegC,Psys: LONGREAL);
PROCEDURE ProbeCharProps(TdegC:LONGREAL);
PROCEDURE PolymerSpecVol(VAR SpVol,Alpha: LONGREAL;
                        TdegC,WtFrEVA: LONGREAL);
PROCEDURE MassFromMol(VAR wm2,wm3:LONGREAL; MolFr2:LONGREAL);
PROCEDURE SegmtFromMol(VAR ws2,ws3:LONGREAL; MolFr2:LONGREAL);
PROCEDURE MolFromMass(VAR mf2,mf3:LONGREAL; WtFr2:LONGREAL);
PROCEDURE PolymerProps(TdegC,WtFrEVA:LONGREAL);
END rjmutils.

```

IMPLEMENTATION MODULE rjmutils;

(* amended 14th October to avoid the need for displaying the probe menu *)

(* amended 15th August to include Debug parameters 12,13 for RosWalsh *)

(* amended 13th August to include procedures for obtaining mass fractions from mol fractions;
segment fractions from mole fractions and mol fractions from mass fractions *)

(** optimize(i386 => on) *)

(** optimize(i387 => on) *)

(** debug(vid => full) *)

(** check(index => on) *)

(** check(stack => on) *)

```

PROCEDURE CubeRoot(x:LONGREAL): LONGREAL;
  VAR
    xroot          :LONGREAL;
    w              :Words;

  BEGIN
    IF x <= 0.0 THEN
      w[0] := 'CubeRoot called with argument <= zero';
      bbmutils.Pause(w,0,1);
    ELSE
      xroot := Exp(Log(x)/3.0);
    RETURN xroot;
  END;
END CubeRoot;

```

```
PROCEDURE SetDebugParams(nLines:CARDINAL);
```

```
VAR
```

```

  nx,ny,n,xc1,yc1,xc2,yc2,j,k,LastLine,
  j0,k0,m                                :CARDINAL;
  ok                                       :BOOLEAN;
  ch1,ch2                                  :CHAR;
  w                                         :Words;
  m0                                       :Window.WinType;
  d0                                       :Window.WinDef;
```

```
BEGIN
```

```

w[0] := 'Display of Numerical Data';
w[1] := 'Do you wish values from ProbePhysProps (y/n) ?';
w[2] := 'Do you wish values from VPmmHg (y/n) ?';
w[3] := 'Do you wish values from HBT (y/n) ?';
w[4] := 'Do you wish values from RackettSD (y/n) ?';
w[5] := 'Do you wish values from AlphaCalc (y/n) ?';
w[6] := 'Do you wish values from RSD (y/n) ?';
w[7] := 'Do you wish values from ProbeCharProps (y/n) ?';
w[8] := 'Do you wish values from PolymerProps (y/n) ?';
w[9] := 'Do you wish values from Bvirial (y/n) ?';
w[10] := 'Do you wish values from ChiCalc (y/n) ?';
w[11] := 'Do you wish values from XijBar (y/n) ?';
w[12] := 'Do you wish values from PartDerivs (y/n) ?';
w[13] := 'Do you wish values from Spinodal (y/n) ?';
```

```

d0 := Window.WinDef(0,0,79,24,Window.LightBlue,Window.Black,
  FALSE,FALSE,FALSE,TRUE,Window.SingleFrame,
  Window.Yellow,Window.Black);
```

```

m0 := Window.Open(d0);
Window.CursorOn;
bbmutils.NewWindow(w,0,nLines,m0,xc1,yc1,xc2,yc2);
ny := 1; LastLine := yc2 - yc1 - 2;
bbmutils.LocateStr(w[0],0,xc2-xc1,ny);
INC(ny);
bbmutils.OffSet(w[1],j,k,0,xc2-xc1);
n := 0;
w[21] := 'To change other debug commands enter y else n';
bbmutils.OffSet(w[21],j0,k0,xc1,xc2);
```

```
REPEAT
```

```

  INC(n); INC(ny); m := nLines-n+1;
  j := Str.Length(w[m]);
  Window.DirectWrite(k,ny,ADR(w[m]),j);
  Window.GotoXY(j+k-1,ny);
  REPEAT
```

```

    ch1 := CAP(IO.RdKey());
    UNTIL (ch1 = 'Y') OR (ch1 = 'N');
    Debug[m] := ch1 = 'Y';
    Window.DirectWrite(k0,LastLine,ADR(w[21]),j0);
    Window.GotoXY(j0+k0+2,LastLine);
  REPEAT
```

```

    ch2 := CAP(IO.RdKey());
    UNTIL (ch2 = 'Y') OR (ch2 = 'N');
    Window.GotoXY(1,LastLine);
    Window.ClrEol;
```

```

  UNTIL (n = nLines) OR (ch2 = 'N');
  Window.Close(m0);
```

```
END SetDebugParams;
```

```

PROCEDURE CancelDebug;
  VAR n :CARDINAL;
  BEGIN
    FOR n := 1 TO 20 DO Debug[n] := FALSE END;
  END CancelDebug;

PROCEDURE SolventChoice(VAR SolventRefNo:CARDINAL;
  DisplayMenu:BOOLEAN; VAR SolventName:String);
  LABEL skip;
  VAR
    nx1,nx2,nx3,nline,n1,n2,n3,j,k :CARDINAL;
    ch :CHAR;
    s,t,w :Words;
    range :CardSet;
    m0 :Window.WinType;
    d0 :Window.WinDef;

  BEGIN
    s[1] := 'Methanol';          t[1] := 'Methyl Alcohol';
    s[2] := 'Ethanol';          t[2] := 'Ethyl Alcohol';
    s[3] := 'Benzene';          t[3] := 'Benzol';
    s[4] := 'Dichloromethane';  t[4] := 'Methylene Chloride';
    s[5] := 'Carbon Tetrachloride'; t[5] := 'Tetrachloromethane';
    s[6] := 'Cyclohexane';      t[6] := 'Hexamethylene';
    s[7] := 'Pentane';          t[7] := 'Amyl Hydride';
    s[8] := 'Hexane';           t[8] := 'Caproyl Hydride';
    s[9] := 'Heptane';          t[9] := 'Heptyl Hydride';
    s[10] := 'Octane';          t[10] := 'Octyl Hydride';
    s[11] := 'Toluene';         t[11] := 'Methyl Benzene';
    s[12] := '2-Butanone';      t[12] := 'Methyl Ethyl Ketone';
    s[13] := 'Trichloromethane'; t[13] := 'Chloroform';
    s[14] := 'Tetrahydrofuran'; t[14] := 'Tetramethylene Oxide';
    s[15] := 'Methyl Acetate';  t[15] := ' ';
    s[16] := '2-Propanone';     t[16] := 'Acetone';
    s[17] := 'Isopropanol';     t[17] := 'Isopropyl Alcohol';
    s[18] := 'Ethyl Acetate';   t[18] := ' ';

    w[1] := 'Systematic Name';
    w[2] := 'Trivial Name';
    w[3] := 'Reference No';
    w[4] := 'Enter the reference number for the solvent ';
    w[5] := 'Your choice was outside the permitted range - try again!';

    (* Note if the menu is not displayed then the user program must ensure the
    value of SolventRefNo is within {1..18} while excluding 3 and 14 *)

    IF NOT DisplayMenu THEN GOTO skip END;

    n1 := 5;  w[6] := spaces[n1];
    n2 := 14; w[7] := spaces[n2];
    n3 := 15; w[8] := spaces[n3];
    Str.Concat(w[9],w[6],w[1]);
    Str.Append(w[9],w[7]);
    Str.Append(w[9],w[2]);
    Str.Append(w[9],w[8]);
    Str.Append(w[9],w[3]);
  
```

```
d0 := Window.WinDef(0,0,79,24,Window.LightBlue,Window.Black,
FALSE,FALSE,FALSE,TRUE,Window.SingleFrame,
Window.Yellow,Window.Black);
```

```
m0 := Window.Open(d0);
Window.CursorOn;
nline := 1;
Window.DirectWrite(1,nline,ADR(w[9]),Str.Length(w[9]));
ch := CHR(196);
w[10] := spaces[78];
FOR j := 1 TO 78 DO w[10,j] := ch END;
INC(nline);
Window.DirectWrite(1,nline,ADR(w[10]),Str.Length(w[10]));
nx1 := 6; nx2 := 35; nx3 := 67;
```

```
FOR j := 1 TO 18 DO
  INC(nline);
  Window.DirectWrite(nx1,nline,ADR(s[j]),Str.Length(s[j]));
  Window.DirectWrite(nx2,nline,ADR(t[j]),Str.Length(t[j]));
  Window.GotoXY(nx3,nline);
  IO.WrCard(j,2);
END;
```

```
range := CardSet{1,3..18};
INC(nline,2);
bbmutils.OffSet(w[4],j,k,0,79);
REPEAT
  Window.TextColor(Window.LightBlue);
  Window.GotoXY(1,nline);
  Window.ClrEol;
  bbmutils.LocateStr(w[4],0,79,nline);
  Window.GotoXY(j+k,nline);
  SolventRefNo := IO.RdCard();
  IF NOT (SolventRefNo IN range) THEN
    Window.TextColor(Window.Yellow);
    bbmutils.LocateStr(w[5],0,79,nline+1)
  END;
UNTIL SolventRefNo IN range;
Window.Close(m0);
```

```
skip: SolventName := s[SolventRefNo];
END SolventChoice;
```

```
PROCEDURE ProbePhysProps(SolventRefNo:CARDINAL);
```

```
VAR
```

nx,ny,j,k,xc1,yc1,xc2,yc2	:CARDINAL;
s	:String;
wh,wd	:Words;
d	:Data;
np	:SigFigs;

BEGIN

CASE SolventRefNo OF

- 1: (* Methanol, RPS 62, RPP 117 *)
 MolWt := 32.042; Tcrit := 513.15; Pcrit := 80.9;
 Omega := 0.556; OmegaSRK := 0.5536;
 Rho20 := 0.7914; ZRa := 0.23230; Vast := 0.1198;
 VpA := -8.54796; VpB := 0.76982;
 VpC := -3.10850; VpD := 1.54481;
 b0 := -0.17507994; b1 := 0.37661262; b2 := -1.96633786;
 SolubilityParameter := 0.000;
 StoVRatio1 := 2.3909E-10;
- 2: (* Ethanol, RPS 102, RPP 170 *)
 MolWt := 46.069; Tcrit := 516.16; Pcrit := 61.4;
 Omega := 0.644; OmegaSRK := 0.6378;
 Rho20 := 0.7893; ZRa := 0.25041; Vast := 0.1752;
 VpA := -8.51838; VpB := 0.34163;
 VpC := -5.73683; VpD := 8.32581;
 b0 := -0.75487486; b1 := 6.22885505; b2 := -13.27808137;
 SolubilityParameter := 0.000;
- 3: (* Benzene, RPS 242, RPP 343 *)
 MolWt := 78.011; Tcrit := 562.16; Pcrit := 48.9;
 Omega := 0.212; OmegaSRK := 0.2137;
 Rho20 := 0.8765; ZRa := 0.26967; Vast := 0.2564;
 VpA := -6.98273; VpB := +1.33213;
 VpC := -2.62863; VpD := -3.33399;
 b0 := -0.37822731; b1 := +0.61790557; b2 := -0.30460014;
 SolubilityParameter := 9.147;
 StoVRatio1 := 2.3980E-10;
- 4: (* Dichloromethane, RPS 53, RPP 107 *)
 MolWt := 84.933; Tcrit := 510.00; Pcrit := 63.0;
 Omega := 0.199; OmegaSRK := 0.1959;
 Rho20 := 1.3266; ZRa := 0.26793; Vast := 0.1767;
 VpA := -7.35739; VpB := +2.17546;
 VpC := -4.07038; VpD := +3.50701;
 b0 := -0.40527635; b1 := +0.19403877; b2 := -0.82176584;
 SolubilityParameter := 9.879;
 StoVRatio1 := 2.9857E-10;
- 5: (* Carbon Tetrachloride, RPS 42, RPP 94 *)
 MolWt := 153.823; Tcrit := 556.40; Pcrit := 45.6;
 Omega := 0.193; OmegaSRK := 0.1875;
 Rho20 := 1.594; ZRa := 0.28008;
 VpA := -7.07139; VpB := +1.71497; Vast := 0.2754;
 VpC := -2.89930; VpD := -2.49466;
 b0 := -0.94192552; b1 := -0.78952035; b2 := -1.27972279;
 SolubilityParameter := 8.582;
 StoVRatio1 := 1.8290E-10;
- 6: (* Cyclohexane, RPS 249, RPP 353 *)
 MolWt := 84.162; Tcrit := 553.54; Pcrit := 40.7;
 Omega := 0.212; OmegaSRK := 0.2128;
 Rho20 := 0.7785; ZRa := 0.27286;
 VpA := -6.96009; VpB := +1.31328; Vast := 0.3090;
 VpC := -2.75683; VpD := -2.45491;
 b0 := -0.32696438; b1 := +0.66426287; b2 := -0.29882136;
 SolubilityParameter := 8.182;
 StoVRatio1 := 2.3354E-10;

- 7: (* Pentane, RPS 223, RPP 311 *)
 MolWt := 72.151; Tcrit := 469.65; Pcrit := 33.7;
 Omega := 0.251; OmegaSRK := 0.2522;
 Rho20 := 0.6262; ZRa := 0.26853; Vast := 0.3113;
 VpA := -7.28936; VpB := +1.53679;
 VpC := -3.08367; VpD := -1.02456;
 b0 := -0.34472727; b1 := +0.75926287; b2 := -0.26023873;
 SolubilityParameter := 7.012;
 StoVRatio1 := 2.2937E-10;
- 8: (* Hexane, RPS 271, RPP 379 *)
 MolWt := 86.178; Tcrit := 507.43; Pcrit := 30.1;
 Omega := 0.299; OmegaSRK := 0.3007;
 Rho20 := 0.6603; ZRa := 0.26355; Vast := 0.3682;
 VpA := -7.46765; VpB := +1.44211;
 VpC := -3.28222; VpD := -2.50941;
 b0 := -0.34109856; b1 := +0.76502185; b2 := -0.35116533;
 SolubilityParameter := 7.242;
 StoVRatio1 := 2.2328E-10;
- 9: (* Heptane, RPS 308, RPP 429 *)
 MolWt := 100.205; Tcrit := 540.26; Pcrit := 27.4;
 Omega := 0.349; OmegaSRK := 0.3507;
 Rho20 := 0.6837; ZRa := 0.26074; Vast := 0.4304;
 VpA := -7.46768; VpB := +1.37068;
 VpC := -3.53620; VpD := -3.20243;
 b0 := -0.33914149; b1 := +0.66524786; b2 := -0.84928651;
 SolubilityParameter := 7.423;
 StoVRatio1 := 2.0565E-10;
- 10: (* Octane, RPS 354, RPP 483 *)
 MolWt := 114.232; Tcrit := 568.83; Pcrit := 24.9;
 Omega := 0.398; OmegaSRK := 0.3998;
 Rho20 := 0.7025; ZRa := 0.25678; Vast := 0.4904;
 VpA := -7.91211; VpB := +1.38007;
 VpC := -3.80435; VpD := -4.50132;
 b0 := -0.34577078; b1 := +0.84347227; b2 := -0.50695659;
 SolubilityParameter := 7.554;
 StoVRatio1 := 2.1990E-10;
- 11: (* Toluene, RPS 286, RPP 400 *)
 MolWt := 92.141; Tcrit := 591.79; Pcrit := 41.0;
 Omega := 0.263; OmegaSRK := 0.2651;
 Rho20 := 0.8669; ZRa := 0.26455; Vast := 0.3137;
 VpA := -7.28607; VpB := +1.38091;
 VpC := -2.83433; VpD := -2.79186;
 b0 := -0.35415461; b1 := +0.87470561; b2 := -0.28391941;
 SolubilityParameter := 8.907;
 StoVRatio1 := 2.5886E-10;
- 12: (* 2-Butanone, RPS 167, RPP 243 *)
 MolWt := 72.107; Tcrit := 536.78; Pcrit := 42.1;
 Omega := 0.320; OmegaSRK := 0.3188;
 Rho20 := 0.8054; ZRa := 0.26248; Vast := 0.2523;
 VpA := -7.71476; VpB := +1.71061; (* ZRa calculated *)
 VpC := -3.68770; VpD := -0.75169;
 b0 := +0.21880959; b1 := +2.64087032; b2 := +0.41155558;
 SolubilityParameter := 9.038;
 StoVRatio1 := 2.3244E-10;

- 13: (* Trichloromethane, RPS 50, RPP 103 *)
 MolWt := 119.378; Tcrit := 536.40; Pcrit := 53.7;
 Omega := 0.218; OmegaSRK := 0.2181;
 Rho20 := 1.4832; ZRa := 0.27498; Vast := 0.2245;
 VpA := -6.95546; VpB := +1.16625;
 VpC := -2.13970; VpD := -3.44421;
 b0 := -0.21654695; b1 := +1.28817983; b2 := +0.27776848;
 SolubilityParameter := 9.240;
 StoVRatio1 := 1.8777E-10;
- 14: (* Tetrahydrofuran, RPS 168, RPP 244 *)
 MolWt := 72.107; Tcrit := 540.15; Pcrit := 51.9;
 Omega := 0.217; OmegaSRK := 0.2227;
 Rho20 := 0.8892; ZRa := 0.25523; Vast := 0.2308;
 VpA := +9.1069; VpB := +2768.38; VpC := -46.9;
 (* Uses RPP equation 3 *)
 b0 := +0.00000000; b1 := +0.00000000; b2 := +0.00000000;
 SolubilityParameter := 9.317;
 StoVRatio1 := 2.0000E-10;
- 15: (* Methyl Acetate, RPS 129, RPP 203 *)
 MolWt := 74.080; Tcrit := 506.80; Pcrit := 46.9;
 Omega := 0.326; OmegaSRK := 0.3205;
 Rho20 := 0.933; ZRa := 0.55238; Vast := 0.2262;
 VpA := -8.05406; VpB := +2.56375;
 VpC := -5.12994; VpD := +0.16125;
 b0 := -0.73216340; b1 := -0.36768303; b2 := -1.92009995;
 SolubilityParameter := 0.000;
 StoVRatio1 := 2.0000E-10;
- 16: (* Acetone, RPS 122, RPP 196 *)
 MolWt := 58.080; Tcrit := 508.15; Pcrit := 47.0;
 Omega := 0.304; OmegaSRK := 0.3149;
 Rho20 := 0.790; ZRa := 0.24494; Vast := 0.2080;
 VpA := -7.45514; VpB := +1.20200;
 VpC := -2.43926; VpD := -3.35590;
 b0 := -0.34055397; b1 := +0.82971338; b2 := -1.49459151;
 SolubilityParameter := 9.712;
 StoVRatio1 := 2.0000E-10;
- 17: (* Isopropanol, RPS 134, RPP 208 *)
 MolWt := 60.096; Tcrit := 508.76; Pcrit := 47.6;
 Omega := 0.665; OmegaSRK := 0.6637;
 Rho20 := 0.786; ZRa := 0.24962; Vast := 0.2313;
 VpA := -8.16927; VpB := -9.43213E-2;
 VpC := -8.10040; VpD := +7.85;
 b0 := -0.44005976; b1 := -0.01017017; b2 := -3.30505211;
 SolubilityParameter := 0.000;
 StoVRatio1 := 2.0000E-10;
- 18: (* Ethyl Acetate, RPS 172, RPP 249 *)
 MolWt := 88.107; Tcrit := 523.20; Pcrit := 38.3;
 Omega := 0.362; OmegaSRK := 0.3595;
 Rho20 := 0.901; ZRa := 0.25389; Vast := 0.2853;
 VpA := -7.68521; VpB := -1.36511;
 VpC := -4.08980; VpD := -1.75342;
 b0 := -0.66912027; b1 := -0.31486861; b2 := -1.72062881;
 SolubilityParameter := 9.044;
 StoVRatio1 := 2.0000E-10;

```
ELSE
END;
```

```
IF Debug[1] THEN
```

```
  wh[0] := 'Physical Properties of ';
  Str.Append(wh[0],SolventName);
  wd[1] := 'Molecular Weight   '; d[1] := MolWt;   np[1] := 3;
  wd[2] := 'Critical Temperature'; d[2] := Tcrit;   np[2] := 2;
  wd[3] := 'Critical Pressure   '; d[3] := Pcrit;   np[3] := 1;
  wd[4] := 'Acentric Factor     '; d[4] := Omega;   np[4] := 4;
  wd[5] := 'Acentric Factor(SRK)'; d[5] := OmegaSRK; np[5] := 4;
  wd[6] := 'Density at 20 degC  '; d[6] := Rho20;   np[6] := 4;
  wd[7] := 'Rackett Z value     '; d[7] := ZRa;     np[7] := 5;
  wd[8] := 'VpA                 '; d[8] := VpA;     np[8] := 5;
  wd[9] := 'VpB                 '; d[9] := VpB;     np[9] := 5;
  wd[10] := 'VpC                '; d[10] := VpC;    np[10] := 5;
  wd[11] := 'VpD                '; d[11] := VpD;    np[11] := 5;
  wd[12] := 'b0                 '; d[12] := b0;     np[12] := 8;
  wd[13] := 'b1                 '; d[13] := b1;     np[13] := 8;
  wd[14] := 'b2                 '; d[14] := b2;     np[14] := 8;
  wd[15] := 'Solubility Param.  ';
  d[15] := SolubilityParameter;   np[15] := 4;
  wd[16] := '1.0E10 * StoVRatio1';
  d[16] := StoVRatio1*1.0E10;     np[16] := 4;
  bbmutils.ShowData(wh,wd,d,np,1,16);
```

```
END;
```

```
END ProbePhysProps;
```

```
PROCEDURE VPmmHg(VAR VP:LONGREAL; TdegC:LONGREAL;
  SolventRefNo:CARDINAL);
```

```
VAR
```

```
  x,x15,x3,x6,f1,f2,t           :LONGREAL;
  r                             :CardSet;
  wh,wd                         :Words;
  d                              :Data;
  np                             :SigFigs;
```

```
BEGIN
```

```
  t := TdegC + CtoK;
  r := CardSet{1..13,15..18};
  IF SolventRefNo IN r THEN
    x := 1.0 - t/Tcrit; x15 := x*Sqrt(x);
    x3 := x15*x15; x6 := x3*x3;
    f1 := (VpA*x + VpB*x15 + VpC*x3 + VpD*x6)/(1.0 - x);
    f2 := Pcrit*Exp(f1);
```

```
ELSE
```

```
  f1 := VpA - VpB/(t + VpC);
  f2 := Exp(f1);
```

```
END;
```

```
VP := 750.0*f2;
```

```
IF Debug[2] THEN
```

```
  wh[0] := 'Test Output from Procedure VPmmHg';
  wd[1] := 'Temperature (degC)   ';
  wd[2] := 'Vapour Pressure (mmHg)';
  d[1] := TdegC; np[1] := 2;
  d[2] := VP;   np[2] := 1;
  bbmutils.ShowData(wh,wd,d,np,1,2);
```

```
END;
```

```
END VPmmHg;
```

PROCEDURE HBT(VAR Vsat,Kval:LONGREAL; TdegC,Psystem:LONGREAL);

(* The calculation of liquid saturated molar volumes using the Hankinson-Brost-Thomson technique as detailed in Reid, Prausnitz and Polling, pp 55 et seq. *)

(* Extended in an attempt to calculate the isothermal compressibility K *)

CONST

a = -1.52816; e = -0.296123;
 b = +1.43907; f = +0.386914;
 c = -0.81446; g = -0.0427258;
 d = +0.190454; h = -0.0480645;

aa = -9.070217; bb = +62.45326; dd = -135.1102;
 ff = +4.79594; gg = +0.250047; hh = +1.14188;
 jj = +0.0861488; kk = +0.0344483;

VAR

VrZero,Vrdelta,Tr,x1,x2,x3,x4,Vstar,
 cc,ee,beta,V1,V2,V3,dP,Pbar :LONGREAL;
 wh,wd :Words;
 v :Data;
 np :SigFigs;

BEGIN

(* The value of the Debug Parameter is 3 *)

(* This procedure cannot be used without re-introducing OmegaSRK into the Physical Constants Procedure *)

VPmmHg(VP,TdegC,SolventRefNo);

VP := VP/750.0; (* convert to Bar *)

(*

(* Use Rho20 to calculate Vstar *)

Tr := (20.0 + CtoK)/Tcrit;
 x3 := 1.0 - Tr; x1 := CubeRoot(x3); x2 := x1*x1; x4 := x3*x1;
 VrZero := 1.0 + a*x1 + b*x2 + c*x3 + d*x4;
 Vrdelta := (e + Tr*(f + Tr*(g + Tr*h)))/(Tr - 1.00001);
 Vstar := MolWt/(Rho20*VrZero*(1.0 - OmegaSRK*Vrdelta));

*)

Tr := (TdegC + CtoK)/Tcrit;
 x3 := 1.0 - Tr; x1 := CubeRoot(x3); x2 := x1*x1; x4 := x3*x1;
 VrZero := 1.0 + a*x1 + b*x2 + c*x3 + d*x4;
 Vrdelta := (e + Tr*(f + Tr*(g + Tr*h)))/(Tr - 1.00001);
 Vsat := 1000.0*Vast*VrZero*(1.0 - OmegaSRK*Vrdelta); (* cm3/mol *)

(* Next evaluate the terms that are independent of Pressure *)

cc := jj + kk*OmegaSRK;
 ee := Exp(ff + OmegaSRK*(gg + OmegaSRK*hh));
 beta := Pcrit*(-1.0 + aa*x1 + bb*x2 + dd*x3 + ee*x4);

Pbar := 1.01325*Psystem; dP := 0.05*Pbar;

IF dP < 0.5 THEN dP := 0.5 END;

V1 := Vsat*(1.0 - cc*Log((beta + Pbar - dP)/(beta + VP)));
 V2 := Vsat*(1.0 - cc*Log((beta + Pbar)/(beta + VP)));
 V3 := Vsat*(1.0 - cc*Log((beta + Pbar + dP)/(beta + VP)));

(* K is defined as $-(1/V)(dV/dP)$ *)

Kval := -0.5*(V3 - V1)/V2/dP;

```

IF Debug[3] THEN
  wh[0] := 'Test Output from Procedure HBT';
  wd[1] := 'Temperature (degC)      ';
  wd[2] := 'Vast (cm3/mol)          ';
  wd[3] := 'Vsat (cm3/mol)         ';
  wd[4] := 'Volume at 0.5 bar      ';
  wd[5] := 'Volume at 1.0 bar     ';
  wd[6] := 'Volume at 1.5 bar     ';
  wd[7] := 'Estimate of 1.0E6*K   ';

  v[1] := TdegC;      np[1] := 2;
  v[2] := 1000.0*Vast; np[2] := 3;
  v[3] := Vsat;       np[3] := 3;
  v[4] := V1;         np[4] := 3;
  v[5] := V2;         np[5] := 3;
  v[6] := V3;         np[6] := 3;
  v[7] := 1.0E6*Kval; np[7] := 2;
  bbmutils.ShowData(wh,wd,v,np,1,7);
END;
END HBT;

```

```

PROCEDURE RackettSD(VAR Vsat:LONGREAL; TdegC:LONGREAL);
CONST r = 0.285714285;
VAR
  phi,Tr,TrRef,f1,f2          :LONGREAL;
  wh,wd                       :Words;
  v                            :Data;
  np                           :SigFigs;
BEGIN
  Tr := (TdegC + CtoK)/Tcrit; TrRef := (20.0 + CtoK)/Tcrit;
  phi := Exp(r*Log(1.0-Tr)) - Exp(r*Log(1.0-TrRef));
  Vsat := (MolWt/Rho20)*Exp(phi*Log(ZRa));

  IF Debug[4] THEN
    wh[0] := 'Test Output from Procedure RackettSD';
    wd[1] := 'Temperature (degC)      ';
    wd[2] := 'Calculated Vsat (cm3/mol)';

    v[1] := TdegC;  np[1] := 2;
    v[2] := Vsat;   np[2] := 2;
    bbmutils.ShowData(wh,wd,v,np,1,2);
  END;
END RackettSD;

```

```

PROCEDURE AlphaCalc(VAR alpha:LONGREAL; TdegC:LONGREAL);
VAR
  v0,v1,v2,t1,t2             :LONGREAL;
  wh,wd                       :Words;
  d                            :Data;
  np                           :SigFigs;
BEGIN
  (* Debug parameter is 5 *)

```

(* The liquid phase volumes have been calculated from the RackettSD equation in preference to the Hankinson-Brost-Thomson technique because the former gave results which were in better agreement with the only available test data:

alpha = 0.001487 for acetone at 20 degC
 RSD gave 0.001462 while HBT gave 0.001516

*)

```

RackettSD(v0,TdegC);  t1 := TdegC-0.5;
RackettSD(v1,t1);    t2 := TdegC+0.5;
RackettSD(v2,t2);
alpha := (v2-v1)/v0;

IF Debug[5] THEN
  wh[0] := 'Output from Procedure AlphaCalc';
  wd[1] := 'Temperature (degC)  ';
  wd[2] := 'Calculated Alpha (/deg)  ';

  d[1] := TdegC;          np[1] := 2;
  d[2] := alpha;         np[2] := 8;
  bbmutils.ShowData(wh,wd,d,np,1,2);
END;
END AlphaCalc;

```

```
PROCEDURE RSD(VAR vt,alpha,kval:LONGREAL; TdegC,Psystem:LONGREAL);
```

```
VAR
```

```

Tr,Pr,Kt,Kr,Tref,Pbar,dP,
Rhotandp,Rhotm,Rhotp,Rhopp      :LONGREAL;
Bi                                :ARRAY [0..4],[0..3] OF LONGREAL;
wh,wd                             :Words;
d                                  :Data;
np                                 :SigFigs;

```

```
PROCEDURE FuncAi(Pr:LONGREAL; i:CARDINAL):LONGREAL;
```

```
VAR
```

```

n                                :CARDINAL;
sum,x                            :LONGREAL;

```

```
BEGIN
```

```

sum := 0.0;
FOR n := 0 TO 4 DO
  IF n = 0 THEN x := 1.0 ELSE x := Pr*x END;
  sum := sum + Bi[n,i]*x;
END;
RETURN sum;

```

```
END FuncAi;
```

```
PROCEDURE FuncK(Tr,Pr:LONGREAL):LONGREAL;
```

```
VAR
```

```

n                                :CARDINAL;
sum,x,Ai                          :LONGREAL;

```

```
BEGIN
```

```

sum := 0.0;
FOR n := 0 TO 3 DO
  Ai := FuncAi(Pr,n);
  IF n = 0 THEN x := 1.0 ELSE x := Tr*x END;
  sum := sum + Ai*x;
END;
RETURN sum;

```

```
END FuncK;
```

BEGIN

```
Bi[0,0] := +1.6368;           Bi[1,0] := -0.04615;
Bi[2,0] := +2.1138*1.0E-3;   Bi[3,0] := -0.7845*1.0E-5;
Bi[4,0] := -0.6923*1.0E-6;
```

```
Bi[0,1] := -1.9693;          Bi[1,1] := +0.21874;
Bi[2,1] := -8.0028*1.0E-3;   Bi[3,1] := -8.2823*1.0E-5;
Bi[4,1] := +5.2604*1.0E-6;
```

```
Bi[0,2] := +2.4638;          Bi[1,2] := -0.36461;
Bi[2,2] := +12.8763*1.0E-3;  Bi[3,2] := +14.8059*1.0E-5;
Bi[4,2] := -8.6895*1.0E-6;
```

```
Bi[0,3] := -1.5841;          Bi[1,3] := +0.25136;
Bi[2,3] := -11.3805*1.0E-3;  Bi[3,3] := +9.5672*1.0E-5;
Bi[4,3] := +2.1812*1.0E-6;
```

(* This procedure for the adjustment of known liquid density for temperature and pressure is by Rea, Spencer and Danner (1973) and is quoted by Walas in Phase Equilibria in Chemical Engineering, Butterworth. It can be made to yield values of both isobaric thermal expansion and isothermal compressibility; the system pressure is assumed to be in atmospheres but note that Pc is in bar hence Psystem is multiplied by 1.01325 *)

(* Calculate alpha *)

```
Tref := 20.0 + CtoK; Pbar := 1.01325*Psystem;
Tr := Tref/Tcrit; Pr := Pbar/Pcrit;
Kr := FuncK(Tr,Pr);
```

```
Tr := (TdegC + CtoK)/Tcrit;
Kt := FuncK(Tr,Pr);
Rhotandp := Rho20*Kt/Kr; (* density at TdegC, 1 atm *)
Tr := (TdegC + 0.5 + CtoK)/Tcrit;
Kt := FuncK(Tr,Pr);
Rhotp := Rho20*Kt/Kr; (* density at TdegC+0.5 *)
Tr := (TdegC - 0.5 + CtoK)/Tcrit;
Kt := FuncK(Tr,Pr);
Rhotm := Rho20*Kt/Kr; (* density at TdegC-0.5 *)
```

```
alpha := (1.0/Rhotp - 1.0/Rhotm)/(1.0/Rhotandp);
```

(* Calculate isothermal compressibility: determine a value for dP (say) 5% of Psystem but never less than 0.5 bar *)

```
dP := 0.05*Pbar;
IF dP < 0.5 THEN dP := 0.5 END;
Tr := (TdegC + CtoK)/Tcrit;
Pr := (Pbar + dP)/Pcrit;
Kt := FuncK(Tr,Pr);
Rhopp := Rho20*Kt/Kr; (* density at Psys+dP *)
Pr := (Pbar - dP)/Pcrit;
Kt := FuncK(Tr,Pr);
Rhopm := Rho20*Kt/Kr; (* density at Psys-dP *)
```

```
kval := -0.5*(1.0/Rhopp - 1.0/Rhopm)/(1.0/Rhotandp)/dP;
```

```

IF Debug[6] THEN
    wh[0] := 'Output from Procedure RSD      ';
    wd[1] := 'Density at 20C and Psystem    ';
    wd[2] := 'Density at T and Psystem      ';
    wd[3] := 'Density at T+0.5 and Psystem  ';
    wd[4] := 'Density at T-0.5 and Psystem  ';
    wd[5] := 'Density at T and Psystem+dP   ';
    wd[6] := 'Density at T and Psystem-dP   ';

    wd[7] := 'Calculated Alpha*1.0E3 (/deg) ';
    wd[8] := 'Calculated Kval*1.0E6 (/bar)  ';

    d[1] := Rho20;          np[1] := 5;
    d[2] := Rhotandp;      np[2] := 8;
    d[3] := Rhotp;         np[3] := 8;
    d[4] := Rhotm;         np[4] := 8;
    d[5] := Rhopp;         np[5] := 8;
    d[6] := Rhopm;         np[6] := 8;
    d[7] := alpha*1.0E3;   np[7] := 4;
    d[8] := kval*1.0E6;    np[8] := 4;
    bbmutils.ShowData(wh,wd,d,np,1,8);
END;
END RSD;

```

```
PROCEDURE ProbeCharProps(TdegC:LONGREAL);
```

```
VAR
```

```

    x,alpha,f,TdegK,Pval,Psat,DeltaSq,Kval :LONGREAL;
    wh,wd                                  :Words;
    d                                        :Data;
    np                                       :SigFigs;

```

```
BEGIN
```

```
(* Debug parameter is 7 *)
```

```

TdegK := TdegC + CtoK;
AlphaCalc(alpha,TdegC);
f := alpha*TdegK;
x := (3.0 + 4.0*f)/(3.0 + 3.0*f);
vred1 := x*x*x;

```

```

RackettSD(v1,TdegC);
v1 := v1/MolWt;
vstar1 := v1/vred1;
Tred1 := (x - 1.0)/x/vred1;
Tstar1 := TdegK/Tred1;

```

```
IF SolubilityParameter > 0.0 THEN
```

```
DeltaSq := SolubilityParameter*SolubilityParameter;
```

```
Pstar1 := 10.0*DeltaSq*vred1*vred1*4.1868; (* bar *)
```

```
ELSE
```

```
HBT(Psat,Kval,TdegC,1.0);
```

```
Pstar1 := alpha*vred1*vred1*TdegK/Kval;
```

```
END;
```

```

IF Debug[7] THEN
  wh[0] := 'Procedure ProbeCharProps - Data for ';
  Str.Append(wh[0],SolventName);
  wd[1] := 'Temperature (degC)';
  wd[2] := 'Calculated vred1';
  wd[3] := 'Calculated v1 (cm3/g)';
  wd[4] := 'Calculated vstar1 (cm3/g)';
  wd[5] := 'Calculated vstar1 (cm3/mol)';
  wd[6] := 'Calculated Tred1';
  wd[7] := 'Calculated Tstar1 (K)';
  wd[8] := 'Calculated Pstar1 (Bar)';
  wd[9] := 'Calculated Pstar1 (J/cm3)';

  d[1] := TdegC;      np[1] := 2;
  d[2] := vred1;      np[2] := 4;
  d[3] := v1;         np[3] := 4;
  d[4] := vstar1;     np[4] := 4;
  d[5] := MolWt*vstar1; np[5] := 2;
  d[6] := Tred1;      np[6] := 8;
  d[7] := Tstar1;     np[7] := 0;
  d[8] := Pstar1;     np[8] := 1;
  d[9] := 0.1*Pstar1; np[9] := 1;
  bbmutils.ShowData(wh,wd,d,np,1,9);
END;
END ProbeCharProps;

```

```

PROCEDURE PolymerSpecVol(VAR SpVol,Alpha: LONGREAL;
  TdegC,WtFrEVA: LONGREAL);

```

(* The specific volume is a function of composition and temperature; the data were first correlated in terms of mass fraction EVA and the relationship was found to be linear. The resulting coefficients were then plotted against temperature and it was decided to use a linear function for a0 and a quadratic for a1. *)

```

VAR
  a0,a1,deriv      :LONGREAL;
  debug            :BOOLEAN;
  wh,wd            :Words;
  d                :Data;
  np               :SigFigs;

```

```

BEGIN
  a0 := a0b0 + a0b1*TdegC;
  a1 := a1b0 + TdegC*(a1b1 + a1b2*TdegC);
  SpVol := a0 + a1*WtFrEVA;
  deriv := a0b1 + WtFrEVA*(a1b1 + 2.0*a1b2*TdegC);
  Alpha := deriv/SpVol;

  debug := FALSE;
  IF debug THEN
    wh[0] := 'Debug Results for PolymerSpecVol';
    wd[1] := 'a0';      d[1] := a0;      np[1] := 8;
    wd[2] := 'a1';      d[2] := a1;      np[2] := 8;
    wd[3] := 'SpVol';   d[3] := SpVol;   np[3] := 5;
    wd[4] := 'Alpha';   d[4] := Alpha;   np[4] := 8;
    bbmutils.ShowData(wh,wd,d,np,1,4);
  END;
END PolymerSpecVol;

```

```

PROCEDURE MassFromMol(VAR wm2,wm3:LONGREAL; MolFr2:LONGREAL);
  VAR numerator,denominator :LONGREAL;
  BEGIN
    numerator := MolFr2*NoAvMolWt2;
    denominator := numerator + (1.0 - MolFr2)*NoAvMolWt3;
    wm2 := numerator/denominator; wm3 := 1.0 - wm2;
  END MassFromMol;

```

```

PROCEDURE SegmtFromMol(VAR ws2,ws3:LONGREAL; MolFr2:LONGREAL);
  VAR numerator,denominator :LONGREAL;
  BEGIN
    numerator := MolFr2*SegMolWt2;
    denominator := numerator + (1.0 - MolFr2)*SegMolWt3;
    ws2 := numerator/denominator; ws3 := 1.0 - ws2;
  END SegmtFromMol;

```

```

PROCEDURE MolFromMass(VAR mf2,mf3:LONGREAL; WtFr2:LONGREAL);
  VAR numerator,denominator :LONGREAL;
  BEGIN
    numerator := WtFr2/NoAvMolWt2;
    denominator := numerator + (1.0 - WtFr2)/NoAvMolWt3;
    mf2 := numerator/denominator; mf3 := 1.0 - mf2;
  END MolFromMass;

```

```

PROCEDURE PolymerProps(TdegC,WtFrEVA:LONGREAL);
  VAR
    TdegK,alpha,alpha2,alpha3,p,xw2,xw3,
    delta2,delta3,g2at25c,g3at25c,g2,g3,S2toS3,
    v2at25c,v3at25c,dToverT,a2at25c,a3at25c :LONGREAL;
    nx,ny,n,xc1,yc1,xc2,yc2,j,k :CARDINAL;
    ok :BOOLEAN;
    s0,s1,s2 :String;
    PP,Ph :Words;
    PPvals :Data;
    np :SigFigs;
  BEGIN
    (* The Debug parameter is 8 *)
    (* Step 1 - calculate volume functions *)
    TdegK := TdegC + CtoK;
    PolymerSpecVol(v2,alpha2,TdegC,1.0);
    PolymerSpecVol(v3,alpha3,TdegC,0.0);
    p := alpha2*TdegK;
    xw2 := (3.0+4.0*p)/(3.0+3.0*p);
    vred2 := xw2*xw2*xw2;
    p := alpha3*TdegK;
    xw3 := (3.0+4.0*p)/(3.0+3.0*p);
    vred3 := xw3*xw3*xw3;
    vstar2 := v2/vred2; vstar3 := v3/vred3;

    (* According to paper by Rostami and Walsh, p319, the
    product rbar*N*vstar is calculated as vrbarN *)

```

```

xw2 := WtFrEVA; xw3 := 1.0 - xw2;
vrbarN := xw2*vstar2 + xw3*vstar3;
PPvals[10] := vrbarN;
PolymerSpecVol(v23,alpha,TdegC,WtFrEVA);
p := alpha*TdegK;
p := (3.0+4.0*p)/(3.0+3.0*p);
vred23 := p*p*p; vstar23 := v23/vred23;

```

```
IF Debug[8] THEN
```

```

PPvals[1] := v2; PP[1] := 'v2 ';
PPvals[2] := vred2; PP[2] := 'vred2 ';
PPvals[3] := vstar2; PP[3] := 'vstar2 ';
PPvals[4] := v3; PP[4] := 'v3 ';
PPvals[5] := vred3; PP[5] := 'vred3 ';
PPvals[6] := vstar3; PP[6] := 'vstar3 ';
PPvals[7] := v23; PP[7] := 'v23 ';
PPvals[8] := vred23; PP[8] := 'vred23 ';
PPvals[9] := vstar23; PP[9] := 'vstar23 ';
PPvals[10] := vrbarN; PP[10] := 'vrbarN ';
Ph[0] := 'Volume Functions';
Ph[1] := ' at ';
Str.FixRealToStr(TdegC,0,Ph[2],ok);
Ph[3] := ' degC';
bbmutils.bbMConcat(Ph[5],Ph,1,3);
Str.Append(Ph[0],Ph[5]);
Ph[1] := 'For EVA, FVA and Blends';
FOR n := 1 TO 10 DO np[n] := 5 END;
bbmutils.ShowData(Ph,PP,PPvals,np,2,10);

```

```
END;
```

- (* Step 2 - calculate the characteristic pressures. *)
 (* The first step is to calculate the gamma values at 25oC *)

```

PolymerSpecVol(v2at25c,a2at25c,25.0,1.0);
PolymerSpecVol(v3at25c,a3at25c,25.0,0.0);
delta2 := sigmaG2/SegMolWt2/v2at25c;
delta3 := sigmaG3/SegMolWt3/v3at25c;
g2at25c := delta2*delta2/298.15;
g3at25c := delta3*delta3/298.15;

```

- (* The next step is to calculate the temperature correction for gamma in accordance with the method given by Rostami *)

```

dToverT := (TdegK - 298.16)/TdegK;
g2 := g2at25c*(1.0 - (1.0 + 2.0*a2at25c*TdegK)*dToverT);
g3 := g3at25c*(1.0 - (1.0 + 2.0*a3at25c*TdegK)*dToverT);

```

- (* Pressures obtained from the relationship $P_{star} = \gamma * v_{red} * v_{red} * T_{degK}$ are in units of cal/cm³; to convert to bar multiply by 10.0 * 4.1868 *)

```

Pstar2 := 41.868*g2*TdegK*vred2*vred2;
Pstar3 := 41.868*g3*TdegK*vred3*vred3;

```

- (* Step 3 - calculate the temperature functions. *)

```

p := CubeRoot(vred2);
Tred2 := (p - 1.0)/(vred2*p); Tstar2 := TdegK/Tred2;
p := CubeRoot(vred3);
Tred3 := (p - 1.0)/(vred3*p); Tstar3 := TdegK/Tred3;

```

```

IF Debug[8] THEN
  PPvals[1] := Tred2;      PP[1] := 'Tred2 ';  np[1] := 8;
  PPvals[2] := Tstar2;    PP[2] := 'Tstar2 '; np[2] := 1;
  PPvals[3] := Tred3;    PP[3] := 'Tred3 ';  np[3] := 8;
  PPvals[4] := Tstar3;    PP[4] := 'Tstar3 '; np[4] := 1;
  PPvals[5] := Pstar2;    PP[5] := 'Pstar2 '; np[5] := 1;
  PPvals[6] := Pstar3;    PP[6] := 'Pstar3 '; np[6] := 1;
  Ph[0] := 'Temperature and Pressure Functions';
  Ph[1] := 'for EVA, FVA and Blends';
  Str.Append(Ph[1],Ph[5]);
  bbmutils.ShowData(Ph,PP,PPvals,np,2,6);
END;

```

(* Step 4 - Calculate the volume/segment fractions together with the surface fractions. Note the phi values are based on number average molecular weights. *)

```

StoVRatio2 := 2.0000E-10; StoVRatio3 := 1.0000E-10;
S2toS3 := 2.0000;
xw2 := WtFrEVA; xw3 := 1.0 - xw2;
phi3 := xw3*v3/v23;
phi2 := xw2*v2/v23;

phistar3 := xw3*vstar3/(xw2*vstar2 + xw3*vstar3);
phistar2 := 1.0 - phistar3;
g2 := 1.0/S2toS3;
theta3 := g2*phistar3/(g2*phistar3 + phistar2);
theta2 := 1.0 - theta3;

```

```

IF Debug[8] THEN
  PPvals[1] := phi2;      PP[1] := 'Phi2      ';
  PPvals[2] := phi3;      PP[2] := 'Phi3      ';
  PPvals[3] := phistar2;  PP[3] := 'Phistar2  ';
  PPvals[4] := phistar3;  PP[4] := 'Phistar3  ';
  PPvals[5] := theta2;    PP[5] := 'Theta2    ';
  PPvals[6] := theta3;    PP[6] := 'Theta3    ';
  FOR n := 1 TO 6 DO np[n] := 6 END;
  PPvals[7] := 1.0E10*StoVRatio2;
  np[7] := 4;             PP[7] := 'StoVRatio2 ';
  PPvals[8] := 1.0E10*StoVRatio3;
  np[8] := 4;             PP[8] := 'StoVRatio3 ';
  Ph[0] := 'Segment and Surface Area Functions';
  bbmutils.ShowData(Ph,PP,PPvals,np,2,8);
END;

```

END PolymerProps;

BEGIN

CancelDebug;

END rjmutils.

MODULE X23Optim;

```
(** optimize( i386 => on ) *)
(** optimize( i387 => on ) *)
(** debug( vid => full ) *)
(** check( index => on ) *)
(** check( stack => on ) *)
```

```
(* An optimization program for X23 - 24th May 1990 *)
(* sum of squares of the error term using Brent method *)
```

```
IMPORT Window,Str,bbmutils,rjmutils,IO,Graph;
FROM bbmutils IMPORT ShowData,Words,String,spaces,Data,SigFigs;
FROM MATHLIB IMPORT Exp,Log,Sqrt;
FROM rjmutils IMPORT CubeRoot,SetDebugParams,SolventChoice,
ProbePhysProps,VPmmHg,HBT,RackettSD,
AlphaCalc,RSD,ProbeCharProps,PolymerProps;
```

```
FROM rjmutils IMPORT
CtoK, GasConst, (* J/(mol K) *)
MolWt,Tcrit,Pcrit,ZRa,Omega,Rho20,OmegaSRK,
VpA,VpB,VpC,VpD,b0,b1,b2,VP,TdegC,Vast,
SolubilityParameter,
v1,vred1,vstar1,Pstar1,Pred1,Tred1,Tstar1,
v2,vred2,vstar2,v3,vred3,vstar3,Pstar2,Pstar3,
Pred2,Pred3,Tred2,Tred3,Tstar2,Tstar3,
v23,vred23,vstar23,vrbarN,
P,Pstarb,Predb,TdegK,Tstarb,Tredb,
phi2,phi3,phistar2,phistar3,
theta2,theta3,dPred,dTred,dvred,
SolventRefNo,SolventName,Vret,Debug;
```

```
TYPE CharSet = SET OF CHAR;
CardSet = SET OF CARDINAL;
```

```
VAR
Error,X23,t1,t2,t3 :LONGREAL;
ch :CHAR;
wh,wd :Words;
s :String;
j,k,n,nx,ny,xc1,xc2,yc1,yc2,nData1,nData2 :CARDINAL;
m0,m1 :Window.WinType;
d0,d1 :Window.WinDef;
ok,db :BOOLEAN;
dHData,WtFr,X23vals,dHCalc,d :Data;
np :SigFigs;
```

```
PROCEDURE Func(X23:LONGREAL; n1,n2:CARDINAL):LONGREAL;
VAR
t0,t1,t2,t3,t4,Error :LONGREAL;
j,k,n :CARDINAL;
BEGIN
Error := 0.0;
FOR n := n1 TO n2 DO
IF n <= 8 THEN TdegC := 75.5 ELSE TdegC := 86.1 END;
PolymerProps(TdegC,WtFr[n]);
```

(* Pstar is in bar thus each term in the RHS will have units of cm³ bar/g hence the dHData must be multiplied by 10 to convert J/g to cm³.bar/g *)

```
t0 := 10.0*dHData[n]/vrbarN;
t1 := phi2*Pstar2*(1.0/vred2 - 1.0/vred23);
t2 := phi3*Pstar3*(1.0/vred3 - 1.0/vred23);
t3 := phi2*theta3*X23/vred23;
t4 := t0 - t1 - t2 - t3;
Error := Error + t4*t4;
```

```
END;
RETURN Error;
```

```
END Func;
```

```
PROCEDURE Brent(VAR Answer,Error:LONGREAL;
                ax,bx,cx,tol:LONGREAL; Display:BOOLEAN);
```

```
  LABEL Finish;
```

```
  CONST
```

```
    itmax = 100; zeps = 1.0E-8; cgold = 0.3819660;
```

```
  VAR
```

```
    a,b,d,e,etemp,fu,fv,fw,fx,
    p,q,r,tol1,tol2,u,v,w,x,xm      :LONGREAL;
    iter                             :CARDINAL;

    xc1,xc2,yc1,yc2,j,k,nx,ny,ni    :CARDINAL;
    sw                               :Words;
    s1,s2,s3                         :String;
    ch                               :CHAR;
    m0                               :Window.WinType;
    d0                               :Window.WinDef;
    ok                               :BOOLEAN;
```

```
  PROCEDURE Sign(a,b:LONGREAL):LONGREAL;
```

```
    BEGIN
```

```
      IF b >= 0.0 THEN RETURN ABS(a)
      ELSE RETURN ABS(b)
```

```
    END;
```

```
  END Sign;
```

```
BEGIN
```

```
  IF Display THEN
```

```
    d0 := Window.WinDef(0,0,79,24,Window.LightBlue,Window.Black,
                        FALSE,FALSE,FALSE,TRUE,Window.SingleFrame,
                        Window.Yellow,Window.Black);
```

```
    m0 := Window.Open(d0);
```

```
    Window.CursorOn;
```

```
    xc1 := 15; xc2 := 65; yc1 := 1; yc2 := 23;
```

```
    Window.Change(m0,xc1,yc1,xc2,yc2);
```

```
    ni := 2;
```

```
    s2 := 'Press any key to continue';
```

```
    s3 := ' N           x           F(x)';
```

```
    Window.DirectWrite(5,1,ADR(s3),Str.Length(s3));
```

```
  END;
```

```

(* a and b must be in ascending order *)
  IF ax < cx THEN a := ax ELSE a := cx END;
  IF ax > cx THEN b := ax ELSE b := cx END;

(* initialization *)
  v := bx; w := v; x := v; e := 0.0;
  fx := Func(x,nData1,nData2);
  fv := fx; fw := fx;

(* Main Program Loop *)
  FOR iter := 1 TO itmax DO
    xm := 0.5*(a+b); tol1 := tol*ABS(x) + zeps; tol2 := tol1 + tol1;

    IF ABS(x - xm) <= tol2 - 0.5*(b-a) THEN
      Answer := x; Error := fx;
      IF Display THEN
        bbmutils.Offset(s2,j,k,xc1,xc2);
        Window.DirectWrite(k,yc2-2,ADR(s2),j);
        Window.GotoXY(k+j+1,yc2-2);
        ch := IO.RdKey();
      END;
      GOTO Finish;
    ELSE
      IF Display THEN
        INC(ni);
        nx := 4;
        Window.GotoXY(nx,ni); IO.WrCard(iter,3);
        INC(nx,10);
        Str.FixRealToStr(x,10,s1,ok);
        Window.DirectWrite(nx,ni,ADR(s1),Str.Length(s1));
        IF fx < 0.0 THEN INC(nx,19) ELSE INC(nx,20) END;
        Str.FixRealToStr(fx,10,s1,ok);
        Window.DirectWrite(nx,ni,ADR(s1),Str.Length(s1));
        IF ni > 19 THEN
          ni := 2;
          bbmutils.Offset(s2,j,k,0,50);
          Window.DirectWrite(k,yc2-2,ADR(s2),j);
          Window.GotoXY(k+j+1,yc2-2);
          ch := IO.RdKey();
          Window.Clear;
          Window.DirectWrite(5,1,ADR(s3),Str.Length(s3));
        END;
      END;
    END;
  END;

  IF ABS(e) > tol1 THEN
    r := (x-w)*(fx-fv);
    q := (x-v)*(fx-fw);
    p := (x-v)*q - (x-w)*r;
    q := 2.0*(q-r);
    IF q > 0.0 THEN p := -p END;
    q := ABS(q); etemp := e; e := d;
  END;

```

(* Construct trial parabolic fit *)

```

IF (ABS(p) >= ABS(0.5*q*etemp)) OR (p <= q*(a-x)) OR (p >= q*(b-x))
THEN IF x >= xm THEN e := a-x ELSE e := b-x END;
    d := cgold*e;
ELSE
    d := p/q; u := x+d;
    IF (u-a < tol2) OR (b-u < tol2) THEN d := Sign(tol1,xm-x) END;
END;
    (* of IF ABS(p) > ..loop*)
ELSE
    IF x >= xm THEN e := a-x ELSE e := b-x END;
    d := cgold*e;
END;
    (* of IF ABS(e) > tol12 ....loop *)

IF ABS(d) >= tol1 THEN u := x + d ELSE u := x + Sign(tol1,d) END;
fu := Func(u,nData1,nData2);

IF fu <= fx THEN
    IF u >= x THEN a := x ELSE b := x END;
    v := w; fv := fw; w := x; fw := fx;
    x := u; fx := fu;
ELSE
    IF u < x THEN a := u ELSE b := u END;
    IF (fu <= fw) OR (w = x) THEN v := w; fv := fw; w := u; fw := fu;
    ELSE
        IF (fu <= fv) OR (v = x) OR (v = w)
        THEN v := u; fv := fu END;
    END;
END;
    (* of IF (fu <= fx) condition.*)
END;
    (* of FOR loop *)

```

```

sw[0] := 'Permitted number of iterations exceeded';
sw[1] := ' ';
sw[2] := 'Current best answer is ';
sw[3] := ' ';
Str.FixRealToStr(b,10,sw[4],ok);
Str.Append(sw[2],sw[4]);
bbmutils.Pause(sw,3,0);
Answer := x; Error := fx;

```

Finish:

```
IF Display THEN Window.Close(m0) END;
```

END Brent;

BEGIN

(* Data at 75.5 degC - all data in Joules/gram *)

```

WtFr[1] := 0.1193;   dHData[1] := 3.804E-2;
WtFr[2] := 0.2432;   dHData[2] := 7.162E-2;
WtFr[3] := 0.2987;   dHData[3] := 9.005E-2;
WtFr[4] := 0.3610;   dHData[4] := 10.596E-2;
WtFr[5] := 0.4752;   dHData[5] := 10.007E-2;
WtFr[6] := 0.4786;   dHData[6] := 10.047E-2;
WtFr[7] := 0.6353;   dHData[7] := 9.496E-2;
WtFr[8] := 0.8333;   dHData[8] := 3.257E-2;

```

(* Data at 86.1 degC *)

```

WtFr[9] := 0.2991;   dHData[9] := 5.390E-2;
WtFr[10] := 0.3613;  dHData[10] := 7.703E-2;
WtFr[11] := 0.4786;  dHData[11] := 6.259E-2;

```

```

wh[0] := 'Estimation of X23 by Minimisation of Error';
wd[1] := 'The value of X23 for data at 75.5C is';
wd[2] := 'The value of X23 for data at 86.1C is';
wd[3] := 'The value of X23 for combined data is';
wd[4] := 'To continue, press any key';

```

```

SetDebugParams(8);
db := TRUE;
nData1 := 1; nData2 := 8;
Brent(X23,Error,0.0,5.0,10.0,1.0E-6,db);
X23vals[1] := X23;

```

```

nData1 := 9; nData2 := 11;
Brent(X23,Error,0.0,5.0,10.0,1.0E-6,db);
X23vals[2] := X23;

```

```

nData1 := 1; nData2 := 11;
Brent(X23,Error,0.0,5.0,10.0,1.0E-6,db);
X23vals[3] := X23;

```

```

FOR n := 1 TO 3 DO np[n] := 8 END;
ShowData(wh,wd,X23vals,np,1,3);

```

(* The recalculation of the dHData values using the optimised values of X23 *)

```

FOR n := 1 TO 11 DO
  IF n <= 8 THEN TdegC := 75.5 ELSE TdegC := 86.1 END;
  IF n <= 8 THEN X23 := X23vals[1] ELSE X23 := X23vals[2] END;
  PolymerProps(TdegC,WtFr[n]);
  t1 := phi2*Pstar2*(1.0/vred2 - 1.0/vred23);
  t2 := phi3*Pstar3*(1.0/vred3 - 1.0/vred23);
  t3 := phi2*theta3*X23/vred23;

```

(* As calculated, the energy term will have units of cm³ bar / g
thus to convert J/g it is necessary to multiply by 0.1 *)

```

  dHCalc[n] := 0.1*vrbarN*(t1 + t2 + t3);
END;

```

```

wh[0] := 'A comparison of the experimental heat of mixing';
wh[1] := ' data with the values recalculated using the ';
wh[2] := ' optimised X23 values at 75.5 and 86.1 degC. ';
wh[3] := ' dHData dHCalc ';

```

```

FOR n := 1 TO 11 DO
  Str.FixRealToStr(100.0*dHData[n],4,wd[n],ok);
  d[n] := 100.0*dHCalc[n]; np[n] := 4;

```

```

END;
bbmutils.AddSpaces(wd,11);
ShowData(wh,wd,d,np,4,11);

```

END X23Optim.

```
(** data(stack_size=>9000H)*)
MODULE XbarAll;
```

```
(* Last edited Tuesday 14th August 1990 *)
```

```
(** optimize( i386 => on ) *)
(** optimize( i387 => on ) *)
(** debug( vid => full ) *)
(** check( index => on ) *)
(** check( stack => on ) *)
```

```
IMPORT      bbmutils,rjmutils,retvols,IO,FIO,MATHLIB,Window,Str;

FROM FIO      IMPORT      File;
FROM MATHLIB IMPORT      Exp,Log,Sqrt;

FROM rjmutils  IMPORT      CubeRoot,SetDebugParams,SolventChoice,
                          ProbePhysProps,VPmmHg,HBT,RackettSD,
                          AlphaCalc,RSD,ProbeCharProps,
                          PolymerSpecVol,MassFromMol,SegmtFromMol,
                          MolFromMass,PolymerProps;

FROM retvols   IMPORT      RetentVols80,RetentVols100,RetentVols120;

FROM bbmutils  IMPORT      Words,String,spaces,Data,SigFigs;

FROM rjmutils  IMPORT      CtoK, GasConst, (* J/(mol K) *)
                          SegMolWt2,sigmaG2,SegMolWt3,
                          sigmaG3,NoAvMolWt2,NoAvMolWt3,
                          MolWt,Tcrit,Pcrit,ZRa,Omega,Rho20,OmegaSRK,
                          VpA,VpB,VpC,VpD,b0,b1,b2,VP,TdegC,Vast,
                          SolubilityParameter,
                          v1,vred1,vstar1,Pstar1,Pred1,Tred1,Tstar1,
                          v2,vred2,vstar2,v3,vred3,vstar3,Pstar2,Pstar3,
                          Pred2,Pred3,Tred2,Tred3,Tstar2,Tstar3,
                          v23,vred23,vstar23,vrbarN,
                          P,Pstar23,Pred23,TdegK,Tstar23,Tred23,phi2,phi3,
                          phistar2,phistar3,theta2,theta3,
                          StoVRatio1,StoVRatio2,StoVRatio3,
                          WtFr,dPred,dTred,dvred,
                          SolventRefNo,SolventName,
                          Debug;
FROM retvols   IMPORT      Vret;
```

```
TYPE
    CharSet = SET OF CHAR;
    CardSet = SET OF CARDINAL;
```

```
LABEL Omit;
```

```
VAR
    B11,Vret2,Vret3,Chi12,Chi13 Chi12star,
    Chi13star,X12bar,X13bar,error      :LONGREAL;
    nSet                                :CardSet;
    w,PP,wtfr                           :Words;
    s,ResFile                             :String;
    Chi23,Chi23prime,Chi23star,Chi23sandp,
    Chi123,Chi123star,X23bar,Q23        :Data;
    FileOutput                            :BOOLEAN;
    FileHandle                            :File;
```

```

n,nx,ny,xc1,xc2,yc1,yc2,j,k,nDegC,nprobe : CARDINAL;
ch                                           : CHAR;
d                                           : Data;
np                                           : SigFigs;
m0                                          : Window.WinType;
d0                                          : Window.WinDef;

```

```

PROCEDURE FileData(VAR wh,w: Words; d: Data; np: SigFigs;
                  nh,nd: CARDINAL;FileHandle: File);

```

```

VAR
    n           : CARDINAL;
    ok          : BOOLEAN;
    ch          : CHAR;
    s           : String;

```

```

BEGIN

```

```

(* This procedure is intended to write numerical data to a file identified by
FileHandle; the array w should contain identifiers for the numerical data
held in array d. nd should not exceed 20 though no protection is provided. *)

```

```

FOR n := 1 TO nh-1 DO
    FIO.WrStr(FileHandle,wh[n-1]);
    FIO.WrLn(FileHandle);

```

```

END;

```

```

FIO.WrCard(FileHandle,nd,2);
FIO.WrLn(FileHandle);

```

```

s := wh[nh-1];
FOR n := 1 TO Str.Length(wh[nh-1]) DO s[n] := CHR(196) END;
FIO.WrStr(FileHandle,wh[nh-1]);
FIO.WrLn(FileHandle);
FIO.WrStr(FileHandle,s);
FIO.WrLn(FileHandle);

```

```

FOR n := 1 TO nd DO
    FIO.WrStr(FileHandle,w[n]);
    IF d[n] > 0.0 THEN s := spaces[6] ELSE s := spaces[5] END;
    FIO.WrStr(FileHandle,s);
    Str.FixRealToStr(d[n],np[n],s,ok);
    FIO.WrStr(FileHandle,s);
    FIO.WrLn(FileHandle);

```

```

END;
FIO.WrLn(FileHandle);

```

```

END FileData;

```

```

PROCEDURE Bvirial(VAR B11: LONGREAL; TdegC: LONGREAL);

```

```

VAR
    f0,f1,tr1,tr2,tr3,tr8,br1,br2,
    Bbbm,Btsonop           : LONGREAL;
    ok                     : BOOLEAN;
    Bw,Bh                  : Words;
    Bv                     : Data;
    np                     : SigFigs;

```

```

BEGIN
  (*the Debug Parameter is 9 *)

  tr1 := (TdegC + CtoK)/Tcrit;
  tr2 := tr1*tr1; tr3 := tr2*tr1; tr8 := tr3*tr3*tr2;
  f0 := 0.1445 - 0.330/tr1 - 0.1385/tr2 - 0.0121/tr3 - 0.000607/tr8;
  f1 := 0.0637 + 0.331/tr2 - 0.423/tr3 - 0.008/tr8;
  br1 := f0 + Omega*f1;

  f0 := Log(tr1)/tr1;
  br2 := b0 + f0*(b1 + f0*b2);

  f1 := Pcrit/GasConst/Tcrit;
  Bbbm := br2/f1; Btsonop := br1/f1;
  IF (SolventRefNo = 14) OR (SolventRefNo = 15)
    THEN B11 := Btsonop
    ELSE B11 := Bbbm
  END;

  IF Debug[9] THEN
    Bh[0] := 'Estimated values of 2nd Virial Coefficients';
    Bh[2] := 'at a temperature of ';
    Str.FixRealToStr(TdegC,0,Bh[3],ok);
    Bh[4] := ' degC';
    bbmutils.bbmConcat(Bh[1],Bh,2,4);

    Bv[1] := Bbbm; Bw[1] := 'Bvir from exptl data (cm3/mol)';
    Bv[2] := Btsonop; Bw[2] := 'Bvir from correlation (cm3/mol)';
    np[1] := 1; np[2] := 1;
    bbmutils.ShowData(Bh,Bw,Bv,np,2,2);
  END;
END Bvirial;

PROCEDURE ChooseTdegC(nDegC: CARDINAL): LONGREAL;
VAR
  tdegc : LONGREAL;
BEGIN
  IF nDegC = 1 THEN tdegc:=-80.0
  ELSIF nDegC = 2 THEN tdegc:=-100.0
  ELSE tdegc:=-120.0
  END;
  RETURN tdegc;
END ChooseTdegC;

PROCEDURE ChiValues(VAR Npts: CARDINAL; nDegC, SolventRefNo: CARDINAL;
  FileOutput: BOOLEAN; FileHandle: File);

CONST
  GasConst = 83.144; (* Bar cm3 / (Mol K) *)

  (* as vapour pressure data have been amended to bar it
  is convenient to redefine R in appropriate units. *)

```

```

VAR
  f0,f1,V1,V2,V3,Vstar1,Vstar2,Vstar3,w2,
  Veva,Vfva,w3,TdegC,TdegK,
  term1,term2,term3,term4,r,rstar
                                     : LONGREAL;
  n,m
                                     : CARDINAL;
  ok,debug
                                     : BOOLEAN;
  Cw,Ch
                                     : Words;
  Cv,WF
                                     : Data;
  np
                                     : SigFigs;

PROCEDURE F1(a,b,c: LONGREAL): LONGREAL;
  BEGIN
    RETURN Log(a*b/c);
  END F1;

PROCEDURE S1(a,b,c: LONGREAL): LONGREAL;
  BEGIN
    RETURN a-b-c;
  END S1;

BEGIN
  (* Debug parameter is 10 *)
  debug := FALSE;
  TdegC := ChooseTdegC(nDegC);
  TdegK := TdegC+CtoK;
  ProbePhysProps(SolventRefNo);
  ProbeCharProps(TdegC);

  VPmmHg(VP,TdegC,SolventRefNo); VP := VP/750.061; (* to bar *)
  Bvirial(B11,TdegC);

  (* Load the values of the retention volumes. *)

  IF nDegC = 1 THEN Npts := 9; RetentVols80(SolventRefNo);
  ELSIF nDegC = 2 THEN Npts := 8; RetentVols100(SolventRefNo);
  ELSE Npts := 8; RetentVols120(SolventRefNo);
  END;

  (* Chi12 and Chi13 values from Eqn 2 of Bhatt.. et al
  after obtaining v2 and v3 for pure polymers *)

  f0 := VP/GasConst;
  V1 := v1*MolWt;
  f1 := CtoK/V1/f0;
  term2 := f0*(B11 - V1)/TdegK;

  (* For 100% EVA the weight fraction is always 1.0 and
  the retention volume is always Vret[2,Npts] *)

  WF[Npts] := 1.0000; Veva := Vret[2,Npts];
  PolymerProps(TdegC,1.0);
  V2 := v2*NoAvMolWt2; (* only evaluated once *)
  term3 := 1.0 - V1/V2;
  term1 := F1(f1,v2,Veva);
  Chi12 := S1(term1,term2,term3);

```

```

(* For 100% FVA the weight fraction is always 0.0 and
the retention volume is always Vret[2,1] *)

WF[1] := 0.0000; Vfva := Vret[2,1];
V3 := v3*NoAvMolWt3; (* only evaluated once *)
term3 := 1.0 - V1/V3;
term1 := F1(f1,v3,Vfva);
Chi13 := S1(term1,term2,term3);
r := V2/V1; (* only evaluated once *)

(* Chi23prime values from Eqn 3 *)
FOR n := 2 TO Npts-1 DO

  (* Convert the mol fraction Vret[1,n] to mass
  fractions prior to the call to PolymerProps *)

  MassFromMol(w2,w3,Vret[1,n]);
  WF[n] := w2;
  PolymerProps(TdegC,w2);
  term1 := Exp(phi2*Log(v2))*Exp(phi3*Log(v3));
  term2 := Exp(phi2*Log(Veva))*Exp(phi3*Log(Vfva));
  term3 := w2*v2 + w3*v3;
  Chi23prime[n] := Log((term1*Vret[2,n])/(term2*term3))/(phi2*phi3);

  (* Chi23 values now obtained by multiplying prime
  values by the ratio V2/V1 *)

  Chi23[n] := r*Chi23prime[n];
END;

IF Debug[10] OR FileOutput THEN

  (* The first 3 sections need only be done once for all the output sections *)

  Ch[4] := 'for '; Ch[5] := SolventName; Ch[6] := ' at ';
  Str.FixRealToStr(TdegC,0,Ch[7],ok); Ch[8] := ' degC';
  bbmutils.bbmConcat(Ch[1],Ch,4,8);

  Ch[4] := ' Wt.Fr'; Ch[5] := spaces[9]; Ch[6] := 'Chi ';
  bbmutils.bbmConcat(Ch[2],Ch,4,6);

  FOR n := 1 TO Npts DO Str.FixRealToStr(WF[n],4,Cw[n],ok) END;
  FOR n := 1 TO Npts DO np[n] := 4 END;

  Ch[0] := 'Values of Chi12, Chi13 and Chi23prime';
  Cv[Npts] := Chi12; Cv[1] := Chi13;
  FOR n := 2 TO Npts-1 DO Cv[n] := Chi23prime[n] END;
  IF Debug[10] THEN bbmutils.ShowData(Ch,Cw,Cv,np,3,Npts) END;
  IF FileOutput THEN FileData(Ch,Cw,Cv,np,3,Npts,FileHandle) END;

  Ch[0] := 'Values of Chi12, Chi13 and Chi23';
  FOR n := 2 TO Npts-1 DO Cv[n] := Chi23[n] END;
  IF Debug[10] THEN bbmutils.ShowData(Ch,Cw,Cv,np,3,Npts) END;
  IF FileOutput THEN FileData(Ch,Cw,Cv,np,3,Npts,FileHandle) END;
END;

```

(* Chi12star and Chi13star values from Eqn 2 of Bhatt.. et al *)

```
Vstar1 := vstar1*MolWt; (* only evaluated once *)
f1 := CtoK/Vstar1/f0;
term2 := f0*(B11 - Vstar1)/TdegK;
Vstar2 := vstar2*SegMolWt2; (* only evaluated once *)
term3 := 1.0 - Vstar1/Vstar2;
term1 := F1(f1,vstar2,Veva);
Chi12star := S1(term1,term2,term3);
Vstar3 := vstar3*SegMolWt3; (* only evaluated once *)
term3 := 1.0 - Vstar1/Vstar3;
term1 := F1(f1,vstar3,Vfva);
Chi13star := S1(term1,term2,term3);
rstar := Vstar2/Vstar1;
```

(* Chi23sandp values from Eqn 3 *)

```
FOR n := 2 TO Npts-1 DO
  (* convert mol fractions to mass fractions *)
  MassFromMol(w2,w3,Vret[1,n]);
  (* call procedure to get phistar2,phistar3 *)
  PolymerProps(TdegC,w2);
  term1 := Exp(phistar2*Log(vstar2))*Exp(phistar3*Log(vstar3));
  term2 := Exp(phistar2*Log(Veva))*Exp(phistar3*Log(Vfva));
  term3 := w2*v2 + w3*v3;
  Chi23sandp[n] := Log((term1*Vret[2,n])/(term2*term3))/(phi2*phi3);
```

(* Chi23star values now obtained by multiplying
prime values by the ratio Vstar2/Vstar1 *)

```
Chi23star[n] := rstar*Chi23sandp[n];
```

END;

IF Debug[10] OR FileOutput THEN

```
Ch[0] := 'Values of Chi12star, Chi13star and Chi23sandp';
Cv[Npts] := Chi12star; Cv[1] := Chi13star;
FOR n := 2 TO Npts-1 DO Cv[n] := Chi23sandp[n] END;
IF Debug[10] THEN bbmutils.ShowData(Ch,Cw,Cv,np,3,Npts) END;
IF FileOutput THEN FileData(Ch,Cw,Cv,np,3,Npts,FileHandle) END;
```

```
Ch[0] := 'Values of Chi12star, Chi13star and Chi23star';
FOR n := 2 TO Npts-1 DO Cv[n] := Chi23star[n] END;
IF Debug[10] THEN bbmutils.ShowData(Ch,Cw,Cv,np,3,Npts) END;
IF FileOutput THEN FileData(Ch,Cw,Cv,np,3,Npts,FileHandle) END;
```

END;

(*Calculation of Chi123 *)

```
f1 := CtoK/f0/V1;
term2 := f0*(B11 - V1)/TdegK;
FOR n := 2 TO Npts-1 DO
  (* calculate wt.frs. from mol frs. *)
  MassFromMol(w2,w3,Vret[1,n]);
  PolymerProps(TdegC,w2);
  term3 := (1.0 - V1/V2)*phi2;
  term4 := (1.0 - V1/V3)*phi3;
  term3 := term2 + term3 + term4;
  Chi123[n] := Log(f1*v23/Vret[2,n]) - term3;
```

END;

(* Calculation of Chi123star *)

```
f1 := CtoK/f0/Vstar1;
term2 := f0*(B11-Vstar1)/TdegK;
FOR n := 2 TO Npts-1 DO
  (* calculate wt.frs. from mol frs. *)
  MassFromMol(w2,w3,Vret[1,n]);
  PolymerProps(TdegC,w2);
  term3 := (1.0 - Vstar1/Vstar2)*phistar2;
  term4 := (1.0 - Vstar1/Vstar3)*phistar3;
  term3 := term2 + term3 + term4;
  Chi123star[n] := -Log(f1*vstar23/Vret[2,n]) - term3;
END;
```

```
IF Debug[10] OR FileOutput THEN
  Ch[0] := 'Values of Chi12, Chi13 and Chi123';
  Cv[Npts] := Chi12; Cv[1] := Chi13;
  FOR n := 2 TO Npts-1 DO Cv[n] := Chi123[n] END;
  IF Debug[10] THEN bbmutils.ShowData(Ch,Cw,Cv,np,3,Npts) END;
  IF FileOutput THEN FileData(Ch,Cw,Cv,np,3,Npts,FileHandle) END;
  Ch[0] := 'Values of Chi12star, Chi13star and Chi123star';
  Cv[Npts] := Chi12star; Cv[1] := Chi13star;
  FOR n := 2 TO Npts-1 DO Cv[n] := Chi123star[n] END;
  IF Debug[10] THEN bbmutils.ShowData(Ch,Cw,Cv,np,3,Npts) END;
  IF FileOutput THEN FileData(Ch,Cw,Cv,np,3,Npts,FileHandle) END;
END;
END ChiValues;
```

```
PROCEDURE Xijbar(nDegC,SolventRefNo: CARDINAL;
  FileOutput: BOOLEAN; FileHandle: File);
```

```
CONST
  GasConst = 83.144; (* Bar cm3 / (Mol K) *)
```

```
VAR
  t0,t1,t2,t3,t4,Vstar1,TdegK,w2,w3,r,
  OptimValue,f0,p0,q0,p1,q1,p2,q2 : LONGREAL;
  n,Npts : CARDINAL;
  ok : BOOLEAN;
  s : String;
  Cw,Ch,Ctemp : Words;
  Cv,Cwf : Data;
  np : SigFigs;
```

```
BEGIN
  OptimValue := 5.566; (* units bar using only data at 75.5 degC *)
```

```
ChiValues(Npts,nDegC,SolventRefNo,FALSE,FileHandle);
```

```
TdegC := ChooseTdegC(nDegC);
TdegK := TdegC + CtoK;
f0 := GasConst*TdegK;
```

(* X12bar and X13bar are calculated from Eq 5 *)

```

(* X12bar *)
Vstar1 := vstar1*MolWt;
p0 := (CubeRoot(vred1) - 1.0);
t0 := p0/(CubeRoot(vred2) - 1.0);
q0 := Pstar1*Vstar1;
p1 := 1.0/vred1 + 3.0*Tred1*Log(t0);
t1 := q0*(p1 - 1.0/vred2);
t2 := f0*Chi12star;
X12bar := (vred2/Vstar1)*(t2 - t1); Cwf[Npts] := 1.000;

(* X13bar *)
t0 := p0/(CubeRoot(vred3) - 1.0);
t1 := q0*(p1 - 1.0/vred3);
t2 := f0*Chi13star;
X13bar := (vred3/Vstar1)*(t2 - t1); Cwf[1] := 0.000;

(* X23bar is calculated from Eq 9 *)
p2 := X12bar*theta2 + X13bar*theta3;
q2 := theta2*theta3;

FOR n := 2 TO Npts-1 DO
  MassFromMol(w2,w3,Vret[1,n]); Cwf[n] := w2;
  PolymerProps(TdegC,w2);
  t0 := p0/(CubeRoot(vred23) - 1.0);
  t1 := q0*(p1 - 1.0/vred23);
  t2 := f0*Chi123star[n];
  t3 := (vred23/Vstar1)*(t2-t1) - p2;
  X23bar[n] := - (t3*StoVRatio2/StoVRatio1)/q2;
  Q23[n] := (OptimValue - X23bar[n])/(TdegK*vred23);
END;

IF Debug[11] OR FileOutput THEN
  (* Develop Heading *)
  Ch[0] := 'Calculated values for X23bar and Q23';
  Ch[1] := ' Probe - '; Ch[2] := SolventName;
  Ch[3] := ' at ';
  Str.FixRealToStr(TdegC,0,Ch[4],ok);
  Ch[5] := ' degC';
  bbmutils.bbmConcat(s,Ch,1,5);
  Ch[1] := s;
  Ch[2] := 'X23bar is in bar and Q23 in bar/K';
  Ch[3] := spaces[2];
  Ch[4] := 'WtFr '; Ch[5] := spaces[7];
  Ch[6] := ' Xijbar'; Ch[7] := spaces[6];
  Ch[8] := ' Q23'; Ch[9] := spaces[2];
  bbmutils.bbmConcat(s,Ch,3,9);
  Ch[3] := s;
  FOR n := 1 TO Npts DO Str.FixRealToStr(Cwf[n],4,Cw[n],ok)END;
  bbmutils.AddSpaces(Cw,Npts);
  FOR n := 1 TO Npts DO Str.Append(Cw[n],spaces[5]) END;
  Str.FixRealToStr(X13bar,4,Ctemp[1],ok);
  Str.FixRealToStr(X12bar,4,Ctemp[Npts],ok);
  FOR n := 2 TO Npts-1 DO
    Str.FixRealToStr(X23bar[n],4,Ctemp[n],ok)
  END;
  bbmutils.AddSpaces(Ctemp,Npts);
  FOR n := 1 TO Npts DO Str.Append(Cw[n],Ctemp[n])END;

```

```

    Cv[1] := 0.0; Cv[Npts] := 0.0;
    FOR n := 2 TO Npts-1 DO Cv[n] := Q23[n] END;
    FOR n := 1 TO Npts DO np[n] := 4 END;
    IF Debug[11] THEN bbmutils.ShowData(Ch,Cw,Cv,np,3,Npts)END;
    IF FileOutput THEN FileData(Ch,Cw,Cv,np,4,Npts,FileHandle) END;
END;
END Xijbar;

BEGIN
  SetDebugParams(11);
  nSet := CardSet{1,2,3};

  w[0] := 'Do you wish to write the results to a file (y/n)? ';
  w[2] := 'Enter the file name (up to 8 chars)';
  w[4] := 'Enter an integer {1,2 or 3} to select a';
  w[6] := 'temperature of 80, 100 or 120 degC: ';
  w[8] := 'Do you wish to repeat with another probe (y/n)?';
  FOR n := 1 TO 7 BY 2 DO w[n] := ' ' END;

  d0 := Window.WinDef(0,0,79,24,Window.LightBlue,Window.Black,
    FALSE,FALSE,FALSE,TRUE,Window.SingleFrame,
    Window.Yellow,Window.Black);
  m0 := Window.Open(d0);
  Window.CursorOn;
  bbmutils.NewWindow(w,0,6,m0,xc1,yc1,xc2,yc2);
  Window.Clear;
  ny := 2;
  bbmutils.OffSet(w[0],j,nx,xc1,xc2);
  Window.DirectWrite(nx,ny,ADR(w[0]),j);
  Window.GotoXY(nx+j+1,ny);
  REPEAT
    ch := CAP(IO.RdKey());
    FileOutput := ch = 'Y';
  UNTIL FileOutput OR (ch = 'N');
  Window.GotoXY(1,ny);
  Window.ClrEol;

  IF FileOutput THEN
    INC(ny,2);
    j := Str.Length(w[2]);
    Window.DirectWrite(nx,ny,ADR(w[2]),j);
    Window.GotoXY(nx+j+1,ny);
    IO.RdStr(ResFile);
    Str.Append(ResFile,'Res');
    FileHandle := FIO.Create(ResFile);
  END;

  INC(ny,2);
  Window.DirectWrite(nx,ny,ADR(w[4]),Str.Length(w[4]));
  INC(ny,2);
  j := Str.Length(w[6]);
  REPEAT
    Window.DirectWrite(nx,ny,ADR(w[6]),j);
    Window.GotoXY(j+nx+1,ny);
    Window.ClrEol;
    Window.GotoXY(j+nx+1,ny);
    nDegC := IO.RdCard();
  UNTIL nDegC IN nSet;

```

```
Window.Clear;
Window.Hide(m0);

TdegC := ChooseTdegC(nDegC);

FOR nprobe := 3 TO 18 DO
  IF nprobe = 14 THEN GOTO Omit END;
  SolventRefNo := nprobe;
  SolventChoice(SolventRefNo,FALSE,SolventName);
  Xijbar(nDegC,SolventRefNo,FileOutput,FileHandle);
Omit:
  END;

  IF FileOutput THEN FIO.Close(FileHandle) END;

END XbarAll.
```

```
(*# data(stack_size => 6000H) *)
```

```
MODULE Spinodal;
```

```
(* Re-edited Wednesday 15th August 1990 *)
```

```
(*# optimize( i386 => on ) *)
```

```
(*# optimize( i387 => on ) *)
```

```
(*# debug( vid => full ) *)
```

```
(*# check( index => on ) *)
```

```
(*# check( stack => on ) *)
```

```
IMPORT bbmutils,rjmutils,retvols,IO,FIO,MATHLIB,Window,Str;
```

```
FROM FIO IMPORT File;
```

```
FROM MATHLIB IMPORT Exp,Log,Sqrt;
```

```
FROM rjmutils IMPORT CubeRoot,SetDebugParams,SolventChoice,
ProbePhysProps,VPmmHg,HBT,RackettSD,
AlphaCalc,RSD,ProbeCharProps,
PolymerSpecVol,MassFromMol,SegmtFromMol,
MolFromMass,PolymerProps;
```

```
FROM retvols IMPORT RetentVols80,RetentVols100,RetentVols120;
```

```
FROM bbmutils IMPORT Words,String,spaces,Data,SigFigs;
```

```
FROM rjmutils IMPORT CtoK,SegMolWt2,sigmaG2,SegMolWt3,sigmaG3,
NoAvMolWt2,NoAvMolWt3,
MolWt,Tcrit,Pcrit,ZRa,Omega,Rho20,OmegaSRK,
VpA,VpB,VpC,VpD,b0,b1,b2,VP,TdegC,Vast,
SolubilityParameter,
v1,vred1,vstar1,Pstar1,Pred1,Tred1,Tstar1,
v2,vred2,vstar2,v3,vred3,vstar3,Pstar2,Pstar3,
Pred2,Pred3,Tred2,Tred3,Tstar2,Tstar3,
v23,vred23,vstar23,vrbarN,
P,Pstarb,Predb,TdegK,Tstarb,Tredb,
phi2,phi3,phistar2,phistar3,theta2,theta3,
WtFr,dPred,dTred,dvred,
StoVRatio1,StoVRatio2,StoVRatio3,
SolventRefNo,
SolventName,
Debug;
```

```
FROM retvols IMPORT Vret;
```

```
TYPE CharSet = SET OF CHAR;
```

```
CardSet = SET OF CARDINAL;
```

```
CONST GasConst = 83.144;
```

```
(* redefined as bar cm3 / (mol K) *)
```

```
VAR
```

```
X23,Q23,wtr
```

```
:LONGREAL;
```

```
j,k,n,nx,ny,xc1,xc2,yc1,yc2
```

```
:CARDINAL;
```

```
m0,m1
```

```
:Window.WinType;
```

```
d0,d1
```

```
:Window.WinDef;
```

```
ok
```

```
:BOOLEAN;
```

```
ch
```

```
:CHAR;
```

```
s
```

```
:String;
```

```
w
```

```
:Words;
```

```
d
```

```
:Data;
```

```
np
```

```
:SigFigs;
```

```

PROCEDURE ShowReal(Var s:String; r:LONGREAL; nplaces,nx,ny:CARDINAL);
  VAR
    ok                                     :BOOLEAN;
  BEGIN
    Str.FixRealToStr(r,nplaces,s,ok);
    Window.DirectWrite(nx,ny,ADR(s),Str.Length(s));
  END
  ShowReal;

PROCEDURE PartDerivs(Ttrial:LONGREAL);
  VAR
    v3red23,factor,B,C,D,x,y,z,p,q,vroot      :LONGREAL;
    j,k,n                                       :CARDINAL;
    PDvals                                       :Data;
    s,s1                                        :String;
    w,PD,Ph                                     :Words;
    np                                          :SigFigs;
  BEGIN
    (* Using the nomenclature derived by Zhikuan et al, Polymer, 1983, Vol 24, 263 *)

    Pstarb := Pstar2*phistar2 + Pstar3*phistar3
            - phistar2*theta3*X23; (* R&W Eqn 5 *)
    p := phistar2*Pstar2/Tstar2;
    q := phistar3*Pstar3/Tstar3;
    Tstarb := Pstarb/(p + q); (* R&W Eqn 6 *)
    Predb := P/Pstarb; Tredb := Ttrial/Tstarb;
    B := P/(Pstarb*Pstarb)*
        (Pstar2 - Pstar3 - X23*theta3*(1.0 - theta2/phistar3));
    dPred := B; (* R&W Eqn 27 *)

    C := Tredb*B/Predb + (Pstar3*Tred3 - Pstar2*Tred2)/Pstarb;
    dTred := C; (* R&W Eqn 28 *)
    v3red23 := vred23*vred23*vred23; vroot := CubeRoot(vred23);
    x := B - C*(Predb/Tredb + 1.0/(Tredb*vred23*vred23));
    y := Tredb*(3.0*vroot - 2.0);
    z := 3.0*vred23*vroot*vroot*(vroot - 1.0)*(vroot - 1.0);
    D := x/(2.0/v3red23 - y/z);
    dvred := D;

    IF Debug[12] THEN
      Ph[0] := 'Values of Blend Parameters';
      PD[1] := 'Pstarb'; PDvals[1] := Pstarb;
      PD[2] := 'Tstarb'; PDvals[2] := Tstarb;
      PD[3] := 'Predb'; PDvals[3] := Predb;
      PD[4] := 'Tredb'; PDvals[4] := Tredb;
      FOR n := 1 TO 2 DO np[n] := 2 END;
      FOR n := 3 TO 4 DO np[n] := 6 END;
      bbutils.ShowData(Ph,PD,PDvals,np,1,4);

      Ph[0] := 'Values of Partial Derivatives';
      PD[1] := 'dPred/dphistar3'; PDvals[1] := B;
      PD[2] := 'dTred/dphistar3'; PDvals[2] := C;
      PD[3] := 'dvred/dphistar3'; PDvals[3] := D;
      FOR n := 1 TO 3 DO np[n] := 8 END;
      bbutils.ShowData(Ph,PD,PDvals,np,1,3);
    END;
  END
  PartDerivs;

```

```

PROCEDURE ErrorTerm(TrialK:LONGREAL; db:BOOLEAN):LONGREAL;
  VAR
    Vstar2,vroot,TrialC           :LONGREAL;
    j,k,n,xc1,xc2,yc1,yc2       :CARDINAL;
    lc                            :LONGCARD;
    ok                            :BOOLEAN;
    s0,s1                        :String;
    t                              :Data;
    wh,wd                        :Words;
    np                            :SigFigs;
  BEGIN
    (* NOTE Vstar2 is defined as the molar hard core volume of component 2
       - suggest we try NoAvMolWt2*vstar2 *)

    TrialC := TrialK - CtoK;
    PolymerProps(TrialC,WtFr);
    PartDerivs(TrialK);
    Vstar2 := NoAvMolWt2*vstar2;

    t[1] := 2.0*theta3*theta3*theta2/(phistar2*phistar3);
    t[2] := Pstar2*dvred*(1.0/vred23/vred23 + Pred2);
    t[3] := (X23/vred23)*(t[1] - dvred*theta3*theta3/vred23);
    t[4] := t[2] + t[3];

    (* the ratio of r2/r3 has been fixed as 0.73972 *)

    t[5] := (GasConst/Vstar2)*(1.0/phistar2 - (1.0 - 0.73972));
    vroot := CubeRoot(vred23);
    t[6] := Pstar2*dvred/Tstar2/(vred23 - vroot*vroot) - t[1]*Q23;
    t[7] := t[5] + t[6];
    t[8] := t[4]/TrialK - t[7];

    IF db THEN
      wh[0] := 'Value of Terms in Error Function';
      FOR n := 1 TO 8 DO
        Str.CardToStr(VAL(LONGCARD,n),s0,10,ok);
        Str.Concat(wd[n],'Term',s0);
        np[n] := 6;
      END;
      bbmutils.ShowData(wh,wd,t,np,1,8);
    END;
    RETURN t[8];
  END ErrorTerm;

PROCEDURE zBrent(VAR answer:LONGREAL;x1,x2,tol:LONGREAL; Display:BOOLEAN);
  LABEL Finish;
  CONST itmax = 1000; eps = 1.0E-14;
  VAR
    a,b,c,d,e,min1,min2,min,fa,fb,fc,
    p,q,r,s,tol1,xm           :LONGREAL;
    iter                      :CARDINAL;
    xc1,xc2,yc1,yc2,j,k,nx,ny,ni
    w                          :Words;
    s1,s2,s3                  :String;
    ch                        :CHAR;
    m3                        :Window.WinType;
    d3                        :Window.WinDef;
    ok,db                     :BOOLEAN;

```

BEGIN

```

db := FALSE;
a := x1; fa := ErrorTerm(a,db);
b := x2; fb := ErrorTerm(b,db);
IF fa*fb > 0.0 THEN
    w[0] := 'Root must be bracketed in search procedure';
    w[1] := ' ';
    bbmutils.Pause(w,1,0);
    GOTO Finish;
END;

IF Display THEN
    d3 := Window.WinDef(0,0,79,24,Window.LightBlue,Window.Black,
        FALSE,FALSE,FALSE,TRUE,
        Window.SingleFrame,
        Window.Yellow,Window.Black);
    m3 := Window.Open(d3);
    Window.CursorOn;
    xc1 := 15; xc2 := 65; yc1 := 1; yc2 := 24;
    Window.Change(m3,xc1,yc1,xc2,yc2);
    ni := 2;
    s2 := 'Press any key to continue';
    s3 := ' N          x          F(x)';
    Window.DirectWrite(5,1,ADR(s3),Str.Length(s3));
END;

fc := fb;
FOR iter := 1 TO itmax DO
    IF fb*fc > 0.0 THEN c := a; fc := fa; d := b-a; e := d;END;
    IF ABS(fc) < ABS(fb) THEN
        a := b; b := c; c := a;
        fa := fb; fb := fc; fc := fa;
    END;
    tol1 := 2.0*eps*ABS(b) + 0.5*tol;
    xm := 0.5*(c - b);

    IF (ABS(xm) <= tol1) OR (fb = 0.0) THEN
        answer := b;
        IF Display THEN
            bbmutils.OffSet(s2,j,k,xc1,xc2);
            Window.DirectWrite(k,yc2-2,ADR(s2),j);
            Window.GotoXY(k+j+1,yc2-2);
            ch := IO.RdKey();
        END;
        GOTO Finish;
    END;

    IF (ABS(e) >= tol1) AND (ABS(fa) > ABS(fb)) THEN
        s := fb/fa;
        IF a = c THEN p := 2.0*xm*s; q := 1.0 - s;
        ELSE
            q := fa/fc; r := fb/fc;
            p := s*(2.0*xm*q*(q-r) - (b-a)*(r-1.0));
            q := (q-1.0)*(r-1.0)*(s-1.0);
        END;

```

```

      IF p > 0.0 THEN q := -q END;
      p := ABS(p);
      min1 := 3.0*xm*q - ABS(tol1*q);
      min2 := ABS(e*q);
      IF min1 < min2 THEN min := min1
                        ELSE min := min2
      END;
      IF 2.0*p < min THEN e := d; d := p/q;
                        ELSE d := xm; e := d;
      END;
ELSE
  d := xm; e := d;
END;

a := b; fa := fb;
IF ABS(d) > tol1 THEN b := b+d
ELSE
  IF xm >= 0.0 THEN b := b + ABS(tol1)
                  ELSE b := b - ABS(tol1)
  END;
END;

fb := ErrorTerm(b,db);
IF Display THEN
  INC(ni);
  nx := 4;
  Window.GotoXY(nx,ni); IO.WrCard(iter,3);
  INC(nx,10);
  ShowReal(s1,b,10,nx,ni);
  IF fb < 0.0 THEN INC(nx,19) ELSE INC(nx,20) END;
  ShowReal(s1,fb,10,nx,ni);
  IF ni > 20 THEN
    ni := 2;
    bbmutils.OffSet(s2,j,k,0,50);
    Window.DirectWrite(k,yc2-2,ADR(s2),j);
    Window.GotoXY(k+j+1,yc2-2);
    ch := IO.RdKey();
    Window.Clear;
    Window.DirectWrite(5,1,ADR(s3),Str.Length(s3));
  END;
END;

END;

w[0] := 'Permitted number of iterations exceeded';
w[1] := ' ';
w[2] := 'Current best answer is ';
w[3] := ' ';
Str.FixRealToStr(b,10,w[4],ok);
Str.Append(w[2],w[4]);
bbmutils.Pause(w,3,0);
answer := b;
Finish:
IF Display THEN Window.Close(m3) END;
END zBrent;
```

BEGIN

```

SetDebugParams(13);
w[0] := 'The Calculation of the Spinodal Temperature';
w[1] := 'Enter the exptl. temperature      ';
w[2] := 'Enter the wt fr EVA';
w[3] := 'Enter Q23 (bar/K) ';
w[4] := 'Calculated Spinodal Temperature (K)';
w[5] := 'Do you wish to repeat the calculation (y/n)?';

d0 := Window.WinDef(0,0,79,24,Window.LightBlue,Window.Black,
                   FALSE,FALSE,FALSE,TRUE,Window.SingleFrame,
                   Window.Yellow,Window.Black);

m0 := Window.Open(d0);
Window.CursorOn;
bbmutils.NewWindow(w,0,8,m0,xc1,yc1,xc2,yc2);
REPEAT
    Window.Clear;
    ny := 2;
    bbmutils.OffSet(w[0],j,nx,xc1,xc2);
    Window.DirectWrite(nx,ny,ADR(w[0]),j);

    bbmutils.OffSet(w[1],j,nx,xc1,xc2);
    INC(ny,2);
    j := Str.Length(w[1]);
    Window.DirectWrite(nx,ny,ADR(w[1]),j);
    Window.GotoXY(nx+j+1,ny);
    Texptl := IO.RdLngReal();
    INC(ny,2);
    j := Str.Length(w[2]);
    Window.DirectWrite(nx,ny,ADR(w[2]),j);
    Window.GotoXY(nx+j+1,ny);
    WtFr := IO.RdLngReal();
    INC(ny,2);
    j := Str.Length(w[3]);
    Window.DirectWrite(nx,ny,ADR(w[3]),j);
    Window.GotoXY(nx+j+1,ny);
    Q23 := IO.RdLngReal();
    Window.Clear;

    P := 1.01325;          (* atmospheric pressure bar *)
    X23 := 5.667;         (* bar *)

    SolventChoice(SolventRefNo,FALSE,SolventName);
    zBrent(TdegK,5.0,1000.0,0.0001,Debug[13]);

    INC(ny,2);
    j := Str.Length(w[4]);
    Window.DirectWrite(nx,ny,ADR(w[4]),j);
    ShowReal(s,TdegK,2,nx+j+1,ny);
    INC(ny,2);
    bbmutils.OffSet(w[5],j,nx,xc1,xc2);
    Window.DirectWrite(nx,ny,ADR(w[5]),j);
    Window.GotoXY(nx+j+1,ny);
    REPEAT
        ch := CAP(IO.RdKey());
    UNTIL (ch = 'Y') OR (ch = 'N');
    ch = 'N';
UNTIL
END Spinodal.
```